Integrated Diagnostics and Theranostics of Thyroid Diseases

Luca Giovanella
Editor

OPEN ACCESS

Springer

Integrated Diagnostics and Theranostics of Thyroid Diseases

Luca Giovanella
Editor

Integrated Diagnostics and Theranostics of Thyroid Diseases

Springer

Editor
Luca Giovanella
Clinic of Nuclear Medicine and Molecular Imaging
Imaging Institute of Southern Switzerland
Bellinzona, Ticino, Switzerland

ISBN 978-3-031-35212-6 ISBN 978-3-031-35213-3 (eBook)
https://doi.org/10.1007/978-3-031-35213-3

Imaging Institute of Southern Switzerland

This Springer imprint is published by the registered company Springer Nature Switzerland AG
The registered company address is: Gewerbestrasse 11, 6330 Cham, Switzerland

“Care more particularly for the individual patient than for the special features of the disease.” William Osler

Preface

In the last 2 years, the demand for a personalized diagnostic and therapeutic approach has been constantly increasing to refine our diagnosis, better characterize patients' diseases, develop more effective and personalized therapeutic regimens, and improve outcomes avoiding unnecessary treatments. The current scenario of diagnostic medicine is well represented using the "silo metaphor," where laboratory medicine, pathology, and radiology are conceptually separated diagnostic disciplines. On the other hand, progresses in understanding of biochemical-biological-structural interplays in human diseases, compounded with technological advances, are generating relevant multidisciplinary convergences, leading the way to a new frontier, called integrated diagnostics. This new discipline, which is currently defined as convergence of imaging, pathology, and laboratory tests with advanced information technology, has an enormous potential for revolutionizing diagnosis and therapeutic management of human diseases. In addition, theranostics is emerging as an invaluable tool in personalized medicine; it is a treatment strategy in which the same (or very similar) agents are used for both diagnostic and therapeutic purposes. Thyroid disorders are commonly encountered in clinical practice and their diagnosis and therapy typically involve different specialists using different tools. Laboratory tests and imaging procedures are integral to the diagnosis and management of thyroid disease. Finally, radioiodine therapy represents the first clinical theranostics approach and is widely used in clinical practice since 1940s. Accordingly, thyroid diseases represent an ideal platform to develop and test integrated diagnostics and theranostics strategies. Nuclear medicine is ideally placed to play a central role in this field as clinical management of thyroid disease is a daily activity in nuclear medicine departments. Visualization of molecular targets enables the so-called in vivo immunohistochemistry, by which noninvasive biomarkers can be provided to select targeted drugs labeled with therapeutic radionuclides. On the other hand, an appropriate integration of other laboratory, imaging and pathology data is essential to refine patients' selection for theragnostic procedures and predict their effectiveness and potential toxicity. Our scope is to provide essential but exhaustive information on different diagnostic tools actionable in thyroid patients and, especially, their integration. Furthermore, theragnostic applications available for patients with benign and malignant thyroid diseases are also illustrated. This book is aimed at specialists in clinical thyroidology, imaging and theranostics, laboratory, pathology but also at bioinformatics and computer scientists involved in diagnostic and theragnostic

activities. I believe that medical students and biomedical technicians can also benefit from this reading to have an overall view of a discipline that will undoubtedly be part of their future professional daily life.

Bellinzona, Switzerland Luca Giovanella

Acknowledgments

I would like to warmly thank the authors of different chapters in this book. Without their contribution and their availability, it would not have been possible to carry out this project successfully.

Contents

Integrated Diagnostics: The Future of Diagnostic Medicine?

1

Mario Plebani and Giuseppe Lippi

1.1 Introduction

"Care for a medical condition (or a patient population) usually involves multiple specialties and numerous interventions. Value for the patient is created by providers' combined efforts over the full cycle of care. The benefits of any one intervention for ultimate outcomes will depend on the effectiveness of other interventions throughout the care cycle" [1]. This sentence, reported in a seminal paper published by Michael E Porter, highlights the need to avoid the vision of "focused factories" concentrated on narrow groups of interventions to promote integrated practice units that are accountable for the total care for a medical condition and its complications. The progressive transition from the so-called "silos" models to more integrated and patient-centered systems (i.e., more focused on patient journey) in clinical medicine should involve also the practice of diagnostics.

M. Plebani (✉)
Clinical Chemistry and Clinical Molecular Biology, University of Padova, Padua, Italy

University of Texas Medical Branch, Galveston, TX, USA
e-mail: mario.plebani@unipd.it

G. Lippi
Clinical Biochemistry at University of Verona, Verona, Italy

Service of Laboratory Medicine at University Hospital of Verona, Verona, Italy
e-mail: giuseppe.lippi@univr.it

1.2 Diagnosis and Diagnostics

The word "diagnosis" comes from the Greek prefix dia (apart) and gignōskein (discern, know). Taken together, the meaning of the word is to "know thoroughly" or to "know apart" (distinguish from another). In contemporary Western medicine, physicians move toward the closure of diagnostic possibilities through testing and objective analysis and by means of a "rule-out" reasoning (to ensure the life threatening and treatable conditions are quickly identified), which shall ultimately bring physicians to the correct clinical answer [2]. Diagnostic information may originate from any clinical interaction, examination, or test, including the patient's history, signs and symptoms, laboratory and imaging studies, biopsy and other procedures, and physiological and functional assessments. Diagnosis serves as description of a patient's condition and for guiding treatment and prognosis. An increased understanding of the genomic, proteomic, metabolomic, and microbiomic underpinnings of human biology over time has generated greater knowledge of etiology and progression of biological function from a healthy condition to a diseased state. As understanding of the precursors of disease grow more detailed and revealing, the art and science of diagnosis enlarge from detection of present disease to prediction of future illness. "Put in equivalent, positive terms, medical diagnosis moves from characterizing the current state of health to predicting the future state

L. Giovanella (ed.), *Integrated Diagnostics and Theranostics of Thyroid Diseases*,
https://doi.org/10.1007/978-3-031-35213-3_1

of health. Then interventions may be designed to enhance, maintain, and as needed, restore health" [3]. Despite these impressive improvements in understanding the pathophysiology and molecular nature of most acute and chronic diseases, multiple inefficiencies built into the clinical diagnostic testing landscape work against the seamless integration of clinical diagnostic testing into the treatment pathway. These inefficiencies result in slowing the adoption of laboratory and other diagnostic tests, deficient physician education, and delays in the inclusion of diagnostic testing in associated clinical guidelines—ultimately inhibiting the seamless delivery of these critical diagnostic tests [4]. In particular, the business model involved in delivery of laboratory and other diagnostic services seems to be "primarily designed and executed in individual silos driven by internal activities and managed according to performance metrics that match the discipline itself rather than the products of services to improve clinical pathways, clinical and economical outcomes and patient safety" [5, 6]. As such, clinical laboratories are increasingly organized as focused factories, with the goal of maximizing productivity, improving internal efficiency (e.g., by reducing the cost per test), and consolidating structures in megalaboratories or even outsourcing testing to independent facilities. Several initiatives propose a rigorous team-building transformational organizational change, with a radical departure from the current hierarchical, silo-oriented, medical practice model focused on physician-centered tools, models, concepts, and the language to implement transformational patient-centered medical care [7].

1.3 Integrated Diagnostics

According to the World Health Organization (WHO), health services should be "managed and delivered so that people receive a continuum of health promotion, disease prevention, diagnosis, treatment, disease-management, rehabilitation and palliative care services, coordinated across the different levels and sites of care within and beyond the health sector, and according to their needs throughout the life course" [8]. "Integrated diagnostics" has been defined as "convergence of imaging, pathology, and laboratory tests with advanced information technology (IT)" [9]. In their paper, the authors emphasized that "diagnoses depend on multiple components that include not only imaging, but also clinical observation, pathology, laboratory, and genomic tests. To date, there is too little coordination between the medical specialties responsible for ordering and performing these tests, nor is there enough consideration as to the optimal order of tests. This will change in a world of integrated diagnostics, where, instead of relying on individual provider bias in the selection of tests, data from diverse sources will be used to determine the most efficient diagnostic algorithms. Imaging will be incorporated judiciously into these integrated diagnostic algorithms, complementing other diagnostic techniques in order to maximise efficiency and minimise waste." Other authors emphasized the evidence that "Under the current paradigm of diagnostic medicine, pathologists and radiologists function as members of distinct disciplines, with no direct linkage between their workflows or reporting systems. Even when both departments belong to the same institution, their respective reports on the same patient are only loosely associated with one another by identifiers such as patient's name and medical record number. Despite this complete bifurcation of reporting, the synthesis of both specialties' data must establish diagnosis, determine prognosis, drive patient management and serve as the primary means for assessing response to treatment" [10]. Therefore, the better comprehension of several biological pathways, coupled with emerging technological advances, has recently fostered a paradigm shift in the way diagnostics have been for a long time acknowledged, paving the way to a new model of healthcare based on integration of different data coming from multiple and often independent sources. This, in turn, may allow a more rapid, efficient, and accurate clinical decision-making process, thus ultimately assuring better clinical and economical outcomes. Irrespective of clinical and environmental scenarios, several lines of evidence now attest that the role of the so-called "integrated diagnostics" will overwhelmingly emerge in the foreseeable future, allowing not

only to make earlier and more accurate diagnoses, but also to save a large amount of human and economic resources [11]. In their article, the authors have reported several examples of the fundamental value of integrated diagnostics in most of the leading causes of morbidity and mortality in Western Countries such as acute myocardial infarction, stroke, venous thromboembolism, cancer, and infectious diseases. More recently, the coronavirus disease 2019 (COVID-19) pandemic has reinforced the need for more and better integration between all subdisciplines of laboratory medicine, as well as between pathology, genomic, and radiology [12]. The possible convergence of laboratory, pathology, and imaging test results within the same medical report is, therefore, a valuable goal to foster earlier and more accurate diagnoses, and personalized medicine. However, the enormous volumes of different information (the so-called "big-data") should challenge the mind of clinicians and healthcare professionals. Reinforcement of clinical decision support through expert systems and algorithms based on machine learning and artificial intelligence will become unavoidable [13, 14], and is a major point for the education and training of the new generation of diagnostic professionals. The combination of big data and artificial intelligence, referred by some as the fourth industrial revolution, will change laboratory, radiology, and pathology along with other medical specialties. As predicted by some authors, because pathology and radiology have a similar past and a common destiny, these specialties should perhaps be merged into a single entity, the "information specialist," whose responsibility will not be exclusively to extract information from laboratory data, images, and histology, but to manage the information extracted by artificial intelligence in the clinical context of the patient [15]. The integration of laboratory and pathology services with the creation of the acronym "PALM" (Pathology and Laboratory Medicine) has been recommended by Michael Wilson and Colleagues as a fundamental tool for assuring "accurate diagnosis and detection of disease, informing prognosis and guiding treatment, contributing to disease screening, public health surveillance and disease registries, and supporting medical-legal systems" [16]. A further challenge is represented by the need to integrate, particularly as concerns laboratory tests, the data from decentralized testing (point-of-care, near-patient, and home testing) and wearables [17], as shown in Fig. 1.1.

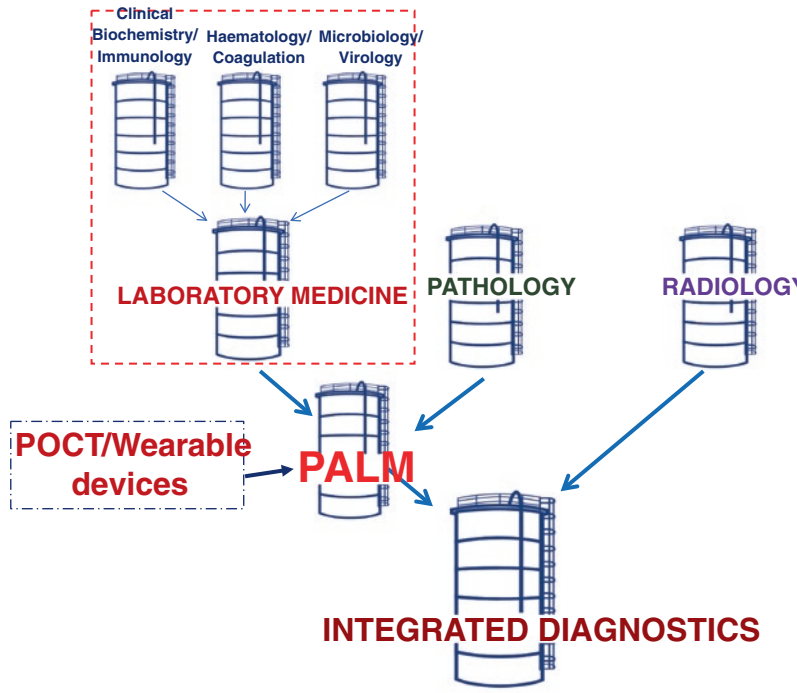

Fig. 1.1 Integrated diagnostics: convergence of laboratory medicine, pathology, radiology, and decentralized testing

1.4 Conclusions

The quest for diagnostic excellence currently encounters many obstacles, including shortcomings in healthcare delivery that limit an efficient integration between several sources of information. The generation of a vast amount of data from the clinical laboratory, pathology genomics, and radiology does not automatically convert to meaningful conclusions and higher effectiveness in both diagnosis and patient treatment. Diagnostic integration and generation of unified medical reports, coupled with machine learning techniques, especially suited to analyze large amounts of data in real time, should be now adopted to foster an optimal diagnostic process and more specific, accurate, and complete diagnostic assessment. However, a combination of machine learning and human judgement should be taken for granted [18].

References

1. Porter ME. What is value in health care? N Engl J Med. 2010;363(26):2477–81.
2. Maitra A, Verghese A. Diagnosis and the illness experience: ways of knowing. JAMA. 2021;326(19):1907–8.
3. Yang D, Fineberg HV, Cosby K. Diagnostic excellence. JAMA. 2021;326(19):1905–6.
4. Keeling P, Clark J, Finucane S. Challenges in the clinical implementation of precision medicine companion diagnostics. Expert Rev Mol Diagn. 2020;20(6):593–9.
5. Price CP, John AS, Christenson R, Scharnhorst V, Oellerich M, Jones P, et al. Leveraging the real value of laboratory medicine with the value proposition. Clin Chim Acta. 2016;462:183–6.
6. Plebani M. Charting the course of medical laboratories in a changing environment. Clin Chim Acta. 2002;319(2):87–100.
7. Plebani M. Quality and future of clinical laboratories: the Vico's whole cyclical theory of the recurring cycles. Clin Chem Lab Med. 2018;56(6):901–8.
8. WHO. Framework on integrated people-centred health services. Report by the secretariat (document A69/39). Geneva: Sixty-ninth World Health Assembly; 2016. 23–28 May 2016. https://apps.who.int/gb/ebwha/pdf_ fles/WHA69/A69_39-en.pdf. Accessed 28 Dec 2022.
9. Krestin GP, Grenier PA, Hricak H, Jackson VP, Khong PL, Miller JC, Muellner A, Schwaiger M, Thrall JH. Integrated diagnostics: proceedings from the 9th biennial symposium of the International Society for Strategic Studies in Radiology. Eur Radiol. 2012;22(11):228394.
10. Sorace J, Aberle DR, Elimam D, Lawvere S, Tawfik O, Wallace WD. Integrating pathology and radiology disciplines: an emerging opportunity? BMC Med. 2012;10:100.
11. Lippi G, Plebani M. Integrated diagnostics: the future of laboratory medicine? Biochem Med. 2020;30:1–13.
12. Plebani M. Laboratory medicine in the COVID-19 era: six lessons for the future. Clin Chem Lab Med. 2021; https://doi.org/10.1515/cclm-2021-0367.
13. Plebani M, Laposata M, Lippi G. A manifesto for the future of laboratory medicine professionals. Clin Chim Acta. 2019;489:49–52.
14. Padoan A, Plebani M. Artificial intelligence: is it the right time for clinical laboratories? Clin Chem Lab Med. 2022;60(12):1859–61.
15. Jha S, Topol EJ. Adapting to artificial intelligence: radiologists and pathologists as information specialists. JAMA. 2016;316(22):2353–4.
16. Wilson ML, Fleming KA, Kuti MA, Looi LM, Lago N, Ru K. Access to pathology and laboratory medicine services: a crucial gap. Lancet. 2018;391(10133):1927–38.
17. Mukherjee S, Suleman S, Pilloton R, Narang J, Rani K. State of the art in smart portable, wearable, ingestible and implantable devices for health status monitoring and disease management. Sensors (Basel). 2022;22(11):4228.
18. Fineberg HV, Song S, Wang T. The future of diagnostic excellence. JAMA. 2022;328(11):1039–40.

2 Artificial Intelligence and Machine Learning in Integrated Diagnostic

Lisa Milan

2.1 Background

High-quality patient care relies on the delivery of high-quality and comprehensive medical treatments, meeting the needs of each patient. It comprises a wide range of healthcare services, including diagnosis, treatment, and management of illnesses, as well as preventive care and health promotion. Physician's experience is a key factor in providing valuable standard of care and in taking accurate decisions. Obviously, this is a long process requiring both financial and time investments through practice and continuous education. Artificial Intelligence (AI) and Machine Learning (ML) can offer great support to the experienced physicians, by providing them with additional insights that otherwise they may not have had direct access to. AI can also help to automate routine tasks and identify potential issues early, assisting expert physicians in their diagnostic process and decision-making. If a radiologist may review approximately 225,000 magnetic resonance (MR) or computed tomography (CT) exams during his career [1], AI algorithms can process millions of scans in a short period; this leads to a higher probability to identify subtle abnormalities that may have been missed by radiologists. This high potential can be exploited in "integrated diagnostics," a term used to define the convergence of imaging, pathology, and laboratory tests with advanced information technology [2]. AI can contribute to creating new models, boosting the integration of these different data toward a more efficient and straightforward healthcare [3]. One of the main areas where AI is exploited in integrated diagnostics is in the analysis of medical images. AI algorithms can be trained to analyze images from multiple modalities, such as X-ray, CT, MR, positron emission tomography (PET), single photon emission computer tomography (SPECT), and ultrasound (US) images and detect phenotyping information that may not be obvious to the human eye.

AI is also used in the analysis of genomic data. The cost of sequencing a patient's genome has decreased over the years, with the consequent exponential increase of the available genomic data [4]. AI algorithms analyze these data and identify genetic variations that may be associated not only with cancers but also with common non-cancer diseases [5]. This can lead to the development of personalized precision medicine and a better understanding of the underlying causes of disease. AI can also be used in the analysis of electronic health records (EHRs). EHR includes information about a patient's health history, such as diagnoses, medicines, tests, allergies, immunizations, treatment plans, personalized medical care, and improvement of medical quality and

L. Milan (✉)
Clinic of Nuclear Medicine and Molecular Imaging, Imaging Institute of Southern Switzerland, Ente Ospedaliero Cantonale, Bellinzona, Switzerland
e-mail: Lisa.Milan@eoc.ch

L. Giovanella (ed.), *Integrated Diagnostics and Theranostics of Thyroid Diseases*,
https://doi.org/10.1007/978-3-031-35213-3_2

safety [6]. Through AI, it would be possible to accurately classify diseases, reclassify preexisting disease categories according to individual characteristics, quickly analyze images and medical data in EMR, and provide appropriate services [6]. In addition, AI assists in the interpretation of lab test results, such as pathology reports, and other diagnostic data. Digital image analysis in pathology can identify and quantify specific cell types quickly and accurately evaluating histological features, morphological patterns, and biologically relevant regions of interest [7, 8]. Quantitative image analysis tools also enable the capturing of data from tissue slides that may not be accessible during manual assessment via routine microscopy reducing the analysis time and avoiding human error [9, 10]. The power of AI to analyze large amounts of data quickly can significantly speed up the discovery of novel features that may help predict how a patient's disease will progress and how the patient will likely respond to a specific treatment [11–14].

2.2 Artificial Intelligence and Machine Learning

McCarthy and colleagues coined the term "Artificial Intelligence" during a conference in the 1950s and they referred to all the mathematical algorithms that attempt to perform tasks that normally require human cognitive abilities [15–17]. It encompasses a wide range of technologies and techniques, including machine learning, natural language processing, computer vision, and expert systems. AI systems can be trained using a variety of techniques, such as supervised learning, unsupervised and reinforcement learning. They can also be implemented using a variety of architectures, such as neural networks, decision trees, and genetic algorithms. In general, the first step in the creation of an AI model starts with collecting the data and checking for their goodness and lack of bias. The data has to be harmonized and only after they can be used to train the algorithm. The training phase consists of a set of iterations executing mathematical functions and is aimed to correlate the input of the endpoint of interest with a high level of probability. The accuracy of the created model has to be evaluated with another dataset called testing set, which allowed for adjusting the model parameters. Finally, the model has to be confirmed with internal and/or external validation datasets, in order to evaluate the performance with a new and independent dataset.

The most common types of AI in diagnostic medicine include:

1. Machine learning: ML algorithms are used to identify patterns and make predictions based on data by multiple layers of analysis. The models produced by ML algorithms are inferences made from statistical analysis of very large datasets, expressed as the likelihood of a relationship between variables [18]. According to how the ML algorithms are trained, they can be divided into supervised, unsupervised, and reinforcement learning. Supervised learning requires a set of input data as well as their corresponding output information, in order to identify a function linking inputs to outputs [19]. On the other hand, unsupervised learning does not need labels, since it searches for patterns that can separate the input data into subsets with similar characteristics [20]. The supervised learning algorithms can be broadly divided into regression and classification based on prediction of a quantitative or categorical variable [21]. Unsupervised learning is often used for feature extraction, while supervised learning is suitable for predictive modelling [22]. Different methods can be used for unsupervised learning. For example, clustering is one of the most famous methods in which data are split into groups according to their peculiarities [23]. The third category of AI algorithm is reinforcement learning, which learns by taking in feedback the result of its action. It consists of an agent that executes an action and the environment in which the action is performed. It is based on the concept of reward: an agent learns to interact with the environment aiming to achieve the best reward. The

environment sends a signal to the agent that performs a specific action. Once the action is performed, the environment reacts with a reward signal, so the agent can update and evaluate its last action. The cycle repeats until the environment sends a stop feedback. This workflow mirrors what happens in clinical situations, where a doctor has to adopt an action depending on the patient's condition [24]. Reinforcement learning can be used to design a decision support system in order to provide treatment recommendations to physicians [25].

2. Deep learning (DL): DL, a term coined in 1986 by Rina Dechter [26], is a new type of ML method that uses advanced neural networks with multiple layers to analyze the data. A neural network is a set of simple computational units, also called nodes, highly interconnected. Nodes are then organized into layers, i.e., a structure that takes information from the previous layers and then passes it to the next layer. In general, there are input layers, hidden layers, and output layers. As the name suggests, the number of nodes and layers in DL algorithms can be very high. DL is particularly useful for analyzing images and other types of data that have complex structures and presents not simply linear relationships [27]. Different from traditional feature-based ML approaches (Fig. 2.1), DL is able to achieve diagnosis automation, avoiding human intervention [28]. In medical applications, DL algorithms are exploited, for example, in the detection and characterization of different tissues (normal vs pathological) as well as for the analysis of disease progression [26, 29].
3. Natural language processing (NLP): NLP is a branch of AI that is used to understand and interpret written and spoken human language. It can be used to extract information from unstructured data, such as medical records, clinical notes, and other free texts. Understanding human languages constitute some of the most challenging problems faced

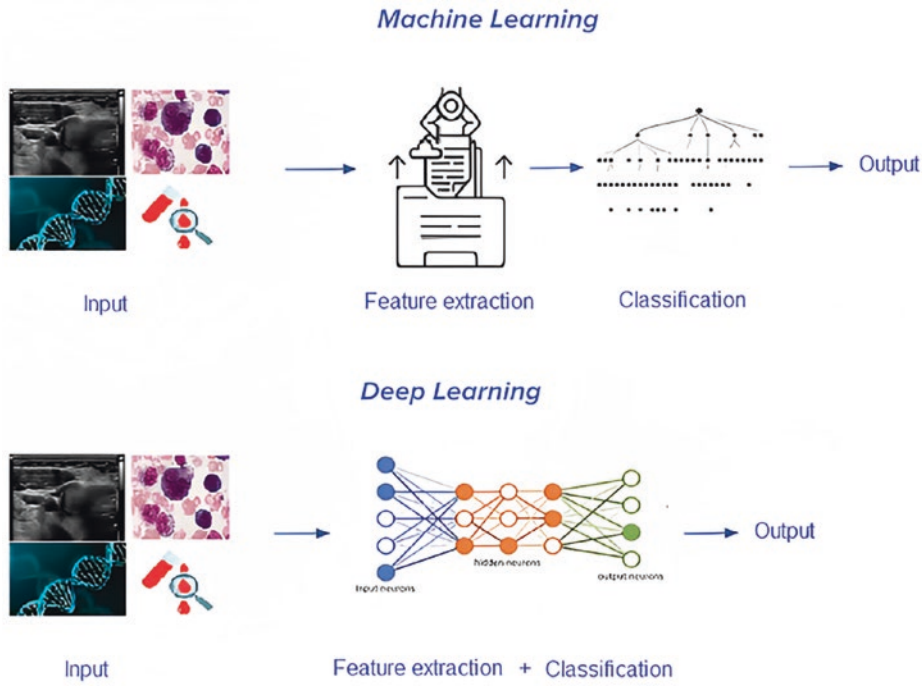

Fig. 2.1 Difference between ML and DL. In contrast to ML, DL does not need to define a priori a set of handcrafted features, but it is able to find complex correlations to predict the output

by AI [30]. As well as for the other AI methods, often the amount of available data is not sufficient and the effort to evaluate their goodness by the experts can be very huge and expensive. This is particularly true for Clinical NLP; in fact, it requires a very important amount of time for the revision of these unstructured data. Moreover, domain knowledge has also been shown to be important for understanding biomedical texts, such as in interpreting linguistic structures [31]. The knowledge is commonly represented as ontologies, that organize domain knowledge into structures that computers can read, and humans can understand. The size and extent of background knowledge needed to make inferences are great [31]. However, clinical NLP benefits from the availability of massive knowledge resources, such as, for example, medical vocabularies.

2.3 AI in Integrated Diagnostic: Challenges and Future Prospects

Recent reports confirm that approximately 86% of healthcare organizations use ML solutions, and more than 80% of healthcare organization leaders have an AI plan for the future [32, 33]. Looking at the articles published in the last 10 years, it is possible to estimate the growing interest and effort in the application of AI in healthcare (Fig. 2.2). The integrated diagnostic field is included in this big picture. In fact, the integration of the different diagnostic information, e.g., from pathology, imaging, EHRs, and its analysis by AI systems is expected to improve diagnostic precision and the therapeutic path [34]. Until now, many AI models have been used in the mentioned disciplines to detect cancers [35], cardiovascular diseases [36], neurological disorders [37], orthopedic conditions [38], pulmonary diseases [39, 40], skin diseases [41], sequencing genomic [42, 43], drug interactions and side effects [44, 45], and so on.

Unfortunately, the integration of the totality of diagnostic information into a clinical routine is limited by the lack of a suitable information technology infrastructure, the absence of high-quality unbiased data, and difficulties to access and exchange data [34]. AI methods need a very large database in order to avoid overfitting; however, this can be challenging, especially in small institutions or in the case of rare diseases. Additionally, the data must be as good as possible; in fact, the model will be a mirror of the type of data used to train it. Moreover, it can be possible, especially in clinical datasets, to have class imbalance negatively affecting the AI algorithms' performance. For example, if an AI system is trained on a dataset that is mostly composed of images from a certain race or gender, it may not perform well on images from other populations. This particular

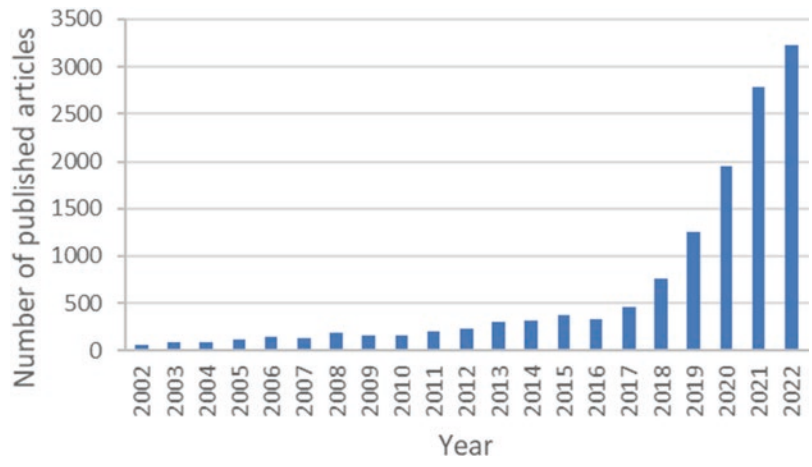

Fig. 2.2 Number of articles retrieved in PubMed by using the search terms "Artificial Intelligence" and "healthcare," grouped by year of publication. A search performed at the end of January 2023

aspect put light on the necessity of AI to be ethical: the performance of the AI solutions must be the same independent of race, gender, and age.

Explainability and transparency are other big problems of AI methods; AI-based systems can be difficult to interpret and understand, making it challenging to explain the taken decisions to patients and physicians. This can lead to uncertainty and a lack of acceptance of the technology. That is why there is a growing interest in developing AI systems that can provide explanations for their decisions, known as "explainable AI" or "XAI" [46].

AI-based diagnostic systems should be clinically validated and approved by regulatory agencies before they are used in clinical practice to ensure safety and efficacy [47]. A recent literature review reported that most studies assessing AI did not include the recommended design features for the robust validation of AI [48]. There is, therefore, a need to develop frameworks for the robust validation of the performance and safety of AI with reliable external datasets [49, 50]. The regulatory environment for AI in healthcare is still evolving and there are currently no clear guidelines for the development, validation, and deployment of AI-based diagnostic systems [51]. Additionally, there is a lack of standardization in the field, which can make it difficult for different systems to communicate and work together. It is a very difficult task, especially considering the dynamism of this technology. ML algorithm can be re-trained and improve its performance as soon as additional data are at disposal; but regularization system does not allow that a medical device changes without first undergoing a reauthorization process. Moreover, there is a need to protect patient privacy: strong privacy protection is realizable when institutions are structurally encouraged to cooperate to ensure data protection [52]. Commercial implementations of healthcare AI can be manageable for the purposes of protecting privacy, but it introduces competing goals. Manufacturers may not be sufficiently encouraged to maintain privacy protection if they can monetize the data or otherwise gain from them, and if the legal penalties are not high enough to offset this behavior. Because of these and other concerns, there have been calls for systemic oversight of big data health research and technology [51, 53].

2.4 Conclusions

In conclusion, AI is playing a growing role in the diagnosis and management of diseases through integrated diagnostics. By analyzing images, blood test results, and genomic data, AI algorithms can assist in the detection and diagnosis, leading to more accurate and personalized treatment plans. However, there are also limitations to consider, including the need for large amounts of data to train AI algorithms and the need for more research to validate the use of AI. Nevertheless, the future of AI in integrated diagnostics is promising and holds great potential to improve patient outcomes. For the broad implementation of AI and integrated diagnostics, central organizations (at the national or even international level) that ensure common structures, standards, and data safety have to be set up.

References

1. Yokota H, Goto M, Bamba C, et al. Reading efficiency can be improved by minor modification of assigned duties: a pilot study on a small team of general radiologists. Jpn J Radiol. 2017;35:262–8.
2. Lippi G, Plebani M. Integrated diagnostics: the future of laboratory medicine? Biochem Med (Zagreb). 2020;30(1):010501.
3. Neumaier M, Watson ID. The end of laboratory medicine as we know it? Clin Chem Lab Med. 2019;57:305–7. https://doi.org/10.1515/cclm-2018-1264.
4. Wetterstrand MS. The cost of sequencing a human genome. 2021. https://www.genome.gov/about-genomics/fact-sheets/Sequencing-Human-Genome-cost.
5. Dlamini Z, Francies FZ, Hull R, Marima R. Artificial intelligence (AI) and big data in cancer and precision oncology. Comput Struct Biotechnol J. 2020;18:2300–11.
6. Lee S, Kim HS. Prospect of artificial intelligence based on electronic medical record. J Lipid Atheroscler. 2021;10(3):282–90.
7. Bera K, Schalper KA, Rimm DL, Velcheti V, Madabhushi A. Artificial intelligence in digital

pathology – new tools for diagnosis and precision oncology. Nat Rev Clin Oncol. 2019;16:703–15.
8. Tumeh PC, et al. Liver metastasis and treatment outcome with anti-PD-1 monoclonal antibody in patients with melanoma and NSCLC. Cancer Immunol Res. 2017;5:417–24.
9. Barisoni L, Lafata KJ, Hewitt SM, Madabhushi A, Balis UGJ. Digital pathology and computational image analysis in nephropathology. Nat Rev Nephrol. 2020;16:669–85.
10. Neltner JH, et al. Digital pathology and image analysis for robust high-throughput quantitative assessment of Alzheimer disease neuropathologic changes. J Neuropathol Exp Neurol. 2012;71:1075–85.
11. Aeffner F, et al. Introduction to digital image analysis in whole-slide imaging: a white paper from the digital pathology association. J Pathol Inform. 2019;10:9.
12. Serag A, et al. Translational AI and deep learning in diagnostic pathology. Front Med. 2019;6:185.
13. Barsoum I, Tawedrous E, Faragalla H, Yousef GM. Histo-genomics: digital pathology at the forefront of precision medicine. Diagnosi. 2019;6:203–12.
14. Baxi V, Edwards R, Montalto M, Saha S. Digital pathology and artificial intelligence in translational medicine and clinical practice. Mod Pathol. 2021;35(1):23–32.
15. McCarthy JJ, Minsky ML, Rochester N. Artificial intelligence. Research Laboratory of Electronics (RLE) at the Massachusetts Institute of Technology (MIT); 1959.
16. McCarthy J, Minsky ML, Rochester N, Shannon CE. A proposal for the Dartmouth summer research project on artificial intelligence. AI Mag. 1955;27(4):12.
17. Iqbal MJ, Javed Z, Sadia H, Qureshi IA, Irshad A, Ahmed R, Malik K, Raza S, Abbas A, Pezzani R, et al. Clinical applications of artificial intelligence and machine learning in cancer diagnosis: looking into the future. Cancer Cell Int. 2021;21:1–11.
18. Rowe M, Frankish K, Ramsey WM. An introduction to machine learning for clinicians the Cambridge handbook of artificial intelligence. Cambridge: Cambridge University Press; 2017.
19. Wernick MN, Yang Y, Brankov JG, Yourganov G, Strother S. Machine learning in medical imaging. IEEE Signal Process Mag. 2010;27:25–38.
20. Castiglioni I, Rundo L, Codari M, Di Leo G, Salvatore C, Interlenghi M, Gallivanone F, Cozzi A, D'Amico NC, Sardanelli F. AI applications to medical images: from machine learning to deep learning. Phys Med. 2021;83:9–24.
21. Sarker IH. Machine learning: algorithms, real-world applications and research directions. SN Comput Sci. 2021;2:160.
22. Jiang F, Jiang Y, Zhi H, et al. Artificial intelligence in healthcare: past, present and future. Stroke Vasc Neurol. 2017;2. https://doi.org/10.1136/svn-2017-000101.
23. Sinharay S. An overview of statistics in education. In: International encyclopedia of education. 3rd ed. Amsterdam: Elsevier; 2010.
24. Zhang Z. Reinforcement learning in clinical medicine: a method to optimize dynamic treatment regime over time. Ann Transl Med. 2019;7(14):345.
25. Riachi E, Mamdani M, Fralick M, Rudzicz F. Challenges for reinforcement learning in healthcare; 2021. arXiv:210305612.
26. Hosny A, Parmar C, Quackenbush J, Schwartz LH, Aerts H. Artificial intelligence in radiology. Nat Rev Cancer. 2018;18:500–10.
27. Walter W, Haferlach C, Nadarajah N, et al. How artificial intelligence might disrupt diagnostics in hematology in the near future. Oncogene. 2021;40:4271–80.
28. Aggarwal R, Sounderajah V, Martin G, Ting DSW, Karthikesalingam A, King D, Ashrafian H, Darzi A. Diagnostic accuracy of deep learning in medical imaging: a systematic review and meta-analysis. NPJ Digit Med. 2021;4:65.
29. Chartrand G, Cheng PM, Vorontsov E, Drozdzal M, Turcotte S, Pal CJ, Kadoury S, Tang A. Deep learning: a primer for radiologists. Radiographics. 2017;37:2113–31.
30. Wu H, Wang M, Wu J, et al. A survey on clinical natural language processing in the United Kingdom from 2007 to 2022. NPJ Digit Med. 2022;5:186.
31. Tian S, Yang W, Le Grange JM, Wang P, Huang W, Ye Z. Smart healthcare: making medical care more intelligent. Glob Health J. 2019;3:62–5.
32. HealthITAnalytics. 86% of healthcare companies use some form of AI. *Healthcare IT News*; 2017. https://www.healthcareitnews.com/news/86-healthcare-companies-use-some-form-ai.
33. HealthITAnalytics. Over 80% of health execs have artificial intelligence plans in place. *HealthITAnalytics*; 2020. https://healthitanalytics.com/news/over-80-of-health-execs-have-artificial-intelligence-plans-in-place.
34. Bukowski M, Farkas R, Beyan O, et al. Implementation of eHealth and AI integrated diagnostics with multidisciplinary digitized data: are we ready from an international perspective? Eur Radiol. 2020;30:5510–24.
35. Khanyile R, Marima R, Mbeje M, Mutambirwa S, Montwedi D, Dlamini Z. AI tools offering cancer clinical applications for risk predictor, early detection, diagnosis, and accurate prognosis: perspectives in personalised care. In: Dlamini Z, editor. Artificial intelligence and precision oncology. Cham: Springer; 2023.
36. Moradi H, Al-Hourani A, Concilia G, et al. Recent developments in modeling, imaging, and monitoring of cardiovascular diseases using machine learning. Biophys Rev. 2023;15:19.
37. Chandra J, Rangaswamy M, Banerjee B, Prajapati A, Akhtar Z, Sakauye K, Joseph A. Applications of artificial intelligence to neurological disorders: current technologies and open problems. In: Neurological disorder prediction and rehabilitation using artificial intelligence. London: Academic Press; 2022. p. 243–72. ISBN 9780323900379.
38. Kumar V, Patel S, Baburaj V, Vardhan A, Singh PK, Vaishya R. Current understanding on artificial intel-

ligence and machine learning in orthopaedics – a scoping review. J Orthop. 2022;34:201–6. ISSN 0972-978X.
39. Naz Z, Khan MUG, Saba T, Rehman A, Nobanee H, Bahaj SA. An explainable AI-enabled framework for interpreting pulmonary diseases from chest radiographs. Cancers. 2023;15(1):314.
40. Ghaffar Nia N, Kaplanoglu E, Nasab A. Evaluation of artificial intelligence techniques in disease diagnosis and prediction. Discov Artif Intell. 2023;3(1):5.
41. Escalé-Besa A, Yélamos O, Vidal-Alaball J, Fuster-Casanovas A, Catalina QM, Börve A, …, Marin-Gomez FX. Use of artificial intelligence as a diagnostic support tool for skin lesions in primary care: feasibility study in clinical practice; 2023.
42. Williams AM, Liu Y, Regner KR, Jotterand F, Liu P, Liang M. Artificial intelligence, physiological genomics, and precision medicine. Physiol Genomics. 2018;50(4):237–43.
43. Dias R, Torkamani A. Artificial intelligence in clinical and genomic diagnostics. Genome Med. 2019;11:70.
44. Jang HY, Song J, Kim JH, et al. Machine learning-based quantitative prediction of drug exposure in drug-drug interactions using drug label information. NPJ Digit Med. 2022;5:88.
45. Hung TNK, Le NQK, Le NH, Van Tuan L, Nguyen TP, Thi C, Kang JH. An AI-based prediction model for drug-drug interactions in osteoporosis and Paget's diseases from SMILES. Mol Inform. 2022;41(6):e2100264.
46. Ahmad MA, Eckert C, Teredesai A. Interpretable machine learning in healthcare. In: Proceedings of the 2018 ACM international conference on bioinformatics, computational biology, and health informatics; 2018. pp. 559–60.
47. Park SH, Kressel HY. Connecting technological innovation in artificial intelligence to real-world medical practice through rigorous clinical validation: what peer-reviewed medical journals could do. J Korean Med Sci. 2018;33:e152.
48. Kim DW, Jang HY, Kim KW, Shin Y, Park SH. Design characteristics of studies reporting the performance of artificial intelligence algorithms for diagnostic analysis of medical images: results from recently published papers. Korean J Radiol. 2019;20:405–10.
49. The Lancet null. Artificial intelligence in health care: within touching distance. Lancet. 2018;390:2739.
50. Park SH, Han K. Methodologic guide for evaluating clinical performance and effect of artificial intelligence technology for medical diagnosis and prediction. Radiology. 2018;286:800–9.
51. Murdoch B. Privacy and artificial intelligence: challenges for protecting health information in a new era. BMC Med Ethics. 2021;22:122.
52. Canadian Association of Radiologists (CAR) Artificial Intelligence Working Group. Canadian Association of Radiologists white paper on ethical and legal issues related to artificial intelligence in radiology. Can Assoc Radiol J. 2019;70(2):107–18.
53. Vayena E, Blasimme A. Health research with big data: time for systemic oversight. J Law Med Ethics. 2018;46(1):119–29.

3 Biochemical Diagnosis of Thyroid Dysfunctions

Luca Giovanella, Federica D'Aurizio, and Petra Petranović Ovčariček

3.1 Introduction

Thyroid disorders are commonly encountered in clinical practice and laboratory tests are integral to their diagnosis and management, including assessment of disease severity and response to therapy. This chapter details the pathophysiological background of thyroid function and the in vitro laboratory tests used in different thyroid diseases. Interpretation criteria, inappropriate or redundant testing, and relevant pitfalls are also reviewed, and guidance for rational test ordering and integration between clinical, laboratory, and imaging data is provided.

L. Giovanella (✉)
Clinic for Nuclear Medicine and Competence Center for Thyroid Diseases, Imaging Institute of Southern Switzerland, Ente Ospedaliero Cantonale, Bellinzona, Switzerland
e-mail: luca.giovanella@eoc.ch

F. D'Aurizio
Department of Laboratory Medicine, University Hospital of Udine, Udine, Italy
e-mail: federica.daurizio@asufc.sanita.fvg.it

P. P. Ovčariček
Department of Oncology and Nuclear Medicine, University Hospital Center Sestre milosrdnice, Zagreb, Croatia

3.2 Physiological Basis of Thyroid Function Laboratory Assessment

Thyroid hormone synthesis is finely tuned by the hypothalamus–pituitary–thyroid axis. In physiologic conditions, thyroid-stimulating hormone (TSH) regulates cellular activity, stimulating thyrocytes to express proteins necessary for thyroid hormones production and to increase thyroid hormones synthesis and secretion. Intracellular iodine transport across the follicular thyroid cell is generated by the Na^+/K^+ ATPase pump, which provides the transmembrane Na^+ gradient. The natrium iodide symporter transports one iodide ion together with two sodium ions, resulting in a significantly higher iodine concentration in the follicular cells (up to 500 times) compared with the bloodstream. Subsequently, through different membrane channels located at the apical membrane (e.g., pendrin, anoctamin, and chloride channel ClC5), iodine passes from the cytoplasm of the follicular cell into the lumen [1].

At the same time, the glycoprotein thyroglobulin moves from the apical membrane and enters into the follicular lumen (i.e., exocytosis). The thyroid follicular lumen consists of a colloidal suspension of thyroglobulin (concentration up to 750 mg/mL). Thyroglobulin serves as the backbone for thyroid hormones [2].

Iodine is then oxidated via action of the enzyme thyroid peroxidase (TPO): hydrogen peroxide, a

L. Giovanella (ed.), *Integrated Diagnostics and Theranostics of Thyroid Diseases*,
https://doi.org/10.1007/978-3-031-35213-3_3

substrate for TPO, is synthesized at the apical external surface of follicular thyroid cells. Oxidation is followed by organification (i.e., oxidized iodine links covalently to tyrosyl residues of thyroglobulin), enabling the biosynthesis of diiodotyrosines (DITs) and monoiodotyrosines (MITs), respectively. Under modulation by TPO, DITs and MITs are coupled to form triiodothyronine (T3), while two DITs form thyroxine (T4) (Fig. 3.1) [3].

The hormones T3 and T4 are phenolic rings coupled by an ether link and iodinated at three (3,5,3′-tri-iodo-L-thyronine, i.e., T3) or four (3,5,3′,5′-tetra-iodo-L-thyronine, i.e., T4) positions on the phenolic ring [4].

Thyroid hormones are stored in the lumen of follicular cells and, when required, the thyroglobulin–thyroid hormone complex internalizes to the cytoplasm and undergoes enzymatic disintegration, hydrolysis, and transport via the basolateral membrane across the monocarboxylate transporter 8.

Under normal conditions, the thyroid secretes ~90% T4, ~8–10% T3, and < 2% reverse T3. During intense TSH receptor stimulation, or in the case of iodine deficiency, the ratio of T3 formation increases [4]. More than 99% of circulating T4 and T3 molecules bind to carrier proteins (e.g., thyroxine-binding globulin, transthyretin, and albumin) and only small amounts circulate as free hormones (free thyroxine [FT4], free triiodothyronine [FT3]). These free hormones act on target tissues and bind thyroid receptors in the nuclei of target cells [5].

T3 is the bioactive thyroid hormone, with about 30 times higher affinity than T4 for the thyroid hormone receptor and is derived mostly from peripheral conversion of T4 via deiodinase activity [4]. Thyroid hormones also provide negative feedback to both the hypothalamus and the pituitary gland, closing the finely regulated homeostatic thyroid hormone biosynthesis loop. The relationship between TSH and FT4 is genetically determined and influenced by age and other

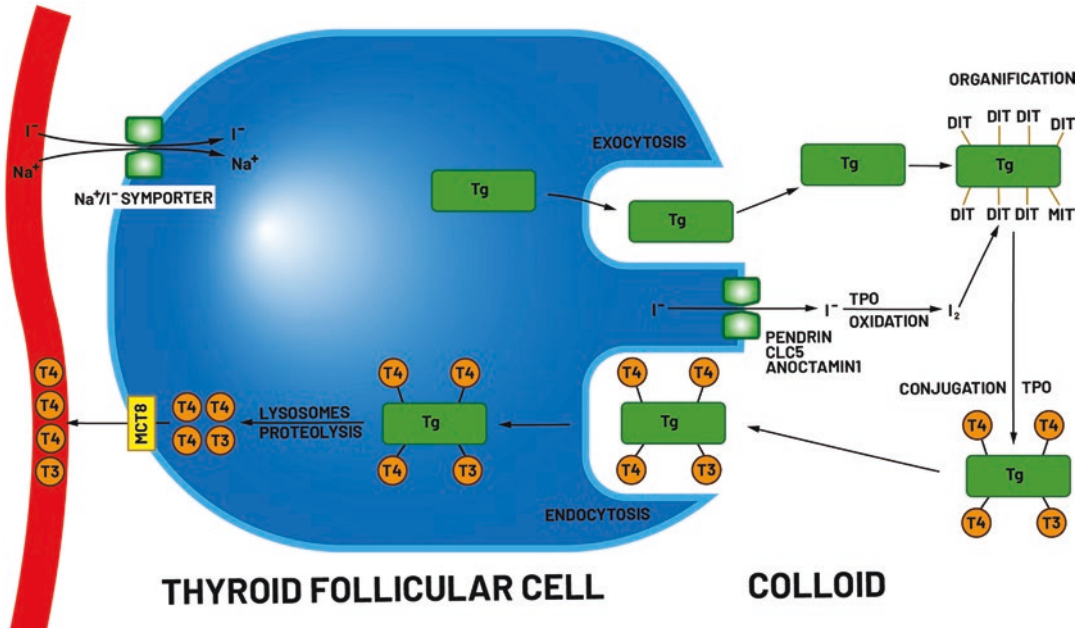

Fig. 3.1 Biosynthesis of thyroid hormones. *DIT* diiodotyrosine, *MCT8* monocarboxylate transporter 8, *MIT* monoiodotyrosine, *T3* triiodothyronine, *T4* thyroxine, *Tg* thyroglobulin, *TPO* thyroid peroxidase. Reproduced from D'Aurizio et al. Free thyroxine measurement in clinical practice: how to optimize indications, analytical procedures, and interpretation criteria while waiting for global standardization. Crit Rev. Clin Lab Sci 2022; doi: 10.1080/10408363.2022.2121960 [in press]

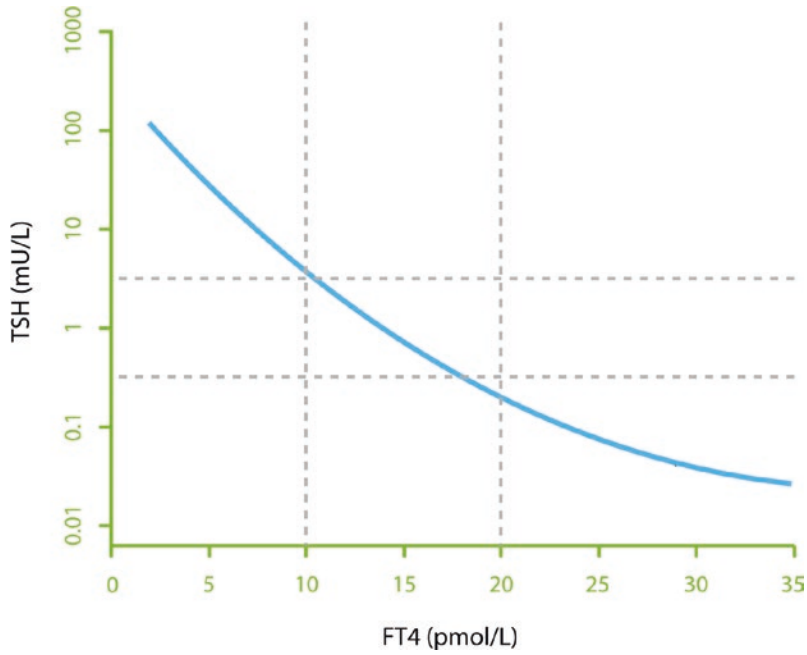

Fig. 3.2 The log–linear inverse relationship between TSH and FT4. The blue line represents an approximate relationship between TSH and FT4. The dotted gray lines represent the normal values for TSH (horizontal) and FT4 (vertical). *TSH* thyroid-stimulating hormone, *FT4* free thyroxine. Reproduced from D'Aurizio et al. Free thyroxine measurement in clinical practice: how to optimize indications, analytical procedures, and interpretation criteria while waiting for global standardization. Crit Rev. Clin Lab Sci 2022; doi: 10.1080/10408363.2022.2121960 [in press]

factors such as smoking status. With few exceptions, the TSH–free thyroid hormone relationship is largely inverse log-linear [6] (Fig. 3.2).

TSH secretion is highly sensitive to small fluctuations in thyroid hormone levels, and abnormal TSH levels indicate early thyroid dysfunction, well before clear actual hormone abnormalities emerge.

Notably, currently used FT4 (and FT3) immunoassays are binding protein-dependent and their performance may be suboptimal at low or high thyroid hormone concentrations. Liquid chromatography-tandem mass spectrometry (LC-MS/MS), for the most part, avoids the inherent shortcomings of competitive immunoassays, as demonstrated by the stronger TSH–FT4 relationship when FT4 is measured by LC-MS/MS versus conventional immunoassays [7]. However, LC-MS/MS remains largely unavailable in clinical laboratories, and selective and appropriate use of FT4 and FT3 testing based on TSH results remains pivotal to avoiding diagnostic pitfalls.

3.3 Thyroid Function Tests

Thyroid function is assessed by measuring TSH and free thyroid hormones. As previously discussed, TSH and FT4 have a complex, nonlinear relationship, and small changes in FT4 result in relatively large changes in TSH [8]. With some rare exceptions (i.e., central hypothyroidism, resistance to thyroid hormones, TSH-secreting pituitary adenoma [TSH-oma], treated hyperthyroidism, and nonthyroidal illness syndrome), TSH measurement is a sensitive first-line test for thyroid dysfunction. Guidelines from the American Thyroid Association [9], the American Association of Clinical Endocrinologists [10], and the National Academy of Clinical Biochemistry [11] have endorsed TSH measure-

ment as the best first-line strategy for detecting thyroid dysfunction in most clinical settings. However, TSH levels are relatively inadequate in evaluating the severity of thyroid dysfunction, and FT4 (with or without FT3) should be tested when abnormal TSH levels are found. To reduce the overuse of FT4 testing without compromising the detection of overt thyroid dysfunction, FT4 may be added to existing requests, either automatically on the basis of algorithms (i.e., reflex testing) or by laboratory professionals (i.e., reflective testing). These strategies have proven to be clinically appropriate and cost-effective in the first-line assessment of thyroid function [12, 13].

3.3.1 Performance Characteristics of Thyroid Function Assays

Most thyroid function tests are performed by immunoassays on automated platforms. Immunoassays for FT4 and FT3 are competitive, as the small size of thyroid hormones precludes the use of sandwich immunometric assays [13]. However, competitive thyroid hormone assays are occasionally affected by cross-reactivities, and the dynamic range limitations create a difficult task for manufacturers of producing assays that are very accurate at both low and high concentrations [14] (Tables 3.1 and 3.2).

Conversely, immunoassays used to measure TSH are largely sandwich immunometric assays. This assay architecture offers advantages over competitive assays, such as reduced cross-reactivity, better detection sensitivity, and a wider dynamic measurement range. Currently available TSH assays have detection sensitivities of <0.01–0.02 mIU/L, a 4 Log^{10}, and a more dynamic range, respectively [13] (Table 3.3). Finally, they also have no cross-reactivity with pituitary glycoproteins luteinizing hormone and follicle-stimulating hormone, and the human chorionic gonadotropin, respectively.

Table 3.1 Main analytical characteristics of the most frequently used FT4 immunoassays, as quoted by manufacturers

Manufacturer/Assay	Assay principle	LOD (pmol/L)	LOQ (pmol/L)	Assay range (pmol/L)	Imprecision (CV %) (intra-assay; inter-assay; total)	Reference interval[a] (pmol/L)
Abbott Alinity i Free T4	CMIA, competitive	3.60	5.41	5.41–64.5	1.7–3; 2–3.1; ND	9.0–19.1
Beckman Coulter Access Free T4	CLIA, competitive	3.22	ND	3.22–77.20	1.8–4.4; 3.3–8.1; 4.3–9.2	7.86–14.41
DiaSorin Free T4	CLIA, competitive	1.29	ND	1.29–28.70	2.0–3.3; 2.0–4.4, ND	10.29–21.88
Mindray FT4	CLIA, competitive	3.86	ND	3.86–77.23	2.05–3.17; 1.58–1.98; 4.38–4.64	7.72–15.45
Ortho Vitros FT4	CLIA, competitive	0.88	ND	0.88–90.0	1.6–2.8; 2.4–5.8; 2.5–6.2	10.0–28.2
Roche cobas Elecsys FT4 IV	ECLIA, competitive	0.5	1.3	0.5–100.0	1.6–5.0; 1.9–6.3; ND	11.9–21.6
Siemens Healthineers Atellica IM FT4	CLIA, competitive	1.3	ND	1.3–154.8	1.2–4.7; 2.2–6.8; ND	11.5–22.7
SNIBE Maglumi FT4	CLIA, competitive	1.9	ND	1.9–154.5	2.76–4.99; 1.51–6.17; 3.15–7.94	11.5–22.1

[a]Reference intervals were calculated in a population of apparently healthy adults. Information updated to August 2022
CLIA chemiluminescent assay, *CMIA* chemiluminescent microparticle immunoassay, *CV* coefficient of variation, *ECLIA* electrochemiluminescence assay, *FT4* free thyroxine, *LOD* limit of detection, *LOQ* limit of quantitation, *ND* not disclosed

Table 3.2 Main analytical characteristics of the most frequently used FT3 immunoassays, as quoted by manufacturers

Manufacturer/Assay	Assay principle	LOD (pmol/L)	LOQ (pmol/L)	Assay range (pmol/L)	Imprecision (CV %) (intra-assay; inter-assay; total)	Reference interval[a] (pmol/L)
Abbott Alinity i Free T3	CMIA, competitive	1.46	1.92	2.30–30.72	2.4–3.8; ND; 3.6–4.8	2.43–6.00
Beckman Coulter Access Free T3	CLIA, competitive	1.40	ND	1.40–46.00	2.6–6.6; 1.3–8.0; 5.3–10.4	3.8–6.0
DiaSorin Free T3	CLIA, competitive	0.46	1.54	0.46–46.2	2.6–4.7; 2.4–4.7, ND	3.39–6.47
Mindray FT3	CLIA, competitive	1.35	ND	1.35–46.20	1.89–2.65; 2.16–2.41; 2.62–3.31	3.54–6.16
Ortho Vitros FT3	CLIA, competitive	0.77	ND	0.77–35.00	1.1–4.0; 2.0–11.3; 2.3–14.7	4.26–8.10
Roche cobas Elecsys FT3 III	ECLIA, competitive	0.6	1.5	0.6–50.0	1.4–7.6; 1.6–8.3; ND	3.1–6.8
Siemens Healthineers Atellica IM FT3	CLIA, competitive	0.31	ND	0.31–30.80	0.67–7.59; ND; 1.07–9.14	3.5–6.5
SNIBE Maglumi FT3	CLIA, competitive	0.62	ND	0.62–77.00	2.64–4.63; 1.77–6.12; 3.68–7.67	3.10–6.47

[a]Reference intervals were calculated in a population of apparently healthy adult males and females. Information updated to August 2022

CLIA chemiluminescent assay, *CMIA* chemiluminescent microparticle immunoassay, *CV* coefficient of variation, *ECLIA* electrochemiluminescence assay, *FT3* free triiodothyronine, *LOD* limit of detection, *LOQ* limit of quantitation, *ND* not disclosed

Table 3.3 Main analytical characteristics of the most frequently used TSH immunoassays, as quoted by manufacturers

Manufacturer/Assay	Assay principle	IRP	LOD (mIU/L)	LOQ (mIU/L)	Assay range (mIU/L)	Imprecision (CV %) (intra-assay; inter-assay; total)	Reference interval[a] (mIU/L)
Abbott Alinity i TSH	CMIA, non-competitive	ND	0.0036	0.0083	0.0083–100	1.3–1.6; ND; 1.5–2.1	0.35–4.94
Beckman Coulter Access TSH 3rd IS	CLIA, non-competitive	81/565	0.005	0.01	0.005–50	2–4; 0.2–2; 3–6	0.38–5.33
DiaSorin Liaison TSH	CLIA, non-competitive	80/558	0.004	0.02	0.004–100	0.7–1.9; 1.6–5.1; ND	0.3–3.6
Mindray TSH	CLIA, non-competitive	81/565	0.005	0.02	0.005–100	1.75–2.39; 1.40–1.65; 2.32–3.13	0.35–5.1
Ortho Vitros TSH	CLIA, non-competitive	80/558	0.014	0.097	0.014–150	0.9–5.3; 1.7–7.4; 2.0–8.8	0.47–4.68
Roche cobas Elecsys TSH	ECLIA, non-competitive	80/558	0.005	0.005	0.005–100	0.7–3.4; 1.5–11.2; ND	0.27–4.20
Siemens Healthineers Atellica IM TSH3-UL	CLIA, non-competitive	81/565	0.008	0.008	0.008–150	1.5–3.6; 2.9–4.5; ND	0.55–4.78
SNIBE Maglumi TSH	CLIA, non-competitive	81/565	0.006	ND	0.006–100	1.76–2.53; 1.40–2.04; 2.25–3.71	0.3–4.5

[a]Reference intervals were calculated in a population of apparently healthy adult males and females. Information updated to August 2022

CLIA chemiluminescent assay, *CMIA* chemiluminescent microparticle immunoassay, *CV* coefficient of variation, *ECLIA* electrochemiluminescence assay, *IRP* international reference preparation, *LOD* limit of detection, *LOQ* limit of quantitation, *ND* not disclosed, *TSH* thyroid-stimulating hormone

3.3.2 Thyroid-Stimulating Hormone

As previously discussed, Thyroid-Stimulating Hormone (TSH) is the single most useful test of thyroid function in most patients. Generally, no further testing is indicated when TSH appears within the normal range. Nevertheless, several issues should be considered when interpreting a TSH value, the importance of which requires that a clinical decision not be made based on a single TSH value when it is within or close to the normal range [13].

3.3.2.1 Normal Range

Considerable literature exists regarding the "normal" range for TSH, which is generally quoted to be between 0.40 and 4.00 mIU/mL [15, 16]. However, the accuracy of any given immunoassay can strongly affect TSH cutoffs, as inter-method differences of about 1 mU/L at concentrations of 4–5 mU/L have been reported [17]. The lack of interchangeability of laboratory results and cutoffs (due to poor harmonization of TSH assays) does not allow standardized cutoffs to be used in clinical practice. Therefore, each clinical laboratory must establish reliable cutoffs based on their adopted method. Adopted cutoffs may differ based on population and clinical context. In the general population, the approach is to adopt cutoffs that facilitate the greatest reduction in the frequency of FT4 testing; in other clinical settings, a different cutoff may be preferable to avoid missing hypo- and/or hyperthyroidism diagnoses.

3.3.2.2 Circadian Variability

Though not usually accounted for in clinical practice TSH secretion follows a circadian rhythm, with maximal levels in the early morning and a nadir in the late afternoon to mid-evening. Generally, TSH levels remain within the normal range, but variation in TSH by a mean of 0.95–2.00 mIU/mL can be observed and may affect clinical decisions [18].

3.3.2.3 Individual Variation

Individual variation in TSH levels may occur without an obvious cause. In a study assessing TSH values monthly for 1 year in healthy men, random variations occurred, with a mean TSH of 0.75 mIU/mL and a range of 0.2–1.6 mIU/mL [19]. Thus, variation in TSH of up to 40–50% within the normal range does not necessarily indicate a change in thyroid function or status [10, 19].

Overall, the "reflex TSH" strategy highlights an opportunity to improve appropriateness in test requests and save unjustified costs for healthcare systems. However, caution must be exercised when using solely TSH tests for subclinical thyroid dysfunction and for secondary hypothyroidism, and during the initial phases of medical therapy for hyper- and hypothyroidism [20].

3.3.3 Free Thyroid Hormones

Measurement of FT4 levels is integral in both the diagnosis and management of relevant central dysfunctions, as well as therapy monitoring in hyperthyroid patients treated with antithyroid drugs or radioiodine. FT3 measurement may also add useful information in patients with suppressed TSH and normal FT4 levels to distinguish subclinical hyperthyroidism (i.e., normal FT3) from T3-thyrotoxicosis (i.e., high FT3). The accuracy of FT4 and FT3 tests depends greatly on the assay used. Unfortunately, the assays used in the vast majority of clinical laboratories are still hindered by some limitations and pitfalls. Although considerable progress has been made in the standardization of FT4 procedures, some challenges remain, including establishing clinical decision limits in varying patient populations and education of stakeholders [21]. As such, different assays and reference values cannot be interchanged at present. Two-way communication between laboratory and clinical specialists is vital in choosing a reliable FT4 assay, establishing local reference ranges, investigating discordant results, and monitoring the analytical and clinical performance of the assay over time.

3.4 Diagnosis of Thyroid Dysfunctions

Symptoms of thyroid dysfunction may be nonspecific with minimal signs; thus, the use of thyroid function tests in patient evaluation is vital. While testing TSH alone is sufficient for general screening, both FT4 and TSH assays are needed for diagnosing subclinical thyroid dysfunction, central hypothyroidism, drug effects, and hospitalized patients, as well as for accurate assessment of treatment effects. Close communication between the bedside and bench-side is crucial for the successful interpretation of thyroid function test results, particularly when inconsistent results are rendered. An algorithm for thyroid function test interpretation is presented in Fig. 3.3.

3.4.1 Subclinical Thyroid Dysfunctions

Increased frequency of screening and routine blood tests have resulted in more patients being diagnosed with subclinical thyroid dysfunction. In subclinical hyperthyroidism, TSH level is low/suppressed and FT4 level is within the normal range. FT3 should be measured to rule out T3 toxicosis in these cases. Patients with subclinical hyperthyroidism should be further screened and considered for treatment, especially if they are elderly and/or at risk for atrial fibrillation or osteoporosis [22].

In subclinical hypothyroidism, TSH level is elevated and the FT4 level is within the normal range. Levothyroxine should be started if the TSH level exceeds 10 mIU/L. Treatment may also be considered in other situations, such as in patients with consistent symptoms, poorly controlled hypercholesterolemia, or subfertility [9].

3.4.2 Overt Thyroid Dysfunctions

3.4.2.1 Hyperthyroidism

Hyperthyroid patients may present with symptoms such as palpitations, tremors, anxiety, weight loss, and heat intolerance. Clinicians should in the first instance confirm biochemical thyrotoxicosis by testing both TSH and FT4 [23].

Most patients with thyrotoxicosis have primary hyperthyroidism, giving a typical constellation of elevated FT4 and suppressed TSH. The most frequent cause of thyroid hyperfunction is Graves' disease, the diagnosis of which is typically obvious upon clinical examination in many cases. In other cases, however, it may be challenging to distinguish Graves' disease from other

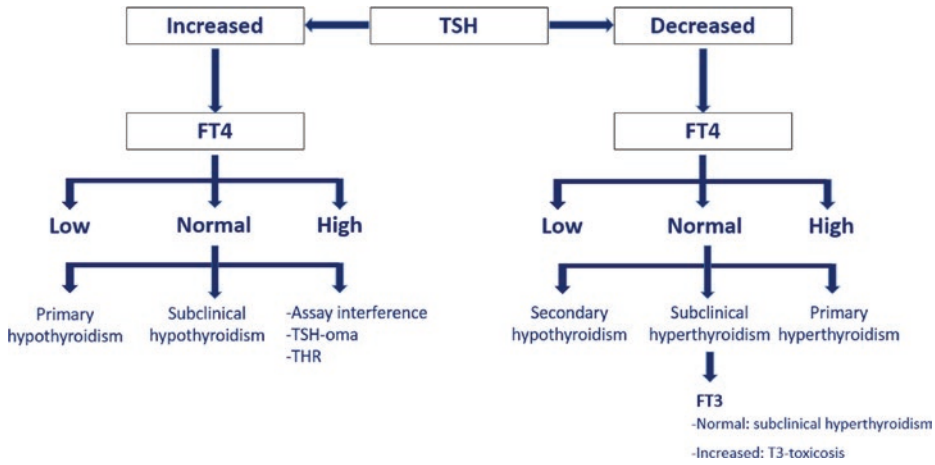

Fig. 3.3 Algorithm for thyroid function test interpretation. *FT3* free triiodothyronine, *FT4* free thyroxine, *T3* triiodothyronine, *THR* thyroid hormone receptor, *TSH* thyroid-stimulating hormone, TSH-oma, TSH-secreting pituitary adenoma

forms of thyrotoxicosis, and several etiologies should be considered before making a definitive diagnosis and starting treatment [24, 25] (Table 3.4). In unclear cases, thyroid scintigraphy, TSH receptor antibody (TRAb) measurement, or ultrasound with Doppler analysis of thyroid vascularity are recommended, depending on local availability and clinical preferences [23]. In addition to aiding diagnosis of Graves' disease, the magnitude of TRAb elevation can serve as a prognostic indicator of remission during medical treatment. In pregnant women with current or previous Graves' disease, TRAb should be tested during the later stages of gestation to assess the risk of fetal/neonatal thyrotoxicosis [24].

Table 3.4 Causes of thyrotoxicosis: etiology and pathophysiology

Cause	Etiology	Pathophysiology
Graves' disease	Autoimmune	TSH-R stimulation
Thyroid functional autonomy	Somatic mutations	Overactive TSH-R and/or Gsα subunit
Subacute thyroiditis	Viral	Inflammatory destruction
Painless thyroiditis	Autoimmune	Immune-mediated destruction
Drug-induced	Iodine overload type 1	Pathologic escape from Wolff-Chaikoff effect
	Iodine overload type 2	Iodine-induced destructive thyroiditis
	TKI, ICPI	Destructive thyroiditis
	Factitious thyrotoxicosis	T4, T3, TH analogs
Tumor	Struma ovarii	Ovarian TH biosynthesis
	Thyroid cancer	Functioning metastasis
	Germinal tumors	βHCG overproduction
Central	Pituitary resistance	THR mutation (TRβ)
	Pituitary adenoma	TSH-secreting tumor

HCG human chorionic gonadotropin, *ICPI* immune checkpoint inhibitors, *T3* triiodothyronine, *T4* thyroxine, *TH* thyroid hormone, *THR* TH receptor, *TKI* tyrosine kinase inhibitors, *TRAb* TSH receptor antibody, *TSH* thyroid-stimulating hormone, *TSH-R* TSH-receptor

In some cases, patients may present with an elevated FT4 level and elevated or inappropriately normal TSH level. While laboratory assay imprecision and/or interferences may explain this abnormality when thyrotoxicosis symptoms are absent, two differential diagnoses should be considered: secondary hyperthyroidism from TSH-oma [prevalence 0.85/1 million] and resistance to thyroid hormone-β (RTHβ) [prevalence 1/40,000]. Patients with TSH-oma have elevated levels of alpha-subunit, a high alpha-subunit/TSH ratio, and a blunted response to thyrotropin-release hormone (TRH) stimulation. Magnetic resonance imaging of the pituitary gland reveals an adenoma (typically a macroadenoma) [26].

Resistance to thyroid hormone (RTH) is a rare genetic syndrome that affects the thyroid hormone receptor isoforms β and α. RTHβ must be considered in patients with unexplained elevated FT4 and unsuppressed TSH levels (inappropriately normal or elevated). Most patients have a positive family history (autosomal dominant inheritance) and show decreased serum FT4/T3 ratio and normal or exaggerated response to TRH stimulation [27].

Finally, it is important to keep in mind that FT4 responds faster to antithyroid therapy and radioiodine than TSH. Consequently, TSH recovery can lag behind FT4 recovery by several months. Clinical actions, such as antithyroid drug titration or introduction of thyroid substitution, should be undertaken according to improvement in FT4 levels in these cases (Table 3.5).

3.4.2.2 Hypothyroidism

Patients who present with overt symptoms of hypothyroidism have low FT4 and elevated TSH levels. The most common cause of primary hypothyroidism in iodine-replete regions is autoimmune thyroiditis (Hashimoto's thyroiditis). Antithyroid peroxidase antibodies (TPOAb) may be tested to confirm the diagnosis. Previous neck surgery, radioactive iodine therapy, and antithyroid drug therapy are also frequent causes of primary hypothyroidism. Patients with secondary hypothyroidism have

Table 3.5 Measurement of FT4: clinical indications

Indication	Aim
Suppressed TSH	To differentiate subclinical from overt hyperthyroidism To assess the degree of overt hyperthyroidism
Increased TSH	To differentiate subclinical from overt hypothyroidism
ATD therapy	To monitor response in the initial months of therapy
RAI therapy	To monitor response in the initial months after RAI therapy
Pituitary disease	To evaluate/monitor patients (TSH not reliable)

ATD antithyroid drug, *FT4* free thyroxine, *TSH* thyroid-stimulating hormone, *RAI* radioactive iodine

low FT4 and low or inappropriately normal TSH levels. After exclusion of assay imprecision or interferences, when a normal TSH level is found alongside low/low-normal T4 but high/high-normal T3 levels, it is important to rule out hypopituitarism and consider resistance to thyroid hormone α-subtype (RTHα). Notably, during early treatment of secondary hypothyroidism with levothyroxine, FT4 levels improve while TSH levels remain low/low-normal, thus making TSH unsuitable for patient monitoring. In these cases, measurement of FT4 alone is recommended (Table 3.5). In pregnant women with hypothyroidism, the usual levothyroxine dose is increased by 30% due to physiological changes. Thyroid function must be monitored closely (every 4–6 weeks) during pregnancy, as maternal hypothyroidism is associated with suboptimal obstetric outcomes and poor fetal neurocognitive development [28].

3.5 Management of Inconsistent Results

Although thyroid function tests are routine examinations, the analytical procedure for determining TSH, FT3, and FT4 remains a major challenge due to multiple interference factors. Notably, most inconsistent thyroid test results are related to nonspecific fluctuations, assay imprecision, or inappropriate reference range rather than clinically relevant dysfunctions [29]. Indeed, falsely increased or decreased thyroid hormone measurements caused by interference factors in immunoassays may result in a considerable number of possible misinterpretations of laboratory findings [30, 31].

3.5.1 Analytical Interferences in Immunoassays

Numerous factors may interfere with immunoassay measurements of TSH, FT3, and FT4, such as macromolecules (frequency < 1:100) [32], interfering antibodies (frequency < 1.1:100) [33], and amino acids and/or glycosylation variants (frequency < 1:100,000), respectively [34, 35]. The use of high-dose biotin (100–300 mg/day) for multiple sclerosis and inherited metabolic disorders has attracted the attention of laboratorians and clinicians, as it can cause inexplicable thyroid test results. Biotin is also advertised and sold for healthy nails and hair and may be present in supplements for this purpose in doses of up to 10 mg per tablet. As most manufacturers have enhanced the biotin tolerance of their assays in recent years, this effect is mainly theoretical unless patients are taking very large doses of biotin or have concomitant renal failure [36, 37]. Nevertheless, it is important that endocrinologists understand the risks of potential interactions with exogenous biotin. Some drugs (e.g., aspirin, furosemide, and phenytoin) may displace the equilibrium between thyroid hormones and binding proteins; others may increase (e.g., estrogen, fluorouracil, and tamoxifen) or inhibit (e.g., androgens, glucocorticoids, and nicotinic acid) the synthesis of thyroxine-binding globulin, leading to dubious method-dependent results in the measurement of FT4 [8]. The administration of heparin may also cause an artificial elevation in FT4 by displacing thyroid hormones from binding proteins via rapidly generated non-esterified fatty acids, especially when FT4 is measured via equilibrium dialysis [38].

3.5.2 Nonthyroidal Illness

Interpretation of thyroid function tests can be confounded by several factors in critically ill patients, depending on the onset, severity, and duration of the critical illness [39]. During critical illness, FT3 levels are the first to decrease, typically within the first 24 h (i.e., low T3 syndrome). FT4 levels decrease subsequently, followed by a decrease in TSH. During the recovery phase, TSH increases early and can transiently exceed the normal range; however, normalization of free thyroid hormones will ensue. These changes in thyroid hormones in critical illness may be due to several factors, such as reduced deiodinase activity, reduced thyroid hormone-binding protein concentrations, increased circulating pro-inflammatory cytokines, and use of certain medications, such as dopamine and glucocorticoids. Whether these changes are a form of beneficial or maladaptive response remains unclear. From a practical point of view, thyroid function tests should be performed during critical illness only if strictly necessary and interpreted with great caution. Otherwise, it is recommended to postpone thyroid testing until the resolution of the acute illness phase.

3.6 Conclusion

Laboratory tests are integral in the management of thyroid dysfunction, and their rational use and proper interpretation may greatly simplify management of patients, and avoid inappropriate diagnostic procedures and clinical actions, including drug administration. In most clinical situations, a concrete understanding of thyroid physiology and the various thyroid tests suffices for the proper and accurate interpretation of the test results. However, unexpected and inconsistent results should be interpreted with caution; clinicians and laboratorians should consider laboratory assay interferences, concurrent medications, pregnancy, nonthyroidal illness, and older age, and interpret results according to the clinical setting. Close communication between all members of the care team is vital.

Acknowledgments Editorial assistance was provided by Erin Slobodian, BA, of Ashfield MedComms, an Inizio company, funded by the Clinic for Nuclear Medicine and Molecular Imaging, Imaging Institute of Southern Switzerland, Ente Ospedaliero Cantonale, Bellinzona, Switzerland.

References

1. Carvalho DP, Dupuy C. Thyroid hormone biosynthesis and release. Mol Cell Endocrinol. 2017;458:6–15.
2. Ulianich L, Suzuki K, Mori A, Nakazato M, Pietrarelli M, Goldsmith P, et al. Follicular thyroglobulin (TG) suppression of thyroid-restricted genes involves the apical membrane asialoglycoprotein receptor and TG phosphorylation. J Biol Chem. 1999;274:25099–107.
3. Kronenberg HM, Melmed S, Larsen PR, et al. Principles of endocrinology. In: Melmed S, Polonsky KS, Larsen PR, Kronenberg HM, editors. Williams textbook of endocrinology. Philadelphia: Elsevier Saunders; 2011.
4. Larsen PR, Zavacki AM. The role of the iodothyronine deiodinases in the physiology and pathophysiology of thyroid hormone action. Eur Thyroid J. 2012;1:232–42.
5. Cody V. Thyroid hormone interactions: molecular conformation, protein binding, and hormone action. Endocr Rev. 1980;1:140–66.
6. Larsen PR. Thyroid-pituitary interaction: feedback regulation of thyrotropin secretion by thyroid hormones. N Engl J Med. 1982;306:23–32.
7. van Deventer HE, Mendu DR, Remaley AT, Soldin SJ. Inverse log-linear relationship between thyroid-stimulating hormone and free thyroxine measured by direct analog immunoassay and tandem mass spectrometry. Clin Chem. 2011;57:122–7.
8. Koulouri O, Moran C, Halsall D, Chatterjee K, Gurnell M. Pitfalls in the measurement and interpretation of thyroid function tests. Best Pract Res Clin Endocrinol Metab. 2013;27:745–62.
9. Jonklaas J, Bianco AC, Bauer AJ, Burman KD, Cappola AR, Celi FS, et al. Guidelines for the treatment of hypothyroidism: prepared by the American Thyroid Association Task Force on Thyroid Hormone Replacement. Thyroid. 2014;24:1670–751.
10. Garber JR, Cobin RH, Gharib H, Hennessey JV, Klein I, Mechanick JI, et al. Clinical practice guidelines for hypothyroidism in adults: cosponsored by the American Association of Clinical Endocrinologists and the American Thyroid Association. Endocr Pract. 2012;18:988–1028.
11. Demers LM, Spencer CA. Laboratory medicine practice guidelines: laboratory support for the diagnosis and monitoring of thyroid disease. Clin Endocrinol. 2003;58:138–40.
12. Plebani M, Giovanella L. Reflex TSH strategy: the good, the bad and the ugly. Clin Chem Lab Med. 2019;58:1–2.

13. Sheehan MT. Biochemical testing of the thyroid: TSH is the best and, oftentimes, only test needed – a review for primary care. Clin Med Res. 2016;14:83–92.
14. Faix JD. Principles and pitfalls of free hormone measurements. Best Pract Res Clin Endocrinol Metab. 2013;27:631–45.
15. Hollowell JG, Staehling NW, Flanders WD, Hannon WH, Gunter EW, Spencer CA, et al. Serum TSH, T(4), and thyroid antibodies in the United States population (1988 to 1994): National Health and nutrition examination survey (NHANES III). J Clin Endocrinol Metab. 2002;87:489–99.
16. Brabant G, Beck-Peccoz P, Jarzab B, Laurberg P, Orgiazzi J, Szabolcs I, et al. Is there a need to redefine the upper normal limit of TSH? Eur J Endocrinol. 2006;154:633–7.
17. Kahapola-Arachchige KM, Hadlow N, Wardrop R, Lim EM, Walsh JP. Age-specific TSH reference ranges have minimal impact on the diagnosis of thyroid dysfunction. Clin Endocrinol. 2012;77:773–9.
18. Sviridonova MA, Fadeyev VV, Sych YP, Melnichenko GA. Clinical significance of TSH circadian variability in patients with hypothyroidism. Endocr Res. 2013;38:24–31.
19. Andersen S, Pedersen KM, Bruun NH, Laurberg P. Narrow individual variations in serum T(4) and T(3) in normal subjects: a clue to the understanding of subclinical thyroid disease. J Clin Endocrinol Metab. 2002;87:1068–72.
20. Li H, Yuan X, Liu L, Zhou J, Li C, Yang P, et al. Clinical evaluation of various thyroid hormones on thyroid function. Int J Endocrinol. 2014;2014:618572.
21. Kratzsch J, Baumann NA, Ceriotti F, Lu ZX, Schott M, van Herwaarden AE, et al. Global FT4 immunoassay standardization: an expert opinion review. Clin Chem Lab Med. 2021;59:1013–23.
22. Bowers J, Terrien J, Clerget-Froidevaux MS, Gothié JD, Rozing MP, Westendorp RG, et al. Thyroid hormone signaling and homeostasis during aging. Endocr Rev. 2013;34:556–89.
23. Ross DS, Burch HB, Cooper DS, Greenlee MC, Laurberg P, Maia AL, et al. 2016 American Thyroid Association guidelines for diagnosis and management of hyperthyroidism and other causes of thyrotoxicosis. Thyroid. 2016;26:1343–421.
24. Kahaly GJ, Bartalena L, Hegedüs L, Leenhardt L, Poppe K, Pearce SH. 2018 European Thyroid Association guideline for the management of Graves' hyperthyroidism. Eur Thyroid J. 2018;7:167–86.
25. Smith TJ, Hegedüs L. Graves' disease. N Engl J Med. 2016;375:1552–65.
26. Beck-Peccoz P, Persani L, Mannavola D, Campi I. Pituitary tumours: TSH-secreting adenomas. Best Pract Res Clin Endocrinol Metab. 2009;23:597–606.
27. Singh BK, Yen PM. A clinician's guide to understanding resistance to thyroid hormone due to receptor mutations in the TRα and TRβ isoforms. Clin Diabetes Endocrinol. 2017;3:8.
28. Soh SB, Topliss DJ. Thyroid dysfunction in pregnancy: optimising obstetric outcomes. Endocrinol Today. 2013;4:8–16.
29. Külz M, Fellner S, Rocktäschel J, Ceglarek U, Willenberg A, Kratzsch J. Dubiously increased FT4 and FT3 levels in clinically euthyroid patients: clinical finding or analytical pitfall? Clin Chem Lab Med. 2022;60:877–85.
30. Grebe SKG. Laboratory testing in thyroid disorders. In: Markus L, Duntas LH, Wartofsky L, editors. The thyroid and its diseases: a comprehensive guide for the clinician. 1st ed. Oxford: Springer; 2019.
31. Favresse J, Burlacu MC, Maiter D, Gruson D. Interferences with thyroid function immunoassays: clinical implications and detection algorithm. Endocr Rev. 2018;39:830–50.
32. Hattori N, Ishihara T, Shimatsu A. Variability in the detection of macro TSH in different immunoassay systems. Eur J Endocrinol. 2016;174:9–15.
33. Ismail AAA, Walker PL, Barth JH, Lewandowski KC, Jones R, Burr WA. Wrong biochemistry results: two case reports and observational study in 5310 patients on potentially misleading thyroid-stimulating hormone and gonadotropin immunoassay results. Clin Chem. 2002;48:2023–9.
34. Drees JC, Stone JA, Reamer CR, Arboleda VE, Huang K, Hrynkow J, et al. Falsely undetectable TSH in a cohort of South Asian euthyroid patients. J Clin Endocrinol Metab. 2014;99:1171–9.
35. Estrada JM, Soldin D, Buckey TM, Burman KD, Soldin OP. Thyrotropin isoforms: implications for thyrotropin analysis and clinical practice. Thyroid. 2014;24:411–23.
36. Mzougui S, Favresse J, Soleimani R, Fillée C, Gruson D. Biotin interference: evaluation of a new generation of electrochemiluminescent immunoassays for high-sensitive troponin T and thyroid-stimulating hormone testing. Clin Chem Lab Med. 2020;58:2037–45.
37. Choi J, Yun SG. Comparison of biotin interference in second- and third-generation Roche free thyroxine immunoassays. Ann Lab Med. 2020;40:274–6.
38. Jaume JC, Mendel CM, Frost PH, Greenspan FS, Laughton CW. Extremely low doses of heparin release lipase activity into the plasma and can thereby cause artifactual elevations in the serum-free thyroxine concentration as measured by equilibrium dialysis. Thyroid. 1996;6:79–83.
39. van den Berghe G. Non-thyroidal illness in the ICU: a syndrome with different faces. Thyroid. 2014;24:1456–65.

4 Integrated Thyroid Imaging: Ultrasound and Scintigraphy

Simone A. Schenke, Daniel Groener, Michael Grunert, and Alexander R. Stahl

4.1 Basics of Thyroid Imaging

Modern integrated imaging of thyroid diseases combines multiparametric thyroid ultrasound as morphological imaging method and molecular imaging with radiopharmaceutical substances to assess the structure and the functional status of the thyroid gland or thyroid lesions. This chapter provides an overview of thyroid ultrasound and molecular imaging for diffuse and nodular thyroid diseases.

The original version of the chapter has been revised. A correction to this chapter can be found at https://doi.org/10.1007/978-3-031-35213-3_11.

S. A. Schenke (✉)
Department of Nuclear Medicine, City Hospital Bayreuth, Bayreuth, Germany

Clinic of Radiology and Nuclear Medicine, Department of Nuclear Medicine, University Hospital Magdeburg, Magdeburg, Germany

D. Groener
Department of Nuclear Medicine, University Hospital Frankfurt, Frankfurt, Germany
e-mail: Daniel.groener@kgu.de

M. Grunert
Department of Nuclear Medicine, German Armed Forces Hospital Ulm, Ulm, Germany
e-mail: Michael.grunert@uni-ulm.de

A. R. Stahl
Department of Nuclear Medicine, Radiologie im Zentrum – RIZ, Augsburg, Germany

4.1.1 Sonography

Since its initial description by Fujimoto et al. in 1967, ultrasound (US) has gained a critical role in the evaluation of diffuse and nodular thyroid diseases. With today's high-resolution systems, ultrasound examinations are among the most widely used imaging methods worldwide. Ultrasound is cost-effective, free of radiation, can be repeated as often as required, is easy to learn, and allows versatile use. Modern ultrasound devices are equipped with transducers that have a frequency spectrum of typically 2–20 Megahertz (MHz), with the choice of frequency depending on the target structure (location and depth within the body). For thyroid ultrasound high-resolution linear transducers with a frequency of 7–15 MHz have been used. Besides brightness-mode (B-mode, gray-scale ultrasound), multiparametric ultrasound (MPUS) also integrates vascularization (spectral/color/power Doppler ultrasound, SDUS/CDUS/PDUS, superb microvascular imaging, SMI, and contrast-enhanced ultrasound, CEUS) and tissue stiffness (ultrasound elastography) [1–4].

4.1.1.1 B-Mode Sonography (Gray-Scale Ultrasound)

B-mode sonography is the standard imaging method for the structured examination of thyroid morphology. The thyroid gland as a whole (i.e., position, enlargement, shape, echogenicity, and

L. Giovanella (ed.), *Integrated Diagnostics and Theranostics of Thyroid Diseases*,
https://doi.org/10.1007/978-3-031-35213-3_4

composition) as well as focal lesions (i.e., size, localization, echogenicity, shape, margins, composition, and calcification) can be described in detail; B-mode sonography is usually displayed in gray-scale mode. B-mode sonography is useful for the assessment of diffuse thyroid disorders (DTD), thyroid nodules, and other thyroid lesions, e.g., inflammatory disorders. The following objectives reflect the indications for thyroid ultrasound set out by the American Thyroid Association (ATA) and American Association of Clinical Endocrinology (AACE):

I. To characterize thyroid nodules to differentiate between benign and malignant lesions (Table 4.1).
II. To evaluate diffuse changes in thyroid parenchyma.
III. To differentiate thyroid lesions from other cervical structures like cervical cysts or a thyroglossal duct.
IV. To detect and to follow up cervical lymph nodes and recurrent disease in patients with thyroid malignancy.

Table 4.1 Ultrasound criteria for thyroid nodule assessment [9–11]

Ultrasound criterion	Description
Composition	
• Solid	Completely solid nodule or almost completely solid nodule cystic portion <50%
• Predominately solid	Entirely cystic without solid components (including septa), partially cystic (cystic portion >50%)
• Cystic	Predominately (>50%) composed of tiny cystic spaces with numerous septa (microcystic change, honeycomb)
• Predominately cystic	
• Spongiform	
Echogenicity	Compared to normal thyroid tissue/strap and strap muscle
• Markedly hypoechoic	Hypoechoic/decreased relative to anterior neck /strap muscle
	Markedly hypoechoic relative to normal thyroid tissue
• Hypoechoic	Hypoechoic to normal thyroid tissue
• Isoechoic	Comparable to normal thyroid tissue
• Hyperechoic	Hyperechoic/increased compared to normal thyroid tissue
• Anechoic	Completely cystic
Margin	Obviously demarkable from adjacent structures
• Well-circumscribed/ smooth	Hypoechoic rim surrounding the nodule
	Not obviously demarkable from adjacent structures
	Obviously demarkable with jagged appearance
• Halo	Typically nodal conglomerates
• Ill-defined	Obviously demarkable with corrugated appearance
• Irregular/spiculated	Surpassing the thyroid capsule; invasion of adjacent tissue/vascular structure
• Macrolobulated	
• Microlobulated	
• Extrathyroidal extension	
Calcification	Echogenic foci ≤1 mm within a solid portion (typically without posterior acoustic shadowing)
• Microcalcification	Echogenic foci >1 mm with posterior acoustic shadowing
• Macrocalcification	Peripheral echogenic rim (complete/incomplete)
• Rim calcification	Echogenic foci with reverberation artifact (within cystic component)
• Punctate hyperechoic foci with comet-tail artifact	
Shape	Anteroposterior diameter > transverse diameter/
• Taller-than-wide/ long (non-parallel growth)	Anteroposterior diameter > longitudinal diameter
	Anteroposterior diameter < transverse diameter/
• Wider/longer-than-tall (parallel growth)	Anteroposterior diameter < longitudinal diameter

V. To screen high-risk patients with MEN type II, a history of familial thyroid cancer or neck irradiation in childhood.
VI. To guide diagnostic (e.g., fine-needle aspiration cytology, FNAC) and therapeutic (e.g., radiofrequency ablation) procedures [5, 6].

The normal thyroid gland physiologically consists of two lobes and the thyroid isthmus. Occasionally, a residue or rests of the thyroglossal duct (pyramidal lobe) may be seen. The normal thyroid size and volume depend on age, sex, and iodine supply. The volume of the thyroid lobe is approximated by the ellipsoid formula: volume = width (mediolateral) × depth (anteroposterior) × length (craniocaudal) × π/6. In case of enlargement, both, the volume of the thyroid isthmus and the pyramid lobe should be added to the total thyroid volume. The upper limit of the thyroid gland volume in a slightly iodine-deficient area such as Germany is as high as 18 mL and 25 mL in adult women and men, respectively [7]. A lower volume limit is frequently not given. However, some studies have shown that thyroid volumes below 5 mL may not be sufficient for adequate thyroid hormone production. The internal structure of a normal thyroid gland is homogenously bright comparable to the salivary glands and markedly hyperechogenic compared to the adjacent cervical muscles [6, 8].

4.1.1.2 Cine-Mode and Tomographic Ultrasound

Cine-mode ultrasound allows for the continuous acquisition of ultrasound images over time [12]. This provides additional means of documentation and storage of cross-sectional data in multiple planes. With the acquired data sets incorporating the whole thyroid gland, structured assessment can be carried out in retrospective and longitudinal comparison of corresponding image planes becomes more accurate. Continuous image acquisition combined with probe tracking technology provides the basis for tomographic ultrasound imaging [13]. Data acquired in an axial plane can thus be reconstructed in multiple planes and fused with functional imaging data as needed. Integrated SPECT/Ultrasound and PET/Ultrasound fusion imaging have been shown to be feasible and may gain wider use once available on a larger scale [14, 15]. Volume data derived from standardized cine-mode acquisitions are the basis for automatic segmentation algorithms and—in the future—artificial intelligence applications.

4.1.1.3 Color Doppler Ultrasound (CDUS) and Contrast-Enhanced Ultrasound (CEUS)

CDUS gives information about the vascularization of the thyroidal tissue by visualizing intraparenchymal as well as the perithyroidal vessels. The underlying technique is based on the change in frequency of a sound wave once reflected by the motion of red blood cells in vessels. Using color coding (red: toward the transducer, blue: away from the transducer), the direction of blood flow is shown in an overlay of Doppler and grayscale images (Fig. 4.1a). In power Doppler mode only one color (e.g., orange) is used to code both flow directions.

The vascularity patterns of thyroid nodules can be categorized into four types:

I. Type 1: No vascularity (absence of intra-/perinodular vascularity).
II. Type 2: Perinodular vascularity (circumferential vascularity of the nodule).
III. Type 3: Mild intranodular vascularity (with or without perinodular vascularity).
IV. Type 4: Marked intranodular vascularity (with or without perinodular vascularity) [3, 9].

In CEUS, an intravenous microbubble contrast agent is used, which enhances the backscattering of ultrasound waves resulting in an amplification of flow signals. This means, it allows visualization of blood flow in thyroid vessels and within the microvasculature. The enhancement pattern reflects the different vascular phases (i.e., arterial, portal-venous, and venous) comparable to contrast-enhanced computed tomography. CEUS is a safe procedure, however, rarely allergic events are possible [3, 16]. Image evaluation for thyroid nodule assess-

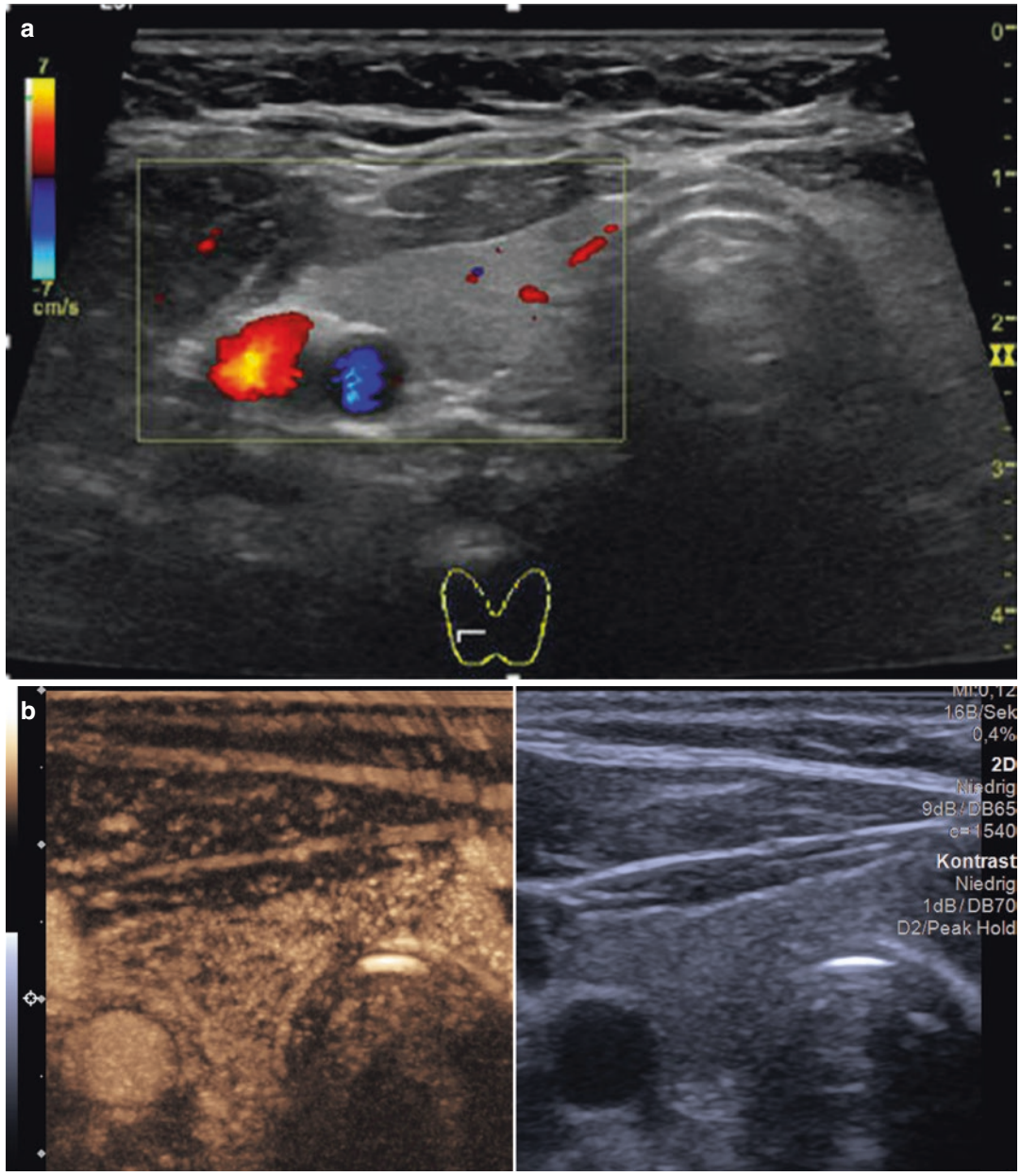

Fig. 4.1 Normal thyroid gland on color Doppler ultrasound (CDUS) (**a**) and contrast-enhanced ultrasound (CEUS) (**b**; left image: after contrast agent application; right image: native B-mode ultrasound). (Courtesy Prof. J. Bojunga, Frankfurt University Hospital)

ment includes qualitative (quality of enhancement, washout behavior, and comparison to the paranodular tissue) and quantitative (time-to-peak, wash-in slope, peak intensity, mean transit time, and area under time-intensity curves) parameters [17]. Normal thyroid tissue shows only small areas with flow termed as "normal background flow" as shown in Fig. 4.1b [18].

4.1.1.4 Ultrasound Elastography

With Ultrasound Elastography (UE) it is possible to measure the elasticity of tissues. The concept of UE was first introduced by Orphir et al. in 1991. The principle is based on an external compression of the tissue, which leads to a measurable deformation. This deformation is more pronounced in soft tissues than in hard structures.

Since a change in the elasticity of tissue typically correlates with pathologic features, UE can aid in differential diagnosis [19]. Three methods are distinguished in UE on the basis of the external stimulus: strain-based UE (USE, mechanically induced force, measuring tissue strain), acoustic radiation force impulse (ARFI, ultrasound induced, measuring tissue displacement), and shear wave-based UE (SWE, ultrasound induced, measuring quantitative shear wave propagation) [20, 21]. UE reflects the histologic composition of a tissue (i.e., cells, membranes, and ultrastructures). Normal thyroid parenchyma presents homogenously soft on UE (in case of USE mostly green, sometimes mixed green/yellow/red, Fig. 4.2). For thyroid nodule elasticity evaluation two qualitative scores are commonly used. The Asteria score ranges from elasticity score 1 representing soft (i.e., benign) tissue to elasticity 4 representing hard (i.e., suspicious) tissue. The

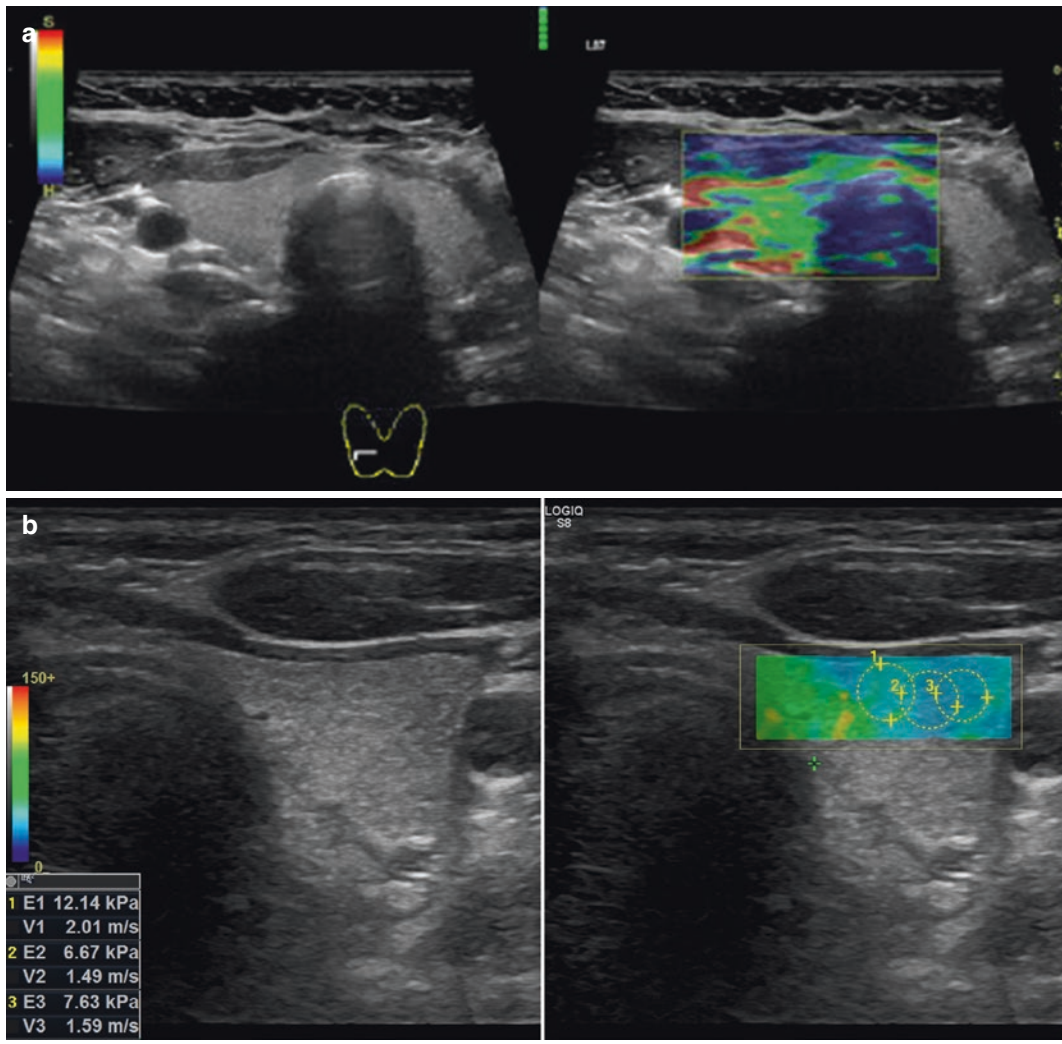

Fig. 4.2 (**a**, **b**) Normal thyroid gland. (**a**) Strain elastography (left: transverse orientation in B-mode sonography; right: superimposed strain elastography) showing a homogenously green/red colored (soft) thyroid lobe and blue colored (hard) trachea. (**b**) Shear wave elastography: transverse image of the left thyroid lobe (left: B-mode sonography and calculated elasticity modulus (kPa) and velocity of the propagation of the shear wave (m/s); right: box with three regions of interest to calculated velocity in the normal thyroid tissue

three-tier Rago Score ranges from an elasticity score 1 representing elasticity in whole or large part of the nodule (i.e., benign) to score 3 without elasticity in the nodule and in the posterior shadowing (i.e., suspicious) [22, 23]. For quantitative SWE it is known, that the stiffer (i.e., suspicious) the tissue is, the higher the propagation of shear waves. Data for normal thyroid tissue are sparse. The World Federation for Ultrasound in Medicine and Biology reported a range for normal thyroid tissue 1.60 ± 0.18 m/s for point-SWE and 2.6 ± 1.8 m/s for 2-D SWE; a single cutoff for differentiation of thyroid nodules are so far not established [24–26].

4.1.2 Radionuclide Imaging

4.1.2.1 ^{99m}Tc-Pertechnetate/^{123}Iodine

Thyroid scintigraphy (TS) allows for global and regional imaging of the sodium iodide transporter (NIS) activity within the thyroid gland in vivo. TS has long been performed with iodine isotopes ($^{131}I^-$, $^{123}I^-$). For standard TS, nowadays, ^{99m}Tc-pertechnetate is preferred over iodine isotopes due to its advantageous physical properties (short physical half-life [6 h], pure gamma emission [140 keV], radiation exposure as low as approx. 1 mSv for a standard application of 70 MBq, i.e., 0.013 mSv/MBq, its easy availability and lower costs. As a mimicker of ionic iodine, ^{99m}Tc-pertechnetate enters the thyroid cell through the basolateral cell via the NIS. In contrast to iodine, ^{99m}Tc-pertechnetate is not further organified and leaves the thyroid cell with a rather short effective half-life (hours) compared to about half a day in $^{123}I^-$ or a couple of days in$^{131}I^-$ [27, 28]. Since the import and the organification of iodine are key for thyroid hormone synthesis, the NIS activity and thus the uptake of ^{99m}Tc-pertechnetate is deemed representative of overall hormone production. TS thus provides overall and regional functional information about the thyroid gland. Under physiological conditions, the activity of the NIS is positively regulated by TSH. Only a small proportion of NIS activity appears to be independent of TSH regulation as indicated by a low (<0.5%, see below), but detectable scintigraphic uptake of ^{99m}Tc-pertechnetate even in subjects with full TSH suppression (physiological background autonomy) [29, 30]. The ^{99m}Tc-pertechnetate uptake can be quantified and is often given as a percentage of injected radioactivity. Sometimes a "normal" range is also given for the "raw" ^{99m}Tc-pertechnetate uptake, e.g., 0.5%–4% [31]. The raw uptake can only be interpreted with knowledge of the current TSH value. To avoid bias by fluctuations of TSH, TSH assessment should be closely connected with scintigraphy—with both exams ideally performed at the same time and at the same institution(s).

The authors suggest calculating ^{99m}Tc-pertechnetate uptake normalized to TSH (i.e., % per mU/L) in addition to raw uptake. The according normal range should be obtained from a site-specific cohort of about 20–30 subjects with normal thyroid function and may range from 0.3–3.0% per mU/L [32]. In addition to TSH regulation, NIS activity is also under inverse regulation by the intrathyroidal iodine concentration ("autoregulation") which in turn is representative of the iodine supply. High iodine concentrations may deteriorate image quality given the inverse effect on NIS activity. The influence of iodine may reach a point, where a scintigraphic image becomes "blocked" (uptake 0%), e.g., after administration of contrast agents containing iodine. This may also occur after the use of NIS blocking agents such as perchlorate. As a conclusion, any "excess" iodine intake should be either avoided prior to scintigraphic imaging or scintigraphy should be postponed for at least 1–3 months in cases of severe iodine contamination to yield high-quality images and usable uptake values.

Thyroid hormones exert their influence on thyroid uptake mainly via TSH regulation. As TSH influence can be accounted for by the use of TSH-normalized uptake values, a properly substituted patient is not necessarily required to withdraw thyroid hormones before TS. However, one should bear in mind that roughly two-thirds of thyroid hormone mass is made up of iodine.

This may result in a somewhat hypernormal iodine status reducing image quality and (normalized) uptake values via "autoregulation" (see above). For this reason, a mild reduction of thyroid hormone substitution may be appropriate before TS. In contrast to ^{99m}Tc-pertechnetate scintigraphy, TS with radioiodine isotopes not only reflects the import of iodine but also organification allowing for late imaging at and beyond 24 h. Owing to organification, thyroid uptake may increase about ten-fold on scintigraphies with radioiodine compared to ^{99m}Tc-pertechnetate resulting in much better thyroid-to-background contrast. Radioiodine scintigraphy is usually performed with $^{123}I^-$ (pure gamma emitter) for its lower radiation burden and better imaging quality compared to $^{131}I^-$ (90% beta- and 10% gamma emitter). $^{131}I^-$ is reserved for thyroid imaging in a therapeutic setting, e.g., testing before and during radioiodine therapy. $^{123}I^-$ TS should be used for evaluating mediastinal or ectopic/dystopic thyroid tissue allowing for better delineation against bloodpool activity (mediastinum) and non-thyroidal uptake (e.g., salivary glands) compared with ^{99m}Tc-pertechnetate (see below). There may be a role of $^{123}I^-$ scintigraphy for delineating small autonomously functioning thyroid nodules (AFTNs) below 1 cm in diameter. As shown below, AFTNs can mimic thyroid cancer on ultrasound imaging. Small AFTNs cannot be reliably diagnosed by ^{99m}Tc-pertechnetate scintigraphy owing to limited contrast resolution and TSH may not be indicative of autonomous function due to limited autonomous volume [33, 34]. Due to the higher contrast on late images, $^{123}I^-$ scintigraphies could delineate such small AFTNs and prevent them from further work-up since AFTNs are presumed to be benign. Another role of $^{123}I^-$ scintigraphy may be ruling out of "trapping only" nodules (see below). Trapping only nodules may mimic true AFTNs by showing a high initial uptake on TS but rapid washout over time as seen on late imaging (e.g., 24 h). Since trapping only nodules harbor a significant risk of malignancy ranging between 5 and 10% it is advised to use $^{123}I^-$ TS if the autonomous nature of a nodule is doubtable [28, 35]. On scintigraphy, the intensity of radionuclide uptake within nodules is visually rated relative to the surrounding thyroid tissue and described as "hyperfunctioning" ("hot"), "hypofunctioning" ("cold"), or isofunctioning ("indifferent"). Note that "hyperfunctioning" indicates a *relatively* increased thyroid hormone synthesis but not automatically an *absolutely* increased one. In fact, when thyroid parenchyma is damaged, e.g., by Hashimoto's thyroiditis, a "hot" nodule may be the only site with normal and preserved hormone synthesis. Vice versa, a cold nodule mostly, but not always indicates a decreased hormone synthesis. In summary, indications for thyroid scintigraphy are shown in Table 4.2.

4.1.2.2 ^{99m}Tc-Methoxy-Isobutyl-Isonitrile (MIBI) Imaging

^{99m}Tc-methoxy-isobutyl-isonitrile (MIBI) is a cationic lipophile complex agent that accumulates in mitochondria by passive diffusion. It has a high first-pass extraction and the MIBI uptake in viable cells depends on the blood flow. Besides its use as a marker for myocardial perfusion and hyperactive parathyroidal tissue, numerous studies have described MIBI uptake in various tumors such as lungs, brain, breast, bone, and thyroid. It is suggested that in addition to the number of mitochondria, their negative membrane potential is also responsible for the binding of MIBI [37–39]. The usefulness of MIBI imaging for risk stratification of hypofunctioning thyroid nodules has been investigated for more than 30 years. For qualitative image evaluation, the MIBI uptake in the thyroid nodule is compared to the MIBI uptake in the paranodular thyroid tissue and classified as hyper-, iso-, and hypointense with the latter ruling out malignancy with high probability. A semiquantitative method has been published by Campenni et al. taking the MIBI kinetics into account also (see below) [40–43]. A further thyroid-specific application for MIBI imaging is to differentiate amiodarone-induced hyperthyroidism (AIT) type 1 and type 2 [44]

Table 4.2 Indications for thyroid scintigraphy with either ^{99m}Tc-pertechnetate or $^{123}I^-$, adapted from [28, 36]

	^{99m}Tc-pertechnetate		$^{123}I^-$	
	Indication	Purpose	Indication	Purpose
Nodules found on ultrasound (predominantly solid)	≥ 1 cm in diameter	Hot nodule: Usually no FNAC; "Cold" nodule: Consider FNAC	≤1 cm but with suspicious ultrasound features[a]	Hot nodule on late imaging: No FNAC
			Hot nodule on ^{99m}Tc-pertechnetate but doubt on autonomous nature[a]	Rule out trapping only nodule
Goiter grade ≥ 2	Iodine administration planned (TSH < 2 mU/L)	Rule out (hidden) focal or diffuse autonomy	Thyroid cannot be fully delineated on Ultrasound	Rule out mediastinal extension
Goiter grade 1	Iodine administration planned (e.g., TSH < 1 mU/L)	Rule out (hidden) focal or diffuse autonomy)	Thyroid gland cannot be fully delineated on Ultrasound	Rule out mediastinal extension
Ectopic and dystopic thyroid tissue (preferably SPECT/CT)	(with limitations)	(detect aberrant tissue)	Base of the tongue, mediastinal, other	Preferred method to detect aberrant thyroid tissue
Suspicion of thyrotoxicosis	E.g., TSH (be)low normal, with and without nodules	Detect focal or diffuse autonomy; discern productive forms of thyrotoxicosis from destructive ones		
Therapeutic management	After radioiodine therapy (benign) or local ablative treatments	Document therapeutic success		
Suppression test	Borderline uptake for autonomy on native scintigram	Distinguish relevant autonomy from non-relevant one. Discern iodine avidity from autonomy in goiters		

[a]Not yet validated

4.1.3 Hybrid Imaging

4.1.3.1 Hybrid Imaging with ^{99m}Tc-Pertechnetate and ^{123}I-NaI

Single photon emission computed tomography (SPECT) with integrated computed tomography (SPECT/CT) enables co-registration of anatomic and functional data and provides accurate attenuation correction of the detected tracer distribution (Table 4.3). It has substantially improved patient care in the management of thyroid cancer. A lot of reported advantages over conventional planar imaging after $^{131}I^-$ post-thyroidectomy radioactive iodine ablation have led to the use of SPECT/CT for precise localization and characterization of radioactive iodine foci and therefore influence staging, risk stratification, and clinical management [45]. SPECT/CT systems use the same gamma camera component generally used for planar and tomographic imaging of single photon emitting radiotracers, without additional radiation exposure for SPECT. In Germany, a volume CT dose index (CTDIvol) of 3 mGy has been defined for auxiliary CT imaging for attenuation correction and anatomic co-registration [46]. For benign thyroid conditions and pretherapeutic thyroid imaging SPECT/CT is not routinely used but SPECT/CT can be helpful in a number of indica-

Table 4.3 Tracer properties according to [36, 46, 48]

Tracer	DRL	Administered activity in MBq for a 75 kg patient	Effective dose equivalent (mSv/MBq)	Effective dose in mSv
^{18}F-FDG	3 MBq/kg	225 i.v.	0.019	4.3
^{99m}Tc-pertechnetate	70 MBq	60–70 i.v.	0.013	0.78–0.91
^{123}I-NaI		5–10 i.v.	0.20	1.0–2.0

tions, especially for substernal or ectopic thyroid tissue [28]. And it can be useful in detecting the dominant nodule in a goiter with multiple nodules and in distinguishing ectopic thyroid tissue from adjacent structures that may physiologically show an elevated iodine concentration, such as salivary glands, salivary collections in the mouth, and swallowed saliva in the esophagus. CT can also provide additional information, e.g., on tracheal compression and shift.

4.1.3.2 Hybrid Imaging with ^{18}F-FDG-PET

Hybrid imaging with positron-emission tomography/computed tomography (PET/CT) and PET/magnetic resonance imaging (PET/MRI) combines imaging of function, e.g., metabolic information, and anatomic structure to provide accurate localization, characterization, and diagnosis in a "one-stop" imaging approach. Under normal conditions, thyroid tissue shows low or absent uptake of FDG. Due to the increase in ^{18}F-fluorodeoxyglucose (^{18}F-FDG)-PET examinations in patients with malignant and non-malignant diseases, incidental FDG uptake in the thyroid gland is seen more frequently and reported in up to 3% of the examinations. FDG uptake patterns in thyroid are generally classified as focal or diffuse. Currently, ^{18}F-FDG-PET/CT is not recommended for initial or preoperative risk assessment of newly detected thyroid nodules or diffuse thyroid diseases. For some thyroid indications, ^{18}F-FDG-PET/CT shows promising results, especially for cytologically indeterminate nodules (see below).

Currently, the radiolabelled glucose analog ^{18}F-FDG-PET/CT is established in clinical practice and widely used for initial staging, restaging, recurrence detection, and assessment of treatment outcomes in a variety of malignant diseases. Combining metabolic and anatomical information, ^{18}F-FDG-PET/CT detects malignant tumor lesions by identifying regions with increased glycolytic metabolism and expression of membrane glucose transporter (GLUT) proteins [47]. However, increased FDG uptake is not only found in malignant diseases but also in infectious or inflammatory conditions. Combined PET/MRI provides complementary data acquired at the same time and offers advantages over PET/CT with regard to increased anatomical details and radiation dose reduction by omitting radiation exposure through the CT component. The radiation exposure related to a PET/CT scan is dependent on the administered activity of FDG and on the intended use of the CT scan. Exposure can be chosen very low for attenuation correction only or mere anatomical correlation, but is higher for a diagnostic CT scan including intravenous contrast agent administration. The effective dose for the CT component thus ranges from 1 to 20 mSv [48]. Scan range can reach from a limited area confined to the tumor, to torso imaging up to whole-body imaging. For Germany, new diagnostic reference levels (DRL) for typical nuclear medicine examinations have been published in 2021. DRL for PET tracers are expressed as administered activity per body weight and for scintigraphies or SPECT as upper threshold levels for activities [46]. The effective dose from FDG application in adults is 0.019 mSv/MBq according to ICRP publication 106, i.e., about 4.3 mSv for an administered activity of 225 MBq [48] (Table 4.3).

4.2 Integrated Imaging of Thyroid Disorders

4.2.1 Diffuse Thyroid Diseases

The most frequent diffuse disorder of the thyroid gland is an enlargement of the glandular volume (goiter). This disorder can easily be assessed by ultrasound using the standard formula for volume calculation (thyroid volume = transverse diameter × anteroposterior diameter × longitudinal diameter × /π/6) [3]. In theory, growth of the thyroid gland is diffuse in first instance but becomes more and more nodular over time. However, nodules mostly occur already in non-enlarged thyroid glands. Up to two-thirds of a population may have thyroid nodules above 5 mm in diameter whereas thyroid gland enlargement affects only 17% in a mildly iodine-deficient population [49]. Therefore, in clinical routine, diffuse growth and development of nodules have a parallel time course rather than a consecutive one. For the sake of clarity, diffuse and nodular growth are treated separately in the following. Goitrous growth is seen in about one-tenth of the world population and it is driven by two main causes: genetic factors and iodine supply [50]. Other factors such as smoking and childbearing have also been shown to play a role [51]. Since iodine deficiency in areas endemic to goiter often dates back over centenaries or even thousands of years [52], it can be hypothesized that longstanding iodine deficiency is also a driving force behind genetic factors promoting goitrous growth. Goiters attributable to iodine deficiency can be assumed to be normofunctioning in the presence of normal or rather high TSH values. TS can demonstrate iodine avidity of the thyroid gland by a rather high uptake (e.g., uptake % twice or more per TSH unit) representing high NIS activity. However, TS is rarely considered necessary for such a diagnosis. Nevertheless, in doubt of the reason for goitrous growth, TS readily distinguishes between iodine deficiency and other reasons such as inflammatory causes (e.g., autoimmune disease, see below) by a high normalized uptake versus a low uptake. This may have implications for the treatment of the goiter–e.g., iodine vs. levothyroxine. In more advanced or longstanding endemic goiters autonomously functioning thyroid tissue above a certain baseline level of autonomy (see above) occasionally develops. By definition, autonomously functioning thyroid tissue produces thyroid hormone without being controlled by TSH regulation. The detection of autonomy is the core indication for TS—mostly performed with ^{99m}Tc-pertechnetate as the preferred radionuclide. In many cases, autonomy can be assigned to a single thyroid nodule or multiple thyroid nodules (i.e., unifocal autonomy and multifocal autonomy, see below) on the basis of an elevated circumscribed uptake on the scintigram. However, the thyroid gland as a whole can also be affected by autonomy, then termed "diffuse" or "disseminated" autonomy. While this disorder is frequently encountered in endemic areas, it is rather uncommon in non-endemic areas. In non-endemic areas, this presentation is often summarized under abortive/antibody-negative forms of Graves' disease (GD) or multinodular autonomy [53, 54]. However, diffuse autonomy exhibits unique features not shared by GD such as a normal echogenicity on thyroid ultrasound, insidious onset, a rather stable clinical course over time and no curative restitution after the use of thyreostatics. Compared to multinodular autonomy there is no focal "hot" lesion on scintigraphy although the scintigraphic appearance may be somewhat patchy. However, diffuse autonomy may occur in combination with AFTN [55] then being named focally- or multifocally-disseminated autonomy. Diffuse thyroid autonomy is a mere scintigraphic diagnosis (see Fig. 4.3). In the absence of serological/biochemical or sonographic hints for GD, diffuse autonomy can be assumed when a goiter shows a moderately increased global uptake (raw uptake typically between 1 and 3%) not attributable to thyroid nodules—in combination with a low or subnormal TSH value. Thyroid antibodies are typically negative. However, in patients with positive TPO antibodies, some overlap with abortive forms of GD exist as well as with iodine avidity in endemic goiter. In goiters without nodules, TS may be considered when TSH is low, e.g., below 1 mU/L, in order to rule out diffuse thyroid

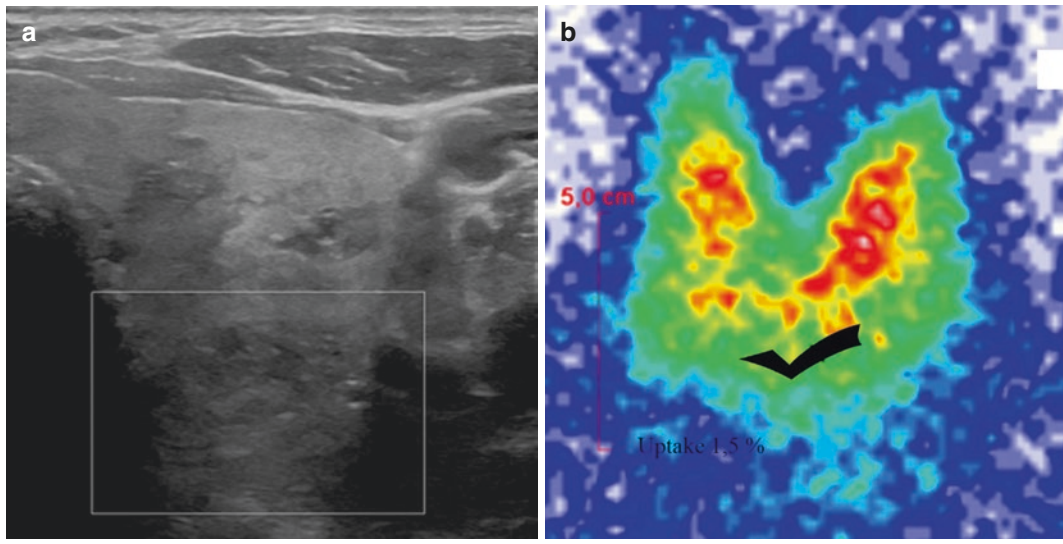

Fig. 4.3 (**a**, **b**) Seventy-year-old man with borderline low TSH over several years. At presentation TSH is 0.23 mU/L. Thyroid antibodies are negative and the patient has no appreciable symptoms. (**a**) Ultrasound examination reveals grade 2–3 goiter (60 mL) with beginning nodular transformation mainly in the caudal portions of the gland. The thyroid parenchyma is otherwise unremarkable on thyroid ultrasound. (**b**) On scintigraphy [the hook marks the jugular groove], the uptake is somewhat inhomogeneous with more pronounced accumulation in the cranial and mid portions, i.e., the portions with the least nodular transformation. The raw uptake (1.5%) appears moderate but normalization to TSH reveals a clearly elevated normalized uptake of 6.5% per mU/L. On the basis of the scintigraphy, the diagnosis of disseminated autonomy is made

autonomy—e.g., in elderly patients before antigoitrous therapy with iodine is initiated or in other instances such as impending iodine contamination from contrast agents or disinfecting agents.

From studies in nodular goiter it is known that thyroid autonomy may occur in the presence of TSH values up to approx. 2 mU/L. This TSH value may also be adopted as a threshold below which diffuse thyroid autonomy may be present in goiters [56, 57]. However, in goiters with TSH in the mid-range TS cannot reliably differentiate between hidden diffuse autonomy and iodine avidity since both exhibit a rather high normalized uptake (see above). A suppression study may be added for a definitive diagnosis (see below). Ruling out disseminated autonomy in large goiters with TSH in the mid-range may have implications for goiter therapy and on how to deal with iodine contamination and its potential to enhance thyroid function. TS is not only able to *detect* autonomy but also to *grade* autonomous functions. The overall excess of hormone production originating from AFTNs and/or diffuse autonomy can be estimated by calculating the radionuclide uptake. As a threshold, a raw uptake between or above 1–2% is considered a relevant autonomy when TSH is suppressed to or below 0.1 mU/L [56]. In this regard, it plays no role whether TSH is suppressed endogenously or exogenously by administering thyroid hormone. The actual uptake threshold may vary between different regions depending on the prevailing iodine supply. Threshold values are lower in regions with sufficient iodine supply (e.g., 1%) as compared to regions with insufficient supply (e.g., 2%) [58, 59]. In subjects with TSH being naturally suppressed by autonomy, raw uptake will almost certainly be above 1%. If not, recent iodine contamination has to be taken into account—possibly lowering or even blocking the uptake [60]. The most common reason for thyrotoxicosis in non-endemic areas is GD [61]. GD is a hormone-productive autoimmune thyroid disease relying on the formation of TSH receptor-stimulating antibodies (TRAbs). Typically, it can readily be

diagnosed by a high uptake on TS (generally ≫ 2%) in combination with a marked thyrotoxicosis, diffuse goiter with lowered echogenicity (Fig. 4.4a) with or without micronodulation, and positive Trabs. If CDUS of the thyroid gland shows a diffuse increase in vascularization ("thyroid inferno," Fig. 4.4b), in such settings TS can be omitted—in particular in juveniles—since the diagnosis is sufficiently certain [3, 8]. The thyroid gland stiffness is significantly higher in GD than in healthy controls [62], but this could also be shown for Hashimoto's thyroiditis (HT) and subacute thyroiditis (SAT) [63–65]. There are mild forms of GD showing only minor ultrasound signs, no elevated vascularization, borderline TRAbs, and high antibodies against thyroid peroxidase (TPO) and/or human Thyroglobulin (hTg). In such cases, differentiation from destructive autoimmune thyroid disease—in particular HT, which can also present with a hypervascularization, and hormone release as the underlying cause for thyrotoxicosis is difficult without TS [3]. Scintigraphy reliably shows an elevated uptake even in mild forms of GD (Fig. 4.4c) vs. a low uptake in destructive thyroid disease [66]. However, the uptake must be related to the TSH

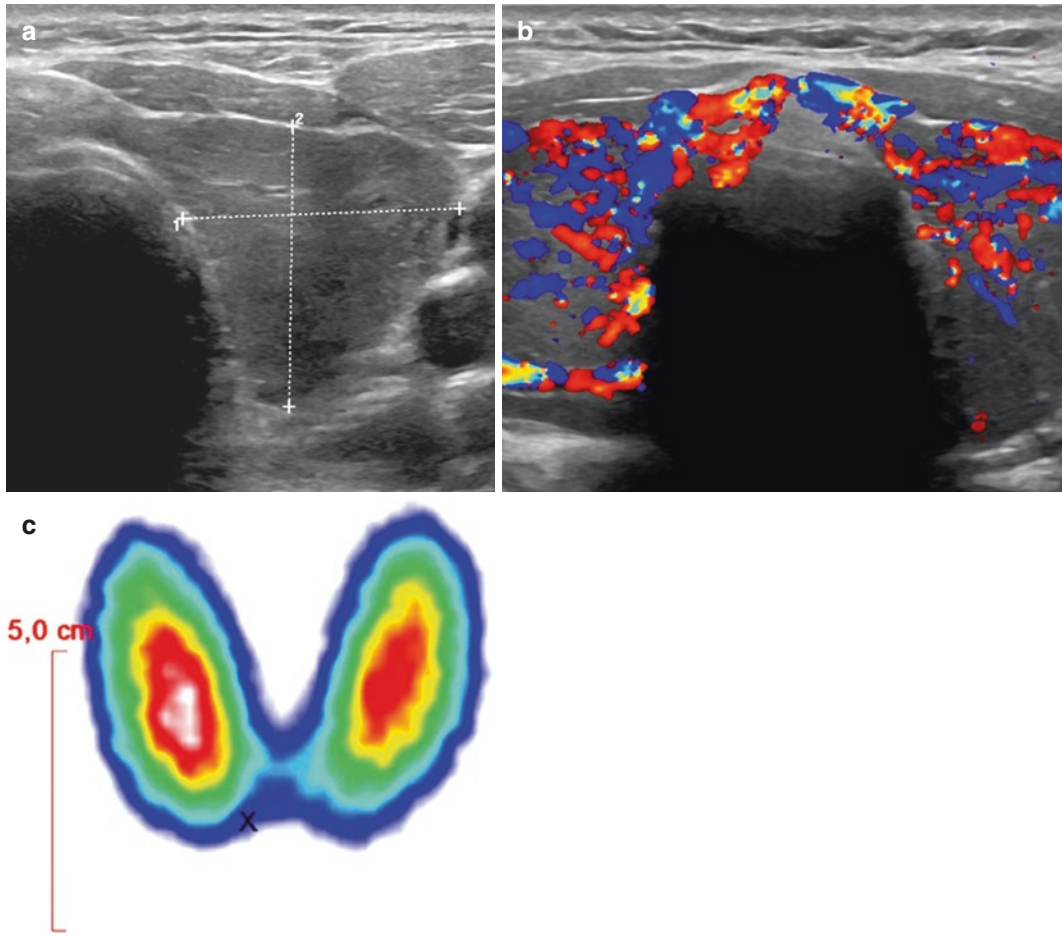

Fig. 4.4 (**a**–**c**) A 30-year-old male presenting with weight loss (20 kg within a few weeks), nervousness, and finger trembling. Pulse rate at 120 bpm. On ultrasound (**a**) the thyroid gland is enlarged with reduced echogenicity—comparable to the overlying strap muscle. Vascularity of the thyroid gland is markedly increased (**b**). Severe hyperthyroidism (TSH suppressed, fT3 31 pg/mL) with high TRAb levels (25 IU/L). On scintigraphic imaging (**c**) there is a markedly increased uptake (11.5%) yielding a normalized uptake (% per mU/L TSH) approaching "infinity"

value ("normalized uptake") in order to become meaningfully interpreted. The only pitfall in this regard may be a recent (<3 months) iodine contamination resulting in a temporarily blocked scintigraphy in GD. CDUS is helpful for the evaluation of disease remission, recurrence, and response to treatment in patients with GD. However, in the early stage of disease, HT shows a diffuse increase in vascularization that decreases in the course of disease due to extensive fibrosis [3].

Autoimmune (destructive) thyroid disease as well as postpartal thyroiditis and silent thyroiditis are the most common causes for acquired hypothyroidism—besides thyroid surgery [67]. The ultrasound patterns of autoimmune thyroiditis are:

- (markedly) hypoechoic and more or less heterogeneous parenchyma
- ("Swiss cheese" or "honeycombing," 1–6 mm) changes
- Pseudomacronodular changes
- Fibrotic (pseudolobulated) changes
- Speckled appearance (infrequently)
- Increased stiffness of the thyroid

Thyroid volume may be normal, increased (HT), or decreased (Ord's disease). Ultrasound may detect perithyroidal satellite lymph nodes in patients with HT (e.g., "Delphian lymph node" above the cranial isthmus) [8, 65, 68].

The onset of autoimmune thyroiditis may be insidious or prompt. The latter often entails an initial interval (some weeks) of thyrotoxicosis as a result of hormone liberation from damaged thyroid follicles. Commonly, the insidious and the prompt form end up in hypothyroidism. TS mostly is not needed for the diagnosis of autoimmune thyroiditis since patients usually present with typical ultrasound and laboratory findings (TPO-antibodies, Tg-antibodies, hypothyroidism). A possible initial interval of thyrotoxicosis frequently goes unnoticed but can otherwise prompt confusion with GD. In this situation, TS is valuable to differentiate GD from early autoimmune thyroiditis by a high vs. a low uptake. As in GD, there are mild (e.g., silent thyroiditis) or even abortive forms of autoimmune thyroiditis (e.g., postpartum thyroiditis) with no recognizable ultrasound signs or without marked elevation of TPO-antibodies (and /or Tg-antibodies). If TSH elevation is borderline there may be doubt whether hypothyroidism is present. Any diagnosis—in favor or against a mild form of thyroiditis—is arbitrary in this situation and may rely on clinical symptoms and signs alone. Although not part of clinical routine work-up, TS may be helpful in selected cases by showing a lowered normalized uptake which reflects parenchymal damage versus a normal uptake in unaffected glands. However, when using TS in this case, high standardization of uptake calculation, site-specific normalized uptake ranges, and exclusion of iodine contamination are mandatory. Subacute thyroiditis (SAT, de Quervain's thyroiditis, Fig. 4.5a–d) is of unclear origin, mostly occurring a few weeks after a viral infection—including COVID-19—and usually exhibiting a painful clinical course over weeks [69]. At the inflammatory stage, even ultrasound examination may be painful for the patient almost always showing rather large, irregularly confined hypoechoic lesions in an enlarged thyroid gland (Fig. 4.5a) and higher stiffness in UE. CDUS shows decreased flow in the hypoechoic areas (Fig. 4.5b). The disease often starts unilaterally but tends to involve both sides over time or to shift to the contralateral side. Within a few months, the ultrasound pattern and enlargement of the thyroid resolve with some strands of fibrosis reflecting the residual thyroid damage. Functionally, SAT mostly has a marked initial interval of thyrotoxicosis [8, 63, 70, 71]. In COVID-19-induced cases, an abortive even painless form of SAT may be seen [72]. If ultrasound features and clinical symptoms are equivocal, TS may be necessary to differentiate SAT from GD. Following the initial phase, a post-inflammatory decline in hormone production often gives rise to increased TSH secretion above normal but usually returns to normal levels within weeks. There is debate over how often a (slight) parenchymal damage after SAT may persist [70]. In individual patients, TS may help to detect thyroid damage on the basis of a decreased normalized uptake (Fig. 4.5c).

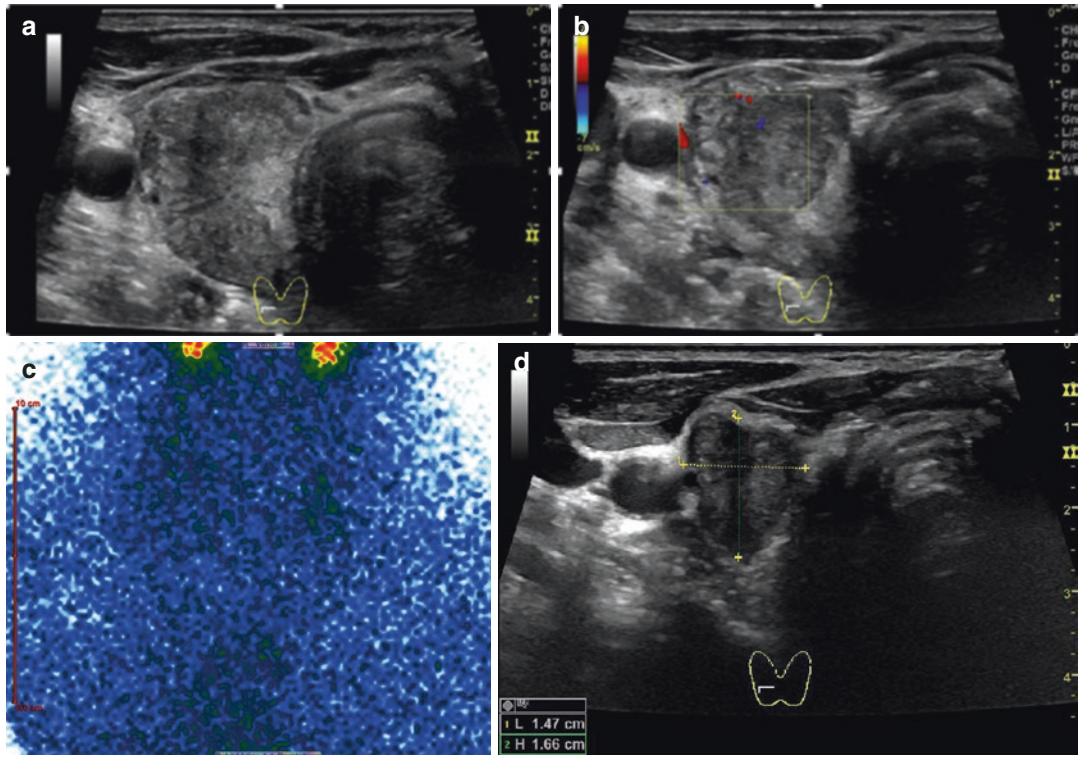

Fig. 4.5 (**a**–**d**) Seventy-three-year-old male patient presenting with neck pain. TSH 0.01 mU/L, free T3 and free T4 normal, thyroid antibodies not elevated. (**a**) B-mode ultrasound (right thyroid lobe, transverse image) showing thyroid gland enlargement (volume right lobe: 17 mL, left lobe: 12 mL) and confluent hypoechoic areas in both lobes. (**b**) CDUS without increased vascularization. (**c**) Absent tracer uptake at thyroid scintigraphy. (**d**) Three months follow-up shows a hypoechoic thyroid shrunken to normal volume (right lobe: 5 mL, left lobe: 5 mL) and TSH 6.15 mU/L and low-free T3 2.35 pg/mL)

4.2.1.1 Diffuse Incidental Thyroid ^{18}F-FDG-Uptake

Diffuse thyroid uptake (Fig. 4.6) is most often associated with benign disease corresponding to inflammatory uptake, e.g., in autoimmune thyroid disorders like HT or hyper-/hypothyroidism [73, 74]. For further clarification, a sonographic examination should be carried out. Sonographically, these patients often show characteristic diffuse heterogeneity; FNAC or intervention is generally not required. In addition, a correlation between thyroid function and the presence of antibodies against thyroid antigens is helpful.

4.2.1.2 Nodular Thyroid Diseases

Autonomously Functioning Thyroid Nodules

As shown by a recent multicenter study, depending on the size, Autonomously Functioning Thyroid Nodules (AFTNs) may constitute up to 27% of all thyroid nodules in Germany [75]. The development of AFTNs is based on somatic mutations. In contrast to many other organs, the thyroid gland harbors a high spontaneous mutation rate which even increases in an environment of iodine deficiency or other goitrogens. As the mutation load increases, clones with positively

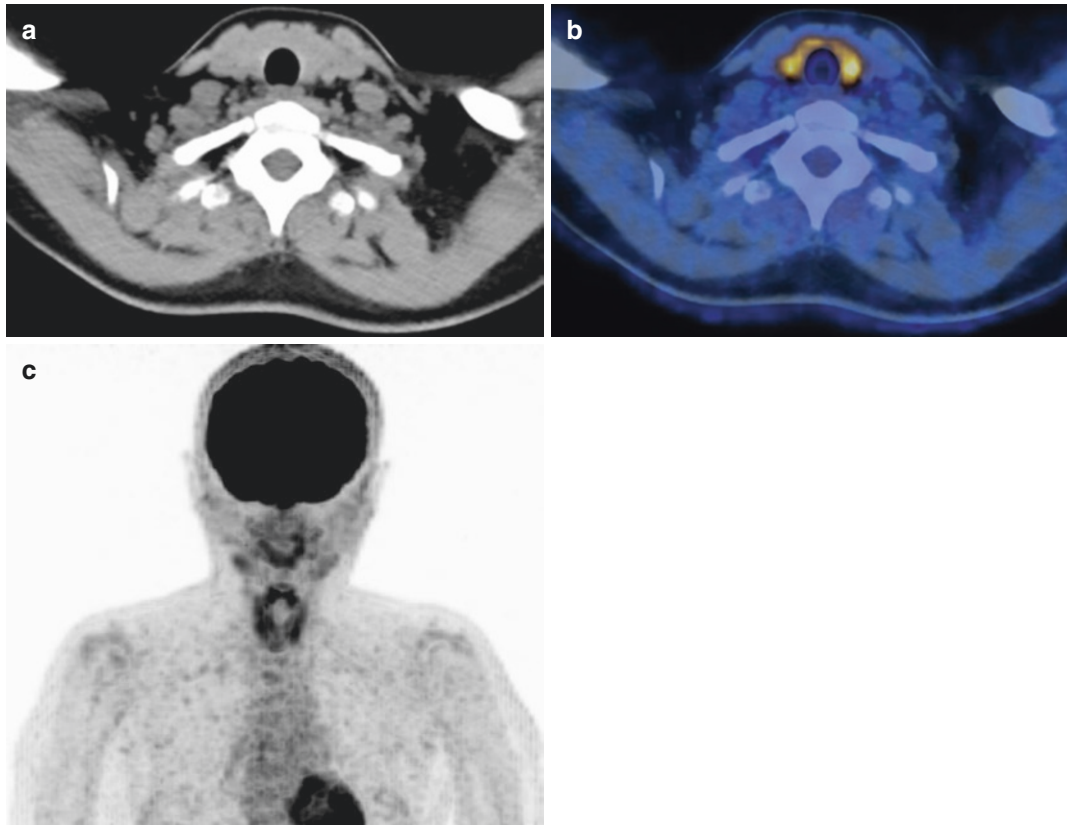

Fig. 4.6 (**a**–**c**) Diffusely increased ^{18}F-FDG uptake in thyroid of 53-year-old woman referred for evaluation of melanoma. Patient is taking Levothyroxine 50 mcg/d. TSH 2.03 mU/L, TPO- and Tg-antibodies were elevated at 649 U/mL (reference range, <60 U/mL) and 66 U/mL (reference range, <29 U/mL) because of known Hashimoto's thyroiditis. (**a**) Transaxial CT image, (**b**) transaxial fused PET/CT image, (**c**) maximum intensity projection image presented diffuse homogeneous tracer uptake, with SUVmax 6.7 in the thyroid gland

activating mutations may outgrowth the surrounding thyroid tissue and give rise to AFTNs with elevated hormone production [76]. Since activated thyroid hormone production leads to an increased import of iodine by the NIS, AFTNs are readily detectable on TS as a "hot spot" (hyperfunctioning). If significant, the increased hormone synthesis in AFTNs leads to TSH downregulation which in turn reduces hormone synthesis in the non-autonomous thyroid tissue. However, TSH secretion by the pituitary gland is mostly not suppressed but normal or low normal [34, 77, 78]. Only, about one-half of AFTNs lead to TSH suppression which often is referred to as a "decompensated" AFTN [75, 78]. On B-mode ultrasound and CDUS, AFTNs may mimic suspicious nodules [33], including cases with a rather high vascularization centrally [79]. In other cases, AFTNs are unremarkable with a small rim-like perfusion [80]. AFTNs cannot be safely identified by thyroid elastography as shown in several studies. Ruhlmann et al. found that up to 70% of the examined AFTNs were rated as hard (i.e., suspicious) according to Rago and Asteria score. A more recent study by Trimboli et al. described that 45% of the AFTNs were hard on UE and 30% showed an intermediate classification [77, 81]. Another study by Ruhlmann and colleagues investigated whether UE can be used to predict the treatment response of AFTNs to radioiodine therapy. They found no significant difference between the groups of responders and non-responders for visual Rago classification [82]. CEUS is not routinely used for the diagno-

sis of autonomous thyroid nodules. AFTNs have a negligibly low malignancy risk—usually below 1% [28, 83]. Overall, AFTNs can be regarded as safely benign and further diagnostic work-up to exclude malignancy is not necessary. As mentioned above, AFTNs develop through mutations. However, in rare instances, a further—inactivating—mutation may occur which disrupts the production line for hormone synthesis. This small subgroup of AFTNs is referred to as "trapping only" nodules and constitutes about 5% of all AFTNs in the presence of a non-suppressed TSH. Trapping only nodules exhibit both an increased iodine import and a decreased organification/hormone synthesis. As a consequence, on ^{99m}Tc-pertechnetate scintigraphy and early phase (up to 4 h after injection) radioiodine scintigraphy trapping only nodules appear hyperfunctioning and indistinguishable from true AFTNs. On delayed radioiodine scintigraphies (e.g., 24 h), however, trapping only nodules become "cold" representing the decreased organification of iodine. Trapping only nodules is functionally not relevant and thus no candidate for radioiodine therapy. The small number of hyperfunctioning thyroid carcinomas is probably attributable to trapping only nodules, since such nodules harbor a significant risk of malignancy of about 30% [35]. The diagnosis of an AFTN should be made with care for its importance with regard to a safe exclusion of malignancy. For this reason, hyperfunctioning nodules with a disproportion between size and intensity on the one hand and TSH level on the other hand should be regarded as potential trapping only nodules. Scintigraphy with $^{123}I^-$ including late-phase scans 24 h after injection can be performed to demonstrate or rule out trapping only nodules. If no late-phase radioiodine scan is available, in a potential trapping only nodule, FNAC should be considered if suspicious sonographic features are present [See Fig. 4.7].

Hyperfunctioning focal lesions in destructive thyroiditis mostly are not AFTNs but rather pseudonodules ("white knight") [84, 85]. Often, they are the only place with preserved hormone synthesis rendering them hyperfunctioning on TS. As with trapping only nodules, further work-up should be considered in such nodules if suspicious sonographic features are present.

4.2.2 Imaging in the Risk Assessment of Thyroid Nodules

4.2.2.1 Ultrasound Risk Stratification Systems (B-Mode Ultrasound, UE, CEUS)

Many lesions within the thyroid gland can be diagnosed as almost safely benign on ultrasound. Cystic lesions often can be excluded from further work-up for risk assessment since thyroid carcinomas are predominantly solid in nature. This applies not only to pure cysts but also to cysts with a concentric solid part at the periphery or with some polygonal solid parts (ATA 2016) (Figs. 4.8 and 4.9). However, with an increasing solid component, evaluation of the solid parts according to Table 4.3 is necessary in order to further assess the risk of malignancy. A spongiform thyroid nodule is almost always benign. It is characterized by close proximity of numerous tiny cystic spaces with membranes in between and only sparse solid parts, giving it the ultrasound appearance of a sponge (Fig. 4.10). Spongiform nodules should also be excluded from further work-up for risk assessment.

In case of significant (e.g., >50%) solid parts within a thyroid lesion, a structured and consistent sonographic risk assessment is recommended according to Table 4.3. As a rule, the risk of malignancy for a thyroid nodule increases as the number of suspicious features increases. However, it is difficult to define the exact number or constellation of sonographic risk factors in order to sharply differentiate benign from malignant nodules since suspicious features are also shared by many benign nodules. According to a low prevalence of malignant thyroid nodes (0.1–1%) in primary care institutions, a higher number of risk factors or the addition of further modalities may be adequate as compared to third-level care centers with an a priori malignancy risk as high 20%.

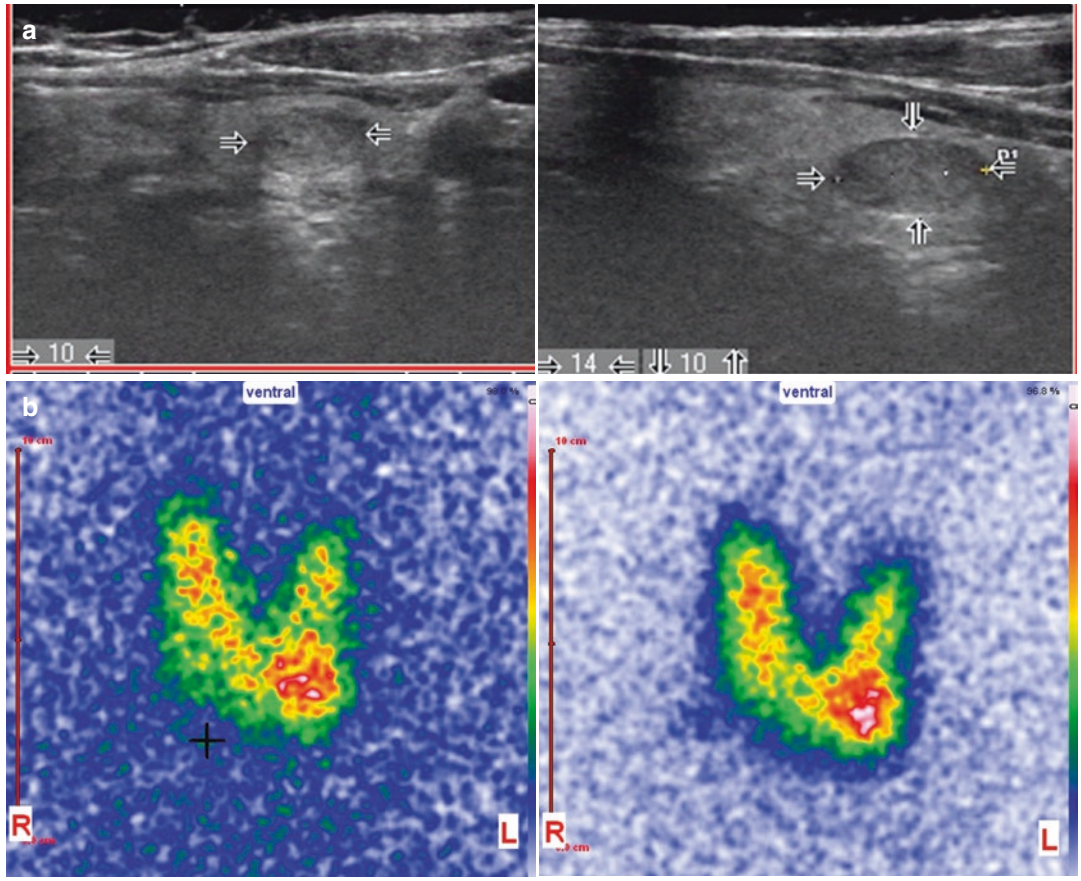

Fig. 4.7 (**a**, **b**) (**a**) Female patient with a hypoechoic and solid thyroid nodule in the left lower lobe (10 × 10 × 14 mm, TSH 0.8 mU/L, left image: transverse orientation, right image: longitudinal orientation). (**b**) $^{123}I^-$ scintigraphy 60 min (left image) and 24 h (right image) after application of 12 MBq $^{123}I^-$ shows a focal tracer uptake in the left lower lobe representing a true AFTN, thus ruling out a trapping only nodule

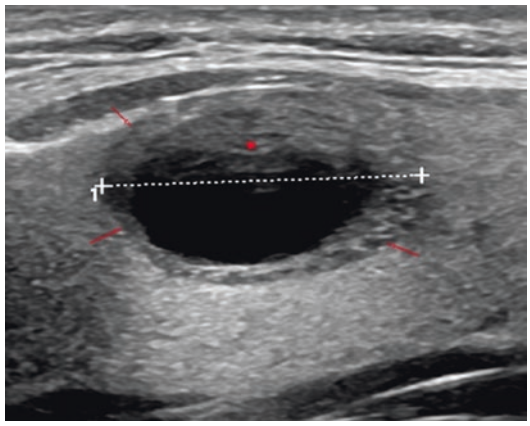

Fig. 4.8 A predominantly cystic lesion with a concentric rim of solid tissue (small arrows) can safely be diagnosed as benign on ultrasound. Note the artifacts from reflections at surfaces from above tissue layers (asterisk) within the cyst and a brightening artifact dorsal to the cyst

Ultrasound risk stratification systems (US-RSSs) such as the Thyroid Imaging Reporting and Data System (TIRADS) are increasingly used in clinical routine for the risk assessment of thyroid nodules in order to select candidates for further diagnostic work-up and reduce unnecessary FNACs. With all US-RSSs the combination and/or the number of certain ultrasound criteria are documented (i.e., composition, echogenicity, margin, spots/calcification, and shape) because no single criterion alone is sufficiently predictive for malignancy [86] (Table 4.4).

The correct application and interpretation of these five ultrasound criteria for the assessment of malignancy risk in thyroid nodules is crucial

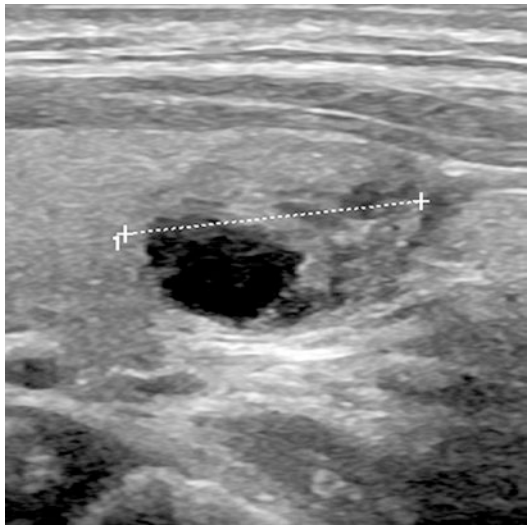

Fig. 4.9 A predominantly solid without suspicious sonographic features such that it can be safely diagnosed as benign on ultrasound. Even when hypofunctioning on TS such nodule needs no FNAC for further risk assessment since the finding is explained by the relevant cystic component in this case

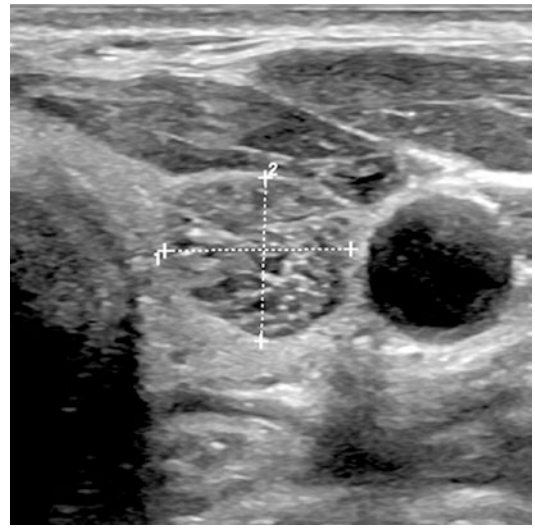

Fig. 4.10 This spongiform nodule is safely benign and needs no FNAC for further work-up, even when cold on scintigram—the latter finding being explained by an abundant content of fluid

Table 4.4 Thyroid ultrasound criteria and diagnostic performance [87]

Criterion according to TIRADS	Suspicious feature	Sensitivity (%)	Specificity (%)
Composition	Solidity (e.g., <10% cystic parts)	92	21
Echogenicity	Hypoechoic nodule	85	52
Margin	Irregular margin	50	92
Echogenic foci/calcification	Microcalcification	55	91
Shape	Taller than wide	33	85

for TIRADS categorization but is more sophisticated than it may look at first glance. The categorization of a nodule as solid is rather straightforward as it relies on the subjective estimation of the cystic proportion of a nodule. For labelling as "solid" a nodule should exhibit less than 10% cystic portions (ATA 2016: <5%). "Solidity" has a sensitivity for the detection of malignancy around 90% but a very low specificity of around 20% [87]. For this reason, solidity cannot serve as a sole criterion for indicating FNAC. Classifying a nodule as hypoechoic heavily relies on subjective assessment since many nodules are heterogenous in pattern, exhibit cystic parts which may lower overall echogenicity or show artifacts from e.g. calcifications. In addition, the assessment is complicated in thyroiditis such that the surrounding thyroid tissue is no longer representative of normal echogenicity. It is not surprising that the assessment of echogenicity has a high interobserver variability (kappa around 0.6) but can be somewhat improved by consensus meetings [88]. Irregular margins including microlobulation and external thyroid extension as a hint for malignancy is a rather inconstant feature of thyroid carcinomas (sensitivity around 50%) but is among the most specific criteria. However, it is difficult to discriminate irregular margins from more ill-defined margins in inflammatory lesions (e.g., SAT) or from macrolobulated margins in composite nodules—again resulting in a high interobserver variability. This variability can substantially be improved by consensus meetings. Microcalcifications are charac-

teristic of papillary thyroid carcinoma and histologically most likely represent psammoma bodies. The assessment of microcalcifications is the most cumbersome among the ultrasound criteria for malignancy. Thus, it has the highest interobserver variability with a kappa of around 0.4 which virtually cannot be improved by consensus meetings [88]. In many nodules, even for specialists, it is difficult to discern microcalcifications from frequent similar findings in benign nodules such as colloidal spots, small macrocalcifications, scars, and ultrasound artifacts resulting from tiny membranes/crystals, etc. (Fig. 4.11).

A taller-than-wide shape of a nodule is defined by a nodule growth more into the depth than into the width on axial imaging. In some settings, this configuration is referred to as "non parallel orientation" in relation to the shape of the thyroid lobe. This antiparallel orientation has been associated with malignant growth [9]. Recently, however, it has been shown that up to 17% of benign nodules also show a taller-than-wide shape. It could be demonstrated that such benign nodules while growing often follow a dorsal protrusion of the thyroid lobe (e.g., Zuckerkandl's tubercle). In this regard, they are still parallel with respect to the anatomically given preconditions (Fig. 4.12). A pole concept of nodule growth (Fig. 4.13) was introduced allowing to exclude the vast majority of taller-than-wide nodules from FNAC [89].

The different US-RSSs are divided into score-based (i.e., ACR TI-RADS and Kwak TIRADS), pattern-based (Horvath TIRADS, ATA Guideline), and mixed systems (EU-TIRADS, K-TIRADS). In combination with the size of the thyroid nodule, a recommendation for the next diagnostic steps is provided (i.e., FNAC or follow-up by ultrasound) [10, 11, 83, 84, 90, 91]. Many studies have investigated the diagnostic performance of the systems and all have been shown to be useful for risk stratification [92–95]. Migda et al. investigated the diagnostic performance of Kwak TIRADS in their meta-analysis including four retrospective and two prospective studies. They found sensitivities, specificities, and diagnostic odds ratios (DOR) of 97–99% (pooled sensitivity 98%), 16–91% (pooled specificity 55%), and 12–372 (pooled DOR 51) [96]. There are significant differences regarding the recommendation for FNAC. In this point, ACR TI-RADS seems to be superior compared to other systems [95, 97]. However, there are limitations that must be considered when using TIRADS. These include the missing integration of TS for functional assessment of the nodules (see below), the varying performance in different histologic subtypes of thyroid cancer (e.g., poor

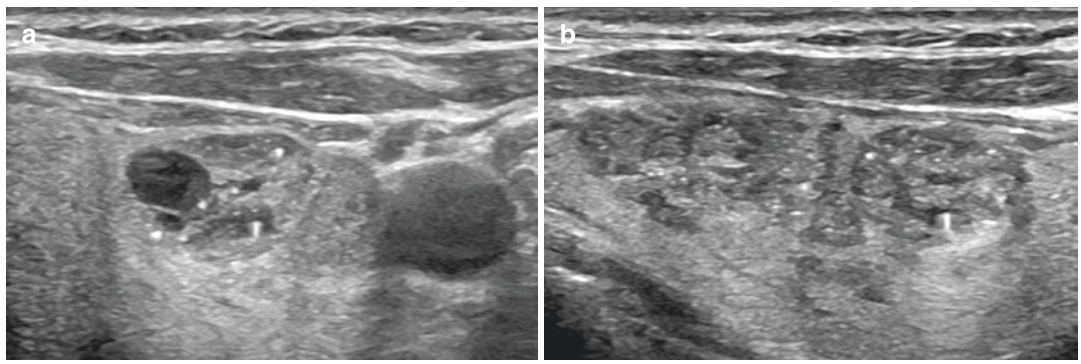

Fig. 4.11 (**a**, **b**) This nodule in the left thyroid lobe (**a**) shows signs of benignity such as a cystic portion >10% and a predominantly isoechogenic appearance of the solid component. However, it shows echogenic foci which may not readily allow discrimination from microcalcification. Whereas most of the foci exhibit no dorsal ultrasound phenomena one such focus does show (a clear dorsal reverberation artifact ("comet tail") classifying it as a benign colloidal spot. The localization within a small cystic collection underlines the colloidal nature. With this spot in mind, the other echogenic spots in this nodule and in further nodules in the same lobe (**b**) should also be classified as most probably colloidal/benign. Otherwise, classification of such tiny hyperechoic foci may be difficult

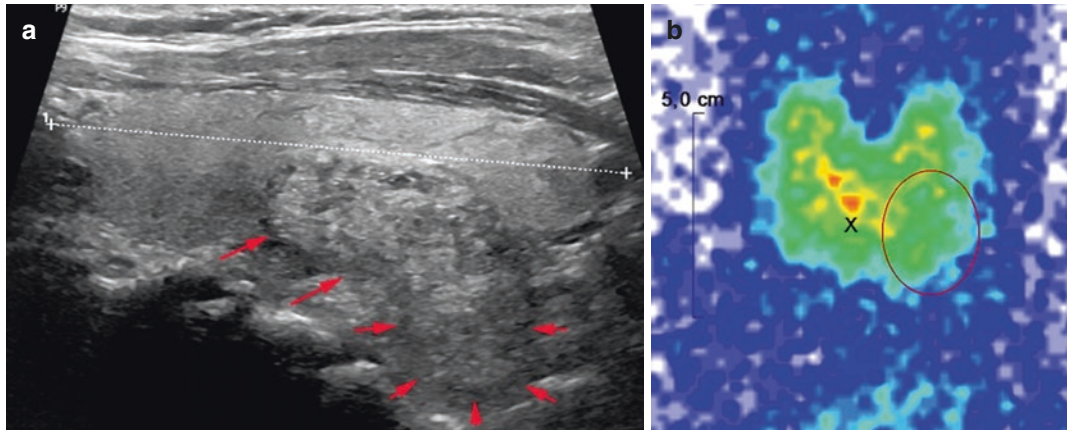

Fig. 4.12 (**a**, **b**) This large nodule in the left lobe is solid, echonormal, without calcifications, and well circumscribed. Its lower part grows toward a posteroinferior direction making it taller than wide (1.6 cm × 2.5 cm, red arrows). Formally, the nodule shows two signs of malignancy (solidity and taller-than-wide shape) and should undergo FNAC. However, the posteroinferior direction of growth is typical for nodules at the posterior surface of the thyroid rendering this feature non-suspicious in this case. At a primary care center, one single sign of malignancy generally does not justify FNAC. Nevertheless, this hypofunctioning (**b**, ^{99m}Tc-pertechnetate scintigraphy) nodule underwent FNAC. FNAC was unremarkable showing regressive changes of otherwise normal follicular epithelium (Bethesda II)

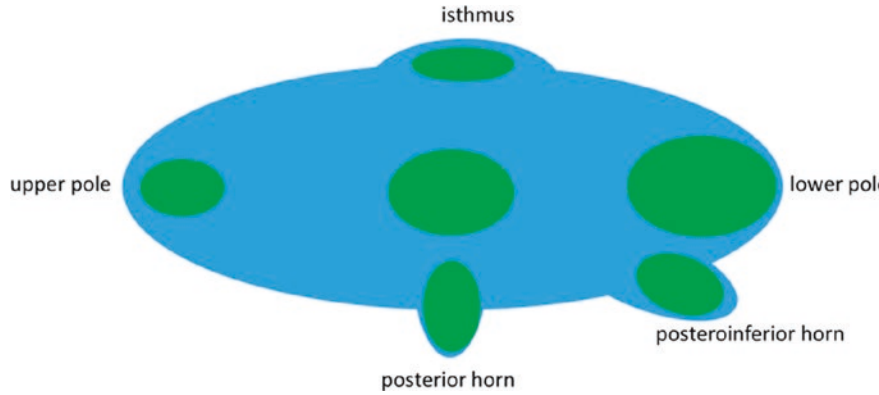

Fig. 4.13 Pole concept of goiter growth. Nodule growth follows the shape of the respective pole. A taller-than-wide configuration of nodules at a posterior or posterior/inferior horn should not be regarded as a suspicious feature without further hints of malignancy. Schematic depiction of nodule growth along the pole model

performance for follicular thyroid cancer), and interobserver variability (see above) [33, 88, 98].

As a complementary method, UE could help with risk stratification of thyroid nodules (Fig. 4.14). In their meta-analysis that included 14 prospective and one retrospective studies, Lin et al. reported sensitivity, specificity, positive predictive value (PPV), and negative predictive value (NPV) for quantitative elastography (SWE and ARFI) of 84%, 88%, 28–45%, and 98–99% [99]. For the group of thyroid nodules with indeterminate results on FNAC, a meta-analysis on a total of 486 thyroid nodules from eight studies showed pooled sensitivity of 69%, specificity of 75%, PPV of 63%, and NPV of 82%, respectively. Thus, the accuracy of elastography appears to be lower for this subset of nodules, but the number of cases was very small [100]. The crucial parameter for the use of UE is the high NPV for a soft nodule, both for qualitative and quantitative elastography. Proper performance of the respective method for UE and knowledge of the

underlying technical principles and limitations is essential. Typical limitations for UE are:

- Presence of calcifications
- Cystic changes (fluid is not compressible)
- Unfavorable location of the nodule (i.e., dorsal position of the thyroid nodule)

Another limitation is—comparable to TIRADS—that follicular thyroid cancer may be soft on UE and therefore lead to false negative results [21]. When comparing different elastographic methods, SWE proves to be less operator-dependent than SE in most studies [4, 20]. With CEUS, the enhancement of ultrasound contrast

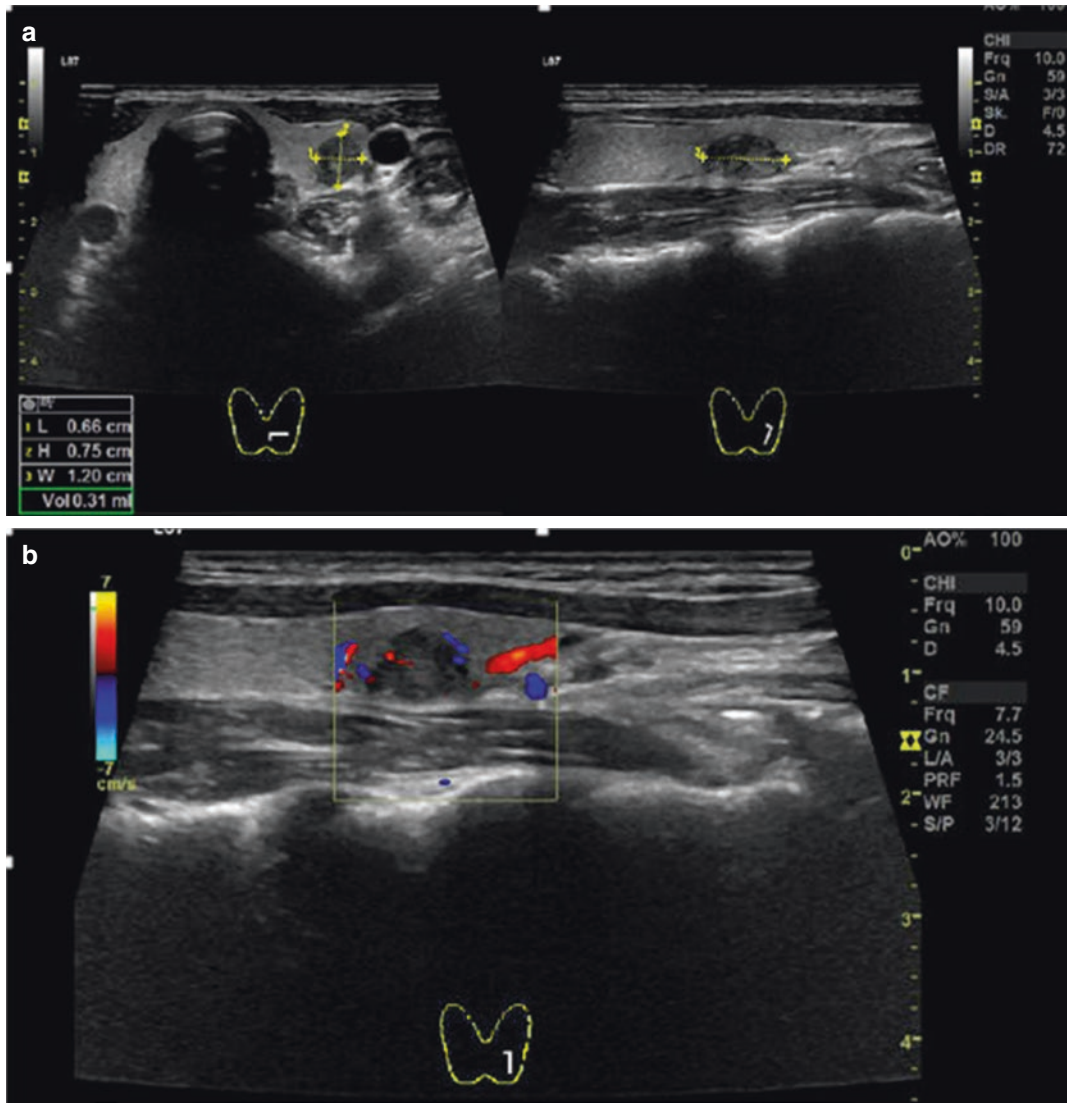

Fig. 4.14 (**a**–**d**) Twenty-seven-year-old female patient, TSH 1.18 mU/L, Calcitonin <1.0 pg/mL; (**a**) B-mode sonography (left: transverse orientation; right: longitudinal orientation) shows a solitary thyroid nodule in the lower left lobe (7 × 8 × 12 mm). EU-TIRADS 5 (hypoechoic and solid composition, taller-than-wide configuration). (**b**) Color Doppler ultrasound of the thyroid nodule shows no hypervascularization; (**c**) Strain elastography shows homogeneous green (soft) normal thyroid tissue and blue (hard) thyroid nodule. (**d**) ^{99m}Tc-pertechnetate scintigraphy shows a reduced tracer uptake in the lower left lobe (i.e., hypofunctioning thyroid nodule). Fine-needle aspiration cytology was non-diagnostic (Bethesda I). Histology revealed papillary thyroid cancer (pT1b pN0)

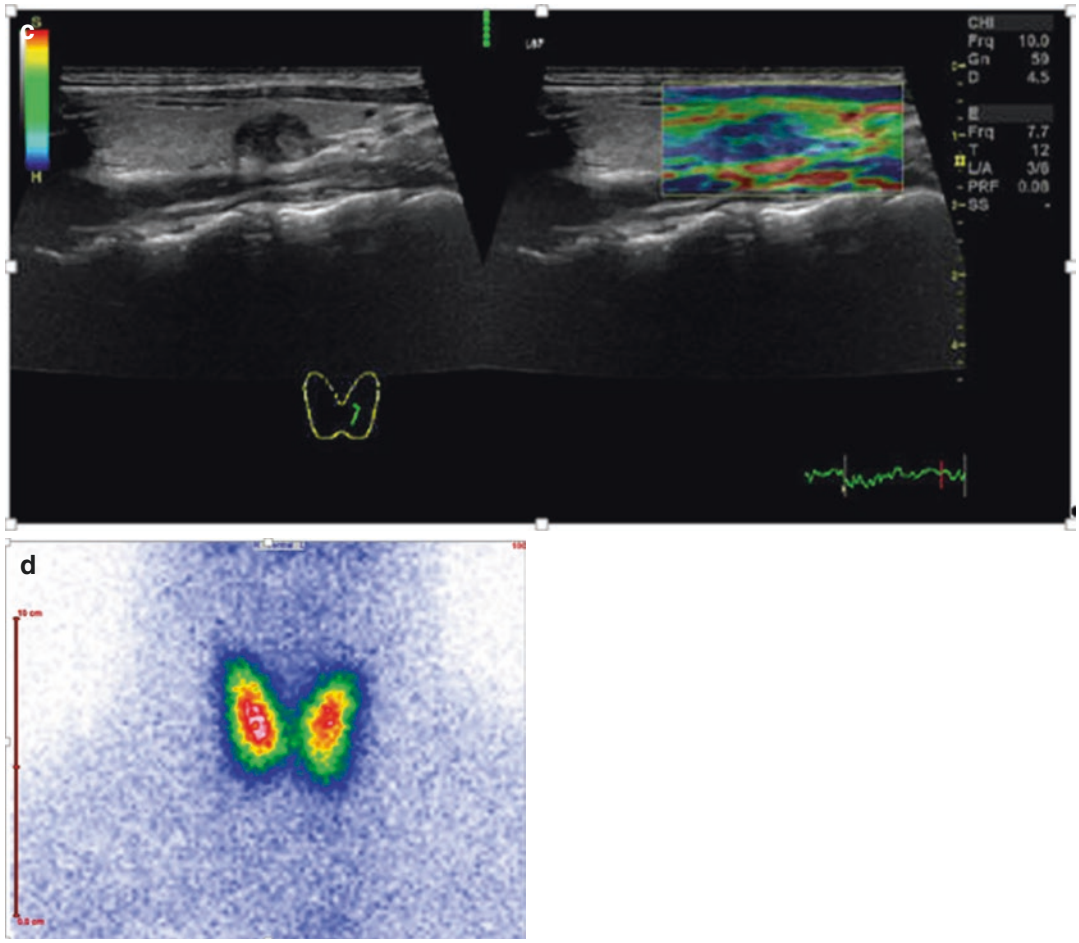

Fig. 4.14 (continued)

agent in the thyroid nodule compared to the paranodular tissue can be described. The qualitative parameters of enhancement include intensity, homogeneity, as well as retention of the contrast agent. Hypoenhancement (sensitivity 82%, specificity 85%, accuracy 84%) and a heterogeneous pattern (sensitivity 88%, specificity 93%, accuracy 90%) as well as early arterial central washout are suspicious for malignancy. The hypoenhancement of malignant nodules goes back to a lack of blood supply because of necrosis and embolus formation within the tumor. A ring enhancement pattern (sensitivity 83%, specificity 94%, accuracy 89%) is suggestive of a benign thyroid nodule. Additionally, quantitative parameters are evaluated including time-intensity curves using a region of interest in the thyroid nodule and comparison to the adjacent thyroid tissues [3, 101, 102]. Trimboli et al. included 1515 thyroid nodules with preoperative CEUS in their systematic review and meta-analysis. For the quantitative methods, the pooled sensitivity and specificity were found to be 85% and 82%, respectively, the pooled PPV was 83% and the NPV 85% [103]. Although performed as a single-center study, the results of a study by Xu et al. combining TIRADS and CEUS are promising in highly preselected cohorts (sensitivity 91%, specificity 90%, PPV 93%, and NPV 87%) [104]. However, to date no single feature has been found to be sufficiently sensitive or specific and CEUS is still an active field of research [101].

4.2.2.2 Value of ^{99m}Tc-Pertechnetate/$^{123}I^-$Scintigraphy

TS, in many guidelines, is no longer a mandatory part of assessing the malignancy risk of a thyroid nodule. Notably, ATA guidelines from 2015 mention TS as an auxiliary but not mandatory tool only in nodules accompanied by a low or lowered TSH [83]. The purpose of TS in such a setting is to virtually rule out malignancy in cases where a nodule is found to be hyperfunctioning on scintigraphy. However, in other countries (e.g., Germany), TS is recommended for all thyroid nodules at ≥1 cm in diameter [36]. How are these differences explicable regarding the purpose of TS? The answer may be found in epidemiologic statistics.

A merely ultrasound-based preselection of thyroid nodules for FNAC is derived from studies with a carcinoma-to-nodule ratio as high as 1:6 [84, 90]. Assessment by FNAC is recommended once a certain malignancy risk can be expected (i.e., PPV), e.g., 2–10% [ultrasound risk category 4a according to Kwak] or 7% [ultrasound risk category 4a according to Horvath]. At institutions with an a priori risk as high as above (1:6), e.g., at tertiary care units, such an ultrasound routine for FNAC preselection results in a reasonably low absolute number of false positive FNAC results (specificity 60–70%) and thus unnecessary surgeries. This is attributable to the rather high predictive values for malignancy of the ultrasound threshold used for indications for FNAC in such settings. In addition, the high sensitivity of FNAC (>90%) would prevent from overlooking a relevant number of thyroid carcinomas. In a non-preselected population, however, carcinoma-to-nodule ratios are as low as 1:1000 [49]. Recalculating the PPV of ultrasound risk category 4a according to Kwak, yields a value as low as roughly 1–2 per thousand for such low risk-settings, i.e., by a factor 20 or more lower as compared to the values from the original study. In such low-risk settings, adopting ultrasound thresholds for FNAC from the above studies with high risk would result in an overwhelming majority of the selected nodules being benign. According to the rather low specificity of FNAC, there would be a great number of unnecessary surgeries, e.g., about 200 per carcinoma vs. 3 per carcinoma in the above study settings. As a consequence, one would be urged to adjust ultrasound criteria toward a more restrictive application in order to reduce unnecessary surgeries but this, in turn, would increase the number of thyroid carcinomas being overlooked. For this reason, in primary care units, the preselection of thyroid nodules by ultrasound alone appears to be suboptimal. TS is necessary to rule out a significant percentage of thyroid nodules (about 25% in Germany) from further diagnostic work-up by the finding of a hyperfunctioning nodule. Such AFTNs harbor a negligible malignancy risk and generally need no cytological or histological examination [28]. In particular, as described previously, AFTNs can present with intermediate or highly suspicious ultrasound features. In the prospective study by Schenke et al., 58% of the AFTNs in the subgroup of euthyroid patients were classified as intermediate (4B) and high risk (4C, 5) according to Kwak TIRADS [33]. Although the rate of AFTNs in the cohort of 1029 euthyroid thyroid nodules retrospectively examined by Noto et al. was low (5% of all nodules), the rate of recommended FNAC for AFTNs for ATA guidelines, EU-TIRADS, and ACR TI-RADS was remarkable (64.7%, 43.1%, and 25.5% respectively). Also, none of the ultrasound features studied was associated with hyperfunctionality, emphasizing the importance of TS as a complementary diagnostic procedure in the diagnostic algorithm [105] (Fig. 4.15).

Even the exclusion of 25% of thyroid nodules from FNAC by identifying AFTNs on TS cannot profoundly reduce the number of unnecessary surgeries when adopting ultrasound criteria from a setting with high risk to a setting with low risk of malignancy. For this reason, TS has long been used in low-risk settings not only to rule out hyperfunctioning nodules but also to rule in hypofunctioning thyroid nodules for further work-up by FNAC. In nodules ≥1 cm in diameter, the sensitivity of a hypofunctioning nodule for malignancy is more than 80% [106]. The addition of a hypofunctioning nodule as a reason for FNAC thus compensates for the loss of sensi-

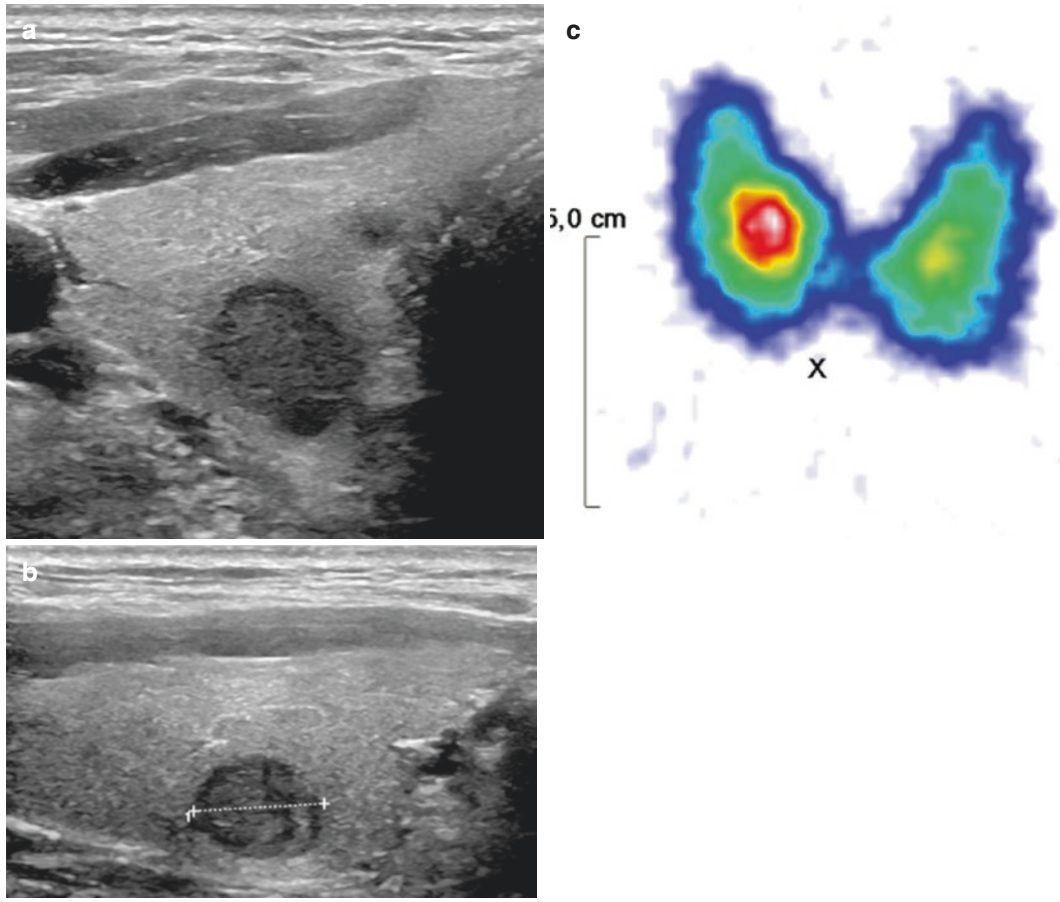

Fig. 4.15 (**a**–**c**) This 60-year-old man has a solitary hypoechoic and solid nodule (10 × 11 × 12 mm) in the dorsal right thyroid lobe (**a**). The configuration of the nodule is slightly taller than wide which may be triggered by the gross protrusion of the thyroid lobe toward the back (**b**, EU-TIRADS 5). Formally, this nodule exhibits three of five ultrasound risk factors making FNAC necessary. However, on TS, the nodule is hyperfunctioning compared to the surrounding tissue (**c**) indicating an AFTN and obviating the need for FNAC. TSH was at 0.8 mU/L× meaning no functional relevance of the autonomy. The non-suppressed TSH as well as a normal normalized uptake (1.6% per mU/L TSH) are plausible owing to the small volume of the nodule and the only slightly elevated uptake therein

tivity by a more restrictive use of ultrasound criteria. The finding of a hypofunctioning nodule, however, in conjunction with substantial cystic proportion should not per se lead to FNAC, since such a finding is readily explicable by the missing uptake in the fluid and thus has no predictive value.

4.2.2.3 Value of MIBI Imaging

Many studies have shown that an absent/low MIBI uptake in hypofunctioning thyroid nodules as well as a high washout of MIBI in semiquantitative analyses are predictive of a benign finding (high NPV) [40, 107]. On the other hand, if a higher uptake of MIBI in a nodule is detected, surgery is recommended to exclude malignancy; but, overall specificity is low, especially for unselected thyroid nodules [42]. To increase specificity it is recommended to select thyroid nodules for MIBI imaging by sonographic appearance (i.e., TIRADS intermediate or high-risk nodules), functional status (exclusion of AFTNs), and FNAC (i.e., indeterminate results) [41, 43, 108]. In a very recent study, the diagnostic performance of MIBI imaging was analyzed at 12 European study sites. The authors included

365 hypofunctioning thyroid nodules, that were classified as intermediate-risk (38%) or high-risk (62%) according to EU-TIRADS and had indeterminate results on FNAC. MIBI imaging evaluation was performed visually and semiquantitatively. As a main result of the study, the authors stated that a negative result on visual image evaluation can rule out malignancy with a very high probability (NPV 96% on planar and SPECT imaging). Additionally, the semiquantitative approach can improve the overall diagnostic performance by providing a more accurate differentiation between malignant and benign thyroid nodules (cutoff -19%: sensitivity 100%, specificity 89%, PPV 82%, NPV 100%, ACC 93%) [109] (Fig. 4.16).

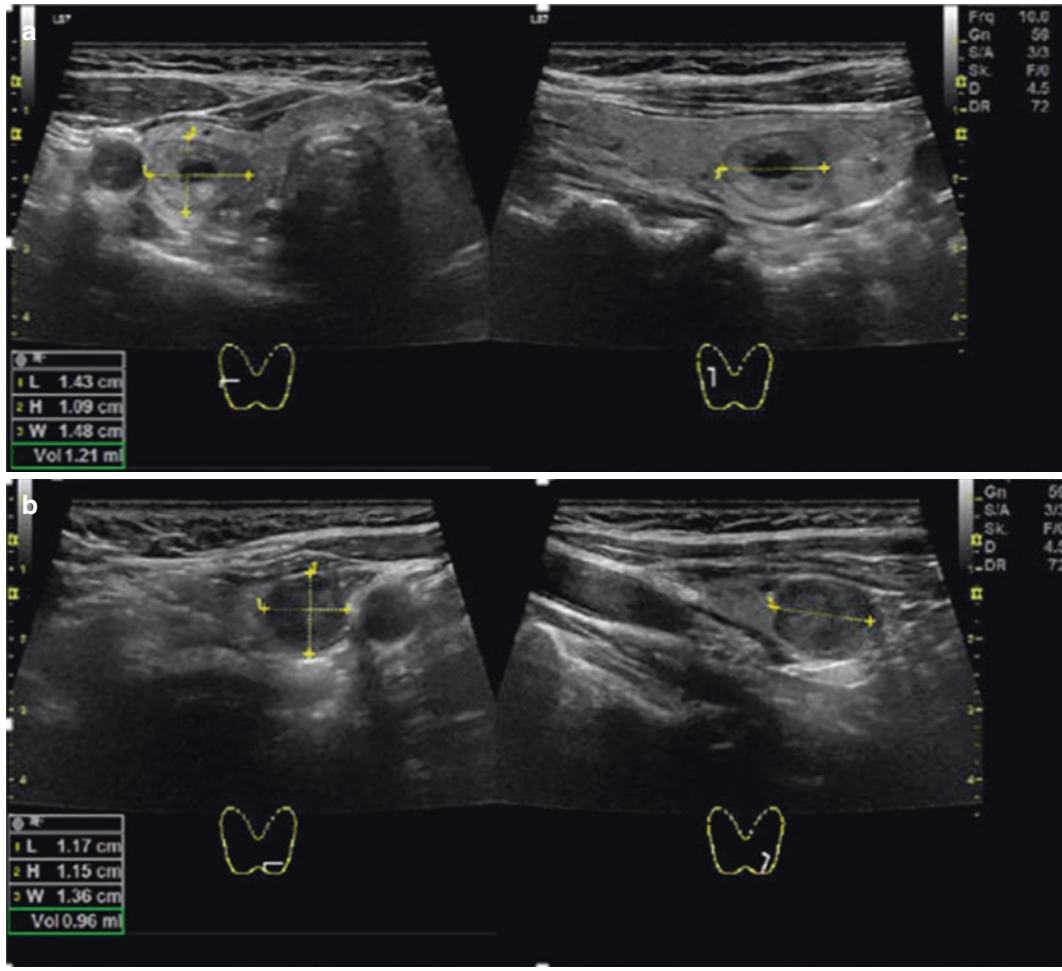

Fig. 4.16 (**a**–**c**) A 59-year-old female patient with multinodular goiter, TSH 0.50 mU/l, Calcitonin <1.0 pg/ml. (**a**) B-mode sonography showed two thyroid nodules (upper images: right central lobe, 14 x 10 x 15 mm, EU-TIRADS 3; lower images: left lower pole, 12x12x14 mm, EU-TIRADS 4). (**c**) ^{99m}Tc-pertechnetate scintigraphy with 64 MBq, both thyroid nodules were identified as hypofunctioning (black circles). (**d**) MIBI imaging: planar early image (left, 10 minutes p.i.) and late image (right, 60 minutes p.i.) show MIBI uptake in the thyroid nodule in the left lobe that visually decreases with time. Semiquantitative analysis reveals a washout index of −28% (MIBI negative). Note: The thyroid nodule in the right lobe is visually MIBI negative in the early and late images. Surgery revealed benign multinodular goiter

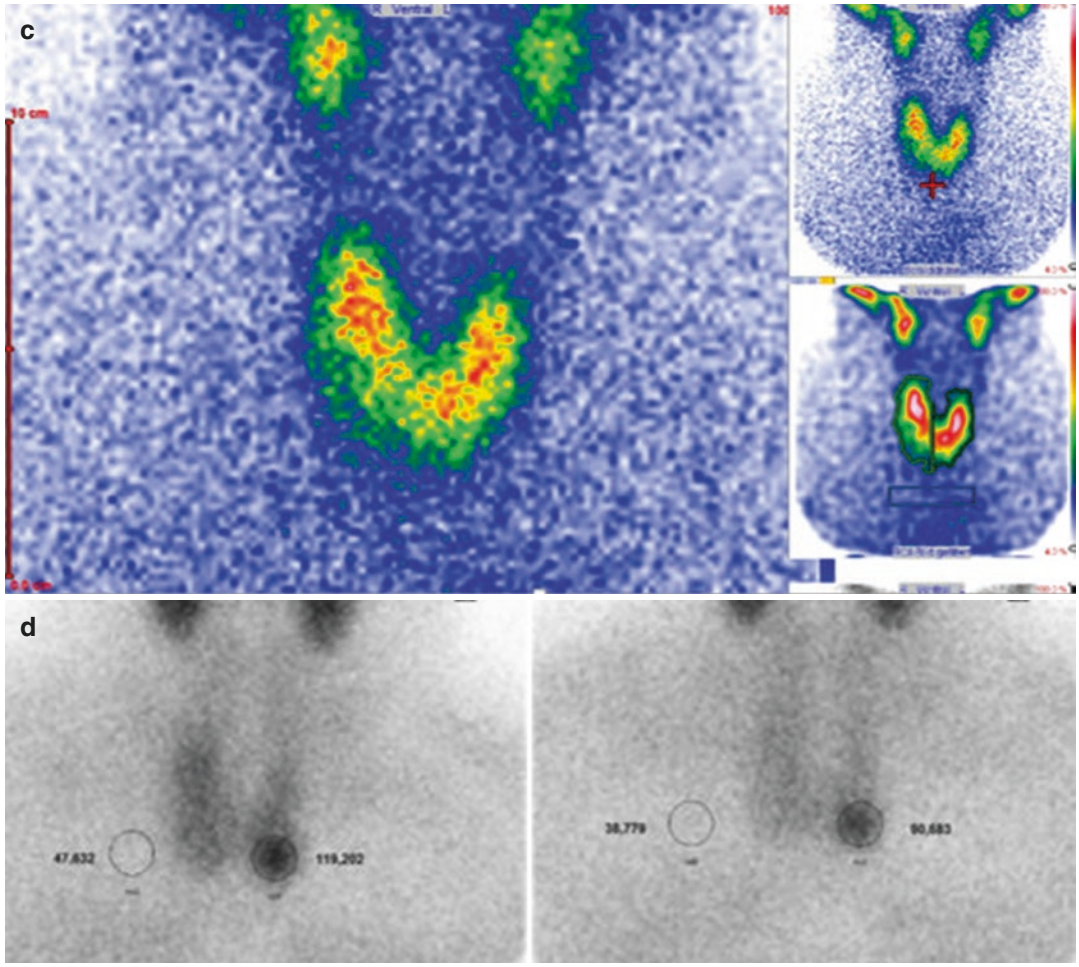

Fig. 4.16 (continued)

4.2.2.4 Incidental Focal Uptake on ^{18}F-FDG Imaging

Focal thyroid incidental FDG uptake (FTI) is detected in 1–2% of patients and defined as an incidentaloma which is in contrast to diffuse uptake associated with a high risk of malignancy ranging 20–40%. A meta-analysis with 34 studies and 215,057 included patients showed a pooled risk of malignancy of 36.2% and a prevalence of FTI of 1.9%. No significant differences among iodine-deficient or iodine-sufficient countries and various geographic regions were found [110]. A systematic review of 125,754 patients without known thyroid disease had an unexpected focal hypermetabolic activity in 2.1%. Approximately one in three (~35%) revealed thyroid malignancy with a higher standardized uptake value (SUV) in malignancies compared to benign nodules (6.9 ± 4.7 vs. 4.8 ± 3.1, $p < 0.001$) [111]. SUV may be helpful in predicting malignant versus benign histology but in clinical settings a reliable discrimination is not always possible. Therefore, an ultrasound exam is recommended for patients with new focal thyroid lesions on ^{18}F-FDG-PET to further assess thyroid tissue, depending on clinical and prognostic contexts. In this case, nodules ≥1 cm with focal ^{18}F-FDG uptake require further work-up and nodules <1 cm should be monitored like thyroid nodules with a high-risk pattern in sonography [83, 112]. We suggest performing TS with ^{99m}Tc-pertechnetate or $^{123}I^-$ to detect AFTNs, rule out

malignancy with a NPV of 96-99% [28], and preselect for FNAC. Additionally, in hypofunctioning nodules molecular imaging with ^{99m}Tc-MIBI may be useful in discriminating malignant from benign nodules.

4.2.2.5 Thyroid Nodules with Indeterminate Cytology

The management of cytologically indeterminate nodules represents a dilemma for thyreologists. The term indeterminate nodule summarizes the results of the FNAC for Bethesda categories III and IV [113]. On the one hand, a 15–40% risk of nodule malignancy leads to overtreatment in most patients when hemithyroidectomy is performed including the risk of operative complications. On the other hand, a conservative management is associated with a residual risk for malignancy. In recent years the utility of ^{18}F-FDG-PET was examined in predicting the correct diagnosis of nodules with indeterminate cytology. The rationale for using the glucose analog FDG is that most malignant tumors characteristically have increased glucose utilization. This is in part related to the overexpression of GLUT glucose transporters and increased hexokinase activity.

In one recent systematic review and meta-analysis which included 225 patients a pooled sensitivity, specificity, PPV, NPV, and accuracy of 95%, 48%, 39%, 96%, and 60% were shown, respectively. Specifically, in patients who had nodules >15 mm sensitivity increased to 100%. A negative ^{18}F-FDG-PET/CT examination can improve diagnostic accuracy in these patients and can reliably exclude T2 thyroid malignancies [114]. Vice versa, an ^{18}F-FDG-PET-positivity did not identify malignant nodules with sufficient certainty, as approximately 50% of these patients had benign lesions. A prospective study in 87 patients compared the preoperative accuracy of ^{18}F-FDG-PET/CT, ultrasound, and ^{99m}Tc-MIBI scan for thyroid nodules with indeterminate cytology. The authors showed that overall sensitivity (94%) and NPV (98%) were significantly higher than with ultrasound and ^{99m}Tc-MIBI imaging. Therefore, a negative ^{18}F-FDG-PET/CT correctly predicts benign nodules and could prevent unnecessary (hemi)thyroidectomies. As in previous studies, ^{18}F-FDG-PET/CT showed a low PPV (37%). Consequently, ^{18}F-FDG-positive nodules should undergo (hemi)thyreoidectomy with histopathological confirmation [115]. Currently, ^{18}F-FDG-PET/CT for preoperative risk assessment shows promising results but needs further evaluation and is not routinely recommended for cytologically indeterminate nodules.

In another preoperative comparison study in hypofunctioning thyroid nodules, in a limited number of patients (n = 23) with larger thyroid nodule size (median 32 mm diameter), a similar NPV and the same sensitivity in detecting malignant nodules was shown for ^{18}F-FDG-PET/CT and MIBI scans. The authors suggest that ^{18}F-FDG-PET/CT imaging is not superior to ^{99m}Tc-MIBI scintigraphy in differentiating thyroid nodules. For the reasons of costs and availability MIBI should thus be the first choice in preoperative evaluation of hypofunctioning thyroid nodules complementary to FNAC [116].

4.2.3 Medication-Induced Thyroid Dysfunction

The antiarrhythmic drug amiodarone is iodine-rich (a single 200 mg tablet contains 75 mg bound iodine and 7 mg free iodine) and lipophilic, thus accumulating in the thyroid gland. It causes thyroid dysfunction in 15–20% of treated patients: amiodarone-induced thyrotoxicosis (AIT), type 1 is an iodine-induced thyrotoxicosis in patients with promoting underlying thyroid abnormalities. Type 2 is a destructive thyroiditis with prolonged hormone liberation and mixed type. Type 1 is typically found in iodine-deficient areas whereas amiodarone-induced hypothyroidism, AIH, is more frequent in iodine-rich areas (Table 4.5).

Differentiation of the type of AIT is important because of the different treatments (Antithyroid drugs vs. oral glucocorticoids) [117, 119, 120]. Besides the laboratory findings, both, ultrasonography and nuclear medicine imaging have been used to confirm the diagnosis of amiodarone-

Table 4.5 Amiodarone-associated thyroid disorders [44, 117, 118]

	Amiodarone-induced thyrotoxicosis (AIT) 1	Amiodarone-induced thyrotoxicosis (AIT) 2	Mixed form of AIT 1/2	Amiodarone-induced hypothyroidism (AIH)
Laboratory constellation	Thyrotoxicosis, thyroid antibodies may be present	Thyrotoxicosis, usually no thyroid antibodies	Thyrotoxicosis	Hypothyroidism, thyroid antibodies may be present
Mechanism	Productive	Cytotoxic effects of amiodarone and its metabolites	Productive and destructive	Wolff-Chaikoff effect (no "escape"), loss of parenchyma
Thyroid uptake scintigraphy	Low, moderate, increased	Low to absent	Low	Low to absent
MIBI imaging	Positive	Negative	Variable	Negative
Color Doppler ultrasound	Present, pattern 1-3	Absent, pattern 0	Variable	Absent, pattern 0
B-mode sonography	Underlying thyroid disease (nodular goiter, Graves' disease)	Normal thyroid tissue	Underlying thyroid disease/ normal	Preexisting chronic thyroiditis/normal

associated thyroid dysfunctions. AIH often occurs in patients with preexisting chronic autoimmune thyroiditis according to typical structural changes on ultrasound. However, a normal appearance on ultrasound may be present. In AIT type 1 underlying (latent) GD or nodular goiter can be detected in thyroid ultrasound whereas AIT type 2 often presents with normal thyroid tissue [117]. Additional CDUS can be helpful by specifying different patterns of blood flow. Pattern 0 (absent vascularity) is associated with AIT type 2, and pattern 1 (uneven patchy parenchymal flow), 2 (diffuse, homogeneous distribution or increased flow, similar to GD), or 3 (marked increased signal and diffuse homogeneous distribution) are typically associated with AIT type 1 [121]. TS with ^{99m}Tc-pertechnetate mostly shows low or absent uptake owing to the high intrathyroidal content of iodine ("autoregulation"). In type 1 AIT, occasionally, there may be appreciable or normal uptake reflecting the underlying disease [117]. In case of unclear findings, molecular imaging with ^{99m}Tc-labelled MIBI can be used. This lipophilic cation complex accumulates in the mitochondria of viable cells and thus in hyperfunctioning thyroid tissue, i.e., toxic nodular goiter and GD, whereas MIBI uptake is reduced in type 2 destructive thyroiditis (Piga et al. 2008, Pattison et al. 2014). In their study of 20 patients with AIT, Piga et al. identified the visual MIBI uptake as the only method to differentiate AIT type 1 from AIT type 2 [44]. A more operator-independent method was published in 2018 by Censi and colleagues. They calculated a target-to-background ratio with a cut-off of 0.482 to differentiate AIT type 1 (> 0.482) from AIT type 2 with a specificity of 100% and a sensitivity of 91.7% [122].

Targeted cancer therapies with immune-checkpoint inhibitors (ICIs) and tyrosine kinase inhibitors (TKIs) play an important role in the therapy of various malignancies. However, during therapy, immune-related adverse effects (irAEs) are common including endocrine disorders (10%). Thyroid dysfunction is the most common endocrine irAE. The overall incidence of primary hypothyroidism and hyperthyroidism is reported as 8% and 3%, respectively. Typically, inflammatory destructive thyroiditis is the most common manifestation with an initial thyrotoxicosis followed by a hypothyroid phase. In rare cases, ICIs and TKI can cause autoimmune-mediated GD, also presenting with thyrotoxicosis in the initial course of the disease. Besides the typical course of thyroid dysfunction, thyroid ultrasound, and TS can help in the differential diagnosis, especially in cases with negative Trab (PD-1 inhibitors). Comparable to other causes of thyroiditis, the CDUS and ^{99m}Tc-pertechnetate uptake is decreased in the destructive form, whereas it is increased in autoimmune-mediated GD. CTLA-4 inhibitors are known to cause an inflammation of the pituitary gland (hypophysi-

tis) that can lead to secondary hypothyroidism with the typical laboratory constellation of a low/normal TSH and low free T4. Also, hypophysitis and thyroiditis can be detected by ^{18}F-FDG-PET/CT showing diffusely increased uptake that could serve as a surrogate prognostic marker during ICI and TKI treatments [123–127].

4.2.4 Aberrant Localization of Thyroid Tissue and Congenital Hypothyroidism

During embryonic development, the thyroid gland arises from endodermal tissue at the pharyngeal floor [128]. It subsequently descends through the foramen cecum at the tongue base, following the anterior trachea before ultimately separating into two lobes. Anywhere along this passage—the so-termed thyroglossal duct—ectopic thyroid tissue can persist. This may present as minimal cellular remnants detectable by scintigraphic imaging only or a macroscopic pyramidal lobe on structural imaging. More rarely cervical cysts remain patent along the thyroglossal duct baring the possibility of benign or malignant thyroid tissue growth over time. Embryonic remnants of thyroid cells at the tongue base can give rise to lingual struma clinically presenting with globus sensation and swallowing complaints in affected patients.

Occasionally, thyroid tissue may be found outside of its ontogenetic path. To make a distinction, such thyroid tissue is referred to as *dystopic* throughout this chapter as compared to *ectopic* tissue within the ontogenetic path and to *orthotopic* location of the thyroid gland next to the second to fifth tracheal ring. Dystopic thyroid tissue often occurs just below the lower poles of any of both thyroid lobes and may easily be overlooked on ultrasound. It is often nodular in nature and may be connected to the lower pole by a fibrous band. Ontogenetically, such dystopic tissue can be considered as having descended too far. It is frequently encountered in the upper anterior but also in the middle mediastinum and may give rise to intrathoracic goiter [129]. Dystopic intrathoracic goiter must be distinguished from extensive downward growth of an a priori orthotopic multinodular goiter. Both, bulky retrosternal goiter (arising from orthotopic goiter) as well as dystopic intrathoracic goiter may impair tracheal, esophageal, or vascular passage. However, as their blood supply differs, retrosternal goiter most often can be removed by a cervical approach, whereas intrathoracic goiter often requires sternotomy.

Rarely, dystopic thyroid tissue may be found within the trachea, within the heart, below the diaphragm or at other sites [130, 131]. Particular ontogenetic incidents may be causative, e.g., dislocation of thyroid cells during separation of the thyroid gland (see above) into the trachea or carriage of thyroid cells within the cardiac precursor tissue.

$^{123}I^-$ is the radionuclide of choice when ectopic or dystopic thyroid tissue is suspected. Due to superior properties such as higher gamma energy (159 keV) compared to ^{99m}Technetium (140 keV), $^{123}I^-$ allows for better penetration of osseous structures and detection of retrosternal, intrathoracic and abdominal thyrogenous masses (Fig. 4.17). Sensitivity and specificity of scintigraphy increase if SPECT/CT hybrid imaging is available for anatomic correlation and attenuation correction [132]. Once sufficient iodine uptake to benign lesions is detected, radioiodine therapy is a therapeutic option. Successful treatment of both retrosternal and lingual strumae has been carried out with radioiodine therapy [133, 134]

Further rare localization of thyroid tissue may be present in ovarian struma. First described by Boettlin et al. in the late nineteenth century, struma ovarii is classified as a rare form of mature teratoma with a predominant fraction of thyroid tissue on histologic assessment. Struma ovarii is mostly detected as an incidental finding after resection of a clinically manifest ovarian mass, in some cases incidental uptake to the ovary is seen in patients undergoing radioiodine therapy for differentiated thyroid cancer. Since up to 5% of all ovarian strumae exhibit features of malignancy histological work-up is warranted [135].

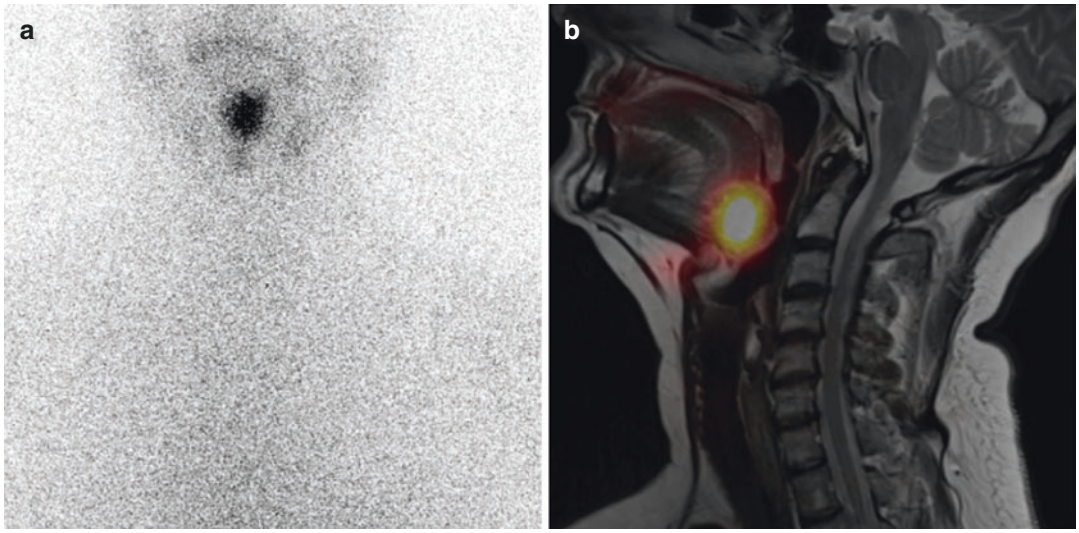

Fig. 4.17 $^{123}I^-$ imaging; (**a**) planar image from anterior, (**b**) SPECT+MRI fusion image showing intense iodine uptake to a benign lingual struma in a 49-year-old patient presenting with swallowing complaints (after having undergone total thyroidectomy for multinodular goiter). The patient underwent partial tongue ground resection and radioiodine therapy

Congenital hypothyroidism is a heterogeneous disorder that can present with either eutopic, dystopic, or dysplastic thyroid tissues. Early diagnosis and treatment are essential to maintain regular neurological and cognitive development in affected infants [136]. Neonatal $^{123}I^-$ scintigraphy can be used to localize functional thyroid tissue in clinically suspected cases. Absent uptake is seen in thyroid aplasia, necessitating lifelong hormone substitution therapy. If $^{123}I^-$ uptake indicates the presence of thyroid tissue, congenital hypothyroidism can remain in a transient state [137].

4.2.5 Tracers Beyond ^{18}F-FDG—Present and Future Directions

In some challenging cases, traditional radiotracers may fail in detecting the presence and extent of disease. Beyond ^{18}F-FDG there are several other PET tracers available, which have been studied and described (Table 4.6). For their use in thyroid nodule risk assessment, there are almost only case reports or studies with a small number of patients.

Table 4.6 Overview of potential PET radiopharmaceuticals in thyroid diseases and their measured effects

PET tracer	Measured effect
^{18}F-fluorodeoxyglucose (FDG)	Aerobic and anaerobic glycolysis, glycolytic metabolism
^{124}I	Iodine kinetics, NIS expression
^{18}F-tetrafluoroborate (TFB)	NIS expression
^{18}F-SiTATE, ^{68}Ga-DOTA-X, ^{64}Cu-DOTA-X in-111-octreotide, ^{68}Ga-somatostatin receptor antagonists	Somatostatin receptor status
^{18}F-fluorodihydroxyphenylalanine (F-DOPA)	Dopamine synthesis, natural amino acid transport
^{18}F-PSMA, ^{68}Ga-PSMA	Prostate-specific membrane antigen
^{11}C-choline, ^{18}F-fluorocholine	Cell membrane metabolism, tumor cell proliferation
^{18}F-FAPI, ^{68}Ga-FAPI	Tumor-associated fibroblast-activated protein

However, the vast expanse of tumor microenvironment provides even more opportunities to exploit several other pathways. The relevant radiopharmaceuticals are listed in Table 4.6. Most PET radiopharmaceuticals are used for the detection of residual disease in malignancy and not for primary risk stratification.

$^{124}I^-$ emits positrons and allows PET/CT or PET/MRI imaging in high resolution and for quantification. It is used as a diagnostic tool to localize disease and also for dosimetry which can be carried out for each individual tumor or metastatic focus without stunning effects [138].

The superiority of low-activity ^{124}I-PET/low-dose CT in functional–morphological assessment of thyroid nodules has been recently showed. A multiobserver study to investigate ^{124}I-PET/Ultrasound fusion imaging demonstrated more hyper- and hypofunctional nodules and less indifferent or not ratable nodules with additional use of ^{124}I-PET/Ultrasound together with conventional imaging vs. using conventional imaging only (ultrasound, TS, and laboratory parameters). The authors showed a significantly lower suggestion of follow-up and more proposals of invasive treatments, e.g., FNAC and surgery [139]. ^{124}I-PET/Ultrasound fusion improves the accuracy of the functional assessment of thyroid nodules even in unfavorable localizations and thus influences the suggested treatment for patients with ambiguous findings in conventional diagnostics.

^{18}F-tetrafluoroborate (^{18}F-TFB) is a promising iodide analog for PET imaging and has been recently proposed as a novel PET tracer for human NIS imaging [140]. ^{18}F-TFB is retained but shows no thyroid organification. Therefore, ^{18}F-TFB may show benefit in so-called "Thyreoglobulin Elevated and Negative Iodine Scintigraphy" (TENIS) while not requiring thyroid-stimulating hormone (TSH) stimulation to detect metastatic lesions after therapy. But clinical evaluation of ^{18}F-TFB is needed in larger patient cohorts [141].

Since the 1990s somatostatin receptors (SSTRs) are known to play a role in regulation and proliferation of normal thyroid cells and tumor tissue [142]. In neuroendocrine tumors (NETs), SSTRs are often overexpressed on the surface of tumor cells. This has led to the development of different radiolabelled somatostatin analogs for diagnostics and/or therapy. Medullary thyroid carcinoma (MTC) is a neuroendocrine tumor arising from parafollicular C-cells of the thyroid glands. The experience in diagnostic performance with ^{68}Ga-labelled DOTA peptides in preoperative MTC staging is very limited. In the situation of disease recurrence, ^{68}Ga-DOTATATE-PET/CT showed promising results, especially in higher levels of tumor marker serum calcitonin [143]. Globally the diagnostic performance is inferior compared with other NETs and ^{68}Ga DOTATATE-PET/CT performs inferior to ^{18}F-DOPA-PET in recurrent MTC lesions [144].

^{18}F-DOPA, which explores amino acid uptake, decarboxylation, and storage, when applied in MTC prior to surgery demonstrated a high sensitivity of 88% in detection of primary tumor sites and sensitivity in detection of central and lateral lymph node metastasis of 53% and 73%, compared to 20% and 39%, respectively, for ultrasonography [145]. At present, neither ^{18}F-FDG-PET/CT nor ^{18}F-DOPA-PET/CT is recommended for primary staging in MTC [146, 147].

PSMA-PET/CT imaging in prostate cancer has become widely established in diagnostics, especially in recurrence situations, due to the precise imaging of the tumor spread. PSMA is a type II transmembrane glycoprotein and is overexpressed in prostate cancer. PSMA could be expressed by vascular endothelium in other solid tumors such as thyroid carcinoma [148].

As ^{18}F-FDG-PET, ^{68}Ga-PSMA- or ^{18}F-PSMA-PET harbor the capability of detecting thyroid lesions (PSMA thyroid incidentalomas - PTI). A systematic review demonstrated among 23 detected thyroid incidentalomas 5 proven primary thyroid carcinomas (4 papillary thyroid carcinomas, 1 follicular thyroid carcinoma) [149].

^{18}F-choline PET/CT is mostly used for evaluation of prostate cancer. But an increased cell membrane choline metabolism can also be seen in other conditions like in patients with primary hyperparathyroidism and thyroid incidentalomas.

In a retrospective study, the authors identified 9 incidentalomas, 8 of them underwent further

investigation and two cases were revealed to be malignant [150].

The percentage of carcinomas identified with choline PET (25%) is similar to FDG-PET (~35%).

However, it must be mentioned that PSMA and choline radiotracers are mainly used in men with prostate cancer and therefore women have so far not been included in these analyses.

Fibroblast activation protein (FAP) is expressed in the stroma of many malignancies and histopathological studies have shown FAP-positive cancer-associated fibroblasts in over 90% of epithelial tumors. FAP inhibitors (FAPIs) specifically bind to the enzymatic domain of FAP with a rapid and almost complete internalization. FAPI-based PET imaging has yielded high uptake and image contrast in several cancers. FAPI as a novel tracer may be helpful in applications from noninvasive tumor characterization up to radioligand therapy. In differentiated thyroid cancers only low-to-moderate FAPI uptake was observed [151]. Currently, major issues are the complementary use of ^{18}F-FDG-PET/CT in localizing disease recurrence and detecting metastatic lesions in patients with "Thyreoglobulin Elevated and Negative Iodine Scintigraphy" (TENIS) [152].

References

1. Fujimoto Y, Oka A, Omoto R, Hirose M. Ultrasound scanning of the thyroid gland as a new diagnostic approach. Ultrasonics. 1967;5:177–80.
2. Chan V, Perlas A. Basics of ultrasound imaging. In: Atlas of ultrasound-guided procedures in interventional pain management. New York: Springer Science + Business Media; 2011. p. 13–9.
3. Chung J, Lee YJ, Choi YJ, Ha EJ, Suh CH, Choi M, et al. Clinical applications of Doppler ultrasonography for thyroid disease: consensus statement by the Korean Society of Thyroid Radiology. Ultrasonography. 2020;39(4):315–30.
4. Zhao CK, Xu HX. Ultrasound elastography of the thyroid: principles and current status. Ultrasonography. 2019;38(2):106–24.
5. Yuen HY, Wong KT, Ahuja AT. Sonography of diffuse thyroid disease. Australas J Ultrasound Med. 2016;19(1):13–29.
6. Dighe M, Barr R, Bojunga J, Cantisani V, Chammas MC, Cosgrove D, et al. Thyroid ultrasound: state of the art part 1 - thyroid ultrasound reporting and diffuse thyroid diseases. Med Ultrason. 2017;19(1):79–93.
7. Dietlein M, Dressler J, Grünwald F, Joseph K, Leisner B, Moser E, et al. Leitlinie zur Schilddrüsendiagnostik - Deutsche Gesellschaft für Nuklearmedizin e.V. [Internet] Deutsche Gesellschaft für Nuklearmedizin eV 2022 [zitiert 18. August 2022]. Verfügbar unter: http://nuklearmedizin.de/leistungen/leitlinien/html/schild_diagn.php?navId=53.
8. Chaudhary V, Bano S. Thyroid ultrasound. Indian J Endocrinol Metab. 2013;17(2):219–27.
9. Shin JH, Baek JH, Chung J, Ha EJ, Kim JH, Lee YH, et al. Ultrasonography diagnosis and imaging-based management of thyroid nodules: revised Korean society of thyroid radiology consensus statement and recommendations. Korean J Radiol. 2016;17(3):370–95.
10. Russ G, Bonnema SJ, Erdogan MF, Durante C, Ngu R, Leenhardt L. European Thyroid Association guidelines for ultrasound malignancy risk stratification of thyroid nodules in adults: the EU-TIRADS. Eur Thyroid J. 2017;6(5):225–37.
11. Tessler FN, Middleton WD, Grant EG, Hoang JK, Berland LL, Teefey SA, et al. ACR thyroid imaging, reporting and data system (TI-RADS): white paper of the ACR TI-RADS Committee. J Am Coll Radiol. 2017;14(5):587–95.
12. Seifert P, Maikowski I, Winkens T, Kühnel C, Gühne F, Drescher R, et al. Ultrasound cine loop standard operating procedure for benign thyroid diseases—evaluation of non-physician application. Diagnostics. 2021;11(1):67.
13. Köhler M, Gomes Ataide EJ, Ziegle J, Boese A, Friebe M. Novel assistive device for tomographic ultrasound neck imaging vs. freehand. Curr Dir Biomed Eng. 2020;6(3):20203008.
14. Freesmeyer M, Winkens T, Kühnel C, Opfermann T, Seifert P. Technetium-99m SPECT/US hybrid imaging compared with conventional diagnostic thyroid imaging with scintigraphy and ultrasound. Ultrasound Med Biol. 2019;45(5):1243–52.
15. Seifert P, Winkens T, Kühnel C, Gühne F, Freesmeyer M. I-124-PET/US fusion imaging in comparison to conventional diagnostics and Tc-99m Pertechnetate SPECT/US fusion imaging for the function assessment of thyroid nodules. Ultrasound Med Biol. 2019;45(9):2298–308.
16. Claudon M, Cosgrove D, Albrecht T, Bolondi L, Bosio M, Calliada F, et al. Guidelines and good clinical practice recommendations for contrast enhanced ultrasound (CEUS) - update 2008. Ultraschall Med. 2008;29(01):28–44.
17. Radzina M, Ratniece M, Putrins DS, Saule L, Cantisani V. Performance of contrast-enhanced ultrasound in thyroid nodules: review of current state and future perspectives. Cancers. 2021;13(21):5469.
18. Clark KJ, Cronan JJ, Scola FH. Color Doppler sonography: anatomic and physiologic assessment of the thyroid. J Clin Ultrasound. 1995;23(4):215–23.

19. Ophir J, Céspedes I, Ponnekanti H, Yazdi Y, Li X. Elastography: A quantitative method for imaging the elasticity of biological tissues. Ultrason Imaging. 1991;13(2):111–34.
20. Bamber J, Cosgrove D, Dietrich C, Fromageau J, Bojunga J, Calliada F, et al. EFSUMB guidelines and recommendations on the clinical use of ultrasound Elastography. Part 1: basic principles and technology. Ultraschall Med. 2013;34(02):169–84.
21. Cantisani V, Grazhdani H, Drakonaki E, D'Andrea V, Di Segni M, Kaleshi E, et al. Strain US Elastography for the characterization of thyroid nodules: advantages and limitation. Int J Endocrinol. 2015;2015:908575.
22. Asteria C, Giovanardi A, Pizzocaro A, Cozzaglio L, Morabito A, Somalvico F, et al. US-elastography in the differential diagnosis of benign and malignant thyroid nodules. Thyroid. 2008;18(5):523–31.
23. Rago T, Scutari M, Santini F, Loiacono V, Piaggi P, Di Coscio G, et al. Real-time elastosonography: useful tool for refining the presurgical diagnosis in thyroid nodules with indeterminate or nondiagnostic cytology. J Clin Endocrinol Metab. 2010;95(12):5274–80.
24. Cosgrove D, Barr R, Bojunga J, Cantisani V, Chammas MC, Dighe M, et al. WFUMB guidelines and recommendations on the clinical use of ultrasound Elastography: part 4. Thyroid. Ultrasound Med Biol. 2017;43(1):4–26.
25. Cantisani V, Lodise P, Grazhdani H, Mancuso E, Maggini E, Di Rocco G, et al. Ultrasound elastography in the evaluation of thyroid pathology. Current status. Eur J Radiol. 2014;83(3):420–8.
26. Giusti M, Orlandi D, Melle G, Massa B, Silvestri E, Minuto F, et al. Is there a real diagnostic impact of elastosonography and contrast-enhanced ultrasonography in the management of thyroid nodules? J Zhejiang Univ Sci B. 2013;14(3):195–206.
27. Mahlstedt J, Schmidt H, Joseph K. Untersuchungen zur Verläßlichkeit des ^{99m}Tc-Speichertests als Schätzer der thyreoidalen Stimulation. RöFo - Fortschritte Auf Dem Geb Röntgenstrahlen Bildgeb Verfahr. 1979;131(11):536–44.
28. Giovanella L, Avram AM, Iakovou I, Kwak J, Lawson SA, Lulaj E, et al. EANM practice guideline/SNMMI procedure standard for RAIU and thyroid scintigraphy. Eur J Nucl Med Mol Imaging. 2019;46(12):2514–25.
29. Meng W. 333460392X - Schilddrüsenerkrankungen. Pathophysiologie, Diagnostik, Therapie - Meng, Wieland [Internet]. 3. Aufl. Jena: Gustav Fischer Verlag GmbH; 1992 [zitiert 21. März 2022]. Verfügbar unter: https://www.eurobuch.com/buch/isbn/333460392X.html.
30. Vassart G, Pardo L, Costagliola S. A molecular dissection of the glycoprotein hormone receptors. Trends Biochem Sci. 2004;29(3):119–26.
31. Atkins HL. Technetium-99m pertechnetate uptake and scanning in the evaluation of thyroid function. Semin Nucl Med. 1971;1(3):345–55.
32. Stahl A, Nagel H, Negele T. Schilddrüse-Atlas.info [Internet]. 2.Auflage. München: Nuk-Verlag; 2021 [zitiert 10. Juli 2022]. Verfügbar unter: https://nuk--verlag.de.
33. Schenke S, Seifert P, Zimny M, Winkens T, Binse I, Goerges R. Risk stratification of thyroid nodules using thyroid imaging reporting and data system (TIRADS): the omission of thyroid scintigraphy increases the rate of falsely suspected lesions. J Nucl Med. 2019;60:342.
34. Görges R, Kandror T, Kuschnerus S, Zimny M, Pink R, Palmedo H, et al [Scintigraphically „hot "thyroid nodules mainly go hand in hand with a normal TSH]. Nuklearmedizin. 2011;50(5):179–88.
35. Reschini E, Ferrari C, Castellani M, Matheoud R, Paracchi A, Marotta G, et al. The trapping-only nodules of the thyroid gland: prevalence study. Thyroid. 2006;16(8):757–62.
36. Dietlein M, Eschner W, Lassmann M, Verburg FA, Luster M. Procedure guideline for thyroid scintigraphy (version 4) 2014. 2014. Verfügbar unter: www.nuklearmedizin.de/leistungen/leitlinien/docs/031-011I_S1_Schiilddrüsenszintigraphie_2014-10.pdf.
37. Rager O, Radojewski P, Dumont RA, Treglia G, Giovanella L, Walter MA. Radioisotope imaging for discriminating benign from malignant cytologically indeterminate thyroid nodules. Gland Surg. 2019;8(Suppl 2):S118–25.
38. Moretti JL, Hauet N, Caglar M, Rebillard O, Burak Z. To use MIBI or not to use MIBI? That is the question when assessing tumour cells. Eur J Nucl Med Mol Imaging. 2005;32(7):836–42.
39. Sarikaya A, Huseyinova G, Irfanoğlu ME, Erkmen N, Cermik TF, Berkarda S. The relationship between 99Tc(m)-sestamibi uptake and ultrastructural cell types of thyroid tumours. Nucl Med Commun. 2001;22(1):39–44.
40. Schmidt M, Schenke S. Update 2019 zur MIBI-Szintigrafie bei hypofunktionellen Schilddrüsenknoten. Nuklearmedizin. 2019;42:174–82.
41. Treglia G, Caldarella C, Saggiorato E, Ceriani L, Orlandi F, Salvatori M, et al. Diagnostic performance of (99m)Tc-MIBI scan in predicting the malignancy of thyroid nodules: a meta-analysis. Endocrine. 2013;44(1):70–8.
42. Kim SJ, Lee SW, Jeong SY, Pak K, Kim K. Diagnostic performance of technetium-99m methoxy-isobutyl-Isonitrile for differentiation of malignant thyroid nodules: a systematic review and meta-analysis. Thyroid. 2018;28(10):1339–48.
43. Campennì A, Siracusa M, Ruggeri RM, Laudicella R, Pignata SA, Baldari S, et al. Differentiatinjg malignant from benign thyroid nodules with indeterminate cytology by 99mTc-MIBI scan: a new quantitative method for improving diagnostic accuracy. Sci Rep. 2017;7(1):6147.
44. Piga M, Cocco MC, Serra A, Boi F, Loy M, Mariotti S. The usefulness of 99mTc-sestaMIBI thyroid scan in the differential diagnosis and manage-

ment of amiodarone-induced thyrotoxicosis. Eur J Endocrinol. 2008;159(4):423–9.
45. Choudhury PS, Gupta M. Differentiated thyroid cancer theranostics: radioiodine and beyond. Br J Radiol. 2018;91(1091):20180136.
46. Bekanntmachung der aktualisierten diagnostischen Referenzwerte für nuklearmedizinische Untersuchungen vom 15. 2021, p. 8.
47. Wahl RL. Targeting glucose transporters for tumor imaging: "sweet" idea, "sour" result. J Nucl Med. 1996;37(6):1038–41.
48. Boellaard R, Delgado-Bolton R, Oyen WJG, Giammarile F, Tatsch K, Eschner W, et al. FDG PET/CT: EANM procedure guidelines for tumour imaging: version 2.0. Eur J Nucl Med Mol Imaging. 2015;42(2):328–54.
49. Guth S, Theune U, Aberle J, Galach A, Bamberger CM. Very high prevalence of thyroid nodules detected by high frequency (13 MHz) ultrasound examination. Eur J Clin Investig. 2009;39(8):699–706.
50. Carlé A, Krejbjerg A, Laurberg P. Epidemiology of nodular goitre. Influence of iodine intake. Best Pract Res Clin Endocrinol Metab. 2014;28(4):465–79.
51. Knudsen N, Brix TH. Genetic and non-iodine-related factors in the aetiology of nodular goitre. Best Pract Res Clin Endocrinol Metab. 2014;28(4):495–506.
52. Spelsberg F, Negele T, Ritter MM. Die Schilddrüse in Klinik und Praxis. Heidelberg: Karl F. Haug Fachbuchverlag; 2000.
53. Kraiem Z, Glaser B, Yigla M, Pauker J, Sadeh O, Sheinfeld M. Toxic multinodular Goiter: A variant of autoimmune hyperthyroidism*. J Clin Endocrinol Metab. 1987;65(4):659–64.
54. Meller J, Jauho A, Hüfner M, Gratz S, Becker W. Disseminated thyroid autonomy or graves' disease: reevaluation by a second generation TSH receptor antibody assay. Thyroid. 2000;10(12):1073–9.
55. Reinhardt MJ, Joe A, von Mallek D, Zimmerlin M, Manka-Waluch A, Palmedo H, et al. Dose selection for radioiodine therapy of borderline hyperthyroid patients with multifocal and disseminated autonomy on the basis of 99mTc-pertechnetate thyroid uptake. Eur J Nucl Med Mol Imaging. 2002;29(4):480–5.
56. Meller J, Becker W. The continuing importance of thyroid scintigraphy in the era of high-resolution ultrasound. Eur J Nucl Med Mol Imaging. 2002;29(S2):S425–38.
57. Giovanella L, D'Aurizio F, Campenni' A, Ruggeri RM, Baldari S, Verburg FA, et al. Searching for the most effective thyrotropin (TSH) threshold to rule-out autonomously functioning thyroid nodules in iodine deficient regions. Endocrine. 2016;54(3):757–61.
58. Happel C, Kranert WT, Bockisch B, Korkusuz H, Grünwald F. 131I- und 99mTc-Uptake in fokalen Schilddrüsenautonomien: Entwicklung in Deutschland seit den 1980er Jahren. Nuklearmedizin. 2016;55(06):236–41.
59. Gotthardt M, Stübinger M, Pansegrau J, Buchwald B, Goecke J, Pfestroff A, et al. Decrease of (99m) Tc-uptake in autonomous thyroid tissue in Germany since the 1970s. Clinical implications for radioiodine therapy. Nukl Nucl. 2006;45(3):122–5.
60. Vassaux G, Zwarthoed C, Signetti L, Guglielmi J, Compin C, Guigonis JM, et al. Iodinated contrast agents perturb iodide uptake by the thyroid independently of free iodide. J Nucl Med. 2018;59(1):121–6.
61. Antonelli A, Ferrari SM, Ragusa F, Elia G, Paparo SR, Ruffilli I, et al. Graves' disease: epidemiology, genetic and environmental risk factors and viruses. Best Pract Res Clin Endocrinol Metab. 2020;34(1):101387.
62. Kılınçer A, Durmaz MS, Baldane S, Kıraç CO, Cebeci H, Koplay M. Evaluation of the stiffness of thyroid parenchyma with shear wave Elastography using a free-region of interest technique in graves disease. J Ultrasound Med. 2020;40:471.
63. Xie P, Xiao Y, Liu F. Real-time ultrasound elastography in the diagnosis and differential diagnosis of subacute thyroiditis. J Clin Ultrasound. 2011;39(8):435–40.
64. Ruchala M, Szczepanek-Parulska E, Zybek A, Moczko J, Czarnywojtek A, Kaminski G, et al. The role of sonoelastography in acute, subacute and chronic thyroiditis: a novel application of the method. Eur J Endocrinol. 2012;166(3):425–32.
65. Kara T, Ateş F, Durmaz MS, Akyürek N, Durmaz FG, Özbakır B, et al. Assessment of thyroid gland elasticity with shear-wave elastography in Hashimoto's thyroiditis patients. J Ultrasound. 2020;23(4):543–51.
66. Ramtoola S, Maisey MN, Clarke SEM, Fogelman I. The thyroid scan in Hashimoto's thyroiditis: the great mimic. Nucl Med Commun. 1988;9(9):639–46.
67. Chaker L, Bianco AC, Jonklaas J, Peeters RP. Hypothyroidism. Lancet. 2017;390(10101):1550–62.
68. Lupo MA, Levine RA. Ultrasound of diffuse thyroid enlargement: thyroiditis. In: Jack Baskin Sr H, Duick DS, Levine RA, Thyroid ultrasound and ultrasound-guided FNA. New York, NY: Springer; 2013. [zitiert 22. März 2022]. S. 99–125. Verfügbar unter: https://doi.org/10.1007/978-1-4614-4785-6_6.
69. Stasiak M, Lewiński A. New aspects in the pathogenesis and management of subacute thyroiditis. Rev Endocr Metab Disord. 2021;22(4):1027–39.
70. Schenke S, Klett R, Braun S, Zimny M. Are there predictive factors for long-term hormone-replacement? Nuklearmedizin. 2013;52(4):137–40.
71. Giovanella L, Ruggeri RM, Ovčariček PP, Campenni A, Treglia G, Deandreis D. Prevalence of thyroid dysfunction in patients with COVID-19: a systematic review. Clin Transl Imaging. 2021;9(3):233–40.
72. Brancatella A, Ricci D, Viola N, Sgrò D, Santini F, Latrofa F. Subacute thyroiditis after Sars-COV-2 infection. J Clin Endocrinol Metab. 2020;105(7):2367–70.
73. Yasuda S, Shohtsu A, Ide M, Takagi S, Takahashi W, Suzuki Y, et al. Chronic thyroiditis: diffuse uptake of FDG at PET. Radiology. 1998;207(3):775–8.

74. Kurata S, Ishibashi M, Hiromatsu Y, Kaida H, Miyake I, Uchida M, et al. Diffuse and diffuse-plus-focal uptake in the thyroid gland identified by using FDG-PET: prevalence of thyroid cancer and Hashimoto's thyroiditis. Ann Nucl Med. 2007;21(6):325–30.
75. Schenke SA, Kreissl MC, Grunert M, Hach A, Haghghi S, Kandror T, et al. Distribution of functional status of thyroid nodules and malignancy rates of hyperfunctioning and hypofunctioning thyroid nodules in Germany. Nuklearmedizin. 2022;61:376.
76. Krohn K, Wohlgemuth S, Gerber H, Paschke R. Hot microscopic areas of iodine-deficient euthyroid goitres contain constitutively activating TSH receptor mutations. J Pathol. 2000;192(1):37–42.
77. Trimboli P, Paone G, Zatelli MC, Ceriani L, Giovanella L. Real-time elastography in autonomously functioning thyroid nodules: relationship with TSH levels, scintigraphy, and ultrasound patterns. Endocrine. 2017;58(3):488–94.
78. Treglia G, Trimboli P, Verburg FA, Luster M, Giovanella L. Prevalence of normal TSH value among patients with autonomously functioning thyroid nodule. Eur J Clin Investig. 2015;45(7):739–44.
79. Reschke K, Klose S, Kopf D, Lehnert H. Role of ultrasound in the diagnosis of thyroid autonomy. Exp Clin Endocrinol Diabetes. 1998;106(Suppl 04):S42–4.
80. Ianni F, Perotti G, Prete A, Paragliola RM, Ricciato MP, Carrozza C, et al. Thyroid scintigraphy: an old tool is still the gold standard for an effective diagnosis of autonomously functioning thyroid nodules. J Endocrinol Invest. 2013;36:233. https://doi.org/10.3275/8471.
81. Ruhlmann M, Stebner V, Görges R, Farahati J, Simon D, Bockisch A, et al. Diagnosis of hyperfunctional thyroid nodules: impact of US-elastography. Nuklearmedizin. 2014;53(5):173–7.
82. Ruhlmann M, Stebner V, Görges R, Bockisch A, Rosenbaum-Krumme SJ, Nagarajah J. Ultrasound-elastography for predicting response of hyperfunctional thyroid nodules to radioiodine therapy: initial results. Austin J Nucl Med Radiother. 2016;3(2):01–4.
83. Haugen BR, Alexander EK, Bible KC, Doherty GM, Mandel SJ, Nikiforov YE, et al. 2015 American Thyroid Association management guidelines for adult patients with thyroid nodules and differentiated thyroid cancer: the American Thyroid Association guidelines task force on thyroid nodules and differentiated thyroid cancer. Thyroid. 2016;26(1):1–133.
84. Horvath E, Majlis S, Rossi R, Franco C, Niedmann JP, Castro A, et al. An ultrasonogram reporting system for thyroid nodules stratifying cancer risk for clinical management. J Clin Endocrinol Metab. 2009;94(5):1748–51.
85. Durfee SM, Benson CB, Arthaud DM, Alexander EK, Frates MC. Sonographic appearance of thyroid cancer in patients with Hashimoto thyroiditis. J Ultrasound Med. 2015;34(4):697–704.
86. Remonti LR, Kramer CK, Leitão CB, Pinto LCF, Gross JL. Thyroid ultrasound features and risk of carcinoma: a systematic review and meta-analysis of observational studies. Thyroid. 2015;25(5):538–50.
87. Seifert P, Schenke S, Zimny M, Stahl A, Grunert M, Klemenz B, Diagnostic Performance of Kwak, EU, ACR, and Korean TIRADS, et al. As well as ATA guidelines for the ultrasound risk stratification of non-autonomously functioning thyroid nodules in a region with long history of iodine deficiency: a German multicenter trial. Cancers. 2021;13(17):4467.
88. Seifert P, Görges R, Zimny M, Kreissl MC, Schenke S. Interobserver agreement and efficacy of consensus reading in Kwak-, EU-, and ACR-thyroid imaging recording and data systems and ATA guidelines for the ultrasound risk stratification of thyroid nodules. Endocrine. 2020;67(1):143–54.
89. Petersen M, Schenke SA, Zimny M, Görges R, Grunert M, Groener D, et al. Introducing a pole concept for nodule growth in the thyroid gland: taller-than-wide shape, frequency, location and risk of malignancy of thyroid nodules in an area with iodine deficiency. J Clin Med. 2022;11(9):2549.
90. Kwak JY, Han KH, Yoon JH, Moon HJ, Son EJ, Park SH, et al. Thyroid imaging reporting and data system for US features of nodules: a step in establishing better stratification of cancer risk. Radiology. 2011;260(3):892–9.
91. Ha EJ, Chung SR, Na DG, Ahn HS, Chung J, Lee JY, et al. 2021 Korean thyroid imaging reporting and data system and imaging-based management of thyroid nodules: Korean Society of Thyroid radiology consensus statement and recommendations. Korean J Radiol. 2021;22(12):2094.
92. Castellana M, Castellana C, Treglia G, Giorgino F, Giovanella L, Russ G, et al. Performance of five ultrasound risk stratification systems in selecting thyroid nodules for FNA. A meta-analysis. J Clin Endocrinol Metab. 2020;105:dgz170.
93. Chung SR, Ahn HS, Choi YJ, Lee JY, Yoo RE, Lee YJ, et al. Diagnostic performance of the modified Korean thyroid imaging reporting and data system for thyroid malignancy: a multicenter validation study. Korean J Radiol. 2021;22(9):1579.
94. Kim PH, Suh CH, Baek JH, Chung SR, Choi YJ, Lee JH. Unnecessary thyroid nodule biopsy rates under four ultrasound risk stratification systems: a systematic review and meta-analysis. Eur Radiol. 2021;31(5):2877–85.
95. Middleton WD, Teefey SA, Reading CC, Langer JE, Beland MD, Szabunio MM, et al. Comparison of performance characteristics of American College of Radiology TI-RADS, Korean Society of Thyroid Radiology TIRADS, and American Thyroid Association guidelines. AJR Am J Roentgenol. 2018;210(5):1148–54.
96. Migda B, Migda M, Migda MS, Slapa RZ. Use of the Kwak thyroid image reporting and data system (K-TIRADS) in differential diagnosis of thyroid

nodules: systematic review and meta-analysis. Eur Radiol. 2018;28(6):2380–8.
97. Xu T, Wu Y, Wu RX, Zhang YZ, Gu JY, Ye XH, et al. Validation and comparison of three newly-released thyroid imaging reporting and data systems for cancer risk determination. Endocrine. 2019;64(2):299–307.
98. Schenke SA, Klett R, Wagner PR, Mott S, Zimny M, Feek U, et al. Characteristics of different histological subtypes of thyroid nodules classified with 99mTc-methoxy-isobutyl-isonitrile imaging and thyroid imaging reporting and data system. Nucl Med Commun. 2021;42(1):73–80.
99. Lin P, Chen M, Liu B, Wang S, Li X. Diagnostic performance of shear wave elastography in the identification of malignant thyroid nodules: a meta-analysis. Eur Radiol. 2014;24(11):2729–38.
100. Trimboli P, Treglia G, Sadeghi R, Romanelli F, Giovanella L. Reliability of real-time elastography to diagnose thyroid nodules previously read at FNAC as indeterminate: a meta-analysis. Endocrine. 2015;50(2):335–43.
101. Sidhu P, Cantisani V, Dietrich C, Gilja O, Saftoiu A, Bartels E, et al. The EFSUMB guidelines and recommendations for the clinical practice of contrast-enhanced ultrasound (CEUS) in non-hepatic applications: update 2017 (long version). Ultraschall Med. 2018;39(02):e2–44.
102. Schleder S, Janke M, Agha A, Schacherer D, Hornung M, Schlitt HJ, et al. Preoperative differentiation of thyroid adenomas and thyroid carcinomas using high resolution contrast-enhanced ultrasound (CEUS). Clin Hemorheol Microcirc. 2015;61(1):13–22.
103. Trimboli P, Castellana M, Virili C, Havre RF, Bini F, Marinozzi F, et al. Performance of contrast-enhanced ultrasound (CEUS) in assessing thyroid nodules: a systematic review and meta-analysis using histological standard of reference. Radiol Med. 2020;125(4):406–15.
104. Xu Y, Qi X, Zhao X, Ren W, Ding W. Clinical diagnostic value of contrast-enhanced ultrasound and TI-RADS classification for benign and malignant thyroid tumors: one comparative cohort study. Medicine (Baltimore). 2019;98(4):e14051.
105. Noto B, Eveslage M, Pixberg M, Gonzalez Carvalho JM, Schäfers M, Riemann B, et al. Prevalence of hyperfunctioning thyroid nodules among those in need of fine needle aspiration cytology according to ATA 2015, EU-TIRADS, and ACR-TIRADS. Eur J Nucl Med Mol Imaging. 2020;47(6):1518–26.
106. Seifert P, Freesmeyer M. Preoperative diagnostics in differentiated thyroid carcinoma. Nuklearmedizin. 2017;56(6):201–10.
107. Wale A, Miles KA, Young B, Zammit C, Williams A, Quin J, et al. Combined (99m) Tc-methoxyisobutylisonitrile scintigraphy and fine-needle aspiration cytology offers an accurate and potentially cost-effective investigative strategy for the assessment of solitary or dominant thyroid nodules. Eur J Nucl Med Mol Imaging. 2014;41(1):105–15.
108. Giovanella L, Campenni A, Treglia G, Verburg FA, Trimboli P, Ceriani L, et al. Molecular imaging with (99m)Tc-MIBI and molecular testing for mutations in differentiating benign from malignant follicular neoplasm: a prospective comparison. Eur J Nucl Med Mol Imaging. 2016;43(6):1018–26.
109. Schenke SA, Campennì A, Tuncel M, Bottoni G, Sager S, Bogovic Crncic T, et al. Diagnostic performance of 99mTc-Methoxy-Isobuty-Isonitrile (MIBI) for risk stratification of hypofunctioning thyroid nodules: a European Multicenter Study. Diagnostics. 2022;12(6):1358.
110. Treglia G, Bertagna F, Sadeghi R, Verburg FA, Ceriani L, Giovanella L. Focal thyroid incidental uptake detected by 18F-fluorodeoxyglucose positron emission tomography: meta-analysis on prevalence and malignancy risk. Nuklearmedizin. 2013;52(04):130–6.
111. Soelberg KK, Bonnema SJ, Brix TH, Hegedüs L. Risk of malignancy in thyroid Incidentalomas detected by ^{18}F-fluorodeoxyglucose positron emission tomography: a systematic review. Thyroid. 2012;22(9):918–25.
112. Hoang JK, Langer JE, Middleton WD, Wu CC, Hammers LW, Cronan JJ, et al. Managing incidental thyroid nodules detected on imaging: white paper of the ACR Incidental Thyroid Findings Committee. J Am Coll Radiol. 2015;12(2):143–50.
113. Cibas ES, Ali SZ. The 2017 Bethesda system for reporting thyroid cytopathology. Thyroid. 2017;27(11):1341–6.
114. Vriens D, de Wilt JHW, van der Wilt GJ, Netea-Maier RT, Oyen WJG, de Geus-Oei LF. The role of [^{18}F]-2-fluoro-2-deoxy-d-glucose-positron emission tomography in thyroid nodules with indeterminate fine-needle aspiration biopsy: systematic review and meta-analysis of the literature. Cancer. 2011;117(20):4582–94.
115. Piccardo A, Puntoni M, Treglia G, Foppiani L, Bertagna F, Paparo F, et al. Thyroid nodules with indeterminate cytology: prospective comparison between 18F-FDG-PET/CT, multiparametric neck ultrasonography, 99mTc-MIBI scintigraphy and histology. Eur J Endocrinol. 2016;174(5):693–703.
116. Sager S, Vatankulu B, Erdogan E, Mut S, Teksoz S, Ozturk T, et al. Comparison of F-18 FDG-PET/CT and Tc-99m MIBI in the preoperative evaluation of cold thyroid nodules in the same patient group. Endocrine. 2015;50(1):138–45.
117. Bartalena L, Bogazzi F, Chiovato L, Hubalewska-Dydejczyk A, Links TP, Vanderpump M. 2018 European thyroid association (ETA) guidelines for the management of amiodarone-associated thyroid dysfunction. Eur Thyroid J. 2018;7(2):55–66.
118. Colunga Biancatelli RM, Congedo V, Calvosa L, Ciacciarelli M, Polidoro A, Iuliano L. Adverse reactions of amiodarone. J Geriatr Cardiol. 2019;16(7):552–66.

119. Tanda ML, Piantanida E, Lai A, Liparulo L, Sassi L, Bogazzi F, et al. Diagnosis and management of amiodarone-induced thyrotoxicosis: similarities and differences between North American and European thyroidologists. Clin Endocrinol. 2008;69(5):812–8.
120. Hoermann R. Amiodaron und Schilddrüsenfunktion. Nuklearmedizin. 2004;27(2):78–85.
121. Tsang W, Houlden RL. Amiodarone-induced thyrotoxicosis: a review. Can J Cardiol. 2009;25(7):421–4.
122. Censi S, Bodanza V, Manso J, Gusella S, Watutantrige-Fernando S, Cavedon E, et al. Amiodarone-induced thyrotoxicosis: differential diagnosis using 99mTc-SestaMIBI and target-to-background ratio (TBR). Clin Nucl Med. 2018;43(9):655–62.
123. Stelmachowska-Banaś M, Czajka-Oraniec I. Management of endocrine immune-related adverse events of immune checkpoint inhibitors: an updated review. Endocr Connect. 2020;9(10):R207–28.
124. Kurimoto C, Inaba H, Ariyasu H, Iwakura H, Ueda Y, Uraki S, et al. Predictive and sensitive biomarkers for thyroid dysfunctions during treatment with immune-checkpoint inhibitors. Cancer Sci. 2020;111(5):1468–77.
125. Hattersley R, Nana M, Lansdown AJ. Endocrine complications of immunotherapies: a review. Clin Med. 2021;21(2):e212–22.
126. Brancatella A, Viola N, Brogioni S, Montanelli L, Sardella C, Vitti P, et al. Graves' disease induced by immune checkpoint inhibitors: a case report and review of the literature. Eur Thyroid J. 2019;8(4):192–5.
127. Petranović Ovčariček P, Deandreis D, Giovanella L. Thyroid dysfunctions induced by molecular cancer therapies: a synopsis for nuclear medicine thyroidologists. Eur J Nucl Med Mol Imaging. 2021;48(11):3355–60.
128. Nilsson M, Fagman H. Development of the thyroid gland. Development. 2017;144(12):2123–40.
129. Zamora E, Ghandili S, Zamora MA, Chun KJ. Incidental primary intrathoracic goiter: dual-isotope scintigraphy and early-MIBI SPECT/CT. World J Nucl Med. 2022;21(2):148–51.
130. Richmond I, Whittaker JS, Deiraniya AK, Hassan R. Intracardiac ectopic thyroid: a case report and review of published cases. Thorax. 1990;45(4):293–4.
131. Theurer S, Siebolts U, Lorenz K, Dralle H, Schmid KW. Ektopes Gewebe der Schilddrüse und der Nebenschilddrüsen. Pathologe. 2018;39(5):379–89.
132. Harisankar CNB, Preethi GR, George M. Hybrid SPECT/CT evaluation of dual ectopia of thyroid in the absence of orthotopic thyroid gland. Clin Nucl Med. 2012;37(6):602–3.
133. Bonnema SJ, Knudsen DU, Bertelsen H, Mortensen J, Andersen PB, Bastholt L, et al. Does radioiodine therapy have an equal effect on substernal and cervical goiter volumes? Evaluation by magnetic resonance imaging. Thyroid. 2002;12(4):313–7.
134. Gandhi A, Wong KK, Gross MD, Avram AM. Lingual thyroid ectopia: diagnostic SPECT/CT imaging and radioactive iodine treatment. Thyroid. 2016;26(4):573–9.
135. Roth LM, Talerman A. The enigma of struma ovarii. Pathology. 2007;39(1):139–46.
136. van Trotsenburg P, Stoupa A, Léger J, Rohrer T, Peters C, Fugazzola L, et al. congenital hypothyroidism: a 2020–2021 consensus guidelines update—an ENDO-European reference network initiative endorsed by the European Society for Pediatric Endocrinology and the European Society for Endocrinology. Thyroid. 2021;31(3):387–419.
137. Schoen EJ, Clapp W, To TT, Fireman BH. The key role of newborn thyroid scintigraphy with isotopic iodide (123I) in defining and managing congenital hypothyroidism. Pediatrics. 2004;114(6):e683–8.
138. Binse I, Poeppel TD, Ruhlmann M, Gomez B, Umutlu L, Bockisch A, et al. Imaging with 124I in differentiated thyroid carcinoma: is PET/MRI superior to PET/CT? Eur J Nucl Med Mol Imaging. 2016;43(6):1011–7.
139. Winkens T, Seifert P, Hollenbach C, Kühnel C, Gühne F, Freesmeyer M. The FUSION iENA study: comparison of I-124-PET/US fusion imaging with conventional diagnostics for the functional assessment of thyroid nodules by multiple observers. Nuklearmedizin. 2019;58(6):434–42.
140. Jiang H, Schmit NR, Koenen AR, Bansal A, Pandey MK, Glynn RB, et al. Safety, pharmacokinetics, metabolism and radiation dosimetry of 18F-tetrafluoroborate (18F-TFB) in healthy human subjects. EJNMMI Res. 2017;7(1):90.
141. Dittmann M, Gonzalez Carvalho JM, Rahbar K, Schäfers M, Claesener M, Riemann B, et al. Incremental diagnostic value of [18F]tetrafluoroborate PET-CT compared to [131I]iodine scintigraphy in recurrent differentiated thyroid cancer. Eur J Nucl Med Mol Imaging. 2020;47(11):2639–46.
142. Salavati A, Puranik A, Kulkarni HR, Budiawan H, Baum RP. Peptide receptor radionuclide therapy (PRRT) of medullary and nonmedullary thyroid cancer using radiolabeled somatostatin analogues. Semin Nucl Med. 2016;46(3):215–24.
143. Tran K, Khan S, Taghizadehasl M, Palazzo F, Frilling A, Todd JF, et al. Gallium-68 Dotatate PET/CT is superior to other imaging modalities in the detection of medullary carcinoma of the thyroid in the presence of high serum calcitonin. Hell J Nucl Med. 2015;18(1):19–24.
144. Treglia G, Castaldi P, Villani MF, Perotti G, de Waure C, Filice A, et al. Comparison of 18F-DOPA, 18F-FDG and 68Ga-somatostatin analogue PET/CT in patients with recurrent medullary thyroid carcinoma. Eur J Nucl Med Mol Imaging. 2012;39(4):569–80.
145. Rasul S, Hartenbach S, Rebhan K, Göllner A, Karanikas G, Mayerhoefer M, et al. [18F]DOPA PET/ceCT in diagnosis and staging of primary medullary thyroid carcinoma prior to surgery. Eur J Nucl Med Mol Imaging. 2018;45(12):2159–69.
146. Wells SA, Asa SL, Dralle H, Elisei R, Evans DB, Gagel RF, et al. Revised American Thyroid

Association guidelines for the management of medullary thyroid carcinoma: the American Thyroid Association guidelines task force on medullary thyroid carcinoma. Thyroid. 2015;25(6):567–610.
147. Giovanella L, Treglia G, Iakovou I, Mihailovic J, Verburg FA, Luster M. EANM practice guideline for PET/CT imaging in medullary thyroid carcinoma. Eur J Nucl Med Mol Imaging. 2020;47(1):61–77.
148. Hofman MS, Hicks RJ, Maurer T, Eiber M. Prostate-specific membrane antigen PET: clinical utility in prostate cancer, normal patterns, pearls, and pitfalls. Radiographics. 2018;38(1):200–17.
149. Bertagna F, Albano D, Giovanella L, Bonacina M, Durmo R, Giubbini R, et al. 68Ga-PSMA PET thyroid incidentalomas. Hormones. 2019;18(2):145–9.
150. Albano D, Durmo R, Bertagna F, Giubbini R. 18F-choline PET/CT incidental thyroid uptake in patients studied for prostate cancer. Endocrine. 2019;63(3):531–6.
151. Kratochwil C, Flechsig P, Lindner T, Abderrahim L, Altmann A, Mier W, et al. 68Ga-FAPI PET/CT: tracer uptake in 28 different kinds of cancer. J Nucl Med. 2019;60(6):801–5.
152. Li M, Younis MH, Zhang Y, Cai W, Lan X. Clinical summary of fibroblast activation protein inhibitor-based radiopharmaceuticals: cancer and beyond. Eur J Nucl Med Mol Imaging. 2022;49(8):2844–68.

5 Non-invasive Imaging Biomarkers of Thyroid Nodules with Indeterminate Cytology

Wyanne A. Noortman, Elizabeth J. de Koster, Floris H. P. van Velden, Lioe-Fee de Geus-Oei, and Dennis Vriens

5.1 Introduction

After stratification by ultrasonography (US), the next step in analysis of a thyroid nodule in a non-hyperthyroid patient is by obtaining cytology. Usually, this is performed by fine-needle aspiration cytology (FNAC) as this procedure is simple, safe, inexpensive, and has high accuracy. The FNAC specimens are categorized into six diagnostic categories according to the Bethesda System for the Reporting of Thyroid Cytology (Table 5.1) [1]. Around 20% of thyroid nodules are cytologically indeterminate, including both atypia of undetermined significance or follicular nodules of undetermined significance (Bethesda III, AUS/FLUS) with a malignancy rate of 6–18% and cytology suspicious for a follicular neoplasm (Bethesda IV, FN/SFN) or Hürthle cell neoplasm (Bethesda IV, HCN/SHCN) together having a malignancy rate of 10–40% [1, 2]. Nodules that are suspicious for malignancy upon FNAC (Bethesda V, SUSP) encounter a malignancy rate of 45–60% and can also be considered cytologically indeterminate [1].

Indeterminate thyroid cytology corresponds to histopathological follicular adenoma (FA), Hürthle cell adenoma (HCA), non-invasive follicular thyroid neoplasm with papillary-like nuclear features (NIFTP), (encapsulated) follicular variant of papillary thyroid carcinoma ((E)FVPTC), follicular thyroid carcinoma (FTC), and Hürthle cell carcinoma (HCC), but can also be seen in papillary thyroid carcinoma (PTC). Unlike histology, cytology does not provide

W. A. Noortman (✉)
Leiden University Medical Center, Department of Radiology, Section of Nuclear Medicine, Leiden, The Netherlands

University of Twente, Biomedical Photonic Imaging Group, Enschede, The Netherlands
e-mail: w.a.noortman@lumc.nl; w.a.noortman@utwente.nl

E. J. de Koster
Leiden University Medical Center, Department of Radiology, Section of Nuclear Medicine, Leiden, The Netherlands

Radboud University Medical Center, Department of Radiology and Nuclear Medicine, Nijmegen, The Netherlands
e-mail: e.j.de_koster@lumc.nl

F. H. P. van Velden · D. Vriens
Leiden University Medical Center, Department of Radiology, Section of Nuclear Medicine, Leiden, The Netherlands
e-mail: f.h.p.van_velden@lumc.nl; d.vriens@lumc.nl

L.-F. de Geus-Oei
Leiden University Medical Center, Department of Radiology, Section of Nuclear Medicine, Leiden, The Netherlands

University of Twente, Biomedical Photonic Imaging Group, Enschede, The Netherlands

Radboud University Medical Center, Department of Radiology and Nuclear Medicine, Nijmegen, The Netherlands
e-mail: l.f.de_geus-oei@lumc.nl

L. Giovanella (ed.), *Integrated Diagnostics and Theranostics of Thyroid Diseases*,
https://doi.org/10.1007/978-3-031-35213-3_5

Table 5.1 The 2017 Bethesda System for reporting thyroid cytopathology [1]. Reported malignancy rates consider NIFTPs as benign

Category	Description	Diagnostic categories	Malignancy rate (%)	Proposed management (ATA guidelines)
I	Non-diagnostic of unsatisfactory	• Cyst fluid only. • Virtually acellular specimen. • Other (obscuring blood, clotting artefact etc.).	5–10	Repeat FNAC with US guidance
II	Benign	• Consistent with a benign follicular nodule (including adenomatoid nodule, colloid nodule etc.). • Consistent with lymphocytic (Hashimoto) thyroiditis in the proper clinical context. • Consistent with granulomatous (subacute) thyroiditis. • Other.	0–3	Clinical and sonographic follow-up
III	Atypia of undetermined significance or follicular lesions of undetermined significance		6–18	Repeat FNAC. If the second Bethesda III result, consider additional tests and/or diagnostic hemithyroidectomy
IV	Follicular neoplasm suspicious for a follicular neoplasm	• Hürthle cell.	10–40	Consider additional tests and/or diagnostic hemithyroidectomy
V	Suspicious for malignancy	• Suspicious for papillary carcinoma. • Suspicious for medullary carcinoma. • Suspicious for metastatic carcinoma. • Suspicious for lymphoma. • Other.	45–60	Thyroid surgery is recommended. Consider pre-operative additional (molecular) testing to determine the extent of surgery
VI	Malignant	• Papillary thyroid carcinoma. • Poorly differentiated carcinoma. • Undifferentiated (anaplastic) carcinoma. • Squamous cell carcinoma. • Carcinoma with mixed features (specify). • Metastatic carcinoma. • Non-Hodgkin lymphoma. • Other.	94–96	Thyroid surgery recommended

insight into tissue structure: it does not show the capsular and/or vascular invasion that distinguishes an FTC from a benign FA. In FVPTC, the growth pattern is follicular and clearly identifying nuclear features of PTC can usually not be distinguished cytologically.

As an alternative to FNAC, the use of core needle *histological* biopsy has recently received

increased interest [3]. Although lower non-diagnostic (Bethesda I) or indeterminate rates are published, core needle *histological* biopsy requires more advanced training for radiologists and histopathologists. Furthermore, this procedure is more painful for patients and has more complications including haematomas and voice changes, and therefore it has not been well-adopted.

The American Thyroid Association (ATA) specified recommendations for the clinical management of the different cytological categories [4]. Repeat FNAC for a Bethesda III nodule may oftentimes result in a Bethesda II result. For nodules that remain Bethesda III after repeat FNAC, or those with Bethesda IV or V cytology, diagnostic hemithyroidectomy is often performed [4]. As the joint malignancy rate in indeterminate nodules is approximately 25%, approximately 75% of these diagnostic surgeries result in a benign histopathological diagnosis. For these benign nodules, the diagnostic surgery can be considered unbeneficial from an oncological perspective, increasing health care consumption expenses and exposing patients to unnecessary surgical risks. In case of malignant histopathology, a completion thyroidectomy might be indicated, putting the patient at a higher risk of two-stage surgical complications and consequently additional costs. Therefore, an additional diagnostic test or combination of tests may prevent unbeneficial diagnostic hemithyroidectomies for benign nodules by ruling out malignancy, and/or prevent two-stage surgery if malignancy can be confirmed pre-operatively.

A multimodal stepwise approach using a sensitive rule-out test and a specific rule-in test might provide the most conclusive diagnosis for indeterminate thyroid nodules [5]. The ATA guidelines state that an ideal "rule-in" test would have a positive predictive value (PPV) similar to a malignant cytologic diagnosis (i.e. 98.6%), and an ideal "rule-out" test would have a negative predictive value (NPV) similar to a benign cytologic diagnosis (i.e. 96.3%) [2, 4]. Diagnostic tests on cytological samples might include molecular tests like gene mutation panels, gene or microRNA expression profiles, immunocytochemistry, and sequencing techniques. Also, several imaging modalities may be used in the workup of indeterminate thyroid nodules in vivo, including anatomical imaging techniques such as US and magnetic resonance imaging (MRI), and molecular imaging techniques such as 2-[^{18}F]fluoro-2-deoxy-D-glucose ([^{18}F]FDG) positron-emission tomography (PET) combined with computed tomography (CT) and hexakis(2-methoxy-2-methylpropylisonitrile) technetium[^{99m}Tc] ([^{99m}Tc]Tc-MIBI, also known as [^{99m}Tc]Tc-sestaMIBI) scintigraphy with single photon emission computed tomography combined with CT (SPECT/CT). Performance of any diagnostic tests is usually expressed by their sensitivity, specificity, PPV, NPV, accuracy, diagnostic odds ratio (dOR), positive likelihood ratio (LR+), negative likelihood ratio (LR-), area under the receiver operating characteristic curve (AUC), and benign call rate, when available (Panel 5.1). The reader should be aware that, albeit clinically very useful, parameters like PPV, NPV but also accuracy and benign call rate are dependent on the a priori risk of a patient suffering from the disease and thus can only be compared between different cohorts if the definition and prevalence of the malignancy are similar. Most studies featured in this chapter present outcome measures of a single cohort, without validation in a separate part of the dataset or (preferably) in an external cohort. When (external) validation was performed, this is specifically mentioned.

This chapter provides an overview of biomarkers obtained using conventional as well as AI-based non-invasive imaging strategies for the differentiation of thyroid nodules with indeterminate cytology. It presents the ability of a test to differentiate between benign and malignant nodules, taking into account the clinical readiness and cost-effectiveness. This chapter presents studies with different definitions of indeterminate cytology: some include Bethesda III and IV, only; others also include Bethesda V; and some have not incorporated the Bethesda System yet. The definition of indeterminate cytology will be specifically reported, when available.

Panel 5.1: Performance Measures of Diagnostic Tests

- $\text{sensitivity} = \dfrac{\text{true positive}}{\text{true positive} + \text{false negative}} = \dfrac{\text{true positive}}{\text{all diseased}};$
- $\text{specificity} = \dfrac{\text{true negative}}{\text{true negative} + \text{false positive}} = \dfrac{\text{true negative}}{\text{all healthy}};$
- $\text{positive predictive value}(\text{PPV}) = \dfrac{\text{true positive}}{\text{true positive} + \text{false positive}} = \dfrac{\text{true positive}}{\text{all positive}};$
- $\text{negative prective value}(\text{NPV}) = \dfrac{\text{true negative}}{\text{true negative} + \text{false negative}} = \dfrac{\text{true negative}}{\text{all negative}};$
- $\text{accuracy} = \dfrac{\text{true positive} + \text{true negative}}{\text{true positive} + \text{true negative} + \text{false positive} + \text{false negative}} = \dfrac{\text{all correct}}{\text{all examined}};$
- $\text{prevalence} = \dfrac{\text{true positive} + \text{false negative}}{\text{rue positive} + \text{true negative} + \text{false positive} + \text{false negative}} = \dfrac{\text{all diseased}}{\text{all examined}}$
- $\text{diagnostic odds ratio}(\text{dOR}) = \dfrac{\text{true positive / false positive}}{\text{false negative / true negative}} = \dfrac{\text{LR}+}{\text{LR}-};$
- $\text{positive likelihood ratio}(\text{LR}+) = \dfrac{\text{true positive} / (\text{true positive} + \text{false negative})}{\text{false positive} / (\text{false positive} + \text{true negative})} = \dfrac{\text{sensitivity}}{1 - \text{specificity}};$
- $\text{negative likelihood ratio}(\text{LR}+) = \dfrac{\text{false negative} / (\text{true positive} + \text{false negative})}{\text{true negative} / (\text{false positive} + \text{true negative})} = \dfrac{1 - \text{sensitivity}}{\text{specificity}};$
- Receiver operating characteristic (ROC) curve: true positive rate (=sensitivity) against the false positive rate (=1-specificity) at various threshold settings;
- Area under the receiver operating characteristic curve (AUC);
- Benign call rate:cytomorphologically indeterminate cases with subsequent benign molecular results.

  $\text{benign call rate} = \dfrac{\text{true negative+false negative}}{\text{true positive+true negative+false positive+false negative}} = \dfrac{\text{all negative}}{\text{all examined}}$

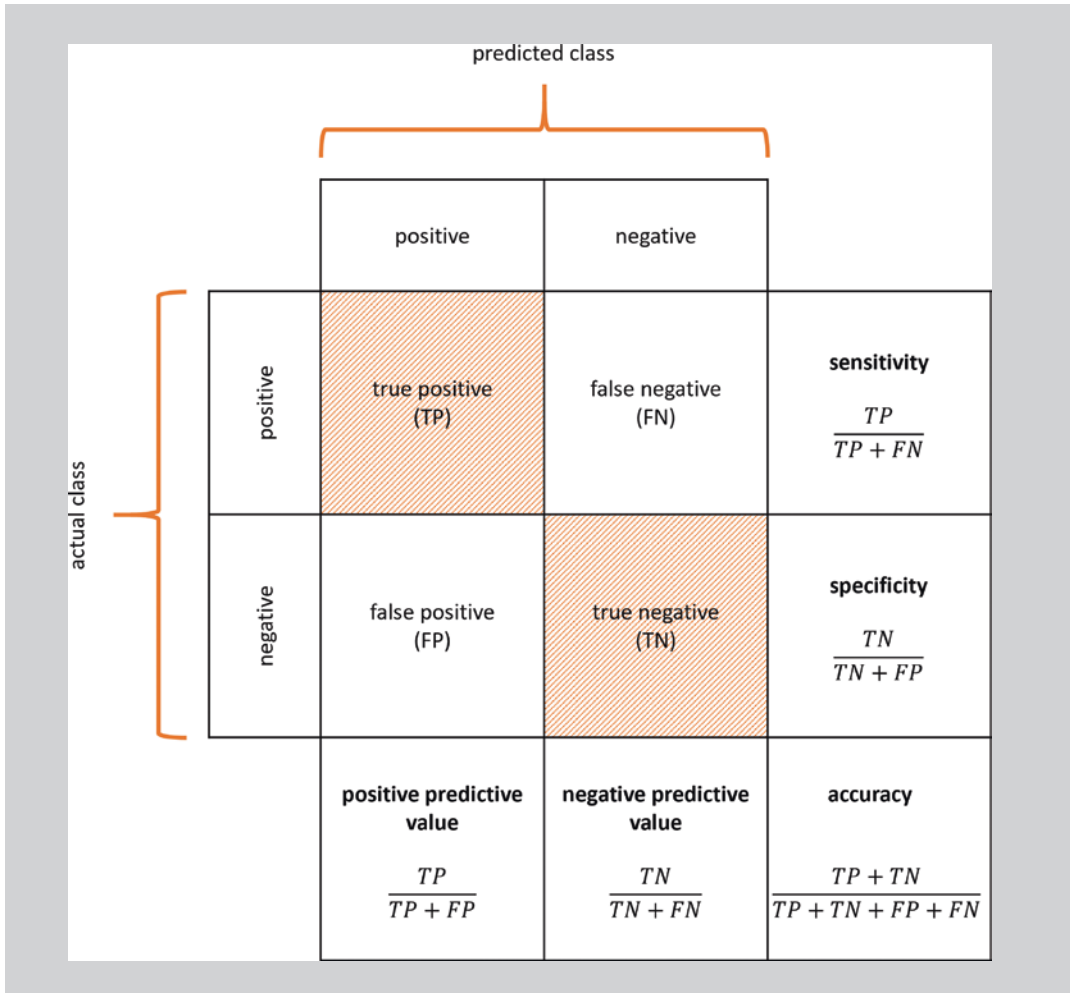

5.2 Uniting Medical Imaging with Artificial Intelligence

Unlike tissue sampling procedures, medical imaging can provide information about the entire lesion, including intra- and interlesional heterogeneity [6], thereby circumventing the shortcoming of sampling error that may occur with FNAC. Visual interpretation of images consists of (qualitative) assessment of signal intensity (e.g. density, echogenicity, radiopharmaceutical uptake, and apparent diffusion coefficient), location, size, shape, deformability (elastography), border (relation with surrounding tissues), patterns or vascularity (e.g. intravenous contrast enhancement, Doppler) of lesions. Medical imaging can stratify nodules before FNAC-procedures and thereby guide the choice of sampling location. Moreover, it can provide circumstantial evidence towards the nature of the nodule, such as suspicious cervical lymphadenopathy.

5.2.1 Quantitative Imaging

Medical images contain much more information about the biology of the lesion hidden in the myriad of voxels of both lesions and healthy tissue than can be assessed visually by a human reader [7]. (Semi-)quantitative analysis of the images provides an objective complement to visual interpretation. The use of quantitative imaging in

(multidevice) studies, and to a lesser extent in clinical management, requires adequate repeatability and reproducibility [8]. Repeatability refers to the likelihood of obtaining the same result in the same patient, when examined more than once on the same system. Reproducibility refers to the ability to yield the same results when that patient is examined on different systems and/or at different imaging sites. Ultimately, quantitative imaging enables the comparison of measurements in a single subject with normative values from a healthy population and permits the monitoring of subtle changes caused by the progression or remission of disease.

PET, as no other, allows for (semi-)quantitative analysis [9]. The standardized uptake value (SUV, unit [g/mL]) expresses the ratio between the local activity concentration and the decay-corrected amount of injected radiotracer per unit of body mass. It indicates the radiotracer concentration factor in a specific region compared to homogeneous distribution of the radiotracer through the body. In case of the radiotracer [^{18}F]FDG, the SUV is generally higher in malignant than in benign lesions. Nevertheless, the SUV is not only determined by tumour biology but also by preparative, procedural and post-procedural factors. The European Association of Nuclear Medicine (EANM) established guidelines for PET tumour imaging with the aim to achieve harmonization in multicentre settings including accreditation programmes (EARL) [8].

CT also allows for quantification, as attenuation coefficients of tissues are linearly transformed to Hounsfield units (HU), where a value of 0 represents the attenuation coefficient of distilled water and a value of −1000 represents the attenuation coefficient of air. However, in practice, deviations in this linearity occur. Increasing the tube voltage and with that the photon energy generally decreases the probability of interactions, i.e. attenuation and, therefore, increases penetration. Also, different scanners deliver different tube currents or photons to the subjects for a given milliamperage × seconds (mAs), as a consequence of differences in beam filtration, variances in tube potential, and rotation times [10]. Consequently, a fixed milliamperage yields different exposures, resulting in noise differences and inconsistencies in HU measurements. Other critical factors include spatial and temporal resolution, reconstruction kernel, subject positioning within the CT scanner bore, breath-holding techniques, and the (frequency of) monitoring of the CT scanner calibrations (i.e. quality control procedures). No central accreditation programmes have been ventured yet, but harmonization has been attempted in specific applications [10].

Quantitative analysis of MRI is even more complex, due to the relative scale of the so-called weighted images. Image contrast is affected by factors intrinsic to the tissue, specific to the examination, and dependent on the hardware. Also, conventional MRI techniques lack biological specificity, i.e. different physiological and pathological substrates can produce similar changes in image contrast. MRI studies can be quantified by obtaining parametric maps of meaningful physical or chemical variables (e.g. apparent diffusion coefficient, ADC) that can be measured in physical units (mm^2/s for ADC) and compared between tissue regions and amongst subjects. As for CT, only local initiatives aim to harmonize images [11, 12].

Conventional US is qualitative in nature, but quantitative US can provide specific numbers related to tissue features that can increase the specificity of image findings [13]. Qualitative bright mode (B-mode) US displays a morphological representation of the tissue, obtained from the radiofrequency data. Quantitative US, on the other hand, processes the raw radiofrequency data from tissue backscatters to characterize and distinguish phenotypic changes at a cellular level. Other US techniques like spectral-based parameterization, elastography, shear wave imaging, flow estimation, and envelope statistics can also be performed quantitatively. However, most clinical devices do not incorporate quantitative US yet.

5.2.2 Artificial Intelligence

Recent developments in computer science have led to advanced artificial intelligence (AI)

approaches, capable of capturing the information concealed in the image in the interest of lesion or disease detection, classification and diagnosis, segmentation, image reconstruction, and quantification [14]. An important breakthrough within AI was the advancement of machine learning, the ability of a system to extract information from raw data and to learn from experience. Decision trees, random forests, and support-vector machines are well-known examples of machine learning algorithms. More recently, deep learning, which is a subset of machine learning that uses a (convolutional) neural network structure loosely inspired by the human brain, emerged, providing even more sophisticated algorithms (Fig. 5.1) [14]. Growing amounts of data and the availability of powerful computational hardware have empowered AI, allowing computers to better represent and interpret complex data [15].

The development and, to a lesser extent, use of AI in oncology are rapidly emerging, also in thyroid cancer. Applications vary from detection of abnormalities, lesions characterization, and the prediction of treatment response [16–19]. Whereas the first AI algorithms performing simple tasks with subhuman performance, more recent algorithms sometimes surpass humans in task-specific applications. As a result, tasks that, until a couple of years ago, could only be performed by humans, can now be executed by AI algorithms. In addition, AI algorithms have the potential to reduce variation, improve efficiency and prevent avoidable medical errors, when integrated in clinical practice as tools to assist clinicians [20]. Quantitative assessment by an algorithm reduces subjectivity that comes with visual assessment, because of the education and experience of a human reader, thereby preventing inter- and intraobserver variability [15]. In addition, a human reader can consider only a few variables at a time, quickly approaching the information processing capacity [21]. In contrast to qualitative assessment by a human reader, AI algorithms evaluate a large number of complex quantitative variables together, consistently, fast, and efficiently. A major challenge of AI, however, is that the quality of a model highly depends on the input data, which is also referred to as "garbage in, garbage out". Furthermore, AI algorithms are often considered as black boxes, since they usually lack an easy and intuitive interpretation that can be interpreted in the domain of biology or radiology [22, 23]. Explainable AI (XAI) is developed to facilitate the interpretation of

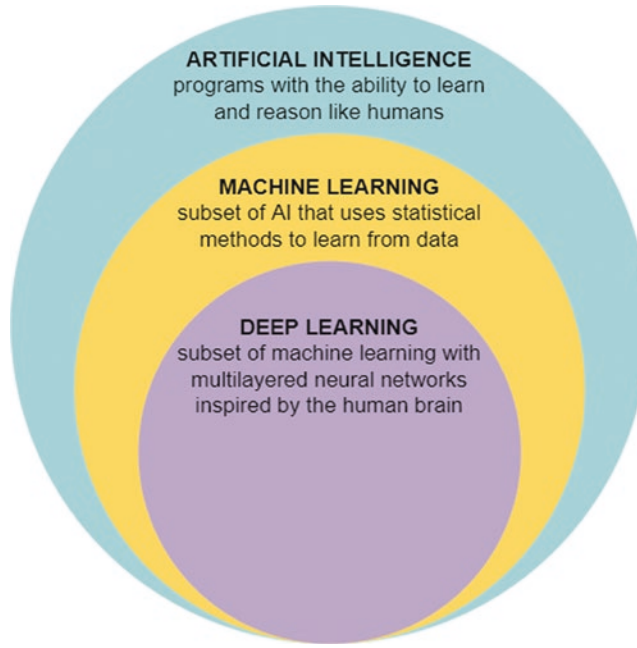

Fig. 5.1 Differences between artificial intelligence, machine learning, and deep learning

data in the context of a specific application and to retrace the results on demand [22]. Moreover, AI methodology is often heterogeneous and not unambiguously reported, complicating validation of the model. Model validation is a crucial step towards clinical translation, verifying whether the model is predictive for the general target population or just for a particular subset of patients. Models must be validated using an independent test set, preferably using data from a different institution. Currently, a lack of this external validation is still one of the major limitations of AI, whilst replication might be of even more scientific value than original discoveries [24].

Since 2012, AI analysis of a large number of quantitative variables derived from medical images has been studied in the field of radiomics [25]. Radiomics consists of the conversion of (parts of) medical images into a high-dimensional set of quantitative features and the subsequent mining of this dataset for potential information useful for the quantification or monitoring of tumour or disease characteristics in clinical practice. The field of radiomics includes the extraction of predefined, handcrafted intensity (i.e. first order), shape and texture features combined with statistical methods or machine learning algorithms for modelling; and more recent deep learning algorithms that both learn features from raw data and perform modelling (Fig. 5.2) [26]. To create a holistic model, in addition to the imaging features, clinical characteristics or other -omics data, like genomics, proteomics, or metabolomics, are also incorporated [27]. Radiomic analysis aims to find stable and clinically relevant image-derived biomarkers for tumour characterization, prognostic stratification, and response prediction, thereby contributing to precision medicine. In this chapter, the umbrella term radiomics encompasses a broad spectrum of image analysis methods, ranging from simple AI-based methods to sophisticated deep learning algorithms.

The promises of radiomics were high. Hypothesizing that medical images contained much more information than could be assessed by the human eye, radiomics was expected to contribute to medical decision-making on a large scale and even to provide new insights into disease processes [7]. Yet, as for any new technology, many (technical and statistical) challenges have to be faced before reaching the goal of large-scale implementation in clinical practice. Radiomic features are sensitive to technical variations in the different steps of the radiomic pipeline (Fig. 5.2), hampering the reproducibility, validation, and clinical translation of radiomic research. These technical variations should be as small as possible in order to attribute differences in feature values to tumour biology instead of technical variation.

Image acquisition and reconstruction largely contribute to data inhomogeneity. Radiomic analysis often consists of retrospective analysis of standard-of-care images and reanalysis of previously published cohorts, where scanners and scan protocols may vary widely between different manufacturers and medical centres. Also, volume of interest segmentation should be performed in a standardized manner, preferably (semi-)automatically using an algorithm to reduce inter- and intraobserver variability [28]. In addition, a lack of standardization in definition and extraction of radiomic features introduced variation. The Image Biomarker Standardisation Initiative (IBSI) made an effort to harmonize this by providing common nomenclature, mathematical definitions, benchmarks for image processing and feature extraction, and reporting guidelines [29, 30]. Similarly, repeatability and reproducibility studies have been performed to identify features that show minimal variations at different time points, under different conditions and with different feature definitions [31, 32].

Besides overcoming technical variations, another challenge of radiomics lies in a large number of features (generally over 100 features per lesion) compared to the number of subjects in a study (varying from several tens to hundreds in typical PET and CT studies, respectively). In contrast to traditional biomarker research, which is hypothesis-driven, radiomic research is of explorative nature. In explorative or data-driven research, a biological rationale of a feature representing certain disease characteristics lacks

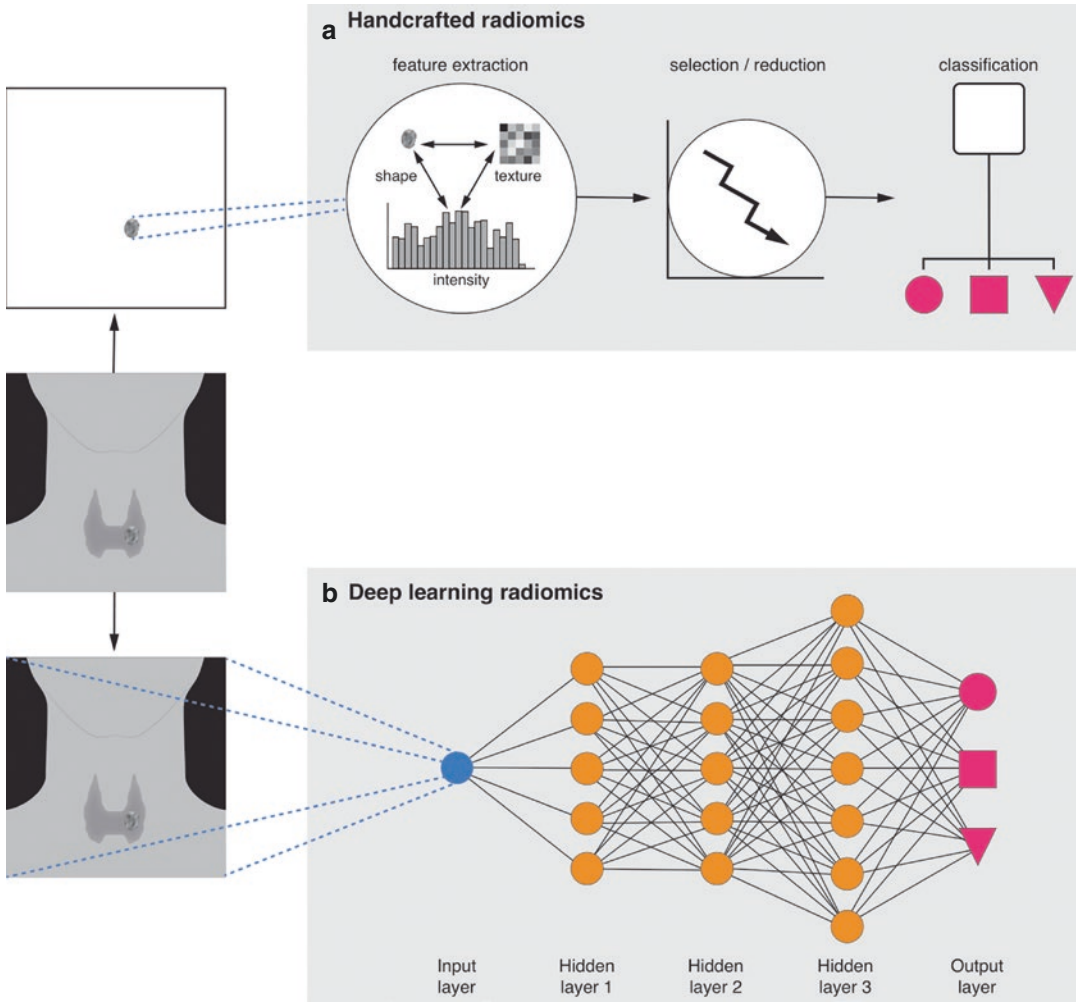

Fig. 5.2 Handcrafted and deep learning radiomics pipeline. (**a**) In the handcrafted pipeline, predefined features are extracted from a manually or (semi-) automatically defined volume of interest (VOI). Feature selection or dimension reduction is performed and these features are consecutively introduced in a statistical or machine learning model. (**b**) Deep learning radiomics does not require VOI delineation, but processes the images in their raw form. The deep learning architecture consists of several hidden layers including convolutional and pooling layers, that extract increasingly complex features and perform feature selection and classification

[33]. Therefore, many features are investigated, under the assumption that some features show association with underlying biology. Simultaneously, because of variations in scan protocols, it is challenging to find sufficiently large homogeneous datasets. When the number of data points (patients or scans) are small compared to the number of features, overfitting occurs, negatively impacting the generalization performance of the radiomic model [34]. Overfitting means that the model is specifically adjusted to the training, or input, dataset, solely reflecting its noise and random fluctuations, and, consequently, it cannot be applied to other datasets, i.e. it is not generalizable. Therefore, before modelling, the number of features should be reduced using feature selection (supervised by outcome) or dimensionality reduction (unsupervised) [35]. In the modelling step, an AI algorithm may be used to fit a function to the input data and compares it with the desired output (e.g. tumour phenotype) minimizing a cost func-

tion [36]. Several (integrated) algorithms for both feature selection/dimensionality reduction and modelling are available, but no consensus on which one to use for radiomic analysis exists. The choice of the algorithm has been shown to affect the prediction performance of the radiomic model and depends on the nature of the data [6]. Many radiomic studies employ multiple AI algorithms, which comes with the risk of multiple testing and thus increasing the false-discovery rate. Multiple-modelling strategies can be justified when comprehensively documented to ensure reproducibility, and when extensively (and externally) validated [37]. In addition to external validation of the radiomic model, another strategy that contributes to clinical translation is the comparison of the performance of a radiomic model with the performance of current approaches, e.g. blood biomarkers or visual interpretation. Also, false discoveries can be minimized by, amongst other things, validation of the results using sham data, i.e. randomly shuffling outcome labels or using radiomic features from healthy tissue, test-retest studies, and by studying the biological rationale, or semantics, of the radiomic features in the model [38, 39].

5.3 Modalities

5.3.1 Ultrasonography

US is an anatomical as well as functional imaging technique that uses pulses of high-frequency (2–15 MHz) sound emitted by a transducer to capture tissue characteristics in real time. The pulses are reflected by the tissue and returned to the transducer. The amplitude and time of the echo represent the reflection properties of specific tissue, which form the images. Conventional B-mode (for brightness) US displays the acoustic impedance of a two-dimensional cross-section of tissue, but other types capture blood flow, tissue motion, the presence of specific molecules, or the stiffness of tissue. Drawbacks of US are its limited field of view, its dependency on skilled operators, and its interobserver variability.

5.3.1.1 Conventional (B-Mode) Ultrasonography

US is an important step in the initial workup of thyroid nodules for its non-invasiveness, cost-effectiveness, and global availability. A large body of literature has investigated the role of US in the stratification of thyroid nodules. Two meta-analyses demonstrated that, in otherwise unselected nodules, US features like composition, hypoechogenicity, microcalcification, irregular margins (i.e. infiltrative or microlobular margins), and a taller-than-wide shape are suspicious for thyroid malignancy [40, 41]. The current ATA guidelines provide a decision tree based on nodule size and other US features with an incremental suspicion for malignancy. These well-known US features are mainly characteristic of PTC, the most prevalent thyroid malignancy. FVPTC and FTC may exhibit other characteristics and may be less easily diagnosed using this decision tree [4, 42, 43]. In an unselected population, no US feature alone is sensitive or specific enough to accurately identify malignancies, but combinations of features might provide new insights [40].

The use of US in thyroid nodules with indeterminate cytology is less widely studied. Both previously mentioned meta-analyses briefly discussed its value in indeterminate nodules (Bethesda System was not taken into account) [40, 41]. As FTC has a higher prevalence in indeterminate nodules, US using the classic characteristics is less accurate in indeterminate nodules than in unselected thyroid nodules, generally demonstrating limited sensitivity. Only solid nodules, in contrast to partially cystic nodules, demonstrated sensitivities above 90% (range: 46%–100%) [5]. The features taller-than-wide shape, presence of irregular margins, presence of microcalcifications, and nodule diameter larger than 4 cm were promising, with specificities ranging from 72% to 99%, 65% to 100%, 36% to 100%, and 69 to 94%, respectively [5]. Remonti et al. presented an increased central vascularization as the best predictor for malignancy, with a specificity of 96%, but other studies showed extremely poor specificities, ranging from 0% to 100% [41].

5.3.1.2 TI-RADS

Since 2009, several US-based risk stratification systems to identify nodules that warrant biopsy or sonographic follow-up have been proposed. Following the BI-RADS classification system that is widely used in breast imaging, the American College of Radiology (ACR) presented the TI-RADS (for Thyroid Imaging, Reporting, and Data System). TI-RADS aims to (1) provide recommendations for reporting incidental thyroid nodules, (2) develop a set of standard terms (lexicon) for US reporting, and (3) propose a TI-RADS risk stratification system on the basis of the lexicon [44]. The ACR TI-RADS scores the composition, echogenicity, shape, margin, and echogenic foci of a thyroid nodule, all consisting of 0 up to 3 points. The total number of points determines whether a nodule is considered benign (TR1, 0 points), not suspicious (TR2, 2 points), mildly suspicious (TR3, 3 points), moderately suspicious (TR4, 4–6 points), or highly suspicious (TR5, ≥7 points) and also guides the decision to perform FNAC or follow-up: no FNAC or follow-up (TR1–2), FNAC if nodule maximum diameter (ø) ≥ 2.5 cm and follow-up if ø ≥ 1.5 cm (TR3), FNAC if ø ≥ 1.5 cm and follow-up if ø ≥ 1.0 cm (TR4) or FNAC if ø ≥ 1 cm and follow-up if ø ≥ 0.5 cm (TR5).

In addition to ACR TI-RADS, the European Thyroid Association and the Korean Society of Thyroid Radiology/Korean Thyroid Association developed similar US risk stratification systems; the EU-TI-RADS and K-TI-RADS, respectively [45, 46]. Also, the ATA and the American Association of Clinical Endocrinologists/American College of Endocrinology/Associazione Medici Endocrinologi propose US risk stratification systems [4, 47]. An international survey investigating the utilization of all five aforementioned risk stratification systems with 875 respondents in 52 countries demonstrated that almost one-third of respondents used more than one risk stratification system in their practice, potentially leading to confusion [48]. Grani et al. compared the risk stratification systems in 477 patients and found that the systems vary widely in their ability to reduce the number of unnecessary thyroid nodule FNACs (17.1 up to 53.4%) [49]. The ACR TI-RADS outperformed the others, classifying more than half of the biopsies as unnecessary with a false-negative rate of 2.2%. The remainder of this chapter focuses on the ACR TI-RADS.

Over recent years, TI-RADS has become fully incorporated in the management of thyroid nodules [4]. As FNAC may be more systematically withheld for patients with a presumed benign nodule with TI-RADS 1, 2, and most 3, the patient population that is selected for additional diagnostic tests has potentially changed. Many of the studies on additional diagnostics have not incorporated TI-RADS yet, and it is currently unclear to say what effect the introduction of TI-RADS may have on the diagnostic accuracy and therapeutic yield of other tests. A different population, or reference class, with a larger proportion of malignant nodules, impacts the PPV and NPV, but also the sensitivity and specificity.

Stratification of cytologically indeterminate nodules according to the risk of malignancy as determined by combining the TI-RADS and Bethesda system might be of interest, notwithstanding a limited body of evidence comprising small retrospective cohorts. Larcher de Almeida et al. investigated the risk of malignancy in indeterminate thyroid nodules by combining the ATA classification with cytological subcategorization (nuclear atypia, architectural atypia, oncocytic atypia) [50]. They found that the risk of malignancy reached almost 80% when both nuclear atypia and ATA-based high-risk US features are present. The presence of these cytological features also increased the risk of malignancy in the ATA-based intermediate-risk category. Architectural atypia and oncocytic patterns were not independently related to higher cancer risk. Moreover, a recent meta-analysis by Staibano et al. including 17 studies investigated sonographic risk criteria (ACR TI-RADS, EU TI-RADS, K-TI-RADS, or ATA) for further prognostication of Bethesda III and IV nodules [51]. In both Bethesda III and Bethesda IV nodules separately, ATA had the highest pooled specificity of 90% and 94% (sensitivity of 52% and 15%), whilst K-TI-RADS had the highest pooled sensitivity of 78% and 91% (specificity of 53%

and 40%), respectively. EU-TI-RADS does not contribute to the clinical management of patients with cytologically indeterminate Hürthle cell nodules, particularly those classified as Bethesda IV [52]. These results underline the combination of cytological subcategorization and US risk stratification in the management of indeterminate nodules. A conservative approach is proposed in nodules with low-risk US suspicion and Bethesda III, whilst additional diagnostics and surgery should be considered for nodules with high-risk US suspicion and Bethesda IV or V [53, 54].

AI has been investigated for the optimization of the ACR TI-RADS risk stratification. Wildman-Tobriner et al. developed AI TI-RADS as a simplification of ACR TI-RADS in unselected nodules, where six features were assigned zero points, using a genetic algorithm inspired by natural selection and its genetic underpinnings [55]. The model was trained using 1325 nodules and validated using 100 nodules, resulting in similar AUCs for ACR TI-RADS and AI TI-RADS of 91% and 93%, respectively. The specificity of AI TI-RADS (65%) was higher than that of ACR TI-RADS (47%).

US radiomics is gaining interest in thyroid nodules. Yoon et al. built a US radiomic score for the differentiation of benign and malignant lesions, retrospectively including 155 nodules with Bethesda III and IV indeterminate cytology [56]. Seven hundred thirty radiomic features were extracted from a square region of interest delineated on a representative 2D image of the initial US. A radiomic score incorporating 15 radiomic features combined with clinical variables (nodule size, gender, age, Bethesda category) performed significantly better than a model composed of clinical variables only with cross-validated AUCs of 84% and 58%, respectively. Major limitations of this study are the use of clinical US images instead of quantitative images and the choice of a representative image by a human reader. Although inherent to US imaging, bias is introduced by the implicit radiologist input in the selection of the 2D slices as described as the Clever Hans effect by Wallis et al. in a widely used MRI dataset [57].

In addition, in unselected nodules, US radiomic analysis has been extensively studied for the differentiation of benign and malignant nodules. A recent meta-analysis by Cleere et al. including 75 studies found a pooled sensitivity of 87% and a pooled specificity of 84%, which indicates that, for some patients, the use of radiomics could possibly circumvent the need for FNAC and surgical resection [58]. For deep learning radiomics using convolutional neural networks (CNN), the pooled sensitivity and specificity were 85% and 82%, significantly lower than for studies using non-CNN (sensitivity: 90%, specificity: 88%), which might be due to a larger required sample size for a deep learning radiomic study (at least 800) compared to a handcrafted radiomic study (around 100) [38]. The meta-analysis only touches upon the heterogeneous methodology of included studies, stating the broad spectrum of analysis methods and interobserver variability of US. Notwithstanding, radiomic features extracted from US images are impacted by the slice variability and preprocessing [59]. To improve feature repeatability, the use of intensity standardization with outlier removal applied to the region of interest and a fixed bin size grey-level discretization could be performed and these and other pre-processing steps should be extensively documented [59]. When standardization of the radiomic methodology is performed and US radiomics is validated in large prospective cohorts, it has the potential to become a non-invasive and cost-effective diagnostic tool in (cytologically indeterminate) thyroid nodules.

5.3.1.3 Elastosonography

One of the key features during palpation of thyroid nodules is the degree of firmness; malignant nodules tend to be firmer than benign ones. Palpation, however, is highly subjective and depends on the size and location of the nodule and on the skill of the practitioner. Elastosonography, a dynamic US technique that is used to evaluate the biomechanical viscoelastic properties of tissue, provides a quantitative method to measure tissue firmness or elasticity. Lyshchik et al. were the first to practice elastosonography for the eval-

uation of the elasticity of thyroid nodules, measuring the tissue distortion whilst applying a standardized dosed external force by the US transducer [60]. Elastosonography methodology is diverse, but it follows the principle of estimating displacement fields in tissue using correlation techniques that track the echo delays in waveforms recorded before and after the quasistatic compression. Qualitative evaluation of the thyroid elasticity is performed by repeated manual compression (also known as strain elastosonography), taking into account the amount of compression and different zones of interest (i.e. healthy tissue should be included in the measurement, which might be complicated in the presence of thyroid diseases or large nodules) [61]. Alternatively, and circumventing the problem that the mechanical compression force applied to the tissue cannot be measured accurately and thus the absolute tissue strain cannot be calculated, shear wave elastosonography has been developed. This technique evaluates tissue stiffness through focused pulses of US instead of mechanical compression [62]. This acoustic force causes horizontal displacements in the tissue, which are called shear waves. These shear waves contain quantitative data about the elastic properties of the tissue that can be measured in propagation speeds of these sheer waves (m/s) or nodule stiffness (kiloPascals). It has the advantages of being more objective, having a higher reproducibility, and having decreased operator dependence.

A colour-coded image superimposed on the grayscale B-mode US images is generated, with colours in the red spectrum representing soft tissues and colours in the blue spectrum representing firm tissues. (Semi)quantitative analysis uses numerical values that correspond to the deformation ratios (strain) or stiffness (sheer wave), scored according to several systems.

A meta-analysis by Nell et al. based on 20 qualitative elastosonography studies concluded that elastosonography could accurately diagnose benign nodules with both a pooled sensitivity and a NPV of 99%, thereby safely dismissing FNAC, on condition that only completely soft nodules are classified as benign (benign call rate 14%) [63]. The role of elastosonography in the preoperative workup of cytologically indeterminate thyroid nodules is limited. Qualitative US based on colour-scales has insufficient sensitivity and specificity and semi-quantitative methods lack validation. A meta-analysis including 20 studies on both qualitative and quantitative techniques and a total of 1.734 indeterminate thyroid nodules reported an overall pooled sensitivity and specificity of 77% and 87%, respectively, with similar diagnostic accuracies for real-time, shear wave and strain ratio elastosonography [64]. The power of the available evidence is negatively impacted by methodological heterogeneity in imaging techniques, image processing, and elasticity scoring methods across studies. Yet, the suggested rule-out capacity of qualitative elastosonography when only completely soft nodules are included is worth validating in indeterminate thyroid nodules, for its easy implementation and potential low costs. Elastosonography can be performed during regular thyroid US with the same equipment, prolonging the procedure to only 5 min. To the best of our knowledge, no cost-effectiveness studies have been carried out in indeterminate thyroid nodules, possibly limited by the heterogeneous methodology.

5.3.2 Computed Tomography

CT is a 3D anatomical imaging technique that reflects X-ray attenuation by different tissues. CT scanners use a rotating X-ray tube and an oppositely placed row of detectors placed in the gantry to measure X-ray photon attenuations, which are reconstructed into tomographic images. Contrast enhancement by iodine-based intravenous contrast may be performed to highlight structures such as blood vessels that otherwise would be difficult to distinguish from their surroundings on native-phase CTs, to obtain functional (perfusion) information about tissues and to improve soft tissue contrast. However, the usage of iodinated intravenous contrast media is relatively contra-indicated as a post-thyroidectomy radioiodine (^{131}I) ablation dose might be indicated in patients suffering from differentiated thyroid cancer. The effectiveness of radioiodine therapy

might decrease by recent use of high doses of iodine and an interval of at least 1 month between iodinated contrast and radioiodine is recommended [65].

CT has not been investigated in thyroid nodules specifically with indeterminate cytology. In unselected nodules, some studies have been performed. Lee et al. found no significant differences between benign and malignant lesions in a number of lesions, lesion size, presence of calcifications, lesion consistency, and lesion attenuation on CT in a dataset of 109 nodules (100 benign, 9 malignant) [66]. Another study in PTC found that CT was inferior to US for the evaluation of thyroid nodules [67]. More recently, AI has been investigated for CT lesion characterization. Peng et al. investigated first-order features for the identification of malignant nodules ($N = 50$), benign nodules ($N = 84$), and healthy controls ($N = 150$), resulting in a sensitivity, specificity, PPV, NPV, and accuracy of 82%, 93%, 92%, 85%, 95%, and 88%, respectively [68]. It should be noted that results have not been validated using a test set. Li et al. developed a deep learning model for automatic recognition and classification of thyroid nodules on iodine contrast-enhanced CTs [69]. The model was trained in a dataset of 786 nodules (543 benign and 243 malignant) and validated in a test set of 137 nodules (103 benign and 34 malignant), resulting in an accuracy of 85%. There is a large class imbalance between benign and malignant nodules, which might have affected the accuracy, but authors state that this was corrected by using class weights.

The role of CT in the pre-operative differentiation of thyroid nodules is limited compared to other imaging techniques. Yet, since CT is an important source of thyroid incidentalomas (incidence: 15% [70]), computer-aided detection systems to automatically recognize and classify thyroid incidentalomas on CT might be of interest.

5.3.3 Magnetic Resonance Imaging

Magnetic resonance imaging (MRI) is a 3D anatomical as well as functional imaging technique based on nuclear magnetic resonance [71]. MRI scanners use strong magnetic fields, magnetic field gradients, and radiofrequency waves to generate images of the organs in the body, with improved soft tissue contrast compared to (contrast-enhanced) CT. Protons (hydrogen atoms) in body tissue that contain water, give off a signal that can be processed into an image. First, a pulse of electromagnetic radiation is used to excite nuclei of atoms in the magnetic field with exactly the right resonance frequency. The excited nuclear spins of the hydrogen nucleus undergo relaxation to the ground state whilst emitting radiofrequency waves, which are measured with a receiving coil. The contrast between different tissues is determined by the speed at which the nuclear spin of excited nuclei returns to the ground state. Since different tissues have different hydrogen densities, details of the anatomy can then be observed.

Different tissue properties can be measured using different pulse sequences of pulsed magnetic field gradients, radiofrequency pulses, intervals between delivery of successive pulses, between pulse delivery and receipt of the echo signal etc. Intravenous contrast, mostly by paramagnetic substances containing gadolinium, enhances relaxation of the excited nuclear spins and thus adds information about tissue perfusion. MRI imaging is less widely available, more complex, lengthy, and costly than US and CT, but provides unsurpassable soft tissue contrast without the use of ionizing radiation.

The classic spin and gradient echo sequences resulting in T1-, T2-, proton density-, and susceptibility-weighted sequences seem to have limited classification value in indeterminate thyroid nodules. Effective T2 mapping (T2* mapping) was explored by Shi et al. in 28 patients with thyroid nodules of different cytological subclasses, subjected to (therapeutic and diagnostic) surgery, describing 100% specificity and 84–90% sensitivity to distinguish malignant and benign thyroid nodules [72]. The use of dynamic gadolinium contrast-enhanced MRI has found conflicting results [73, 74]. A much larger body of evidence has been found for diffusion-weighted MRI (DWI) and proton-magnetic resonance spectroscopy (MRS).

5.3.3.1 Diffusion-Weighted Magnetic Resonance Imaging

DWI is a specific form of MR imaging that is sensitive to the random Brownian motion of water molecules within a voxel of tissue. The easier water molecules diffuse and move around in a region, the higher the isotropic signal will be at higher degrees of diffusion weighting (b-value). Apparent Diffusion Constant (ADC [mm^2/s]) imaging results from a series of conventional DWI sequences with different b-values. The change in signal is proportional to the rate of diffusion. An ADC image thus is an MRI image that more specifically shows diffusion than conventional DWI, by eliminating the T2 weighting that is otherwise inherent to conventional DWI. Contrary to DWI, the standard grayscale of ADC images is to represent a smaller magnitude of diffusion as darker. Generally, highly cellular tissues or those with cellular swelling exhibit lower ADC values.

The use of DWI in cytologically indeterminate thyroid nodules is limited and methodology varies largely. Nakahira et al. evaluated the role of the ADC in 42 nodules, including 15 (36%) with indeterminate cytology (Bethesda System was not taken into account) [75]. The final diagnosis was confirmed by surgery and mean ADCs (acquired with b-values of 0 and 1000 s/mm^2) were compared between benign and malignant nodules (all with indeterminate cytology). Malignant nodules showed significantly lower ADCs than benign nodules. For all nodules, a cut-off value for malignant nodules of 1.60×10^{-3} mm^2/s yielded a sensitivity, specificity, and accuracy of 95%, 83%, and 88%, respectively. It was concluded that ADC measurements could potentially quantitatively differentiate between benign and malignant thyroid nodules, even those of indeterminate cytology [75]. Chung et al. investigated the value of histogram analysis of ADC maps in the differentiation of follicular thyroid carcinoma from follicular adenoma in 17 Bethesda III and IV indeterminate nodules on US-guided core needle biopsy [76]. Histogram parameters were derived from ADC values (acquired with b-values of 0 and 800 s/mm^2) obtained from the entire tumour volume and compared with the histopathological diagnosis. It was found that 10th, 25th, and 50th percentiles of the ADC values were all significantly lower in follicular adenoma than in follicular thyroid carcinoma. ROC curve analysis revealed that the 25th percentile resulted in the highest AUC of 87%, with an optimal cut-off value of 0.353×10^{-3} mm^2/s. A lower ADC value in follicular adenoma compared to follicular carcinoma seems contradictory with results of Nakahira et al., where lower ADCs were found in malignant nodules. The probable reason for this is that Nakahira et al. predominantly included PTC with histological characteristics of calcifications and desmoplastic reactions, which cause restriction of free water movement in the cellular environment and reduce ADC values, whereas follicular neoplasms including Hürthle cell nodules are known for their varying colloid tissue involvement and thus histologically contain more fluid. Thus, DW-MRI would inaccurately provide a more benign image [76, 77].

DWI has been more extensively investigated in the differentiation between benign and malignant unselected thyroid nodules. A 2014 meta-analysis by Wu et al. summarized seven studies with 358 subjects and presented a pooled sensitivity of 91%; a specificity of 93%, a LR+ of 12.24; a LR- of 0.99; a diagnostic OR of 123.78; and an AUC of the summary ROC of 94% [78]. In 2016, a meta-analysis by Chen et al. summarized 15 studies with 765 lesions and presented a pooled sensitivity of 90%; a specificity of 95%; a LR+ of 16.49; a LR- of 0.11; a diagnostic OR of 150.73; and an AUC of the summary ROC of 95% [79]. Most studies showed a significantly lower mean ADC value in malignant lesions compared to benign lesions, because of larger nuclei, denser stroma, and higher cell counts, all of which led to increased cellularity and reduced extracellular space. However, no absolute cut-off was found. This could be attributed to heterogeneous methodology such as varying b-values and differences in ADC measurements. Other explanations could be a diversity in patient population or components with high diffusivity in malignant lesions, like cystic components, central necrosis, or intratumoral haemorrhage.

DWI seems a promising non-invasive, non-radiative, and accurate technique for the pre-operative differentiation of (cytologically indeterminate) thyroid nodules. Nevertheless, whilst the worldwide availability of MRI scanners is growing, MRI is still considered an expensive technique in terms of hardware, overhead costs, and relatively long scan duration. Large-scale trials are necessary to assess and validate its clinical value, to establish harmonization in methodology, to determine cut-off values, and to study cost-effectiveness, specifically in FNAC indeterminate thyroid nodules.

5.3.3.2 Magnetic Resonance Spectroscopy

Magnetic resonance spectroscopy (MRS) is an analytical method used for the in vivo chemical characterization of tissue, measuring the presence and concentration of various metabolites. Magnetic resonance principles are used to detect various nuclei, such as hydrogen-1 (^{1}H), which all can provide valuable metabolic and physiological information [80]. ^{1}H-MRS is able to capture the metabolic profile of a lesion, by determination of the relative concentrations and physical properties of a variety of biochemicals. These include several low molecular weight metabolites such as choline, creatine, glutamate, lactate, and different amino acids. Spectroscopy uses the chemical shift of a nucleus to observe, identify and quantify biologically important compounds in tissue. An anatomical MR image is acquired, on which a volume of interest is selected, and the MR spectrum is acquired. As protons in water are far more abundant than the metabolites of interest (10^4:1), the water signal should be suppressed during MRS-pulse sequences.

The use of MRS specifically in indeterminate thyroid nodules was rather limited. Therefore, we focused on MRS in the differentiation of thyroid carcinoma in general. The use of magnetic resonance principles in thyroid cancer is in fact not new, but originates from ex vivo proteomic and metabolomic research [81]. MRS of cytology and biopsy specimens was attempted to overcome the limitations of FNAC [82, 83]. Also, ex vivo operative specimens have been analyzed, for the identification of the morphologic features of malignancies in the first place; with the advancement of the technology followed by the differentiation between benign and malignant neoplasms [84]. Ex vivo spectra showed lower content of lipids and higher concentrations of amino acids in malignant compared to benign nodules [85].

The first in vivo study by King et al. succeeded in discriminating thyroid carcinomas from normal thyroid tissue based on the 1.5 Tesla ^{1}H-MRS spectra [86]. In their cohort of eight patients (three anaplastic carcinomas, two papillary carcinomas, one follicular carcinoma) and five healthy controls, they found that choline-to-creatine ratio seemed a useful marker for the pre-operative differentiation. This was confirmed by other studies, showing that a choline peak was rather specific for malignancies [87, 88]. It should be noted that these studies considered the absolute choline peak, without the creatine reference. Creatine is considered a convenient internal standard, for its relatively constant level in metabolically active tissues. More recently, the choline-to-creatine ratio was further evaluated by Aghaghazvini et al. in a cohort of 9 malignant (7 papillary, 2 follicular) and 23 benign nodules using 3 Tesla ^{1}H-MRS [89]. At an echo time of 136 ms, a choline-to-creatine ratio of 2.5 corresponded best with histopathology with a sensitivity, specificity, PPV, and NPV of 75%, 100%, 100%, and 92%, respectively.

Whereas the MRS choline-to-creatine ratio seems a promising biomarker for the differentiation of thyroid nodules, all presented studies were performed in small cohorts and with varying methodologies. To the best of our knowledge, only four papers on in vivo MRS in thyroid nodules were published in almost two decades, which might indicate limited clinical interest or limited feasibility. In contrast, the field of MRS is emerging and in recent years, the use of MRS in clinical practice has increased, because of the installation of human MRI systems with high field strengths ($\geq$7 Tesla). Higher field strengths result in spectral dispersion, i.e. a larger frequency between peaks, improving the resolution, which allows more accurate quantification of tissue compounds

in smaller lesions [90]. Future studies should validate these preliminary findings and also cast light on cost-effectiveness.

5.3.3.3 Multiparametric MRI

Both DWI and ^{1}H-MRS seem promising in the evaluation of indeterminate thyroid nodules, but a multiparametric approach has not been extensively studied. Aydin et al. were the first to describe multiparametric MRI, being DW-MRI and ^{1}H-MRS, in unselected thyroid nodules [91]. Other approaches combined ADC values and descriptions of the time-signal intensity curves of dynamic contrast-enhanced MRI, finding an accuracy of 91% [92], used ADC values and T1- and T2-weighted tumour-to-non-tumour ratios with accuracies over 90% [93] or compared DWI with proton transfer imaging and found DWI to be superior [94]. Wang et al. investigated conventional MRI, DWI, and DCE in a retrospective cohort of 181 consecutive subjects (148 benign and 111 *unstratified* malignant nodules, confirmed by pathological results) [95]. The multivariable analysis revealed that ADC value, irregular shape, ring sign in the delayed phase, and cystic degeneration were independent predictors of malignancy, with an AUC, sensitivity, and specificity of these variables combined of 99%, 97%, and 95%, respectively. Song et al. investigated intravoxel incoherent motion MRI and DCE in 38 unstratified nodules and found that parameters were significantly different between benign and malignant nodules [96].

Multiparametric radiomics has also been investigated in a dataset of 120 PTC patients to predict aggressiveness based on 1393 radiomic features extracted from T1-weighted, T2-weighted, and ADC-images. The dataset was split into a training ($N = 96$) and test set ($N = 24$) and machine learning was performed for feature selection and classification, resulting in an AUC in the test set of 92% (compared to 56% for clinical characteristics alone) [97]. Another T1, T2, and ADC radiomics approach in 132 PTC (92 training, 40 tests) used a machine learning algorithm to detect extrathyroidal extension, resulting in an AUC in the test set of 87% [98].

5.3.4 [^{99m}Tc]Tc-MIBI Scintigraphy

Scintigraphy is a 2D functional imaging technique that in vivo localizes gamma-emitting isotopes such as technetium-99 m using a gamma camera. Scintigraphy with the radiopharmaceutical [^{99m}Tc]Tc-MIBI reflects perfusion and the number of active mitochondria in cells [99]. It is primarily known for its use in myocardial perfusion imaging, the evaluation of hyperparathyroidism, and molecular breast imaging. [^{99m}Tc]Tc-MIBI scintigraphy has been investigated for the differentiation between benign and malignant nodules based on the uptake and by assessing an eventual increase in uptake within the nodule over time. [^{99m}Tc]Tc-MIBI is more suitable than [^{99m}Tc]pertechnetate or radioisotopes of iodine (^{123}I, ^{124}I (PET), ^{131}I). Iodine radioisotopes are often used to assess thyroid nodule functioning ("hot" or "cold"), which are unspecific and ineffective for the further stratification of cytologically indeterminate thyroid nodules. Whereas malignant nodules are almost solely cold, as cell dedifferentiation results in a decrease of the sodium-iodide symporter and thereby lower [^{99m}Tc]pertechnetate or radioiodine uptake, benign nodules can be hot as well as cold, whilst far outnumbering carcinomas. [^{99m}Tc]Tc-MIBI uptake is independent of iodine trapping and organification in the thyrocytes.

Increased [^{99m}Tc]Tc-MIBI uptake and late retention are often observed in malignant nodules [100]. A meta-analysis from 2013 by Treglia et al. showed 82% sensitivity and 63% specificity for [^{99m}Tc]Tc-MIBI scintigraphy in clinically suspicious, hypofunctioning, cytologically unselected thyroid nodules [99]. Three studies examined [^{99m}Tc]Tc-MIBI scintigraphy in cytologically indeterminate nodules (Bethesda III/IV/pre-Bethesda) [100–105], based on an early image between 10 and 20 min post-injection and a delayed image between 60 and 120 min post-injection. The uptake in the nodule and retention on the delayed image were assessed and compared with physiological wash-out in normal thyroid tissue. Nodules with increased uptake on early images that persisted or increased on the delayed images were suspicious for malignancy.

The sensitivities and specificities for visual interpretation ranged from 56% to 96% and from 20% to 95%, respectively. Semi-quantitative analysis was performed using the retention index (RI, percentage MIBI uptake reduction in a nodule between the early and the late image, corrected for uptake in the contralateral lobe) and the washout index (WO_{Ind}, percentage MIBI uptake reduction in a nodule between the early and the late image, corrected for uptake in tissue outside the thyroid). At the cut-off determined, for the RI, the sensitivities were 100% and the specificities ranged from 57% to 90% [101, 104]. For the WO_{Ind}, sensitivities were 100% and specificities ranged from 89% to 100% [100, 104, 105]. A recent retrospective multicentre study by Schenke et al. including 365 hypofunctioning Bethesda III and IV nodules in 12 European centres concluded that negative [^{99m}Tc]Tc-MIBI results on visual evaluation is an effective tool to rule-out thyroid malignancy in 18% of negative nodules [105]. Semi-quantitative image analysis may considerably improve the overall diagnostic performance at an optimal WO_{Ind} cut-off of −19%, with a sensitivity, specificity, PPV, NPV, accuracy, and benign call rate of 100%, 89%, 82%, 100%, 93%, and 61%, respectively. These findings cannot be extrapolated to all patients with indeterminate cytology, since preselection of intermediate- or high-risk nodules by EU-TI-RADS and the exclusion of hyperfunctioning nodules, probably by thyroid scintigraphy, is required.

Planar gamma camera imaging is globally widely available. Also, the tracer [^{99m}Tc]Tc-MIBI can be easily complexed using MIBI-kits and an on-site molybdenum-technetium generator. The average costs of [^{99m}Tc]Tc-MIBI scintigraphy range from €119 to €500 in Europe and from $669 to $1156 in the United States [106]. A cost-effectiveness study in 2014 found that [^{99m}Tc]Tc-MIBI-based management was more cost-effective than Afirma® gene expression classifier testing from a German perspective [106], but modelled costs for [^{99m}Tc]Tc-MIBI scintigraphy and thyroid surgery were likely underestimated and performance parameters were extrapolated from unselected nodules. Disadvantages of [^{99m}Tc]Tc-MIBI scintigraphy include the limited spatial resolution of the gamma camera, which limits the test sensitivity in lesions smaller than 30 mm, and the radiation burden is 2–6 millisievert for an adult male (20–30% higher for females) [107].

5.3.5 [^{18}F]FDG PET/CT

PET/CT is a 3D functional imaging technique that in vivo localizes and quantifies positron-emitting isotopes such as fluorine-18. PET imaging with the non-metabolizable glucose analogue [^{18}F]FDG reflects glucose metabolism [9]. After intravenous injection, [^{18}F]FDG is, like D-glucose, taken up in eucaryotic cells by the membrane-bound sodium-dependent glucose transporters (GLUT) family. In the cytosol, it is phosphorylated to [^{18}F]FDG-6-phosphate by members of the hexokinase family. As phosphoglucose isomerase, the enzyme responsible for the second step in the glycolytic pathway, does not interact with deoxyglucose [^{18}F]FDG cannot be degraded further. Moreover, as most mammalian cells lack the enzyme to dephosphorylate [^{18}F]FDG-6-phosphate, it accumulates in the cells, the rate dependent on perfusion, GLUT capacity, and hexokinase activity. Many pathological conditions cause regional alterations in glucose metabolism in tissues, through which [^{18}F]FDG PET/CT is an important tool in the detection and staging of cancer and active inflammations. [^{18}F]PET/CT is an imaging technique using ionizing radiation with high sensitivity, but limited specificity due to other causes of [^{18}F]FDG uptake: coincidental findings may lead to further invasive diagnostics. [^{18}F]FDG PET/CT is an important source of thyroid incidentalomas (i.e. unexpected incidental findings during an [^{18}F]FDG PET/CT for other indications), with a pooled incidence of around 2.5% [108] and a rate of malignancy of around 30% [109]. These incidentalomas require additional workup by FNAC when their diameter exceeds 1 cm [110].

[^{18}F]FDG PET/CT has a limited role in the management of thyroid cancer. Only when radioiodine refractory disease is suspected, [^{18}F]FDG PET/CT plays an important role in disease moni-

toring [4]. In radioiodine refractory disease, differentiated thyroid carcinomas lost the capacity to concentrate radioiodine, but still have measurable thyroglobulin serum values as sign of vital residual disease. [^{18}F]FDG PET/CT is also utilized for the initial staging of poorly differentiated or invasive Hürthle cell carcinoma. Similarly, [^{18}F]FDG PET/CT plays an important role in the staging of undifferentiated forms of thyroid cancer such as anaplastic thyroid cancer.

[^{18}F]FDG PET/CT is mentioned but not routinely advised in the current ATA guidelines for the management of thyroid nodules with indeterminate cytology, despite a growing body of evidence. The first prospective study by Kresnik et al. dates from 2003 and evaluated the usefulness of [^{18}F]FDG PET/CT in the pre-operative assessment of 43 suspicious thyroid nodules with suggestive cytologic results (pre-Bethesda) [111]. They found that thyroid carcinomas, in contrast to most benign thyroid nodules, demonstrate significantly increased glucose metabolism; at a cut-off value of the SUV of 2 g/mL, a 100% sensitivity, 63% specificity, and 100% negative predictive value was reached. However, the study by Kresnik et al. did not represent the general population, because the study was performed in an area of endemic goitre and patients with papillary carcinoma were selected as a positive control group. Subsequently, De Geus-Oei et al. investigated [^{18}F]FDG PET/CT in 44 patients with indeterminate cytology, defined as inconclusive fine-needle aspiration biopsy (pre-Bethesda), who subsequently underwent diagnostic hemithyroidectomy [112]. They demonstrated that a negative [^{18}F]FDG PET/CT could theoretically reduce the number of futile hemithyroidectomies by 66% at a NPV of 100%. A subsequent meta-analysis from 2011 by Vriens et al., including six studies, presented a pooled sensitivity of 95% and a pooled specificity of 48%, resulting in a NPV and PPV of 96% and 39%, respectively (benign call rate: 37%) [113]. In 2017, a review by De Koster et al. reported sensitivities and specificities of [^{18}F]FDG PET/CT to detect thyroid carcinoma in indeterminate thyroid nodules ranging from 77% to 100% and 33% to 64%, respectively [5].

These findings were recently validated in a recent multicentric diagnostic randomized controlled trial that assessed the impact of [^{18}F]FDG PET/CT in the management of thyroid nodules with double-read Bethesda III or IV cytology to rule out malignancy, avoid futile diagnostic surgeries, and improve patient outcomes (*EfFECTS* trial) [114]. De Koster et al. randomized 132 patients with an indeterminate nodule who were scheduled for diagnostic surgery and underwent an [^{18}F]FDG PET/CT scan into a PET/CT-driven arm or a diagnostic surgery arm. In the PET/CT-driven arm, diagnostic surgery was advised in visually [^{18}F]FDG-positive nodules and active surveillance in [^{18}F]FDG-negative nodules. In the diagnostic surgery arm, all patients were advised to continue with the scheduled diagnostic surgery. Patient management was considered unbeneficial (i.e. diagnostic surgery for benign nodules or active surveillance for malignant/borderline nodules) in 42% of patients in the [^{18}F]FDG PET/CT-driven arm and 83% in the diagnostic surgery arm. No wrongful active surveillance for malignant/borderline nodules was reported. As such, [^{18}F]FDG PET/CT-driven management avoided 40% of diagnostic surgeries for benign nodules. Therapeutic yield was the highest (48% reduction in diagnostic surgeries) when only non-Hürthle cell nodules were considered, as nearly all Hürthle cell nodules were [^{18}F]FDG positive on visual interpretation.

Several studies have reported the quantitative assessment of [^{18}F]FDG PET/CT images using the SUV of the indeterminate thyroid nodule, with a higher SUV_{max} reported in thyroid malignancies than in benign lesions [102, 115–120]. Nevertheless, major variations in SUV cut-offs and diagnostic accuracy are found between studies. Deandreis et al. and Rosario et al., respectively, included 56 indeterminate nodules (pre-Bethesda) and 63 Bethesda III/IV nodules and showed that a SUV_{max} cut-off of at least 5 g/mL was 91% specific to detect thyroid carcinoma, NIFTP, and FT-UMP [116, 117]. This was substantiated by Piccardo et al. in 111 indeterminate nodules, but no AUCs or corresponding sensitivity and specificity were reported [118]. Contrarily, Merten et al. demonstrated that a cut-

off of 5 g/mL was only 41% specific but 80% sensitive in their study in 51 Bethesda IV nodules [120]. Pathak et al. reported a SUV_{max} cut-off of 3.25 g/mL best differentiated 42 non-Hürthle cell nodules with 79% sensitivity and 83% specificity [119]. An additional analysis of the *EfFECTS* trial dataset assessed the added value of SUV metrics, SUV ratios (node to contralateral normal thyroid), and radiomics for the pre-operative differentiation [115]. None of these previous studies used ROC curve analysis to determine SUV cut-offs that corresponded to optimal test sensitivity, i.e. a NPV similar to a benign cytologic diagnosis (i.e. 96.3%) as per the ATA recommendations for a useful rule-out test [4]. De Koster et al. performed quantitative analysis and ROC curve analysis of the *EfFECTS* dataset, including 123 patients who underwent [^{18}F]FDG PET/CT according to the EANM guidelines [115]. Quantitative [^{18}F]FDG PET/CT assessment ruled out malignancy in indeterminate thyroid nodules, optimizing the rule-out ability when distinctive SUV cut-offs were applied to Hürthle and non-Hürthle cell nodules. In non-Hürthle cell nodules, malignancy could be ruled out at a SUV_{max} cut-off of 2.1 g/mL (similar to visual interpretation) with a sensitivity of 96% and benign call rate of 18%. In Hürthle cell nodules, a higher cut-off at 5.2 g/mL could rule out malignancy with a sensitivity of 100% and benign call rate of 17%. As such, quantitative analysis appears advantageous over visual analysis in Hürthle cell nodules. Consequently, [^{18}F]FDG PET/CT may be a reliable rule-out test for both non-Hürthle and Hürthle cell nodules, although external validation of these SUV thresholds is required before implementation in clinical practice.

Two recent publications investigated [^{18}F]FDG PET/CT radiomics in cytologically indeterminate thyroid nodules for the classification of malignancies [115, 121]. Giovanella et al. published the first retrospective study in 78 Bethesda III/IV patients (65 non-Hürthle nodules), suggesting a multiparametric model including cytological classification and two radiomic features [121]. The included features were the autocorrelation of the grey-level cooccurrence matrix, a feature that describes the fineness of a texture, and the sphericity of the nodule shape, indicating a taller-than-wide shape. The cross-validated models with the two radiomic features resulted in AUCs of 73% and 73% for all nodules and in a subgroup of non-Hürthle cell nodules, respectively. In non-Hürthle cell nodules, a model with both the radiomic features and the cytological classification resulted in an AUC of 82%. A secondary analysis of the *EfFECTS* dataset performed additional radiomic analysis in [^{18}F]FDG-positive scans *only* [115]. The authors found that radiomic analysis did not contribute to the additional differentiation of [^{18}F]FDG-positive nodules. Both studies concluded that radiomic analysis alone on [^{18}F]FDG PET/CT seems of no added value in the management of indeterminate thyroid nodules. However, implemented in the multiparametric model of two radiomic features and the cytological classification that Giovanella et al. proposed, clinical application of radiomics seems feasible, although validation is required.

The availability of PET-CT scanners and tracers is increasing but varies worldwide. Transport distances are limited due to the short half-life of ^{18}F (~110 min), which is produced in cyclotrons. The radiation exposure of an [^{18}F]FDG PET/CT scan is mainly accounted for by the [^{18}F]FDG dosage, which amounts to about 3.5 millisievert for an administered activity of 185 MBq [8]. The radiation exposure of CT largely varies, but can be less than 0.5 millisievert for a low-dose CT of the neck region only. Costs for an investigation are generally higher than for the other modalities described, because of the costs of PET hardware and the production and transportation of radiopharmaceuticals. Two studies assessed the cost-effectiveness of an [^{18}F]FDG PET/CT-driven management as compared to diagnostic surgery in all Bethesda III/IV patients. A 2014 cost-effectiveness model by Vriens et al. showed that [^{18}F]FDG PET/CT decreased the number of futile surgeries by 47%, thereby reducing the expected 5-year direct medical costs per patient by €822 (from €8804 to €7983) as compared to surgical treatment whilst maintaining health-related quality of life (HRQoL). This study also concluded that, from a European perspective, [^{18}F]FDG PET/CT would be cost-effective over molecular testing [122]. Another cost-effective-

ness study performed by the same group was recently conducted using the observed health care consumption and HRQoL data of the *EfFECTS* trial, which had found a similar reduction in futile surgeries [123]. This study assessed all societal costs over a lifelong horizon, and found that an [^{18}F]FDG PET/CT-driven management reduced the lifelong societal costs by almost €10,000 as compared to diagnostic surgery, with similar HRQoL for both strategies. Whilst diagnostic surgery for a nodule with benign histopathology resulted in more cognitive impairment and physical problems including cosmetic complaints, the reassurance of a negative FDG PET/CT resulted in sustained HRQoL throughout the first year of active surveillance [124].

5.3.6 Combined Approaches

Every currently known engagement point from the genotype to the phenotype of the tumour is being explored. Combined, the various research fields encompass an extensive range of investigative methods. Individually they usually focus on one or two methods only, making one-to-one comparisons of these diagnostics difficult. The 2015 American Thyroid Association (ATA) guidelines suggested several additional tests, but a definitive answer or complete overview of all available tests is still lacking [4]. Alongside higher-level expert discussions and lobbying of MedTech companies, clinical endocrinologists and thyroid surgeons ponder about the best solution for their individual patients. Their choices depend on the characteristics of their patient populations, availability and costs of a certain test, and personal preference. In any case, a useful additional test should be accurate, accessible, affordable, and affect patient management. A multimodal stepwise approach using a sensitive rule-out test and a specific rule-in test might provide the most conclusive diagnosis, e.g. in a specific test a relatively higher threshold value may be recommended to minimize missing malignancy in screening, whilst when appended to another diagnostic test, a relatively lower threshold value may be recommended to reduce false-positive results. Nevertheless, research into combined approaches is limited.

Piccardo et al. compared [^{18}F]FDG PET/CT, multiparametric US (including elastosonography), and [^{99m}Tc]Tc-MIBI scintigraphy in 87 nodules with indeterminate cytology (according to the Società Italiana di Anatomia e Citologia Patologica-International Academy of Pathology classification published in 2010), wherefrom 18 nodules were found to be malignant in histopathology. Separately, [^{18}F]FDG PET/CT outperformed qualitative multiparametric US and [^{99m}Tc]Tc-MIBI scintigraphy for the detection of thyroid malignancy. Also, combined approaches were evaluated, demonstrating that (1) a negative [^{18}F]FDG PET/CT correctly predicted benign findings on histopathology, (2) a positive [^{18}F]FDG PET/CT was significantly associated with malignancy when qualitative [^{99m}Tc]Tc-MIBI scans were rated as negative, and (3) the association of a positive [^{18}F]FDG PET/CT combined with a positive multiparametric US was significantly more specific than [^{18}F]FDG PET/CT alone in identifying differentiated thyroid cancer.

A combined approach by Trimboli et al. investigated whether [^{18}F]FDG PET/CT could play a role in the stratification of nodules with an intermediate risk upon EU-TI-RADS in 93 unselected nodules with EU-TI-RADS 4 and 5, including 38 nodules with indeterminate cytology [125]. They found that thyroid lesions classified as EU-TI-RADS 4 and with no [^{18}F]FDG uptake could be excluded from further examination. Another study by Piccardo et al. also investigated [^{18}F]FDG PET/CT, EU-TI-RADS, and the Italian consensus for the classification and reporting of thyroid cytology (ICCRTC) to distinguish differentiated thyroid cancers and FNs from nodular hyperplasias in 201 Bethesda III and IV thyroid nodules [118]. On multivariate analysis, [^{18}F]FDG PET/CT (OR 9.04), ICCRTC (OR 7.57), and EU-TI-RADS (OR 4.41) were all independent risk factors associated with differentiated thyroid carcinomas and FNs. These studies conclude that [^{18}F]FDG PET/CT could serve as a reliable rule-out test in case of nodules with intermediate risk upon US stratification.

5.4 Future Perspectives

Medical imaging plays an important role in the pre-operative workup of cytologically indeterminate thyroid nodules. A comprehensive overview of imaging biomarkers exemplified in this chapter can be found in Table 5.2. Most biomarkers used in the clinical workup are visual interpretation or basic quantitative metrics. AI applications and radiomic methodologies, on the other hand, are less well established, but are currently developed on a large scale. Extensive external validation should be performed in order to achieve implementation of AI-derived imaging biomarkers in clinical practice.

Many of the imaging biomarkers have either an adequate rule-in or rule-out capacity, but no single biomarker seems to serve both purposes well. A multimodal stepwise approach using a sensitive rule-out test and a specific rule-in test complementing each other might provide the most conclusive diagnosis for indeterminate thyroid nodules [5].

It should be noted that test performance of a test depends on the patient population. With the introduction of US risk stratification systems, FNAC might be withheld more often for patients with a presumed benign nodule, thereby potentially changing the composition of patient population and increasing its associated risk of malignancy. The proportion of Hürthle cell nodules is additionally crucial, as these nodules should be considered a separate entity with varying diagnostic yield of the different imaging modalities [114]. In addition, the prevalence of malignancy and the performance, costs, and feasibility of the imaging techniques might vary globally. Clinical utility should be examined in local implementation studies.

Table 5.2 Overview of imaging biomarkers in the management of cytologically indeterminate thyroid nodules exemplified in this chapter

Technique	Sensitivity	Specificity	Benign call rate (given a prevalence of 26%)	Advantages	Drawbacks	Cost-effectiveness
US	ATA: 52%[a] [51] ACR TI-RADS: 70%[a] [51] EU-TI-RADS: 38%[a] [51] K-TI-RADS: 78%[a] [51]	ATA: 90%[a] [51] ACR TI-RADS: 60%[a] [51] EU-TI-RADS: 81%[a] [51] K-TI-RADS: 53%[a] [51]	ATA: 79% ACR TI-RADS: 52% EU TI-RADS: 76% K-RADS: 45%	• Global availability • Low costs • No ionizing radiation • Possibility of US-guided FNAC	• Operator dependency • Limited prospective clinical validation	Presumed, but unpublished
CT	NA	NA	NA	NA	• Not investigated in indeterminate nodules	NA
MRI	97%[b] [95]	95%[b] [95]	NA	• No ionizing radiation	• High costs • Limited evidence • No methodological consensus • Research ongoing • Limited (but increasing) availability of (high field) MRI scanners	Currently unknown

Table 5.2 Continued

Technique	Sensitivity	Specificity	Benign call rate (given a prevalence of 26%)	Advantages	Drawbacks	Cost-effectiveness
[^{99m}Tc] Tc-MIBI scintigraphy (WO_{ind})	100%[c] [105]	89%[c] [105]	66%[c]	• More widely available and lower costs than PET	• Ionizing radiation • Limited sensitivity in lesions smaller than 30 mm	Unclear
[^{18}F]FDG PET/CT	94% [114]	40% [114]	31% [114]	• High NPV • High benign call rate • Effective reducing futile diagnostic lobectomies	• High costs • Ionizing radiation • Limited but increasing availability of scanners and radiotracers • Incidental findings (low specificity)	Reduced the lifelong societal costs by almost €10,000 as compared to diagnostic surgery [123]

[a]In Bethesda III nodules
[b]In unselected nodules, sensitivity and specificity in indeterminate nodules unknown
[c]Requires pre-selection of hypofunctioning nodules

References

1. Cibas ES, Ali SZ. The 2017 Bethesda System for reporting thyroid cytopathology. Thyroid. 2017;27:1341–6. https://doi.org/10.1089/thy.2017.0500.
2. Bongiovanni M, Spitale A, Faquin WC, Mazzucchelli L, Baloch ZW. The Bethesda System for reporting thyroid cytopathology: a meta-analysis. Acta Cytol. 2012;56:333–9. https://doi.org/10.1159/000339959.
3. Trimboli P, Nasrollah N, Guidobaldi L, Taccogna S, Cicciarella Modica DD, Amendola S, et al. The use of core needle biopsy as first-line in diagnosis of thyroid nodules reduces false negative and inconclusive data reported by fine-needle aspiration. World J Surg Oncol. 2014;12:61. https://doi.org/10.1186/1477-7819-12-61.
4. Haugen BR, Alexander EK, Bible KC, Doherty GM, Mandel SJ, Nikiforov YE, et al. 2015 American Thyroid Association management guidelines for adult patients with thyroid nodules and differentiated thyroid cancer: the American Thyroid Association guidelines task force on thyroid nodules and differentiated thyroid cancer. Thyroid. 2016;26:1–133. https://doi.org/10.1089/thy.2015.0020.
5. de Koster EJ, de Geus-Oei LF, Dekkers OM, van Engen-van Grunsven I, Hamming J, Corssmit EPM, et al. Diagnostic utility of molecular and imaging biomarkers in cytological indeterminate thyroid nodules. Endocr Rev. 2018;39:154–91. https://doi.org/10.1210/er.2017-00133.
6. Parmar C, Grossmann P, Bussink J, Lambin P, Aerts HJWL. Machine learning methods for quantitative radiomic biomarkers. Sci Rep. 2015;5:13087. https://doi.org/10.1038/srep13087.
7. Gillies RJ, Kinahan PE, Hricak H. Radiomics: images are more than pictures, they are data. Radiology. 2016;278:563–77. https://doi.org/10.1148/radiol.2015151169.
8. Boellaard R, Delgado-Bolton R, Oyen WJG, Giammarile F, Tatsch K, Eschner W, et al. FDG PET/CT: EANM procedure guidelines for tumour imaging: version 2.0. Eur J Nucl Med Mol Imaging. 2015;42:328–54.
9. Vriens D, Visser EP, de Geus-Oei LF, Oyen WJ. Methodological considerations in quantification of oncological FDG PET studies. Eur J Nucl Med Mol Imaging. 2010;37:1408–25.
10. Sieren JP, Newell JD Jr, Barr RG, Bleecker ER, Burnette N, Carretta EE, et al. SPIROMICS protocol for multicenter quantitative computed tomography to phenotype the lungs. Am J Respir Crit Care Med. 2016;194:794–806. https://doi.org/10.1164/rccm.201506-1208PP.
11. Pierpaoli C. Quantitative brain MRI. Top Magn Reson Imaging. 2010;21:63. https://doi.org/10.1097/RMR.0b013e31821e56f8.
12. Moon JC, Messroghli DR, Kellman P, Piechnik SK, Robson MD, Ugander M, et al. Myocardial T1 mapping and extracellular volume quantification: a Society for Cardiovascular Magnetic Resonance (SCMR) and CMR Working Group of the European Society of cardiology consensus statement. J

Cardiovasc Magn Reson. 2013;15:92. https://doi.org/10.1186/1532-429X-15-92.
13. Oelze ML, Mamou J. Review of quantitative ultrasound: envelope statistics and backscatter coefficient imaging and contributions to diagnostic ultrasound. IEEE Trans Ultrason Ferroelectr Freq Control. 2016;63:336–51. https://doi.org/10.1109/TUFFC.2015.2513958.
14. McBee MP, Awan OA, Colucci AT, Ghobadi CW, Kadom N, Kansagra AP, et al. Deep learning in radiology. Acad Radiol. 2018;25:1472–80. https://doi.org/10.1016/j.acra.2018.02.018.
15. Hosny A, Parmar C, Quackenbush J, Schwartz LH, Aerts H. Artificial intelligence in radiology. Nat Rev Cancer. 2018;18:500–10. https://doi.org/10.1038/s41568-018-0016-5.
16. Bini F, Pica A, Azzimonti L, Giusti A, Ruinelli L, Marinozzi F, et al. Artificial intelligence in thyroid field—a comprehensive review. Cancers (Basel). 2021:13. https://doi.org/10.3390/cancers13194740.
17. Peng S, Liu Y, Lv W, Liu L, Zhou Q, Yang H, et al. Deep learning-based artificial intelligence model to assist thyroid nodule diagnosis and management: a multicentre diagnostic study. Lancet Digital Health. 2021;3:e250–e9. https://doi.org/10.1016/S2589-7500(21)00041-8.
18. Li L-R, Du B, Liu H-Q, Chen C. Artificial intelligence for personalized medicine in thyroid cancer: current status and future perspectives. Frontiers. Oncology. 2021:10. https://doi.org/10.3389/fonc.2020.604051.
19. Sollini M, Cozzi L, Chiti A, Kirienko M. Texture analysis and machine learning to characterize suspected thyroid nodules and differentiated thyroid cancer: where do we stand? Eur J Radiol. 2018;99:1–8. https://doi.org/10.1016/j.ejrad.2017.12.004.
20. Kelly CJ, Karthikesalingam A, Suleyman M, Corrado G, King D. Key challenges for delivering clinical impact with artificial intelligence. BMC Med. 2019;17:195. https://doi.org/10.1186/s12916-019-1426-2.
21. Halford GS, Baker R, McCredden JE, Bain JD. How many variables can humans process? Psychol Sci. 2005;16:70–6. https://doi.org/10.1111/j.0956-7976.2005.00782.x.
22. Holzinger A, Biemann C, Pattichis CS, Kell DB. What do we need to build explainable AI systems for the medical domain? arXiv preprint arXiv:09923; 2017.
23. Morin O, Vallières M, Jochems A, Woodruff HC, Valdes G, Braunstein SE, et al. A deep look into the future of quantitative imaging in oncology: a statement of working principles and proposal for change. Int J Radiat Oncol Biol Phys. 2018;102:1074–82. https://doi.org/10.1016/j.ijrobp.2018.08.032.
24. Buvat I, Orlhac F. The dark side of radiomics: on the paramount importance of publishing negative results. J Nucl Med. 2019;60:1543. https://doi.org/10.2967/jnumed.119.235325.
25. Lambin P, Rios-Velazquez E, Leijenaar R, Carvalho S, van Stiphout RG, Granton P, et al. Radiomics: extracting more information from medical images using advanced feature analysis. Eur J Cancer. 2012;48:441–6. https://doi.org/10.1016/j.ejca.2011.11.036.
26. Noortman WA, Vriens D, Grootjans W, Tao Q, de Geus-Oei LF, Van Velden FH. Nuclear medicine radiomics in precision medicine: why we can't do without artificial intelligence. Q J Nucl Med Mol Imaging. 2020;64:278–90. https://doi.org/10.23736/s1824-4785.20.03263-x.
27. Zanfardino M, Franzese M, Pane K, Cavaliere C, Monti S, Esposito G, et al. Bringing radiomics into a multi-omics framework for a comprehensive genotype-phenotype characterization of oncological diseases. J Transl Med. 2019;17:337. https://doi.org/10.1186/s12967-019-2073-2.
28. Cook GJR, Azad G, Owczarczyk K, Siddique M, Goh V. Challenges and promises of PET radiomics. Int J Radiat Oncol Biol Phys. 2018;102:1083–9. https://doi.org/10.1016/j.ijrobp.2017.12.268.
29. Zwanenburg A, Leger S, Vallieres M, Lock S. Image biomarker standardisation initiative - feature definitions v11. CoRR. 2019;1612.07003.
30. Frings V, van Velden FHP, Velasquez LM, Hayes W, et al. Repeatability of metabolically active tumor volume measurements with FDG PET/CT in advanced gastrointestinal malignancies: a multicenter study. Radiology. 2014;273:539–48.
31. van Velden FH, Kramer GM, Frings V, Nissen IA, Mulder ER, de Langen AJ, et al. Repeatability of radiomic features in non-small-cell lung cancer [(18)F]FDG-PET/CT studies: impact of reconstruction and delineation. Mol Imaging Biol. 2016;18:788–95.
32. Traverso A, Wee L, Dekker A, Gillies R. Repeatability and reproducibility of Radiomic features: a systematic review. Int J Radiat Oncol Biol Phys. 2018;102:1143–58. https://doi.org/10.1016/j.ijrobp.2018.05.053.
33. O'Connor JP, Aboagye EO, Adams JE, Aerts HJ, Barrington SF, Beer AJ, et al. Imaging biomarker roadmap for cancer studies. Nat Rev Clin Oncol. 2017;14:169–86. https://doi.org/10.1038/nrclinonc.2016.162.
34. Clarke R, Ressom HW, Wang A, Xuan J, Liu MC, Gehan EA, et al. The properties of high-dimensional data spaces: implications for exploring gene and protein expression data. Nat Rev Cancer. 2008;8:37–49. https://doi.org/10.1038/nrc2294.
35. Ang JC, Mirzal A, Haron H, Hamed HNA. Supervised, unsupervised, and semi-supervised feature selection: a review on gene selection. IEEE/ACM Trans Comput Biol Bioinform. 2016;13:971–89. https://doi.org/10.1109/TCBB.2015.2478454.
36. Forghani R, Savadjiev P, Chatterjee A, Muthukrishnan N, Reinhold C, Forghani B. Radiomics and artificial intelligence for biomarker and prediction model development in oncology. Comput Struct Biotechnol

J. 2019;17:995–1008. https://doi.org/10.1016/j.csbj.2019.07.001.
37. Lambin P, Leijenaar RTH, Deist TM, Peerlings J, de Jong EEC, van Timmeren J, et al. Radiomics: the bridge between medical imaging and personalized medicine. Nat Rev Clin Oncol. 2017;14:749–62. https://doi.org/10.1038/nrclinonc.2017.141.
38. Orlhac F, Nioche C, Klyuzhin I, Rahmim A, Buvat I. Radiomics in PET imaging: a practical guide for newcomers. 2021.
39. Tomaszewski MR, Gillies RJ. The biological meaning of radiomic features. Radiology. 2021;298:505–16. https://doi.org/10.1148/radiol.2021202553.
40. Brito JP, Gionfriddo MR, Al Nofal A, Boehmer KR, Leppin AL, Reading C, et al. The accuracy of thyroid nodule ultrasound to predict thyroid cancer: systematic review and meta-analysis. J Clin Endocrinol Metab. 2014;99:1253–63. https://doi.org/10.1210/jc.2013-2928.
41. Remonti LR, Kramer CK, Leitão CB, Pinto LC, Gross JL. Thyroid ultrasound features and risk of carcinoma: a systematic review and meta-analysis of observational studies. Thyroid. 2015;25:538–50. https://doi.org/10.1089/thy.2014.0353.
42. Jeh SK, Jung SL, Kim BS, Lee YS. Evaluating the degree of conformity of papillary carcinoma and follicular carcinoma to the reported ultrasonographic findings of malignant thyroid tumor. Korean J Radiol. 2007;8:192–7. https://doi.org/10.3348/kjr.2007.8.3.192.
43. Lee SH, Baek JS, Lee JY, Lim JA, Cho SY, Lee TH, et al. Predictive factors of malignancy in thyroid nodules with a cytological diagnosis of follicular neoplasm. Endocr Pathol. 2013;24:177–83. https://doi.org/10.1007/s12022-013-9263-x.
44. Tessler FN, Middleton WD, Grant EG, Hoang JK, Berland LL, Teefey SA, et al. ACR thyroid imaging, reporting and data system (TI-RADS): white paper of the ACR TI-RADS Committee. J Am Coll Radiol. 2017;14:587–95. https://doi.org/10.1016/j.jacr.2017.01.046.
45. Russ G, Bonnema SJ, Erdogan MF, Durante C, Ngu R, Leenhardt L. European Thyroid Association guidelines for ultrasound malignancy risk stratification of thyroid nodules in adults: the EU-TIRADS. Eur Thyroid J. 2017;6:225–37. https://doi.org/10.1159/000478927.
46. Shin JH, Baek JH, Chung J, Ha EJ, Kim JH, Lee YH, et al. Ultrasonography diagnosis and imaging-based management of thyroid nodules: revised Korean society of thyroid radiology consensus statement and recommendations. Korean J Radiol. 2016;17:370–95. https://doi.org/10.3348/kjr.2016.17.3.370.
47. Gharib H, Papini E, Garber JR, Duick DS, Harrell RM, Hegedüs L, et al. American association of clinical endocrinologists, american college of endocrinology, and associazione medici endocrinologi medical guidelines for clinical practice for the diagnosis and management of thyroid nodules - 2016 update. Endocr Pract. 2016;22:622–39. https://doi.org/10.4158/ep161208.Gl.
48. Hoang JK, Asadollahi S, Durante C, Hegedüs L, Papini E, Tessler FN. An international survey on utilization of five thyroid nodule risk stratification systems: a needs assessment with future implications. Thyroid. 2022;32:675–81. https://doi.org/10.1089/thy.2021.0558.
49. Grani G, Lamartina L, Ascoli V, Bosco D, Biffoni M, Giacomelli L, et al. Reducing the number of unnecessary thyroid biopsies while improving diagnostic accuracy: toward the "right" TIRADS. J Clin Endocrinol Metab. 2019;104:95–102. https://doi.org/10.1210/jc.2018-01674.
50. Larcher de Almeida AM, Delfim RLC, Vidal APA, Chaves M, Santiago ACL, Gianotti MF, et al. Combining the American Thyroid Association's ultrasound classification with cytological subcategorization improves the assessment of malignancy risk in indeterminate thyroid nodules. Thyroid. 2021;31:922–32. https://doi.org/10.1089/thy.2019.0575.
51. Staibano P, Forner D, Noel CW, Zhang H, Gupta M, Monteiro E, et al. Ultrasonography and fine-needle aspiration in indeterminate thyroid nodules: a systematic review of diagnostic test accuracy. Laryngoscope. 2022;132:242–51. https://doi.org/10.1002/lary.29778.
52. Słowińska-Klencka D, Wysocka-Konieczna K, Klencki M, Popowicz B. Usability of EU-TIRADS in the diagnostics of Hürthle cell thyroid nodules with equivocal cytology. J Clin Med. 2020;9:3410. https://doi.org/10.3390/jcm9113410.
53. Barbosa TLM, Junior COM, Graf H, Cavalvanti T, Trippia MA, da Silveira Ugino RT, et al. ACR TI-RADS and ATA US scores are helpful for the management of thyroid nodules with indeterminate cytology. BMC Endocr Disord. 2019;19:112. https://doi.org/10.1186/s12902-019-0429-5.
54. Maia FF, Matos PS, Pavin EJ, Zantut-Wittmann DE. Thyroid imaging reporting and data system score combined with Bethesda system for malignancy risk stratification in thyroid nodules with indeterminate results on cytology. Clin Endocrinol. 2015;82:439–44. https://doi.org/10.1111/cen.12525.
55. Wildman-Tobriner B, Buda M, Hoang JK, Middleton WD, Thayer D, Short RG, et al. Using artificial intelligence to revise ACR TI-RADS risk stratification of thyroid nodules: diagnostic accuracy and utility. Radiology. 2019;292:112–9. https://doi.org/10.1148/radiol.2019182128.
56. Yoon J, Lee E, Kang SW, Han K, Park VY, Kwak JY. Implications of US radiomics signature for predicting malignancy in thyroid nodules with indeterminate cytology. Eur Radiol. 2021;31:5059–67. https://doi.org/10.1007/s00330-020-07670-3.
57. Wallis D, Buvat I. Clever Hans effect found in a widely used brain tumour MRI dataset. Med Image Anal. 2022;77:102368. https://doi.org/10.1016/j.media.2022.102368.

58. Cleere EF, Davey MG, O'Neill S, Corbett M, O'Donnell JP, Hacking S, et al. Radiomic detection of malignancy within thyroid nodules using ultrasonography—a systematic review and meta-analysis. Diagnostics (Basel). 2022;12:794.
59. Duron L, Savatovsky J, Fournier L, Lecler A. Can we use radiomics in ultrasound imaging? Impact of preprocessing on feature repeatability. Diagn Interv Imaging. 2021;102:659–67. https://doi.org/10.1016/j.diii.2021.10.004.
60. Lyshchik A, Higashi T, Asato R, Tanaka S, Ito J, Mai JJ, et al. Thyroid gland tumor diagnosis at US elastography. Radiology. 2005;237:202–11. https://doi.org/10.1148/radiol.2363041248.
61. Dighe MK. Elastography of thyroid masses. Ultrasound Clin. 2014;9:13–24. https://doi.org/10.1016/j.cult.2013.08.001.
62. Bhatia KS, Tong CS, Cho CC, Yuen EH, Lee YY, Ahuja AT. Shear wave elastography of thyroid nodules in routine clinical practice: preliminary observations and utility for detecting malignancy. Eur Radiol. 2012;22:2397–406. https://doi.org/10.1007/s00330-012-2495-1.
63. Nell S, Kist JW, Debray TP, de Keizer B, van Oostenbrugge TJ, Borel Rinkes IH, et al. Qualitative elastography can replace thyroid nodule fine-needle aspiration in patients with soft thyroid nodules. A systematic review and meta-analysis. Eur J Radiol. 2015;84:652–61. https://doi.org/10.1016/j.ejrad.2015.01.003.
64. Qiu Y, Xing Z, Liu J, Peng Y, Zhu J, Su A. Diagnostic reliability of elastography in thyroid nodules reported as indeterminate at prior fine-needle aspiration cytology (FNAC): a systematic review and Bayesian meta-analysis. Eur Radiol. 2020;30:6624–34. https://doi.org/10.1007/s00330-020-07023-0.
65. Padovani RP, Kasamatsu TS, Nakabashi CC, Camacho CP, Andreoni DM, Malouf EZ, et al. One month is sufficient for urinary iodine to return to its baseline value after the use of water-soluble iodinated contrast agents in post-thyroidectomy patients requiring radioiodine therapy. Thyroid. 2012;22:926–30. https://doi.org/10.1089/thy.2012.0099.
66. Lee C, Chalmers B, Treister D, Adhya S, Godwin B, Ji L, et al. Thyroid lesions visualized on CT: sonographic and pathologic correlation. Acad Radiol. 2015;22:203–9. https://doi.org/10.1016/j.acra.2014.08.007.
67. Kim DW. Computed tomography features of papillary thyroid carcinomas. J Comput Assist Tomogr. 2014;38:936–40. https://doi.org/10.1097/rct.0000000000000149.
68. Peng W, Liu C, Xia S, Shao D, Chen Y, Liu R, et al. Thyroid nodule recognition in computed tomography using first order statistics. Biomed Eng Online. 2017;16:67. https://doi.org/10.1186/s12938-017-0367-2.
69. Li W, Cheng S, Qian K, Yue K, Liu H. Automatic recognition and classification system of thyroid nodules in CT images based on CNN. Comput Intell Neurosci. 2021;2021:5540186. https://doi.org/10.1155/2021/5540186.
70. Russ G, Leboulleux S, Leenhardt L, Hegedüs L. Thyroid incidentalomas: epidemiology, risk stratification with ultrasound and workup. Eur Thyroid J. 2014;3:154–63. https://doi.org/10.1159/000365289.
71. McRobbie DW, Moore EA, Graves MJ, Prince MR. MRI from picture to proton. 2nd ed. Cambridge: Cambridge University Press; 2006.
72. Shi R, Yao Q, Wu L, Zhou Q, Lu Q, Gao R, et al. T2* mapping at 30T MRI for differentiation of papillary thyroid carcinoma from benign thyroid nodules. J Magn Reson Imaging. 2016;43:956–61. https://doi.org/10.1002/jmri.25041.
73. Ben-David E, Sadeghi N, Rezaei MK, Muradyan N, Brown D, Joshi A, et al. Semiquantitative and quantitative analyses of dynamic contrast-enhanced magnetic resonance imaging of thyroid nodules. J Comput Assist Tomogr. 2015;39:855–9. https://doi.org/10.1097/rct.0000000000000304.
74. Sakat MS, Sade R, Kilic K, Gözeler MS, Pala O, Polat G, et al. The use of dynamic contrast-enhanced perfusion MRI in differentiating benign and malignant thyroid nodules. Indian J Otolaryngol Head Neck Surg. 2019;71:706–11. https://doi.org/10.1007/s12070-018-1512-3.
75. Nakahira M, Saito N, Murata S, Sugasawa M, Shimamura Y, Morita K, et al. Quantitative diffusion-weighted magnetic resonance imaging as a powerful adjunct to fine needle aspiration cytology for assessment of thyroid nodules. Am J Otolaryngol. 2012;33:408–16. https://doi.org/10.1016/j.amjoto.2011.10.013.
76. Chung SR, Lee JH, Yoon RK, Sung TY, Song DE, Pfeuffer J, et al. Differentiation of follicular carcinomas from adenomas using histogram obtained from diffusion-weighted MRI. Clin Radiol. 2020;75(878):e13–9. https://doi.org/10.1016/j.crad.2020.07.018.
77. Schueller-Weidekamm C, Kaserer K, Schueller G, Scheuba C, Ringl H, Weber M, et al. Can quantitative diffusion-weighted MR imaging differentiate benign and malignant cold thyroid nodules? Initial results in 25 patients. AJNR Am J Neuroradiol. 2009;30:417–22. https://doi.org/10.3174/ajnr.A1338.
78. Wu LM, Chen XX, Li YL, Hua J, Chen J, Hu J, et al. On the utility of quantitative diffusion-weighted MR imaging as a tool in differentiation between malignant and benign thyroid nodules. Acad Radiol. 2014;21:355–63. https://doi.org/10.1016/j.acra.2013.10.008.
79. Chen L, Xu J, Bao J, Huang X, Hu X, Xia Y, et al. Diffusion-weighted MRI in differentiating malignant from benign thyroid nodules: a meta-analysis. BMJ Open. 2016;6:e008413. https://doi.org/10.1136/bmjopen-2015-008413.
80. van der Graaf M. In vivo magnetic resonance spectroscopy: basic methodology and clinical applica-

tions. Eur Biophysics J. 2010;39:527–40. https://doi.org/10.1007/s00249-009-0517-y.
81. Minuto MN, Shintu L, Caldarelli S. Proteomics, and metabolomics: magnetic resonance spectroscopy for the presurgical screening of thyroid nodules. Curr Genomics. 2014;15:178–83. https://doi.org/10.2174/1389202915999140404100701.
82. Jordan KW, Adkins CB, Cheng LL, Faquin WC. Application of magnetic-resonance-spectroscopy- based metabolomics to the fine-needle aspiration diagnosis of papillary thyroid carcinoma. Acta Cytol. 2011;55:584–9. https://doi.org/10.1159/000333271.
83. Lean CL, Delbridge L, Russell P, May GL, Mackinnon WB, Roman S, et al. Diagnosis of follicular thyroid lesions by proton magnetic resonance on fine needle biopsy. J Clin Endocrinol Metab. 1995;80:1306–11. https://doi.org/10.1210/jcem.80.4.7714105.
84. Mackinnon WB, Delbridge L, Russell P, Lean CL, May GL, Doran S, et al. Two-dimensional proton magnetic resonance spectroscopy for tissue characterization of thyroid neoplasms. World J Surg. 1996;20:841–7. https://doi.org/10.1007/s002689900128.
85. Russell P, Lean CL, Delbridge L, May GL, Dowd S, Mountford CE. Proton magnetic resonance and human thyroid neoplasia. I: discrimination between benign and malignant neoplasms. Am J Med. 1994;96:383–8. https://doi.org/10.1016/0002-9343(94)90071-x.
86. King AD, Yeung DKW, Ahuja AT, Tse GMK, Chan ABW, Lam SSL, et al. In vivo 1H MR spectroscopy of thyroid carcinoma. Eur J Radiol. 2005;54:112–7. https://doi.org/10.1016/j.ejrad.2004.05.003.
87. Gupta N, Kakar AK, Chowdhury V, Gulati P, Shankar LR, Vindal A. Magnetic resonance spectroscopy as a diagnostic modality for carcinoma thyroid. Eur J Radiol. 2007;64:414–8. https://doi.org/10.1016/j.ejrad.2007.03.006.
88. Gupta N, Goswami B, Chowdhury V, RaviShankar L, Kakar A. Evaluation of the role of magnetic resonance spectroscopy in the diagnosis of follicular malignancies of thyroid. Arch Surg. 2011;146:179–82. https://doi.org/10.1001/archsurg.2010.345.
89. Aghaghazvini L, Pirouzi P, Sharifian H, Yazdani N, Kooraki S, Ghadiri A, et al. 3T magnetic resonance spectroscopy as a powerful diagnostic modality for assessment of thyroid nodules. Arch Endocrinol Metab. 2018;62:501–5. https://doi.org/10.20945/2359-3997000000069.
90. Cecil KM. Proton magnetic resonance spectroscopy: technique for the neuroradiologist. Neuroimaging Clin N Am. 2013;23:381–92. https://doi.org/10.1016/j.nic.2012.10.003.
91. Aydin H, Kizilgoz V, Tatar I, Damar C, Guzel H, Hekimoglu B, et al. The role of proton MR spectroscopy and apparent diffusion coefficient values in the diagnosis of malignant thyroid nodules: preliminary results. Clin Imaging. 2012;36:323–33. https://doi.org/10.1016/j.clinimag.2011.09.009.
92. Sasaki M, Sumi M, Kaneko K, Ishimaru K, Takahashi H, Nakamura T. Multiparametric MR imaging for differentiating between benign and malignant thyroid nodules: initial experience in 23 patients. J Magn Reson Imaging. 2013;38:64–71. https://doi.org/10.1002/jmri.23948.
93. Noda Y, Kanematsu M, Goshima S, Kondo H, Watanabe H, Kawada H, et al. MRI of the thyroid for differential diagnosis of benign thyroid nodules and papillary carcinomas. AJR Am J Roentgenol. 2015;204:W332–5. https://doi.org/10.2214/ajr.14.13344.
94. Liu R, Jiang G, Gao P, Li G, Nie L, Yan J, et al. Non-invasive amide proton transfer imaging and ZOOM diffusion-weighted imaging in differentiating benign and malignant thyroid micronodules. Front Endocrinol (Lausanne). 2018;9:747. https://doi.org/10.3389/fendo.2018.00747.
95. Wang H, Wei R, Liu W, Chen Y, Song B. Diagnostic efficacy of multiple MRI parameters in differentiating benign vs. malignant thyroid nodules. BMC Med Imaging. 2018;18:50. https://doi.org/10.1186/s12880-018-0294-0.
96. Song M, Yue Y, Guo J, Zuo L, Peng H, Chan Q, et al. Quantitative analyses of the correlation between dynamic contrast-enhanced MRI and intravoxel incoherent motion DWI in thyroid nodules. Am J Transl Res. 2020;12:3984–92.
97. Wang H, Song B, Ye N, Ren J, Sun X, Dai Z, et al. Machine learning-based multiparametric MRI radiomics for predicting the aggressiveness of papillary thyroid carcinoma. Eur J Radiol. 2020;122:108755. https://doi.org/10.1016/j.ejrad.2019.108755.
98. Wei R, Wang H, Wang L, Hu W, Sun X, Dai Z, et al. Radiomics based on multiparametric MRI for extrathyroidal extension feature prediction in papillary thyroid cancer. BMC Med Imaging. 2021;21:20. https://doi.org/10.1186/s12880-021-00553-z.
99. Treglia G, Caldarella C, Saggiorato E, Ceriani L, Orlandi F, Salvatori M, et al. Diagnostic performance of (99m)Tc-MIBI scan in predicting the malignancy of thyroid nodules: a meta-analysis. Endocrine. 2013;44:70–8. https://doi.org/10.1007/s12020-013-9932-z.
100. Giovanella L, Campenni A, Treglia G, Verburg FA, Trimboli P, Ceriani L, et al. Molecular imaging with (99m)Tc-MIBI and molecular testing for mutations in differentiating benign from malignant follicular neoplasm: a prospective comparison. Eur J Nucl Med Mol Imaging. 2016;43:1018–26. https://doi.org/10.1007/s00259-015-3285-1.
101. Saggiorato E, Angusti T, Rosas R, Martinese M, Finessi M, Arecco F, et al. 99mTc-MIBI imaging in the presurgical characterization of thyroid follicular neoplasms: relationship to multidrug resistance protein expression. J Nucl Med. 2009;50:1785–93. https://doi.org/10.2967/jnumed.109.064980.
102. Piccardo A, Puntoni M, Treglia G, Foppiani L, Bertagna F, Paparo F, et al. Thyroid nodules with

indeterminate cytology: prospective comparison between 18F-FDG-PET/CT, multiparametric neck ultrasonography, 99mTc-MIBI scintigraphy and histology. Eur J Endocrinol. 2016;174:693–703. https://doi.org/10.1530/eje-15-1199.
103. Armefti S, Mettler J, Schmidt M, Faust M, Engels M, Schultheis AM, et al. Could negative Tc-99m-methoxyisobutylisonitrile (MIBI) scintigraphy obviate the need for surgery for Bethesda III and IV. Surgeries. 2021;2:260–7.
104. Campennì A, Siracusa M, Ruggeri RM, Laudicella R, Pignata SA, Baldari S, et al. Differentiating malignant from benign thyroid nodules with indeterminate cytology by (99m)Tc-MIBI scan: a new quantitative method for improving diagnostic accuracy. Sci Rep. 2017;7:6147. https://doi.org/10.1038/s41598-017-06603-3.
105. Schenke SA, Campennì A, Tuncel M, Bottoni G, Sager S, Bogovic Crncic T, et al. Diagnostic performance of (99m)Tc-methoxy-isobuty-isonitrile (MIBI) for risk stratification of hypofunctioning thyroid nodules: a European Multicenter study. Diagnostics (Basel). 2022:12. https://doi.org/10.3390/diagnostics12061358.
106. Heinzel A, Müller D, Behrendt FF, Giovanella L, Mottaghy FM, Verburg FA. Thyroid nodules with indeterminate cytology: molecular imaging with ^{99}mTc-methoxyisobutylisonitrile (MIBI) is more cost-effective than the Afirma gene expression classifier. Eur J Nucl Med Mol Imaging. 2014;41:1497–500. https://doi.org/10.1007/s00259-014-2760-4.
107. Hindié E, Ugur O, Fuster D, O'Doherty M, Grassetto G, Ureña P, et al. 2009 EANM parathyroid guidelines. Eur J Nucl Med Mol Imaging. 2009;36:1201–16. https://doi.org/10.1007/s00259-009-1131-z.
108. Bertagna F, Treglia G, Piccardo A, Giubbini R. Diagnostic and clinical significance of F-18-FDG-PET/CT thyroid incidentalomas. J Clin Endocrinol Metab. 2012;97:3866–75. https://doi.org/10.1210/jc.2012-2390.
109. de Leijer JF, Metman MJH, van der Hoorn A, Brouwers AH, Kruijff S, van Hemel BM, et al. Focal thyroid incidentalomas on (18)F-FDG PET/CT: a systematic review and meta-analysis on prevalence, risk of malignancy and inconclusive fine needle aspiration. Front Endocrinol (Lausanne). 2021;12:723394. https://doi.org/10.3389/fendo.2021.723394.
110. Muñoz Pérez N, Villar del Moral JM, Muros Fuentes MA, López de la Torre M, Arcelus Martínez JI, Becerra Massare P, et al. Could 18F-FDG-PET/CT avoid unnecessary thyroidectomies in patients with cytological diagnosis of follicular neoplasm? Langenbeck's Arch Surg. 2013;398:709–16. https://doi.org/10.1007/s00423-013-1070-9.
111. Kresnik E, Gallowitsch HJ, Mikosch P, Stettner H, Igerc I, Gomez I, et al. Fluorine-18-fluorodeoxyglucose positron emission tomography in the preoperative assessment of thyroid nodules in an endemic goiter area. Surgery. 2003;133:294–9. https://doi.org/10.1067/msy.2003.71.
112. de Geus-Oei LF, Pieters GF, Bonenkamp JJ, Mudde AH, Bleeker-Rovers CP, Corstens FH, et al. 18F-FDG PET reduces unnecessary hemithyroidectomies for thyroid nodules with inconclusive cytologic results. J Nucl Med. 2006;47:770–5.
113. Vriens D, de Wilt JH, van der Wilt GJ, Netea-Maier RT, Oyen WJ, de Geus-Oei LF. The role of [18F]-2-fluoro-2-deoxy-d-glucose-positron emission tomography in thyroid nodules with indeterminate fine-needle aspiration biopsy: systematic review and meta-analysis of the literature. Cancer. 2011;117:4582–94. https://doi.org/10.1002/cncr.26085.
114. de Koster EJ, de Geus-Oei LF, Brouwers AH, van Dam E, Dijkhorst-Oei LT, van Engen-van Grunsven ACH, et al. [(18)F]FDG-PET/CT to prevent futile surgery in indeterminate thyroid nodules: a blinded, randomised controlled multicentre trial. Eur J Nucl Med Mol Imaging. 2022; https://doi.org/10.1007/s00259-021-05627-2.
115. de Koster EJ, Noortman WA, Mostert JM, Booij J, Brouwer CB, de Keizer B, et al. Quantitative classification and radiomics of [18F]FDG-PET/CT in indeterminate thyroid nodules. Eur J Nucl Med Mol Imaging. 2022; https://doi.org/10.1007/s00259-022-05712-0.
116. Deandreis D, Al Ghuzlan A, Auperin A, Vielh P, Caillou B, Chami L, et al. Is (18)F-fluorodeoxyglucose-PET/CT useful for the presurgical characterization of thyroid nodules with indeterminate fine needle aspiration cytology? Thyroid. 2012;22:165–72. https://doi.org/10.1089/thy.2011.0255.
117. Rosario PW, Rocha TG, Calsolari MR. Fluorine-18-fluorodeoxyglucose positron emission tomography in thyroid nodules with indeterminate cytology: a prospective study. Nucl Med Commun. 2019;40:185–7. https://doi.org/10.1097/mnm.0000000000000946.
118. Piccardo A, Puntoni M, Dezzana M, Bottoni G, Foppiani L, Marugo A, et al. Indeterminate thyroid nodules. The role of (18)F-FDG PET/CT in the "era" of ultrasonography risk stratification systems and new thyroid cytology classifications. Endocrine. 2020;69:553–61. https://doi.org/10.1007/s12020-020-02239-y.
119. Pathak KA, Goertzen AL, Nason RW, Klonisch T, Leslie WD. A prospective cohort study to assess the role of FDG-PET in differentiating benign and malignant follicular neoplasms. Ann Med Surg. 2016;12:27–31. https://doi.org/10.1016/j.amsu.2016.10.008.
120. Merten MM, Castro MR, Zhang J, Durski J, Ryder M. Examining the role of preoperative positron emission tomography/computerized tomography in combination with ultrasonography in discriminating benign from malignant cytologically indeterminate

thyroid nodules. Thyroid. 2016;27:95–102. https://doi.org/10.1089/thy.2016.0379.
121. Giovanella L, Milan L, Piccardo A, Bottoni G, Cuzzocrea M, Paone G, et al. Radiomics analysis improves (18)FDG PET/CT-based risk stratification of cytologically indeterminate thyroid nodules. Endocrine. 2021; https://doi.org/10.1007/s12020-021-02856-1.
122. Vriens D, Adang EM, Netea-Maier RT, Smit JW, de Wilt JH, Oyen WJ, et al. Cost-effectiveness of FDG-PET/CT for cytologically indeterminate thyroid nodules: a decision analytic approach. J Clin Endocrinol Metab. 2014;99:3263–74. https://doi.org/10.1210/jc.2013-3483.
123. de Koster EJ, Vriens D, van Aken MO, Dijkhorst-Oei LT, Oyen WJG, Peeters RP, et al. FDG-PET/CT in indeterminate thyroid nodules: cost-utility analysis alongside a randomised controlled trial. Eur J Nucl Med Mol Imaging. 2022; https://doi.org/10.1007/s00259-022-05794-w.
124. de Koster EJ, Husson O, van Dam EWCM, Mijnhout GS, Netea-Maier RT, Oyen WJG, et al. Health-related quality of life following FDG-PET/CT for cytological indeterminate thyroid nodules. Endocr Connect. 2022;11:e220014. https://doi.org/10.1530/ec-22-0014.
125. Trimboli P, Piccardo A, Alevizaki M, Virili C, Naseri M, Sola S, et al. Dedicated neck (18) F-FDG PET/CT: an additional tool for risk assessment in thyroid nodules at ultrasound intermediate risk. Clin Endocrinol. 2019;90:737–43. https://doi.org/10.1111/cen.13949.

6 Diagnostics and Theranostics of Benign Thyroid Disorders

Alfredo Campennì, Rosaria Maddalena Ruggeri, Tomislav Jukić, Massimiliano Siracusa, Marija Punda, Luca Giovanella, and Petra Petranović Ovčariček

6.1 Introduction

Molecular imaging has an important role in the evaluation and management of benign thyroid disorders. Radioisotopes of iodine, i.e., ^{131}I, ^{123}I, and ^{124}I, are crucial for a theragnostic and individualized approach.

In 1941, Saul Hertz applied the first radioiodine therapy to a patient with Graves' disease (GD). For the last 80 years, ^{131}I is successfully used for the treatment of hyperthyroidism, either autoimmune (GD) origin or non-autoimmune, i.e., toxic nodular goiter (TNG) or a toxic multinodular goiter (TMNG). Furthermore, radioiodine therapy is also used as a treatment option for patients with non-toxic nodular goiter (NTG), in order to reduce the thyroid volume [1, 2]. The introduction of radioiodine therapy resulted in a significant shift in the therapeutic approach of benign thyroid disorders, from surgical to radionuclide therapy. Thus, the use of radioiodine has also reduced potential significant side effects of surgery, as well as healthcare costs.

6.2 Radiopharmaceuticals for Thyroid Imaging and Therapy

^{99m}Tc-pertechnetate (Na[^{99m}Tc]Tc0_4) and radioiodine-123 (Na[^{123}I]I) are mainly used tracers in the diagnostic management of benign thyroid disorders. They have a specific affinity for the Sodium Iodide Symporter (NIS) and therefore they are trapped (Na[^{99m}Tc]Tc0_4) in thyroid follicular cells, additionally further organified in case of Na[^{123}I]I. ^{99m}Tc-pertechnetate is the most commonly used diagnostic tracer, while the use of Na[^{123}I]I is limited due to its higher cost.

Both of them are almost pure gamma emitters. Peak energy of ^{99m}Tc is 140 KeV and 159 KeV of ^{123}I. They have a relatively short half-life, 6 h of ^{99m}Tc, compared to 13.2 h of ^{123}I. Most commonly they are administered intravenously, although

A. Campennì (✉) · M. Siracusa
Department of Biomedical and Dental Sciences and Morpho-Functional Imaging, Unit of Nuclear Medicine, University of Messina, Messina, Italy
e-mail: acampenni@unime.it

R. M. Ruggeri
Unit of Endocrinology, Department of Clinical and Experimental Medicine, University of Messina, Messina, Italy
e-mail: rmruggeri@unime.it

T. Jukić · M. Punda · P. P. Ovčariček
Department of Oncology and Nuclear Medicine, University Hospital Center Sestre Milosrdnice, Zagreb, Croatia
e-mail: tomislav.jukic@kbcsm.hr

L. Giovanella
Clinic for Nuclear Medicine, University Hospital and University of Zurich, Zurich, Switzerland

Clinic for Nuclear Medicine, Ente Ospedaliero Cantonale, Imaging Institute of Southern Switzerland, Bellinzona, Switzerland
e-mail: luca.giovanella@eoc.ch

L. Giovanella (ed.), *Integrated Diagnostics and Theranostics of Thyroid Diseases*,
https://doi.org/10.1007/978-3-031-35213-3_6

Na[^{123}I]I may be applied also per os. Scintigraphy is performed 15–20 min following the application of Na[^{99m}Tc]TcO_4 and 2–6 (early phase) and 24 (delayed phase) hours later for Na[^{123}I]I [3]. Both tracers are used for differential diagnosis of thyrotoxicosis and for identifying hyper- or hypofunctioning thyroid nodules. As Na[^{99m}Tc]TcO_4 is only trapped by follicular cells, while Na[^{123}I]I is also organified, in very rare cases, thyroid nodule may be hyperfunctional on Na[^{99m}Tc]TcO_4, while hypofunctional on Na[^{123}I]I scintigraphy due to organification defects in the nodule resulting in fast washout of radioiodine [3, 4]. The so-called "trapping-only nodule" may be associated with an increased risk of malignancy [5].

^{131}I has a half-life of 8.02 days. Its most abundant gamma-ray has an energy of 364 KeV. Besides that, it also emits β-particles with a maximum energy of the main decay of 0.61 MeV, an average energy per transition of 0.192 MeV, and an average path length in the tissue of 0.4 mm. Therefore, Na[^{131}I]I serves as a diagnostic and therapeutic tracer. It is actually the first "theragnostic" tracer.

6.3 Graves' Disease

Graves' disease is a form of hyperthyroidism that affects the whole gland. It is an autoimmune disease caused by loss of immune tolerance to thyroid autoantigens and subsequent production of autoantibodies to TSH receptors (TRAb). They stimulate hyperfunction and growth of the thyroid [6]. GD is the most common cause of non-transient hyperthyroidism in the adult population living in iodine-sufficient areas [7]. It comprises 80% of all cases of hyperthyroidism with an age prevalence between 30 and 60 years and women predominance (5–10) [6, 8–10]. The annual incidence is 20–50 cases per 100,000 people [11, 12]. It is more common among smokers than non-smokers, and more frequently presented with overt than subclinical hyperthyroidism.

GD patients frequently have a family history of autoimmune thyroid disease and may be affected by other autoimmune diseases such as vitiligo, rheumatoid arthritis, and coeliacia [13, 14]. Due to thyroid hormones' influence on most tissues, the signs and symptoms of a hyperthyroid state are various. Younger patients mostly present with hyperactivity, anxiety, tremor, heat intolerance, etc. while older mainly exhibit cardiovascular symptoms and weight loss [13].

Graves' orbitopathy (GO) is the serious and most frequent extra-thyroidal manifestation of GD [15]. It affects almost half of all GD patients and usually exhibits simultaneously with the thyroid disease due to autoreactive T lymphocytes to thyroid-orbit cross-reacting autoantigens [16]. Patients show symptoms of orbital soft tissue inflammation, adipogenesis, and fibrosis of ocular muscles [17, 18].

Diagnosis of GD is based on detailed clinical examination, medical history, and biochemically detected overt or subclinical hyperthyroidism. Increased TRAbs are typical for GD. They have very high sensitivity, as well as specificity (99%). Thyroid ultrasonography (US) usually demonstrates an enlarged gland with different features, such as a diffusely hypoechoic gland, or hypoechoic areas within isoechoic tissue, sometimes also with coexisting nodules. There is usually increased vascularization at Color Doppler (CD). CD flow evaluation is useful in the differential diagnosis between GD and destructive thyroiditis, which is especially important in pregnancy and during lactation [19]. GD is characterized by an increased peak systolic and end-diastolic velocity across *arteria thyreoidea superior et inferior*, compared to normal arterial velocity in destructive thyroiditis [20].

Thyroid scintigraphy with Na[^{99m}Tc]TcO_4 or Na[^{123}I]I is generally indicated in patients with low or low-normal serum TSH values and reference range TRAbs values. In GD it demonstrates diffusely increased uptake in both thyroid lobes.

Na[^{131}I]I uptake (RAIU) is indicated before radioiodine therapy, especially if a dosimetric approach is required and it generally shows increased values in GD patients [21, 22].

The first-line treatment usually consists of anti-thyroid drugs (ATD), i.e., carbimazole, thimazole, and propylthiouracil (PTU). Their purpose is a long-term restoration of the euthyroid

state or preparation for radioiodine therapy or surgery as they decrease the risk of early side effects associated with thyrotoxicosis [23, 24]. Surgical treatment in the form of total thyroidectomy may be the preferred treatment option in patients with: low RAIU, symptomatic and/or large goiters (> 80 g), malignant thyroid nodules (confirmed or suspicious), moderate to severe active GO, as well as in women planning pregnancy within the next 6 months [22]. In GD patients affected by moderate or severe GO, after thyroidectomy, rhTSH-aided radioiodine therapy may be performed to achieve complete thyroid ablation and additionally improve GO [16, 25].

6.4 Toxic Nodular Goiter and Toxic Multi-Nodular Goiter

Thyroid nodules in the form of a single hyperfunctioning nodule, i.e., TNG or multiple hyperfunctioning nodules, i.e., TMNG are the most common cause of hyperthyroidism in elder patients coming from iodine-deficient regions [21, 22, 26, 27]. Hyperfunctioning thyroid nodules represent up to one-tenth of all thyroid nodules. Thyrotropin receptor (TSHR) gene activating mutation as well as mutation of the gene that encodes stimulatory GPT-binding protein are demonstrated as the main causes in the development of hyperfunctioning nodules [28, 29].

TMNG patients usually have non-toxic goiter for many years before the development of hyperfunctioning nodules. Long-term TSH stimulation due to low-iodine intake may result in nodules' enlargement and the development of new nodules with autonomous function. There is usually a slow progression from subclinical to overt hyperthyroidism, which may be potentiated by iodine overload, e.g., iodinated contrast media and amiodarone [9, 21]. Biochemically, the earliest stage of TNG and TMNG may present with T3-toxicosis, i.e., low-normal or suppressed TSH in conjunction with high FT3 and normal FT4, while the thyroid autoantibodies are mainly in reference values [6, 21, 22].

Thyroid ultrasonography is important in the evaluation of thyroid nodules in TNG and TMNG as it detects nodules' size, echographic features, and potentially suspicious nodules. For this latter point, nodules' characteristics should be always analyzed and scored also according to objective criteria [30].

Thyroid scintigraphy obtained with Na[^{99m}Tc]TcO_4 or Na[^{123}I]I is indicated in patients with low-normal or suppressed TSH for detection of hyperfunctioning nodules as well as evaluation of the rest of the thyroid [3, 27].

Na[^{131}I]I uptake test is necessary in case of planned radioiodine therapy, especially in the dosimetry approach. RAIU values are usually normal or high in TNG and TMNG patients [7].

ATD may be given as a first-line treatment to restore euthyroidism and prepare a patient for radioiodine therapy, and also to prepare a patient for surgery [23, 31]. Surgical treatment may be the preferred treatment option in patients with: low RAIU, symptomatic and/or large goiters (>80 g), proven or suspicious malignant thyroid nodules, and in women planning pregnancy within the next 6 months [22]. Surgery may be hemithyroidectomy (TNG, TMNG) or total thyroidectomy (TMNG), depending on the case.

6.5 Radioiodine Therapy for Hyperthyroidism

Patients are preferably treated in a euthyroid state to reduce early side effects of transient thyrotoxicosis that occurs in one-tenth of cases or, rarely, the so-called *"thyroid storm,"* usually occurring in poorly controlled GD [22, 32]. The overt hyperthyroid state should be especially avoided in active GO, in elderly patients, and those with comorbidities, e.g., cardiovascular and cerebrovascular [22, 32]. Therefore, ATD, i.e., thiamazole or carbimazole, is usually excluded 3–7 days before radioiodine therapy, while PTU during 2–8 weeks due to its strong radioprotectivity [31, 33–35], although some authors demonstrated high cure rates of ablative radioiodine therapy in GD patients using short PTU withdrawal periods (2 days) in a dosimetric approach [36].

ATD should be avoided after RIT, if possible, as they may reduce the desirable effect of radioiodine therapy, except in elder patients with cardiovascular comorbidities, which may continue with ATD 3–7 days after therapy administration [22].

Iodine-containing products should be excluded before therapy application, as they may reduce RAIU and the success of radioiodine therapy. The specific time interval depends on the type of iodine-containing product (Table 6.1).

The ß-adrenergic blockers are strongly recommended before and after radioiodine therapy in patients with overt hyperthyroidism, particularly in elder population and those with cardiovascular comorbidities, to avoid side effects, e.g., tachycardia or arrhythmia [37, 38].

In case of NTG and TMNG, radioiodine therapy should be delayed if serum TSH is high-normal or increased to reduce the risk of subsequent hypothyroidism due to the radioiodine effect on extranodular thyroid tissue [22, 39].

In GD patients suffering from comorbidities like diabetes and osteoporosis, and active but mild GO, and absence of risk factors (high TRAb level, smoking), radioiodine therapy without corticoids is an acceptable therapeutic approach. However, corticoids are recommended in the presence of risk factors [22]. In GD patients affected by active moderate to severe GO corticoids are recommended to reduce the risk of exacerbation of ophthalmopathy, mostly in presence of risk factors [7, 40]. The initial dose regimen of corticoids is usually 0.5 g per week for 6 weeks, and subsequently 0.25 g per week for 6 weeks [39, 40]. For GD patients who have a high risk of development or exacerbation of GO and are candidates for radioiodine therapy, corticoids are recommended as prophylaxis. Prednisone is applied per os in a dosage of 0.3–0.5 mg/kg initially, and then slowly withdrawn 3 months later [39]. Corticoid therapy is not recommended in patients with inactive GO and those without apparent GO and no risk factors [22]. It should not be initiated before radioiodine therapy as may decrease RAIU so it is started 1–3 days after the therapy [7, 41].

Lithium is rarely used in hyperthyroidism. Still, it prolongs the biological half-life of ^{131}I in the thyroid and may be used in GD with low RAIU (<20%). It is applied for 7 days starting immediately after the therapy and according to some data may increase its efficiency without inducing side effects such as exacerbation of GO [42]. Recent systematic review and meta-analysis compared the effect of lithium as an add-on therapy with radioiodine alone in increasing the cure rate of hyperthyroidism. There was no significant difference between the two therapy regimens although the dose of 5000–6000 mg of Li might increase the cure rates [43]. However, due to other common side effects, it may be considered only as an alternative treatment option [31].

Low-iodine diet is recommended for 1–2 weeks before radioiodine therapy [7]. Additionally, measurement of iodine in urine is useful in certain cases, i.e., in patients with large iodine intake, those who received iodinated contrast media, etc. [22].

Pregnancy is an absolute contraindication for radioiodine therapy and it has to be avoided 6 months after the therapy, while breastfeeding must be stopped at least 6 weeks before therapy

Table 6.1 Contrast media and medications affecting radioiodine uptake and their recommended time withdrawal before radioiodine therapy

Contrast media and medications	Recommended time withdrawal
Water-soluble intravenous radiographic contrast media	1–2 months
Oil-based intravenous radiographic contrast media	3–6 months
Levothyroxine	4 weeks
Liothyronine	2 weeks
Methimazole, thiamazole	3–7 days
Propylthiouracil	2–8 weeks (2–3 days in case of dosimetric approach)
Iodine solution (Lugol)	4–6 weeks, depending on iodide concentration
Perchlorate	1 week
Topical iodine (antiseptics)	4 weeks
Amiodarone	3–6 months

to reduce high radioiodine uptake in mammary glands [22, 44, 45].

Radionuclide diagnostics and therapy procedures should be in accordance with the safety standards for radiation protection—Chap. VII of the Council Directive 2013/59/Euratom [46]. Na[^{131}I]I may be administered orally (capsule, liquid), or alternatively intravenously. Capsule form enables safer treatment compared to the latter two due to the lower risk of contamination. On the other hand, the liquid form can be used in patients with ingestion problems, it is more affordable and can be divided among more patients. Intravenous application is suitable in patients with the inability to process iodine through the gastrointestinal tract. If case of oral administration patients need to fast before and approximately 2 h after radioiodine therapy. Generally, patients should be advised to take enough fluid for 1–2 days after the therapy to reduce the absorbed dose to the bladder (i.e., *critical organ*) and the rest of the body. They are advised to keep their distance from other people on post-therapy days, particularly children and pregnant women [31, 46].

6.5.1 Radioiodine Therapy in Graves' Disease

Na[^{131}I]I administered activity depends on the purpose (ablative vs. functional) and the approach (fixed dose vs. dosimetric).

Radioiodine therapy is the main therapy option in GD patients older than 10 years, with small to medium goiter and inactive or low to mild active GO; in patients with comorbidities that increase the risk of surgical therapy (especially in elderly); in patients with contraindications to ATD; in patients with relapse after ATD withdrawal or inadequate thyroid surgery; in institutions/regions without high volume endocrine surgeon; in patients with thyroid remnant tissue and severe GO after surgery [22, 47].

On the other hand, there are a few absolute contraindications: pregnancy or breastfeeding; suspicious or proven thyroid malignancy; age 5 years or younger. Relative contraindications are goiter over 80 g; active moderate to severe GO; and high TRAb levels (mainly in smokers) [22, 47, 48].

The main goal of radioiodine therapy in GD is to establish euthyroidism (*"functional dose concept"*) or hypothyroidism (*"ablative dose concept")*. However, ultimate success rate is significantly higher in the current *ablative* concept (>90%) compared to the previous *functional* concept (< 70%) [22, 31, 36]. A secondary goal of radioiodine therapy is a reduction of the thyroid volume due to mechanical and aesthetic issues [7, 49].

The success rate is mainly linked with administered activity and thyroid volume [22, 31, 34, 50]. Recent systematic review and meta-analysis demonstrated that the radiation dose to the thyroid directly positively correlates with the success of therapy [51]. According to the *functional* concept, an absorbed dose of 150 Gy is required to establish euthyroidism [48, 52] while a dose of 200–300 Gy is necessary according to an *ablative* concept [31, 52, 53], although not resolving hyperthyroidism in all patients [53].

Fixed-Activity Approach

The easiest and most widely used method for performing radioiodine therapy with the aim of permanent correction of hyperthyroidism is the fixed-activity method. It is based on the evaluation of thyroid size mainly by thyroid ultrasonography or scintigraphy [7, 31], and measuring RAIU and its turnover in the gland [54]. Most commonly, activities of 370–555 MBq are administered [22, 44, 48] (Fig. 6.1).

Higher activities are considered in case of thyroid volume above 40 cm^3, although in this case dosimetric approach may be preferred [55].

The main advantage of the *fixed-activity approach* is the simplicity of the pre-therapeutic procedure and, additionally, it is less time consuming. Still, there is a potential risk of over- and undertreatment with its consequences in the form of unnecessary radiation exposure and risk of uncured hyperthyroidism [7, 49].

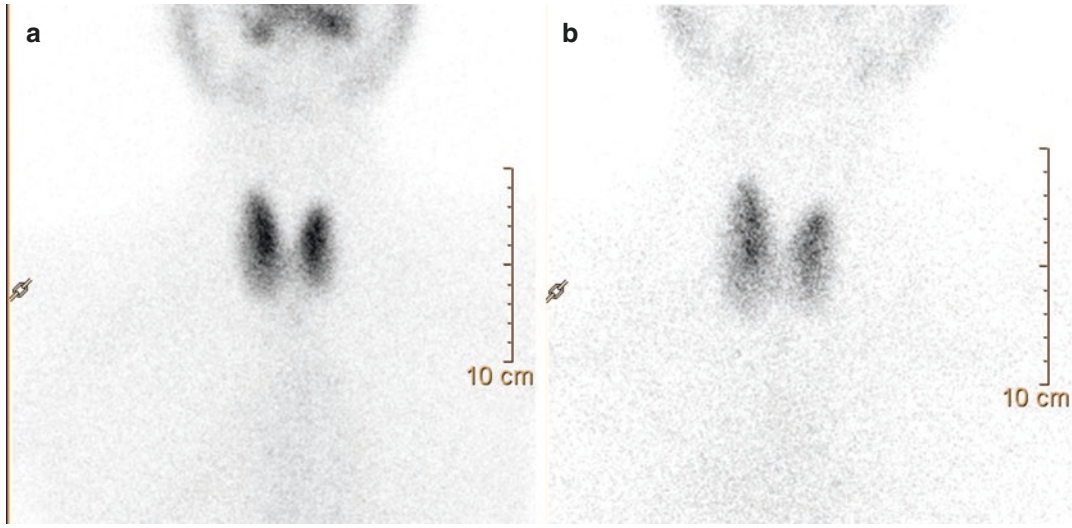

Fig. 6.1 A 44-year-old woman affected by autoimmune overt hyperthyroidism [TSH 0.001 mIU/mL (0.35–4.94), FT3 11.4 pg/mL (1.71–3.71), FT4 4.11 ng/dL (0.70–1.48), anti-thyroglobulin antibody (TgAb) 334 UI/mL (<5), anti-thyroperoxidase antibody (TPOAb) 402 UI/mL (<7), anti-TSH receptor antibody (TRAb) 2.99 U/L (>1.55)] associated with tachycardia, weight loss, asthenia, hyperhidrosis, insomnia, and irritability. Ultrasonography showed a high-normal thyroid volume (with prevalence of the right lobe) with irregularly hypoechoic structure but without nodular lesion and strongly increased blood flow (i.e., thyroid hell). Thyroid scintigraphy (**a**) performed 20 min after ^{99m}Tc-perthecnetate administration (111 MBq) demonstrated intense tracer uptake in both lobes and isthmus. Thus, a toxic diffuse goiter (TDG) was diagnosed. The patient underwent 131-radioiodine treatment (RIT) by fixed-activity approach (407 MBq). Four months after RIT, a clinical and laboratory euthyroid status [TSH 2.80 uIU/mL (0.27–4.2), FT3 2.80 pg/mL (2.02–4.43), FT4 12.90 pg/mL (9.32–17.09)] was diagnosed. At the same time, ^{99m}Tc-perthecnetate thyroid scintigraphy (**b**) showed a significant tracer uptake reduction in the thyroid parenchyma

Dosimetric Approach

A dosimetric approach is performed to determine the exact Na[^{131}I]I activity necessary to deliver the target absorbed dose to the thyroid. Furthermore, it may be used to determine the actual absorbed dose after the administration of radioiodine.

Recent systematic review and meta-analysis demonstrated a positive correlation between success rates of radioiodine therapy for GD and the thyroid absorbed dose. Estimated thyroid absorbed doses of 150 Gy, 200 Gy, and 300 Gy resolve hyperthyroidism in 74%, 81%, and 88% of patients and result in the establishment of a euthyroid state in 38%, 35%, and 29% of them, respectively [51]. An additional risk factor for non-cured hyperthyroidism is a larger gland size, which is linked with fast radioiodine kinetics [53, 56].

A target thyroid dose of a minimum 200 Gy is recommended for the permanent treatment of patients affected by refractory Graves' disease, while up to 300 Gy is used in case of large-volume thyroid and very severe hyperthyroidism in order to resolve the disease quickly. A target dose of 150 Gy may be used in case of mild low recurrence-risk disease with the aim of restoration of a euthyroid state. However, the success of radioiodine therapy is not guaranteed due to interindividual variability. Even if euthyroidism is established after the therapy, hormonal status evaluation should be continued as the rate of hypothyroidism increases over the years.

In case of a shorter half-life, i.e., early and high RAIU, especially in large thyroid glands, underestimation of the thyroid absorbed dose is possible, which may result in significant failure rates [56]. In those cases, estimated absorbed doses over 200 Gy may be required.

6.5.2 Radioiodine Therapy in Patients with Toxic Nodular and Toxic Multi-Nodular Goiter

In patients affected by TNG or TMNG, radioiodine therapy is an efficient and safe therapeutic option to definitively treat hyperthyroidism [7, 57]. It may be the first option in patients with overt or subclinical hyperthyroidism having solitary or multiple hyperfunctioning thyroid nodules without suspicious malignant nodules, particularly in an elderly population, patients with comorbidities that have a higher risk of surgery, those that have undergone previous thyroid surgery or irradiation therapy of the neck, and patients with no access to a high volume endocrine surgeon [7, 22].

On the other hand, absolute contraindications to radioiodine therapy of TNG or TMNG patients are pregnancy or breastfeeding and suspicious or confirmed thyroid cancer. Relative contraindications are large TMNG and symptoms of compression [22].

The first goal of radioiodine therapy is to correct hyperthyroidism, and preferably restoration of euthyroidism. The success rate depends mostly on administered activity, kinetics of radioiodine, and nodule(s) volume [22, 58]. An absorbed thyroid dose of 150–300 Gy is required to resolve the hyperthyroid state [31, 59, 60]. Higher absorbed doses, up to 400 Gy usually improve the success rate [60].

In general, the success rate ranges from 81 to 94% in case of TMNG and TNG, respectively [22, 31, 49, 59, 60]. The risk of persistent/recurrent hyperthyroidism is higher up to 20% in TMNG than in TNG patients [22, 49, 61]. The risk of subsequent hypothyroidism is higher in patients who received higher radioiodine activities, in those with high RAIU, older than 45 years, in patients previously treated with ATD, and in those with incomplete suppression of extranodular parenchyma [22, 62]. The risk of hypothyroidism increases during the next two decades and approximately occurs in two-thirds of TNG and TMNG patients, slightly more common in TMNG [62–64].

The secondary purpose of radioiodine therapy in TNG and TMNG is to reduce larger nodule(s) and thyroid volume to decrease mechanical and esthetic problems. Toxic thyroid nodule(s) reduce in volume by approximately one-third within 3 months, and up to half during 24 months post-therapy [49, 65, 66].

Fixed-Activity Approach

The easiest and most widely used method for performing radioiodine therapy is the fixed-activity method. It is based on the evaluation of thyroid size, RAIU and its biokinetics [54].

However, this method lacks pre-diagnostic accuracy [67] which results in a non-negligible incidence of persistent or recurrent hyperthyroidism (mostly in TMNG) or hypothyroidism (mostly in TNG with non-suppressed extranodular parenchyma) [49, 63]. Activities of 370–740 MBq are most commonly used to treat TNG or TMNG patients [22, 44] (Fig. 6.2).

Still, hyperfunctioning nodule(s) volume larger than 26 cm^3 can hamper the efficiency of radioiodine therapy. In those cases, a dosimetric approach may be more useful [55].

Dosimetric Approach

In the dosimetric approach, it would be preferable to consider the autonomously functioning nodules only (Fig. 6.3).

Measurement of RAIU is reliable only if the healthy thyroid tissue is completely suppressed

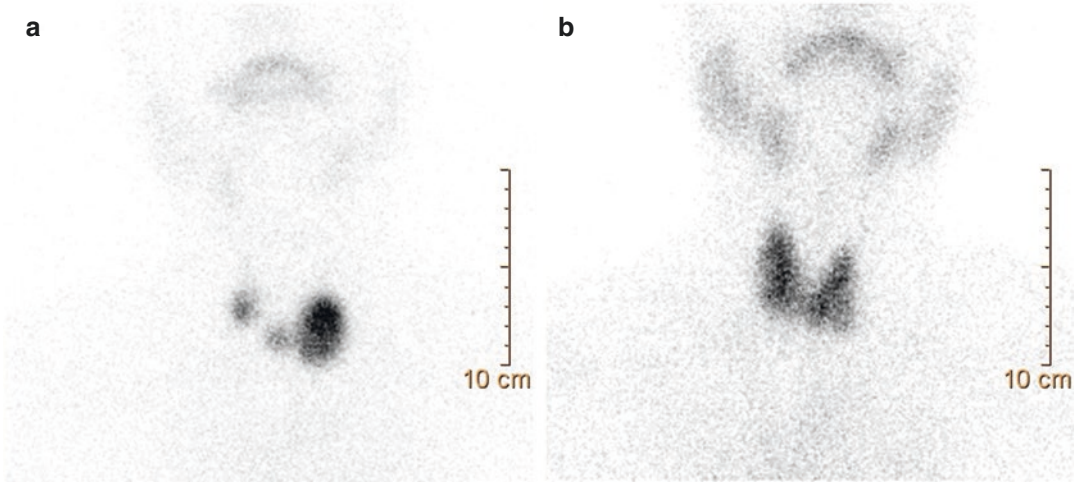

Fig. 6.2 A 75-year-old woman affected by overt hyperthyroidism [TSH 0.006 μIU/mL (0.27–4.20), FT3 8.0 pg/mL (2.00–4.40), FT4 23.12 pmol/L (12.00–22.00)] associated with tachycardia, weight loss, hyperhidrosis, insomnia, and irritability. Thyroid ultrasonography (TU) showed a multinodular goiter with a larger sized isohypoechoic nodule (30 mm in maximum diameter) in the left thyroid lobe. Thyroid scintigraphy (**a**) performed 20 min after ^{99m}Tc-perthecnetate administration (111 MBq) demonstrated three well-defined hyperfunctioning areas located in the left thyroid lobe (prevalent for size and tracer uptake), isthmus, and right lobe (basal region), respectively. No tracer uptake was noted in the extranodular thyroid parenchyma. As per consequence, a toxic multi-nodular goiter (TMNG) inhibiting extranodular parenchyma was diagnosed. The patient underwent 131-radioiodine treatment (RIT) by fixed-activity approach (555 MBq). Five months after RIT, a clinical and laboratory euthyroid status [TSH 3.02 μIU/mL (0.27–4.20), FT3 3.02 pg/mL (2.40–4.22), FT4 14.88 pmol/L (12.00–22.00)] was diagnosed. At the same time, ^{99m}Tc-perthecnetate thyroid scintigraphy (**b**) clearly demonstrated the complete ablation of the hyperfunctioning nodules while restored tracer uptake in the extranodular parenchyma was noted

[52]. Persistent or recurrent hyperthyroidism due to underdosing usually occurs if a significant amount of the measured activity is in the extranodal unsuppressed tissue. Conversely, hypothyroidism occurs if thyroid tissue is incompletely suppressed or in case of too high absorbed dose. In TNG or TMNG with a single or a few correctly measurable nodules, complete dosimetry resolves hyperthyroidism in 85–100% of patients treated with a target dose of 300–400 Gy, while the hypothyroidism occurs in 10%–20% of cases [59, 60]. When a correct volume measurement is not possible, lower target absorbed doses (100–150 Gy) to the entire thyroid are successfully used to determine the adequate radioiodine activity, but still, the proportion of the autonomic tissue should be approximately taken into account as well [59, 68]. If complete dosimetry is not possible, administered activity should be based on the measurement of an early uptake [69]. Target doses are also adjusted according to the degree of hyperthyroidism. Therefore, higher doses are used in patients with more severe hyperthyroidism [70]. Dosimetric approach according to the European standard operational procedure enables the most reliable results regarding achieved and intended target doses [52].

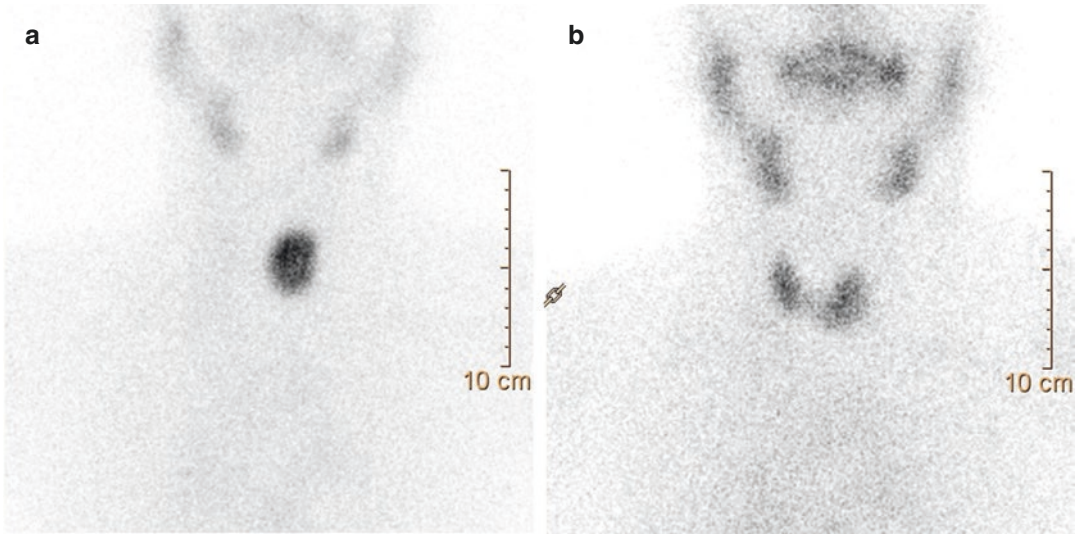

Fig. 6.3 A 75-year-old woman affected by overt hyperthyroidism [TSH 0.003 μIU/mL (0.30–3.07), FT3 5.3 pg/mL (2.40–4.22), FT4 1.22 ng/dL (0.75–1.54)] associated with tachycardia, insomnia, and irritability. Thyroid ultrasonography (TU) showed a large-sized nodule (33*22*20 mm) in the left thyroid lobe, irregularly hypoechoic with the presence of several regression areas. An increased intra-nodular blood flow was also noted. Thyroid scintigraphy (**a**) performed 20 min after ^{99m}Tc-perthecnetate administration (111 MBq) demonstrated a well-defined hyperfunctioning area located in the left thyroid lobe. In this latter, tracer uptake/distribution was quite intense and homogeneous, respectively. On the contrary, no tracer uptake was noted both in the right lobe and isthmus. Thus, a toxic nodular goiter (TNG) with functional inhibition of the remaining thyroid parenchyma was diagnosed. The patient underwent 131-radioiodine treatment (RIT) by dosimetric approach (296 MBq). Three months after RIT, a clinical and laboratory euthyroid status [TSH 2.72 μIU/mL (0.30–3.07), FT3 3.02 pg/mL (2.40–4.22), FT4 0.80 ng/dL (0.75–1.54)] was diagnosed. At the same time, ^{99m}Tc-perthecnetate thyroid scintigraphy (**b**) clearly demonstrated the complete ablation of the hyperfunctioning nodule while restored tracer uptake in the right thyroid lobe and isthmus was noted

6.6 Non-Toxic Goiter

Non-toxic goiter is an enlarged thyroid gland with, or without intrathyroidal nodules, with TSH, FT3, and FT4 values within the reference range.

The prevalence is highest in iodine-deficient regions [22, 71]. On the other hand, NTG incidence in iodine-sufficient areas is very low, with approximately 1/3500000 cases per year [72].

Since therapeutic management of NTG is largely controversial, nuclear medicine physicians must carefully select candidates for RIT taking into account possible treatment failure and patients' preferences. Clinical examination, results of laboratory tests, and imaging procedures are evaluated. Thyroid ultrasonography provides information regarding nodules' location, size, and echographic features. It detects suspicious nodules and in combination with fine-needle aspiration cytology usually rules out malignancy [22]. Alternative morphological procedures, i.e., contrast-free CT or MRI are mainly reserved for patients with large goiter or those with intrathoracic gland extension. They enable reliable evaluation of thyroid volume, its relation to surrounding structures, and the smallest transversal tracheal area. The use of the same imaging study is recommended before and after radioiodine therapy to compare the results of the therapy [73]. Thyroid scintigraphy performed using Na[^{99m}Tc]TcO_4 or Na[^{123}I]I is indicated mainly in patients with low-normal serum TSH, for excluding hyperfunctioning nodules and identifying non-functioning nodules and their location within the gland. RAIU should be measured as well since applied radioiodine activity is adjusted according to its value [71].

There is no ideal treatment for NTG as there is no consensus regarding the best therapeutic management of those patients. Approximately one-third of clinicians use just an observational approach [1, 71]. Iodine supplementation has been suggested as goiter development is associated with iodine deficiency. However, its efficiency is scarcely evaluated. Additionally, its use has been associated with a higher incidence of Hashimoto's thyroiditis, and also thyroid malignancy, i.e., papillary thyroid carcinoma. So the routine use of iodine supplements is not recommended [73].

Levothyroxine therapy is an alternative treatment option [74]. However, there is no consensus regarding its efficiency and a sufficient goiter reduction is detected in a very limited number of patients [73, 75]. Furthermore, goiter reduction is significantly lower in patients on levothyroxine than in those who received radioiodine therapy [76]. Additionally, the thyroid volume usually returns to baseline after levothyroxine withdrawal [77]. Levothyroxine therapy can be considered in younger patients with smaller goiter as it may result in overt hyperthyroidism with its side effects, e.g., cardiovascular [73].

Thyroidectomy is the preferred therapeutic option in patients that require immediate and significant goiter reduction due to severe compression-related symptoms. However, it may have severe side effects in a significant number of patients, especially those with large goiter and substernal gland extension, i.e., hypoparathyroidism, recurrent laryngeal nerve palsy, or tracheomalacia. Furthermore, goiter recurrence may occur in patients who underwent less than subtotal thyroidectomy [73]. In those cases, radioiodine therapy is more favorable compared to second surgical therapy [73, 78, 79] as the risk of vocal cord paralysis and hypoparathyroidism is up to 10x higher [73, 80].

6.7 Radioiodine Therapy of Non-TOXIC Goiter

Radioiodine therapy is a feasible therapeutic option used for the reduction of thyroid or nodule volume in patients with NTG [68, 81].

Candidates for radioiodine therapy are symptomatic NTG patients with a thyroid volume up to 100 cm^3, mostly elderly, patients with comorbidities that raise the risk of thyroid surgery, those that underwent previous neck surgery, and patients with intrathoracic goiter. Conversely, absolute contraindications for radioiodine therapy are pregnancy or breastfeeding, suspicious or confirmed thyroid cancer, and a high degree of tracheal compression, while relative contraindications are RAIU value at 24 h less than 15% (rhTSH may be used in those cases) and thyroid volume larger than 100 cm^3 [81].

Radioiodine therapy in most cases results in a reduction of goiter volume by half 1 year and up to 60% 2–5 years following therapy administration [68, 81–84].

Radioiodine activity of 3.7–14 MBq/g thyroid tissue taking into account RAIU is usually suggested for a target absorbed dose of 100–175 Gy [81–83]. The best results are observed in patients who received the highest thyroid doses, but this approach also results in increased whole-body radiation exposure [81].

Radioiodine efficiency negatively correlates with initial goiter volume. Thus, in large goiters >100 cm^3, the volume reduction rate is lower than usual, i.e., one-third 1 year after the therapy. Furthermore, radioiodine efficiency is reduced in case of low RAIU value [68, 81]. However, additional courses of radioiodine therapy are feasible to obtain a larger goiter reduction.

Preparation for radioiodine therapy in patients with NTNG is same as with hyperthyroid patients. The same is with the procedure.

Patients with NTNG of ≥100 cm^3 volume and severe tracheal constriction, particularly if <1 cm, should be treated under corticoid therapy, e.g., prednisolone, 25 mg/day during 2 weeks [31, 81]. Radioiodine therapy is recommended in an inpatient facility for the elder population and those with comorbidities that may raise the risk of post-therapy complications [31, 82].

Fixed-Activity Approach

The fixed-activity method is the easiest and most common method used for performing radioiodine therapy in NTNG. Goiter volume is measured by

thyroid ultrasonography, CT, or MR. Thyroid scintigraphy is used for functional mapping. RAIU value is determined to extrapolate administered activity [31, 84–86].

Most commonly, activities of 600–1110 MBq are used for the therapy of NTNG patients [81, 84–86].

Dosimetric Approach

Pre-therapeutic dosimetry is performed. The target mean thyroid absorbed dose is approximately 100 Gy [73], and in certain cases up to 150 Gy.

The dosimetric approach according to the European standard operational procedure provides the most precise results regarding the achieved and accomplished target dose [52].

Recombinant Human TSH-Aided Radioiodine Therapy

Recombinant human TSH increases RAIU. Its administration is linked with larger goiter reduction, compared with radioiodine therapy without rhTSH stimulation [87]. However, it is not yet approved for the treatment of NTNG, although it may be administered on an off-label basis. Very large goiters and low thyroid RAIU values are the major causes of therapy failure, and as such, they are the main indications for rhTSH-stimulated radioiodine therapy [88]. In the *superiority* strategy targeted absorbed dose is higher without increasing the radioiodine activity, or alternatively, in the *equality* strategy, administered activity is reduced while maintaining the thyroid dose [89]. rhTSH is administrated 24 h before radioiodine therapy to achieve optimal RAIU [68, 81, 90]. The administered dose of rhTSH depends on the aim of the treatment. The recommended dose in the equality strategy is usually 0.1 mg, whereas, in the superiority strategy, a dose of 0.3 mg is mainly applied. Higher goiter reduction is achieved in superiority than in the equality approach [68].

The risk of hyperthyroidism and acute thyroid enlargement is theoretically increased in rhTSH-stimulated therapy and depends also on applied activity. There is also approximately 5x higher risk of permanent hypothyroidism [88].

However, rhTSH allows reduction of applied radioiodine activity (equality strategy), higher target absorbed dose (superiority strategy), and significant goiter volume reduction.

6.8 Radioiodine Therapy in Pediatric Patients

In pediatric patients, autonomous nodules or NTNG are very rare. Almost all patients referred for radioiodine therapy are diagnosed with ATD refractory GD. According to the recently published European Thyroid Association Guideline for the management of pediatric Graves' disease, Na[^{131}I]I can be used in all age groups except <5 years due to theoretically increased long-term risk of malignancy. A relative contraindication is the age of 5–10 years and therefore ATD should be continued for years until the child reaches adequate age for radioiodine treatment, rather than undergoing surgical therapy [91].

Preparations are equal to those for adults, although parent co-hospitalization might be necessary, depending on the child's age.

Functional ablation is a goal of radioiodine therapy in order to reduce the risk of GD recurrence and possible malignant transformation of viable thyroid cells during the years. There are several therapeutic approaches: fixed-activity strategy using activities 200–800 MBq [31], a weight-based strategy applying 15 MBq Na[^{131}I]I / gram thyroid tissue, and a dosimetric approach with the thyroid target dose of at least 300 Gy [92].

There is no strong evidence of the superiority of one approach over another, although a recently published systematic review and meta-analysis in adult patients demonstrated that higher target doses positively correlate with successful functional ablation [51]. Although fixed-activity concepts are successful, they do carry a risk of overtreatment or undertreatment, which is particularly relevant at a young age. Therefore, thyroid dosimetry is recommended whenever available. In case of therapy failure, radioiodine therapy can be applied again after 3–6 months.

Side effects following radioiodine therapy are very rare. Thyroid tenderness is possible in the first week after the therapy. According to available studies, there is no increased risk of fertility problems or malignancy [93–95].

An alternative definitive treatment option is total thyroidectomy. Generally, surgery is the preferred treatment option in patients with contraindications for radioiodine therapy (i.e., age < 10 years, pregnancy), those with active Graves' ophthalmopathy, large goiter, and patients requiring fast and definitive treatment.

6.9 Side Effects of Radioiodine Therapy

Early Side Effects

Radioiodine therapy is a safe treatment option for benign thyroid disorders. It is most commonly well-tolerated, although acute or late side effects may occasionally occur.

Early side effects occur during the first few weeks following radioiodine therapy. Thyroid swelling is observed in patients with non-toxic, but also large toxic goiter. The main symptom is pain although, in older patients with very large nodular goiter, dyspnea may occur as well [84]. Medical therapy is rarely required, and it is usually symptomatic. In patients with higher risk factors non-steroidal anti-inflammatory drugs may be used for 1–2 days following therapy, while corticoids are given selectively as they may reduce the therapeutic effect of radioiodine [7, 41].

Radiation thyroiditis occurs in approximately 1% of cases during the first weeks following therapy administration. It may cause transient thyrotoxicosis in about 10% of cases [96]. The so-called thyroid storm is very rare nowadays but requires immediate treatment (inorganic iodide, ATD, beta-blockers, corticoids, and antipyretics) [97] and, if medically refractory, prompt thyroidectomy.

Radiation sialadenitis, as an acute or delayed side effect, may occur in case of high administered radioiodine activities. Usual clinical signs and symptoms are salivary glands swelling, xerostomia, pain, and taste dysfunctions that occur in up to a third of cases [98]. Lemon juice or other salivation-inducing products, e.g., lemon candies, consumed 24 h after radioiodine therapy, usually reduce the damage of salivary gland tissue by a faster secretion of radioiodine-containing saliva [99, 100].

The Marine-Lenhart syndrome is a rare side effect occurring in up to 4.1% of cases [101, 102], generally in TNG patients in the first days after therapy administration. Its incidence is higher in patients with initially increased serum thyroid peroxidase antibodies (TPOAb) and those with increased TPOAb following radioiodine administration [101, 103].

Radioiodine, similar to surgery, may cause a transient elevation of TRAb due to follicular cell damage [104]. Activation of existing or new onset GO is the most severe consequence of immune side effects [68].

Late Side Effects

Persistent hypothyroidism is considered a side effect in case of TNG or NTNG patients, but not in case of Graves' disease according to the new "ablative dose concept." Transient hypothyroidism may occur 2–5 months following therapy administration without symptoms of hypothyroidism and with spontaneous regression [7].

Radioiodine therapy is a risk factor for the new onset or deterioration of GO, but the prophylactic application of corticoids is efficient in preventing this side effect [105]. Initially, high TRAb levels, smoking, and untreated post-therapy hypothyroidism are associated with GO development/worsening [106].

Reduction of gonadal function may occur 45 days after radioiodine therapy but it is reversible and normalize after 1 year [107]. It is reasonable to postpone conception for the next 4–6 months in women and 3–4 months in men [7].

References

1. Diehl LA, Garcia V, Bonnema SJ, Hegedüs L, Albino CC, Graf H. Management of the nontoxic multinodular goiter in Latin America: comparison with North America and Europe, an electronic survey. J Clin Endocrinol Metab. 2005;90(1):117–23.

2. Bhagat MC, Dhaliwal SS, Bonnema SJ, Hegedüs L, Walsh JP. Differences between endocrine surgeons and endocrinologists in the management of non-toxic multinodular goitre. Br J Surg. 2003;90(9):1103–12.
3. Giovanella L, Avram AM, Iakovou I, Kwak J, Lawson SA, Lulaj E, et al. EANM practice guideline/SNMMI procedure standard for RAIU and thyroid scintigraphy. Eur J Nucl Med Mol Imaging. 2019;46(12):2514–25.
4. Kusic Z, Becker DV, Saenger EL, Paras P, Gartside P, Wessler T, et al. Comparison of technetium-99m and iodine-123 imaging of thyroid nodules: correlation with pathologic findings. J Nucl Med. 1990;31(4):393–9.
5. Reschini E, Ferrari C, Castellani M, Matheoud R, Paracchi A, Marotta G, et al. The trapping-only nodules of the thyroid gland: prevalence study. Thyroid. 2006;16(8):757–62.
6. Ruggeri R, Giuffrida G, Campennì A. Autoimmune endocrine disease. Minerva Endocrinol. 2018;43(3):305–22.
7. Giovanella L. Nuclear medicine therapy: side effects and complications. In: Nuclear medicine therapy. 1st ed. New York: Springer; 2019.
8. Smith TJ, Hegedüs L. Graves' disease. N Engl J Med. 2016;375(16):488–93.
9. Bartalena L, Masiello E, Magri F, Veronesi G, Bianconi E, Zerbini F, et al. The phenotype of newly diagnosed Graves' disease in Italy in recent years is milder than in the past: results of a large observational longitudinal study. J Endocrinol Investig. 2016;39(12):1445–51.
10. Antonelli A, Ferrari SM, Ragusa F, Elia G, Paparo SR, Ruffilli I, et al. Graves' disease: epidemiology, genetic and environmental risk factors and viruses. Best Pract Res Clin Endocrinol Metab. 2020;34(1):101387.
11. Ippolito S, Cusini C, Lasalvia P, Gianfagna F, Veronesi G, Gallo D, et al. Change in newly diagnosed Graves' disease phenotype between the twentieth and the twenty-first centuries: meta-analysis and meta-regression. J Endocrinol Investig. 2021;44(8):1707–18.
12. Nyström HF, Jansson S, Berg G. Incidence rate and clinical features of hyperthyroidism in a long-term iodine sufficient area of Sweden (Gothenburg) 2003–2005. Clin Endocrinol. 2013;78(5):768–76.
13. Boelaert K, Torlinska B, Holder RL, Franklyn JA. Older subjects with hyperthyroidism present with a paucity of symptoms and signs: a large cross-sectional study. J Clin Endocrinol Metab. 2010;95(6):2715–26.
14. Ruggeri R, Trimarchi F, Giuffrida G, Certo R, Cama E, Campennì A, et al. Autoimmune comorbidities in Hashimoto's thyroiditis: different patterns of association in adulthood and childhood/adolescence. Eur J Endocrinol. 2017;176(2):133–41.
15. Bartalena L, Piantanida E, Gallo D, Lai A, Tanda ML. Epidemiology, natural history, risk factors, and prevention of Graves' orbitopathy. Front Endocrinol (Lausanne). 2020;11:615993.
16. Moleti M, Violi MA, Montanini D, Trombetta C, Di Bella B, Sturniolo G, et al. Radioiodine ablation of postsurgical thyroid remnants after treatment with recombinant human TSH (rhTSH) in patients with moderate-to-severe Graves' orbitopathy (GO): a prospective, randomized, single-blind clinical trial. J Clin Endocrinol Metab. 2014;99(5):1783–9.
17. Bahn RS. Current insights into the pathogenesis of Graves' ophthalmopathy. Horm Metab Res. 2015;47(10):773–8.
18. Davies TF, Andersen S, Latif R, Nagayama Y, Barbesino G, Brito M, et al. Graves' disease. Nat Rev Dis Prim. 2020;6(1):52.
19. Cooper DS. Hyperthyroidism. Lancet. 2003;362(9382):459–68.
20. Zuhur SS, Ozel A, Kuzu I, Erol RS, Ozcan ND, Basat O, et al. The diagnostic utility of color Doppler ultrasonography, Tc-99m pertechnetate uptake, and TSH-receptor antibody for differential diagnosis of Graves' disease and silent thyroiditis: a comparative study. Endocr Pract. 2014;20(4):310–9.
21. Smith TJ, Hegedüs L. Graves' disease. N Engl J Med. 2016;375(16):1552–65.
22. Ross DS, Burch HB, Cooper DS, Greenlee MC, Laurberg P, Maia AL, et al. 2016 American Thyroid Association guidelines for diagnosis and management of hyperthyroidism and other causes of thyrotoxicosis. Thyroid. 2016;26(10):1343–421.
23. Campennì A, Barbaro D, Guzzo M, Capoccetti F, Giovanella L. Personalized management of differentiated thyroid cancer in real life - practical guidance from a multidisciplinary panel of experts. Endocrine. 2020;70(2):280–91.
24. Stokkel MPM, Junak DH, Lassmann M, Dietlein M, Luster M. EANM procedure guidelines for therapy of benign thyroid disease. Eur J Nucl Med Mol Imaging. 2010:2218–28.
25. Leo M, Sabini E, Ionni I, Sframeli A, Mazzi B, Menconi F, et al. Use of low-dose radioiodine ablation for Graves' orbitopathy: results of a pilot, perspective study in a small series of patients. J Endocrinol Investig. 2018;41(3):357–61.
26. Ruggeri R, Campennì A, Sindoni A, Baldari S, Trimarchi F, Benvenga. Association of autonomously functioning thyroid nodules with Hashimoto's thyroiditis: study on a large series of patients. Exp Clin Endocrinol Diabetes. 2011;119(10):621–7.
27. Giovanella L, D'Aurizio F, Campenni' A, Ruggeri R, Baldari S, Verburg F, et al. Searching for the most effective thyrotropin (TSH) threshold to rule-out autonomously functioning thyroid nodules in iodine deficient regions. Endocrine. 2016;54(3):757–61.
28. Vicchio TM, Giovinazzo S, Certo R, Cucinotta M, Micali C, Baldari S, et al. Lack of association between autonomously functioning thyroid nodules and germline polymorphisms of the thyrotropin receptor and Gαs genes in a mild to moderate

iodine-deficient Caucasian population. J Endocrinol Investig. 2014;37(7):625–30.
29. Gozu HI, Lublinghoff J, Bircan R, Paschke R. Genetics and phenomics of inherited and sporadic non-autoimmune hyperthyroidism. Mol Cell Endocrinol. 2010;322(1–2):125–34.
30. Russ G, Bonnema SJ, Erdogan MF, Durante C, Ngu R, Leenhardt L. European thyroid association guidelines for ultrasound malignancy risk stratification of thyroid nodules in adults: the EU-TIRADS. Eur Thyroid J. 2017;6(5):225–37.
31. Stokkel MPM, Handkiewicz Junak D, Lassmann M, Dietlein M, Luster M. EANM procedure guidelines for therapy of benign thyroid disease. Eur J Nucl Med Mol Imaging. 2010;37(11):2218–28.
32. Akamizu T, Satoh T, Isozaki O, Suzuki A, Wakino S, Iburi T, et al. Diagnostic criteria, clinical features, and incidence of thyroid storm based on nationwide surveys. Thyroid. 2012;22(7):661–79.
33. Santos RB, Romaldini JH, Ward LS. Propylthiouracil reduces the effectiveness of radioiodine treatment in hyperthyroid patients with Graves' disease. Thyroid. 2004;14(7):525–30.
34. Bonnema SJ, Bennedbæk FN, Veje A, Marving J, Hegedüs L. Propylthiouracil before 131I therapy of hyperthyroid diseases: effect on cure rate evaluated by a randomized clinical trial. J Clin Endocrinol Metab. 2004;89(9):4439–44.
35. Rostkowska O, Spychalski P, Dobrzycka M, Wilczyński M, Łachiński AJ, Obołończyk Ł, et al. Effects of thyroid hormone imbalance on colorectal cancer carcinogenesis and risk - a systematic review. Endokrynol Pol. 2019;70(2):190–7.
36. Kobe C, Weber I, Eschner W, Sudbrock F, Schmidt M, Dietlein M, et al. Graves' disease and radioiodine therapy. Is success of ablation dependent on the choice of thyreostatic medication? Nuklearmedizin. 2008;47(4):153–6.
37. Klein I, Danzi S. Thyroid disease and the heart. Circulation. 2007;116(15):1725–35.
38. Klein I. Endocrine disorders and cardiovascular disease. In: Libby P, et al., editors. Braunwald's heart disease: a textbook of cardiovascular medicine. 8th ed. Philadelphia: Saunders/Elsevier; 2008. p. 2033–47.
39. Bartalena L, Kahaly GJ, Baldeschi L, Dayan CM, Eckstein A, Marcocci C, et al. The 2021 European group on Graves' orbitopathy (EUGOGO) clinical practice guidelines for the medical management of Graves' orbitopathy. Eur J Endocrinol. 2021;185(4):G43–67.
40. Bartalena L, Baldeschi L, Boboridis K, Eckstein A, Kahaly GJ, Marcocci C, et al. The 2016 European Thyroid Association/European Group on Graves' orbitopathy guidelines for the management of Graves' orbitopathy. Eur Thyroid J. 2016;5(1):9–26.
41. Halstenberg J, Kranert WT, Korkusuz H, Mayer A, Ackermann H, Grünwald F, et al. [Influence of glucocorticoid therapy on intratherapeutic biodistribution of 131I radioiodine therapy in Graves' disease]. Nuklearmedizin. 2018;57(2):43–9.
42. Sekulić V, Rajić M, Vlajković M, Ilić S, Stević M, Kojić M. The effect of short-term treatment with lithium carbonate on the outcome of radioiodine therapy in patients with long-lasting Graves' hyperthyroidism. Ann Nucl Med. 2017;31(10):744–51.
43. Abd-ElGawad M, Abdelmonem M, Ahmed AE, Mohammed OM, Zaazouee MS, Assar A, et al. Lithium carbonate as add-on therapy to radioiodine in the treatment on hyperthyroidism: a systematic review and meta-analysis. BMC Endocr Disord. 2021;21(1):64.
44. Jolanta MD, Bogsrud TV. Nuclear medicine in evaluation and therapy of nodular thyroid. In: Thyroid nodules. Cham: Springer International; 2018.
45. Brzozowska M, Roach PJ. Timing and potential role of diagnostic I-123 scintigraphy in assessing radioiodine breast uptake before ablation in postpartum women with thyroid cancer: a case series. Clin Nucl Med. 2006;31(11):683–7.
46. Council Directive 2013/59/Euratom of 5 December 2013 laying down basic safety standards for protection against the dangers arising from exposure to ionising radiation, and repealing Directives 89/618/Euratom, 90/641/Euratom, 96/29/Euratom, 97/43/Euratom a. Off J EU. 2013;L(13):1–73.
47. Bartalena L, Chiovato L, Vitti P. Management of hyperthyroidism due to Graves' disease: frequently asked questions and answers (if any). J Endocrinol Investig. 2016;39(10):1105–14.
48. De Jong J, Da Huysmans C, de Keizer B. 131I therapy in primary hyperthyroidism and non-toxic (multi) nodular goitre. Procedure Guidelines Nuclear Medicine, Dutch society of nuclear medicine 2016. Part II, page 372–83 (Editor JP Esser) ISBN 978-90-78876-09-0.
49. Tarantini B, Ciuoli C, Di Cairano G, Guarino E, Mazzucato P, Montanaro A, et al. Effectiveness of radioiodine (131-I) as definitive therapy in patients with autoimmune and non-autoimmune hyperthyroidism. J Endocrinol Investig. 2006;29(7):594–8.
50. Santos RB, Romaldini JH, Ward LS. A randomized controlled trial to evaluate the effectiveness of 2 regimens of fixed iodine (^{131}I) doses for Graves' disease treatment. Clin Nucl Med. 2012;37(3):241–4.
51. Taprogge J, Gape PM, Carnegie-Peake L, Murray I, Gear JI, Leek F, et al. A systematic review and meta-analysis of the relationship between the radiation absorbed dose to the thyroid and response in patients treated with radioiodine for Graves' disease. Thyroid. 2021;31(12):1829–38.
52. Hänscheid H, Canzi C, Eschner W, Flux G, Luster M, Strigari M, et al. 2013 EANM dosimetry committee series on standard operational procedures for pre-therapeutic dosimetry II. Dosimetry prior to radioiodine therapy of benign thyroid diseases. Eur J Nucl Med Mol Imaging. 2013;40(7):1126–34.
53. Reinhardt M, Brink I, Joe A, Von Mallek D, Ezziddin S, Palmedo H, et al. Radioiodine therapy in Graves'

disease based on tissue-absorbed dose calculations: effect of pre-treatment thyroid volume on clinical outcome. Eur J Nucl Med. 2002;29(9):1118–24.
54. Arora S, Bal C. Is there any need for adjusting 131 I activity for the treatment of high turnover Graves' disease compared to normal turnover patients? Results from a retrospective cohort study validated by propensity score analysis. Nucl Med Mol Imaging. 2010;55(1):15–26.
55. Vija Racaru L, Fontan C, Bauriaud-Mallet M, Brillouet S, Caselles O, Zerdoud S, et al. Clinical outcomes 1 year after empiric 131I therapy for hyperthyroid disorders: real life experience and predictive factors of functional response. Nucl Med Commun. 2017;38(9):756–63.
56. De Jong JAF, Verkooijen HM, Valk GD, Zelissen PMJ, De Keizer B. High failure rates after (131) I therapy in Graves hyperthyroidism patients with large thyroid volumes, high iodine uptake, and high iodine turnover. Clin Nucl Med. 2013;38(6):401–6.
57. Ross DS. Radioiodine therapy for hyperthyroidism. N Engl J Med. 2011;364(20):1978–9.
58. Amato E, Campennì A, Leotta S, Ruggeri RM, Baldari S. Treatment of hyperthyroidism with radioiodine targeted activity: a comparison between two dosimetric methods. Phys Med. 2016;32(6):847–53.
59. Reiners C, Schneider P. Radioiodine therapy of thyroid autonomy. Eur J Nucl Med Mol Imaging. 2002;29(Suppl 2):S471–8.
60. Reinhardt MJ, Biermann K, Wissmeyer M, Juengling FD, Brockmann H, Von Mallek D, et al. Dose selection for radioiodine therapy of borderline hyperthyroid patients according to thyroid uptake of 99mTc-pertechnetate: applicability to unifocal thyroid autonomy? Eur J Nucl Med Mol Imaging. 2006;33(5):608–12.
61. Kang AS, Grant CS, Thompson GB, Van Heerden JA, Pasieka JL, LoGerfo P, et al. Current treatment of nodular goiter with hyperthyroidism (Plummer's disease): surgery versus radioiodine. Surgery. 2002;132(6):916–23.
62. Zakavi SR, Mousavi Z, Davachi B. Comparison of four different protocols of I-131 therapy for treating single toxic thyroid nodule. Nucl Med Commun. 2009;30(2):169–75.
63. Ceccarelli C, Bencivelli W, Vitti P, Grasso L, Pinchera A. Outcome of radioiodine-131 therapy in hyperfunctioning thyroid nodules: a 20 years' retrospective study. Clin Endocrinol. 2005;62(3):331–5.
64. Yano Y, Sugino K, Akaishi J, Uruno T, Okuwa K, Shibuya H, et al. Treatment of autonomously functioning thyroid nodules at a single institution: radioiodine therapy, surgery, and ethanol injection therapy. Ann Nucl Med. 2011;25(10):749–54.
65. Nygaard B, Hegedüs L, Ulriksen P, Nielsen KG, Hansen JM. Radioiodine therapy for multinodular toxic goiter. Arch Intern Med. 1999;159(12):1364–8.
66. Bonnema SJ, Bertelsen H, Mortensen J, Andersen PB, Knudsen DU, Bastholt L, et al. The feasibility of high dose iodine 131 treatment as an alternative to surgery in patients with a very large goiter: effect on thyroid function and size and pulmonary function. J Clin Endocrinol Metab. 1999;84(10):3636–41.
67. Allahabadia A, Daykin J, Sheppard MC, Gough SCL, Franklyn JA. Radioiodine treatment of hyperthyroidism-prognostic factors for outcome. J Clin Endocrinol Metab. 2001;86(8):3611–7.
68. Bonnema SJ, Hegedüs L. Radioiodine therapy in benign thyroid diseases: effects, side effects, and factors affecting therapeutic outcome. Endocr Rev. 2012;33(6):920–80.
69. Rokni H, Sadeghi R, Moossavi Z, Treglia G, Zakavi SR. Efficacy of different protocols of radioiodine therapy for treatment of toxic nodular goiter: systematic review and meta-analysis of the literature. Int J Endocrinol Metab. 2014;12(2):e14424.
70. Hammes J, van Heek L, Hohberg M, Reifegerst M, Stockter S, Dietlein M, et al. Impact of different approaches to calculation of treatment activities on achieved doses in radioiodine therapy of benign thyroid diseases. EJNMMI Phys. 2018;5(1):32.
71. Gharib H, Papini E, Garber JR, Duick DS, Harrell RM, Hegedüs L, et al. American Association of Clinical Endocrinologists, American College of Endocrinology, and Associazione Medici Endocrinologi medical guidelines for clinical practice for the diagnosis and management of thyroid nodules - 2016 update appendix. Endocr Pract. 2016;22(1):1–60.
72. Sherman SI, Tuttle RM, Ball DW, Byrd D, Clark OH, Daniels GH, et al. NCCN clinical practice guidelines in oncology. Thyroid Carcinoma; 2009. Vol. 1. www.nccn.org.
73. Hegedüs L, Bonnema SJ, Bennedbæk FN. Management of simple nodular goiter: current status and future perspectives. Endocr Rev. 2003;24(1):102–32.
74. Bonnema SJ, Bennedbæk FN, Ladenson PW, Hegedudies L. Management of the nontoxic multinodular goiter: a North American survey. J Clin Endocrinol Metab. 2002;87(1):112–7.
75. Wesche MF, Tiel-v Buul MM, Lips P, Smits NJ, Wiersinga WM. A randomized trial comparing levothyroxine with radioactive iodine in the treatment of sporadic nontoxic goiter. J Clin Endocrinol Metab. 2001;86(3):998–1005.
76. Medeiros-Neto G. Iodine deficiency disorders. In: Jameson JL, De Groot LJ, editors. Endocrinology. Philadelphia: WB Saunders; 2000. p. 1529–39.
77. Berghout A, Wiersinga WM, Touber JL, Smits NJ, Drexhage HA. Comparison of placebo with L-thyroxine alone or with carbimazole for treatment of sporadic non-toxic goitre. Lancet. 1990;336(8709):193–7.
78. Mishra A, Agarwal A, Agarwal G, Mishra SK. Total thyroidectomy for benign thyroid disorders in an endemic region. World J Surg. 2001;25(3):307–10.
79. Hisham AN, Azlina AF, Aina EN, Sarojah A. Total thyroidectomy: the procedure of choice for multinodular goitre. Eur J Surg. 2001;167(6):403–5.

80. Thomusch O, Machens A, Sekulla C, Ukkat J, Lippert H, Gastinger I, et al. Multivariate analysis of risk factors for postoperative complications in benign goiter surgery: prospective multicenter study in Germany. World J Surg. 2000;24(11):1335–41.
81. Bonnema SJ, Fast S, Hegedüs L. The role of radioiodine therapy in benign nodular goitre. Best Pract Res Clin Endocrinol Metab. 2014;28(4):619–31.
82. Bachmann J, Kobe C, Bor S, Rahlff I, Dietlein M, Schicha H, et al. Radioiodine therapy for thyroid volume reduction of large goitres. Nucl Med Commun. 2009;30(6):466–71.
83. Nielsen VE, Bonnema SJ, Boel-Jørgensen H, Grupe P, Hegedüs L. Stimulation with 0.3-mg recombinant human thyrotropin prior to iodine 131 therapy to improve the size reduction of benign nontoxic nodular goiter: a prospective randomized double-blind trial. Arch Intern Med. 2006;166(14):1476–82.
84. Bonnema SJ, Nielsen VE, Boel-Jørgensen H, Grupe P, Andersen PB, Bastholt L, et al. Improvement of goiter volume reduction after 0.3 mg recombinant human thyrotropin-stimulated radioiodine therapy in patients with a very large goiter: a double-blinded, randomized trial. J Clin Endocrinol Metab. 2007;92(9):3424–8.
85. Medeiros-Neto G, Marui S, Knobel M. An outline concerning the potential use of recombinant human thyrotropin for improving radioiodine therapy of multinodular goiter. Endocrine. 2008;33(2):109–17.
86. Paz-Filho GJ, Mesa-Junior CO, Olandoski M, Woellner LC, Goedert CA, Boguszewski CI, et al. Effect of 30 mCi radioiodine on multinodular goiter previously treated with recombinant human thyroid-stimulating hormone. Braz J Med Biol Res. 2007;40(12):1661–70.
87. Huo Y, Xie J, Chen S, Wang H, Ma C. Recombinant human thyrotropin (rhTSH)-aided radioiodine treatment for non-toxic multinodular goitre. Cochrane Database Syst Rev. 2021;12(12):CD010622.
88. Bonnema SJ, Fast S, Hegedüs L. Non-surgical approach to the benign nodular goiter: new opportunities by recombinant human TSH-stimulated 131I-therapy. Endocrine. 2011;40(3):344–53.
89. Fast S, Bonnema SJ, Hegedüs L. Radioiodine therapy of benign non-toxic goitre. Potential role of recombinant human TSH. Ann Endocrinol (Paris). 2011;72(2):129–35.
90. Fast S, Nielsen VE, Grupe P, Bonnema SJ, Hegedüs L. Optimizing 131I uptake after rhTSH stimulation in patients with nontoxic multinodular goiter: evidence from a prospective, randomized, double-blind study. J Nucl Med. 2009;50(5):732–7.
91. Mooij CF, Cheetham TD, Verburg FA, Eckstein A, Pearce SH, Leger J, et al. 2022 European Thyroid Association Guideline for the management of pediatric Graves' disease. Eur Thyroid J. 2021;11:e210073.
92. Silberstein EB, Alavi A, Balon HR, Clarke SEM, Divgi C, Gelfand MJ, et al. The SNMMI practice guideline for therapy of thyroid disease with 131I 3.0. J Nucl Med. 2012;53(10):1633–51.
93. Rivkees SA, Dinauer C. An optimal treatment for pediatric Graves' disease is radioiodine. J Clin Endocrinol Metab. 2007;92(3):797–800.
94. Mizokami T, Hamada K, Maruta T, Higashi K, Tajiri J. Long-term outcomes of radioiodine therapy for juvenile Graves' disease with emphasis on subsequently detected thyroid nodules: a single institution experience from Japan. Endocr Pract. 2020;26(7):729–37.
95. Lutterman SL, Zwaveling-Soonawala N, Verberne HJ, Verburg FA, Van Trotsenburg ASP, Mooij CF. The efficacy and short- and long-term side effects of radioactive iodine treatment in pediatric Graves' disease: a systematic review. Eur Thyroid J. 2021;10(5):353–63.
96. Burch HB, Solomon BL, Cooper DS, Ferguson P, Walpert N, Howard R. The effect of antithyroid drug pretreatment on acute changes in thyroid hormone levels after 131I ablation for Graves' disease. J Clin Endocrinol Metab. 2001;86(7):3016–21.
97. Satoh T, Isozaki O, Suzuki A, Wakino S, Iburi T, Tsuboi K, et al. 2016 guidelines for the management of thyroid storm from The Japan Thyroid Association and Japan Endocrine Society (First edition). Endocr J. 2016;63(12):1025–64.
98. Grewal RK, Larson SM, Pentlow CE, Pentlow KS, Gonen M, Qualey R, et al. Salivary gland side effects commonly develop several weeks after initial radioactive iodine ablation. J Nucl Med. 2009;50(10):1605–10.
99. Van Nostrand D, Bandaru V, Chennupati S, Wexler J, Kulkarni K, Atkins F, et al. Radiopharmacokinetics of radioiodine in the parotid glands after the administration of lemon juice. Thyroid. 2010;20(10):1113–9.
100. Jentzen W, Balschuweit D, Schmitz J, Freudenberg L, Eising E, Hilbel T, et al. The influence of saliva flow stimulation on the absorbed radiation dose to the salivary glands during radioiodine therapy of thyroid cancer using 124I PET(/CT) imaging. Eur J Nucl Med Mol Imaging. 2010;37(12):2298–306.
101. Giuffrida G, Giovinazzo S, Certo R, Vicchio TM, Baldari S, Campennì A, et al. An uncommon case of Marine-Lenhart syndrome. Arq Bras Endocrinol Metabol. 2014;58(4):398–401.
102. Charkes ND. Graves' disease with functioning nodules (Marine-Lenhart syndrome). J Nucl Med. 1972;13(12):885–92.
103. Schmidt M, Gorbauch E, Dietlein M, Faust M, Stützer H, Eschner W, et al. Incidence of postradioiodine immunogenic hyperthyroidism/Graves' disease in relation to a temporary increase in thyrotropin receptor antibodies after radioiodine therapy for autonomous thyroid disease. Thyroid. 2006;16(3):281–8.
104. Chiappori A, Villalta D, Bossert I, Ceresola EM, Lanaro D, Schiavo M, et al. Thyrotropin receptor autoantibody measurement following radiometabolic treatment of hyperthyroidism: comparison

between different methods. J Endocrinol Investig. 2010;33(3):197–201.
105. Li HX, Xiang N, Hu WK, Jiao XL. Relation between therapy options for Graves' disease and the course of Graves' ophthalmopathy: a systematic review and meta-analysis. J Endocrinol Investig. 2016;39(11):1225–33.
106. Bahn RS, Burch HB, Cooper DS, Garber JR, Greenlee MC, Klein I, et al. Hyperthyroidism and other causes of thyrotoxicosis: management guidelines of the American Thyroid Association and American Association of Clinical Endocrinologists. Thyroid. 2011;21(6):593–646.
107. Ceccarelli C, Canale D, Battisti P, Caglieresi C, Moschini C, Fiore E, et al. Testicular function after 131I therapy for hyperthyroidism. Clin Endocrinol. 2006;65(4):446–52.

7 Radioiodine Theranostics of Differentiated Thyroid Carcinoma

Anca M. Avram

7.1 Introduction

DTC is a slow-growing tumor with a very low disease-specific mortality rate for local-regional disease (5-year survival 99.9% for localized disease, and 98.3% for regional metastatic disease), however, distant metastatic disease is associated with significantly worse prognosis (5-year survival 54.9%) [1]. Standard of care management for differentiated thyroid cancer (DTC) includes risk-adapted surgery, post-operative Iodine-131 (^{131}I) therapy, and thyroid hormone therapy. In uncommon cases of radioiodine-refractory tumors, additional therapy may include re-operative surgical intervention, external radiotherapy, and interventional radiology for the treatment of locoregional metastases, and multi-kinase or tyrosine kinase inhibitors for treatment of distant metastatic disease.

Current thyroid cancer guidelines emphasize a patient-individualized approach to therapeutic 131-I administration, recommending against 131-I ablation in low-risk tumors and selective use of 131-I therapy for medium-risk patients [2–4]. Defining the categories of low-, intermediate- and high-risk patients is important for clinical implementation of risk-adapted therapeutic 131-I administration and the 2015 American Thyroid Association (ATA) guidelines introduced the concept of continuum of risk based on estimated risk of structural disease recurrence according to surgical histopathology information [3]. Although referral for post-operative 131-I therapy is predicated on risk stratification based on surgical pathology information, post-operative diagnostic radioiodine (RAI) scintigraphy contributes to the completion of staging and risk stratification itself, thus having the potential to influence 131-I therapeutic strategy [5].

7.2 Diagnosis

The most common clinical presentation of DTC is as an incidental thyroid nodule. Neck ultrasound (US), serum thyroid stimulating hormone (TSH), and thyroid scintigraphy are used to select high-risk nodules for fine-needle aspiration (FNA). Sonographic features have been used to produce a standardized risk assessment for thyroid malignancy named Thyroid Imaging Reporting and Data System (TIRADS) [6, 7]. In the absence of suspicious cervical lymph nodes, FNA is discouraged for nodules less than 1 cm, and the decision to aspirate larger nodules is guided by the TIRADS score in the context of nodule size. The cytologic risk of malignancy is determined using the Bethesda System for Reporting Thyroid Cytopathology [8].

A. M. Avram (✉)
Medicine and Radiology, Case Western Reserve University, Cleveland, OH, USA

Endocrinology Division, MetroHealth Medical Center, Cleveland, OH, USA
e-mail: aavram@metrohealth.org

L. Giovanella (ed.), *Integrated Diagnostics and Theranostics of Thyroid Diseases*,
https://doi.org/10.1007/978-3-031-35213-3_7

7.3 Surgical Treatment

Traditionally, (near-) total thyroidectomy was performed in most DTC patients, with lobectomy reserved for cytologically indeterminate nodules or patients with unifocal micro-PTC < 1 cm. Currently, lobectomy is sometimes suggested for patients with unifocal intrathyroidal low-risk DTC in the absence of additional risk factors (i.e., no clinical evidence of nodal metastases, cN0) [3]. The management of low-risk DTC between 2 and 4 cm is a topic of debate: While a lobectomy may be proposed, total thyroidectomy is still largely advised [9]. Active surveillance is an alternative to lobectomy for unifocal micro-PTC with no extracapsular extension or lymph node metastases [10]. The decision for active surveillance is based primarily on age-related risk of progression, individual surgical risk factors, and patient preference [11]. In all other cases, total thyroidectomy remains the preferred surgical approach [12].

Cervical lymph nodal metastases occur in 20–60% of patients with DTC and this nodal involvement varies from clinically relevant macrometastasis to seemingly clinically irrelevant micrometastases [13, 14]. When lymph nodal metastases are diagnosed pre-operatively, central and/or lateral neck compartment dissection reduces the risk of local-regional recurrence. Prophylactic central neck dissection may improve regional control for invasive tumors (T3–T4), but it is discouraged for low-risk DTC because potentially associated morbidities (i.e., hypoparathyroidism and recurrent laryngeal nerve damage) are not justified by a significant clinical benefit [15].

7.4 Staging and Risk Stratification for Differentiated Thyroid Cancer

The concept of oncologic staging is central for providing a baseline assessment and defining a management strategy in malignant diseases. Staging systems define the mortality risk in thyroid cancer using pTNM classification and the derived AJCC staging (summarized in Tables 7.1 and 7.2) [16].

Table 7.1 TNM classification for differentiated thyroid cancer. TNM UICC/AJCC 8th edition (2017) [16]

		TNM 2017
	Tx	Primary tumor cannot be assessed
T	T0	No evidence of primary tumor
	T1a	T ≤ 1 cm[a]
	T1b	T > 1 cm and ≤ 2 cm[a]
	T2	T > 2 cm and ≤ 4 cm[a]
	T3	T3a: Tumor more than 4 cm in greatest dimension, limited to the thyroid
T3b: Tumor of any size with gross extrathyroidal extension invading only strap muscles (sternohyoid, sternothyroid, thyrohyoid, or omohyoid muscles)		
	T4a	Tumor extends beyond the thyroid capsule and invades any of the following: Subcutaneous soft tissues, larynx, trachea, esophagus, and recurrent laryngeal nerve
	T4b	Tumor invades prevertebral fascia or encases carotid artery or mediastinal vessels
N	Nx	Regional lymph nodes cannot be assessed
	N0	No regional lymph node metastasis
	N1a	Metastases in level VI (pretracheal, paratracheal, and prelaryngeal/Delphian lymph nodes) or upper/superior mediastinum (level VII)[a]

Table 7.1 (Continued)

		TNM 2017
	N1b	Metastasis in other unilateral, bilateral, or contralateral cervical lymph nodes (levels I, II, III, IV, or V) or retropharyngeal
M	M0	No distant metastasis is found
	M1	Distant metastasis is present

[a] In this edition, minor extrathyroidal extension that involves perithyroidal adipose tissue, strap muscles, nerves, or small vascular structures, identified only by microscopy but not clinically appreciated (no gross invasion), is no longer used as a risk factor for staging; superior mediastinal (level VII) nodes are scored N1a

Table 7.2 AJCC prognostic grouping for differentiated thyroid cancer. TNM UICC/AJCC 8th edition (2017) [16]

	AJCC 8th edition (2017)	
	Stage < 55 years old	Stage ≥ 55 years old
Stage I	Any T, any N, M0	T1/T2, N0, M0
Stage II	Any T, any N, M1	T3a/T3b, N0, M0 T1/T2/T3, N1, M0
Stage III	–	T4a, any N, M0
Stage IVA	–	T4b, any N, M0
Stage IVB	–	Any T, any N, M1
Stage IVC	–	–

Table 7.3 Suggested framework for ^{131}I therapy

Strategy	Prescribed ^{131}I activity	Clinical/Pathological context
Risk-adapted ^{131}I therapy	1.11–1.85 GBq (30–50 mCi) ^{131}I[a]	Remnant ablation
Risk-adapted ^{131}I therapy	1.85–3.7 GBq (50–100 mCi) ^{131}I	Adjuvant treatment
Risk-adapted ^{131}I therapy	3.7–5.6 GBq (100–150 mCi) ^{131}I	Treatment of small volume local-regional disease
Risk-adapted ^{131}I therapy	5.6–7.4 GBq (150–200 mCi) ^{131}I	Treatment of advanced local-regional disease and/or small volume distant metastatic disease
Whole body/blood dosimetry	≥ 7.4 GBq (≥ 200 mCi) ^{131}I, maximum tolerable safe ^{131}I activity	Treatment of diffuse distant metastatic disease

[a]FDA approved the use of rhTSH in combination with 100 mCi ^{131}I for remnant ablation in December 2007 [1, 17]. Reproduced with permission from [18]

The risk of structural disease recurrence is defined by ATA as a continuum of risk for structural disease recurrence resulting in a 3-level system of risk stratification described as low-, intermediate-, or high-risk based on surgical pathology and clinical information (summarized in Table 7.3) [3]. Both staging and risk stratification play a crucial role in defining the initial management strategy and subsequent long-term surveillance for patients with thyroid cancer. Due to its indolent nature, thyroid cancer has a very low disease-specific mortality rate for local-regional disease after complete initial therapy (5-year survival 99.9% for localized disease, and 97.8% for regional metastatic disease), however, distant metastatic disease is associated with significantly worse prognosis (5-year survival 55.3%) [19] Therefore, in addition to staging which is used to predict disease-specific survival, secondary outcome variables such as rates of persistent disease, rates of recurrent disease, medico-economic issues, and quality of life outcomes, need to be considered when deciding 131-I therapeutic strategy [20].

7.5 Post-operative Management

Post-operative evaluation includes Tg measurement, neck US and diagnostic radioiodine (^{131}I or ^{123}I) whole-body scan (DxWBS) which is helpful to identify persistent disease and characterize tumor ^{131}I avidity. Institutional management protocols are established by multidisciplinary teams based on the local availability and expertise of the surgical, pathology, radiology, and laboratory components integral to the DTC treatment algorithm [21].

7.6 Post-operative ^{131}I Therapy

The goal of ^{131}I therapy is outlined based on standardized definitions as follows: *remnant ablation, adjuvant treatment, or treatment of known disease* [21, 22]. Upon integration of various parameters including clinical-pathologic, laboratory, and imaging information, ^{131}I therapy is administered for the following reasons:

- *Remnant ablation*, for elimination of the normal thyroid remnant tissue which achieves undetectable or minimal serum Tg levels (in the absence of neoplastic tissue) and facilitates follow-up.
- *Adjuvant treatment*, for elimination of suspected but unproven sites of neoplastic cells with the goal of reducing the risk of disease recurrence.
- *Treatment of known disease*, for treatment of persistent or recurrent metastatic disease.

7.7 Benefits of 131-I Therapy in Thyroid Cancer

The impact of ^{131}I therapy on the clinical outcome of thyroid cancer patients has been demonstrated in several large data series. An analysis of 2936 DTC patients in the National Thyroid Cancer Therapy Cooperative Study Group (NTCTCS) reported improved overall survival and disease-specific survival in patients with advanced tumors and regional and/or distant metastatic disease who received post-operative ^{131}I therapy [23]. An updated analysis of 4941 patients in the NTCTCS study with a median follow-up of 6 years (range 0–25 years) confirmed improved overall survival in stages III and IV patients, and also demonstrated improved disease-free survival for stage II patients receiving ^{131}I therapy [24]. A meta-analysis of 31 patient-cohort studies regarding the effectiveness of ^{131}I therapeutic administration demonstrated a statistically significant effect on improving clinical outcomes at 10 years, with decreased risk for local-regional recurrence (RR 0.31; CI 0.2–0.49) and an absolute risk reduction of 3% for distant metastatic disease [25]. An analysis of the National Cancer Database comprising 21,870 intermediate-risk patients demonstrated that adjuvant ^{131}I treatment improved overall survival, both for the younger (<45 years) and for the older (≥65 years) subsets of patients. Adjuvant ^{131}I therapy was associated with a 29% reduction in the risk of death for all patients [26]. The beneficial effects of post-operative ^{131}I therapy are most evident in patients with local-regionally advanced and distant metastatic disease (stages IV-A, IV-B, and IV-C disease): an analysis of the National Cancer Database comprising 11,832 patients demonstrated that the administration of ^{131}I therapy was associated with significantly improved 5- and 10-year survival for both PTC and FTC patients, regardless of pathological sub-stage (Stage IV A, B, or C), as follows: mortality in the PTC cohort (n = 10,796) at 5 years at 10 years was 11% and 14%, respectively, in patients who received ^{131}I therapy, as compared to 22.7% and 25.5%, respectively, in patients who received none; mortality in the FTC cohort (n = 1036) at 5 years at 10 years was 29.2% and 36.8%, respectively, in patients who received ^{131}I therapy, as compared to 45.5% and 51%, respectively, in patients who received none [27].

7.8 Preparation for ^{131}I Therapy

Evaluation with radioiodine scintigraphy and ^{131}I therapy is scheduled at a minimum of 4 weeks after surgery, which allows time for patient preparation and for reaching post-operative Tg plateau levels, used as a marker for residual thyroid tissue and/or metastatic thyroid cancer after total thyroidectomy. Tg levels must always be interpreted in the context of concomitant TSH level (unstimulated vs. stimulated Tg) and type of TSH stimulation (endogenous vs. exogenous) [28]. Patient preparation for optimal ^{131}I uptake by residual thyroid tissue and metastatic disease includes 1–2 weeks of a low-iodine diet (LID)—see Table 7.2, and adequate TSH stimulation (TSH ≥ 30 mIU/L, measured 1–3 days prior to ^{131}I administration) by either a thyroid hormone

withdrawal (THW) or recombinant human TSH (rhTSH) stimulation [29]. For childbearing females (aged 12–50 years) a negative pregnancy test is required to be obtained within 72 h of ^{131}I administration, or prior to the first rhTSH injection (if employed), unless the patient is status post hysterectomy or postmenopausal.

There are two major approaches for obtaining TSH stimulation which is necessary for increasing Na-I symporter (NIS) expression and function in metastatic lesions (and residual thyroid tissue) with the goal of increasing diagnostic sensitivity of ^{131}I scintigraphy and radiation absorbed dose to target lesions

1. *Endogenous TSH stimulation* is obtained through thyroid hormone deprivation following total thyroidectomy, thus inducing a hypothyroid state: the hypothyroid stimulation protocol (THW) has 2 variants: a) L-T4 (levothyroxine) withdrawal for 4 weeks; this interval is determined by T4 elimination half-life (T4 $t_{1/2}$) of 7 days and the physiologic pituitary response to declining T4 concentrations. b) T4/T3 (levothyroxine/liothyronine) substitution for the first 2 weeks, followed by discontinuation of T3 for 2 weeks; this interval is based on T3 $t_{1/2}$ of 0.75 days.
2. *Exogenous TSH stimulation:* The patient continues T4 treatment and undergoes preparation with low-iodine diet. TSH elevation is obtained through administration of rhTSH (Thyrogen ® Stimulation Protocol): 0.9 mg rhTSH injection is administered intramuscularly on two consecutive days, followed by ^{131}I therapy administration at 48–72 h.

The choice of preparation method (THW vs. rhTSH) needs to be individualized for each patient. There is general agreement that for normal thyroid tissue (i.e., thyroid remnant), rhTSH and THW stimulation are equivalent, because normal thyroid tissue has constitutive high expression of highly functional NIS and does not require prolonged TSH stimulation for adequate ^{131}I uptake and retention. However, metastatic thyroid cancer has lesser density and poorer functionality of NIS, and therefore TSH elevation over time (area under the curve of TSH stimulation) is important to promote increased ^{131}I uptake and retention in tumors [30, 31]. In the setting of distant metastatic disease THW preparation and dosimetry-guided ^{131}I therapy is favored, when clinically safe and feasible [32–34].

7.9 ^{131}I Therapy Administration

There are two approaches to ^{131}I therapy delivery: the theranostic approach which integrates the information obtained with post-operative diagnostic (Dx) radioiodine (^{123}I, ^{131}I or ^{124}I) scans in the management algorithm, and the empirical approach based on clinical-pathologic factors and institutional protocols.

7.9.1 Diagnostic and Post-therapy 131-I Scans with Diagnostic Intent

Historically, post-therapy 131-I imaging had the advantage of superior activity counts statistics (count density) and appeared to provide more diagnostic information than diagnostic 131-I scans. In addition, the issue of stunning by the diagnostic 131-I scan activity was raised (defined as a reduction of 131-I uptake seen on post-therapy scan as compared to the diagnostic scans and interpreted as potentially causing a decreased effect of the subsequent 131-I therapy dose when administered after diagnostic 131-I scans) [35–37]. However, other studies have questioned the clinical relevance of stunning demonstrating little or no clinical evidence of stunning [38–42]. Stunning appears not to be a problem when activities <2 mCi 131-I are utilized for diagnostic scintigraphy and when 131-I therapy is administered within 72 h of the diagnostic 131-I activity [43–45]. It is possible that stunning may be related to a true cytocidal effect of the high 131-I diagnostic activities (5–10 mCi 131-I) used in the past, and therefore an effort to decrease administered diagnostic 131-I activity and optimize the imaging technique to preserve diagnostic sensitivity for disease detection is

important [43]. Progress in gamma camera instrumentation over the past 10 years led to significant improvement in spatial and contrast resolution of modern gamma camera systems making possible the acquisition of high-quality diagnostic 131-I scintigraphic images highly concordant with the post-therapy 131-I scans. McDougall et al. reported in a cohort of 280 patients a 98% concordance rate between the findings obtained with 74 MBq (2 mCi) diagnostic 131-I scans and post-therapy scans obtained at 8 days after 131-I treatment [39]. Furthermore, Avram et al. reported a 92% concordance rate between the findings obtained with 37 MBq (1 mCi) diagnostic 131-I scans and post-therapy scans obtained at 2 days after 131-I treatment. In only 6% of patients, additional foci of activity were detected on post-therapy scans, however, the findings were clinically significant (i.e., upstaged the patient) in only 1.4% of cases [46]. Therefore, it is possible to use diagnostic 131-I scans for identification of regional and distant iodine-avid metastases and for planning activity-adjusted 131-I treatment. Diagnostic 131-I scans performed with modern gamma camera SPECT/CT technology and optimization of imaging protocols have been used post-operatively with good results for assessing the extent of metastatic disease and for guiding therapeutic 131-I administration [47, 48].

7.9.2 Integration of Histopathology, Laboratory, and Scintigraphy Information

Integration of diagnostic and/or post-therapy 131-I scintigraphy information and stimulated thyroglobulin (Tg) levels in the context of surgical pathology is of critical importance for determining disease status by completing initial staging and risk stratification and guiding management decisions. Tg is a glycoprotein exclusively produced by the follicular cells of the thyroid gland and metabolized in the liver. Tg levels can therefore be used as a thyroid cancer biomarker as it declines with a half-life ($t_{1/2}$) of approximately 65 h after total thyroidectomy. Tg levels can become significantly elevated immediately after surgery as compared to preoperative values due to surgical manipulation of thyroid resulting in enhanced wash-out of Tg into the circulation, and it takes approximately 25 days after surgery –10 $t_{1/2}$ for hepatic clearance) for Tg levels to become a reliable marker of residual thyroid tissue and/or metastatic disease [49]. Thyroglobulin autoantibodies (TgAb) are a marker of thyroid autoimmunity and are detected in approximately 20% of DTC patients. Presence of TgAb interferes with reliable measurement of Tg levels causing a falsely low/undetectable Tg. Therefore, every serum specimen for Tg testing needs concomitant TgAb testing to inform that Tg measurement is not compromised by TgAb interference [50]. Tg levels become undetectable in the absence of thyroid remnant and/or persisting disease after total thyroidectomy and 131-I therapy. On the other hand, an increased Tg trend is used as an indicator for residual or recurrent DTC [28].

7.10 Determining the Prescribed Therapeutic ^{131}I Activity

Current practice guidelines recommend routine ^{131}I adjuvant therapy for patients with intermediate to high risk of recurrence (although there are some differences concerning intermediate-risk disease) and avoiding routine ^{131}I therapy for patients with a small (≤1 cm) intrathyroidal DTC and no evidence of locoregional or distant metastatic spread [3, 51]. However, ^{131}I therapy for other low-risk DTC patients (i.e., pT1b-T2) remains controversial: the various iterations of the ATA guidelines advised against the systematic use of ^{131}I in these patients [3], while the 2008 European Association of Nuclear Medicine (EANM) suggests that ^{131}I therapy is helpful, citing the lack of prospective data showing that surveillance without ablation is non-inferior to ^{131}I administration [52].

The decision for ^{131}I therapy and the prescribed ^{131}I activity depends on the goal of ^{131}I therapy as determined by the estimated risk for persistent/recurrent disease. Please see Table 7.3

for suggested treatment ^{131}I activities in the context of therapeutic intent, as follows:

- *Thyroid remnant ablation* in low-risk patients is typically performed with low ^{131}I activity (e.g., 1.1–1.85 GBq; 30 mCi-50 mCi) based on the preponderance of published evidence demonstrating equal effectiveness as compared with higher 131-I activities, with lower rate of adverse events [53–89]. The Federal Drug Administration (FDA) approved the use of rhTSH (Thyrogen ®, Genzyme corporation) in combination with 3.7 GBq (100 mCi) ^{131}I for remnant ablation in December, 2007 [17, 90, 91].
- *Adjuvant ^{131}I therapy* is performed with 1.85–3.7 GBq (50–100 mCi), with some institutions extending this range to 5.6 GBq (150 mCi); there are no comparison data regarding the effectiveness of 3.7 GBq (100 mCi) vs. 5.6 GBq (150 mCi) for adjuvant treatment, while current guidelines advise that the risk for ^{131}I toxicity increases with therapeutic activity escalation [92].
- *Treatment of known disease* is performed with 3.7–5.6 GBq (100–150 mCi) for small volume local-regional disease, and 5.6–7.4 GBq (150–200 mCi) ^{131}I for treatment of advanced local-regional disease and/or small volume distant metastatic disease. Identification of iodine-avid diffuse metastatic disease may lead to escalation of prescribed therapeutic ^{131}I activity to ≥7.4 GBq (200 mCi) guided by dosimetry calculations [48, 93, 94].

A special circumstance is presented by use of ^{131}I therapy (3.7 GBq [100 mCi]) for ablation of a remaining thyroid lobe after lobectomy/hemithyroidectomy as an alternative to completion thyroidectomy [95–97]. Current guidelines propose lobectomy for patients deemed as low-risk for recurrence; however, if the pathology demonstrates a higher risk tumor, then completion thyroidectomy with resection of the contralateral thyroid lobe is recommended with the goal of facilitating post-operative ^{131}I therapy and long-term surveillance. Therapeutic ^{131}I administration as a substitute for completion thyroidectomy is not recommended routinely [3]. However, it can be used to eliminate the residual thyroid lobe in highly selected cases, such as patients who had experienced complications during initial surgery (e.g., recurrent laryngeal nerve paralysis), for whom completion thyroidectomy is contraindicated due to other comorbidities, or for patients who decline additional surgery.

7.11 The Role of Dosimetry for Thyroid Cancer Treatment

There are two approaches for individualization of 131-I treatment based on a pre-therapy study, as follows: (1) blood dosimetry- and (2) lesion dosimetry-based methods. Of these, the classic blood-based method is more widely used, and permits calculation of the maximum tolerated activity (MTA) that can be administered to an individual patient without the risk of severe hematopoietic toxicity. In this dosimetry schema the radiation absorbed dose to the blood is used as a surrogate for the absorbed dose to the red bone marrow, typically considered as the dose limiting critical organ (in some situations, such as extensive pulmonary metastatic disease, the lung could be the critical organ). An upper limit of 2 Gy to the blood is generally used as the threshold that avoids any serious bone marrow toxicity, which is based on the findings of the original study of Benua et al. [98]. Treatment individualization is based on determining the maximum 131-I activity that can be administered to each patient while keeping the absorbed dose to the blood at ≤2 Gy. Blood-based dosimetry is carried out by measuring activity counts in blood samples obtained at specified time points over a 4-day period after the administration of a tracer amount of 131-I as described in a document by the EANM Dosimetry Committee [99]. The contribution to the absorbed dose from beta radiation originating from the activity in the blood, as well as the contribution from gamma-ray emissions originating from the activity throughout the whole-body must be considered, although the latter component is usually <25%. To determine the blood activity, whole blood samples (5 ml hepa-

rinized aliquots) are collected at multiple time points (2, 24, 48, 72, and 96 h) during the first week after administration of tracer amount (e.g., 15–37 MBq [0.4–1 mCi]) 131-I activity and measurements are performed in an accurately calibrated (for 131-I) well counter. To determine the whole-body activity, serial measurements are performed with either a dual-head gamma camera or a scintillation probe. Once time-integrated activities (cumulated activities) for both blood and whole body are determined from the serial measurements, the absorbed dose to the blood per unit administered activity (i.e., Gy/GBq administered activity) can be determined using the S-value-based equations of the MIRD schema [99]. The therapeutic 131-I activity that can be safely administered while maintaining blood radiation absorbed dose ≤2 Gy) can then be determined based on this pre-therapy predicted radiation absorbed dose to the blood [100]. Further restrictions to MTA recommend that the administered therapeutic activity does not exceed 4.44 GBq (120 mCi) 131-I whole-body retention at 48 h, or 2.96 GBq (80 mCi) 131-I whole-body retention at 48 h if pulmonary metastases are present [101].

Maximizing therapeutic effectiveness is highly desirable for the treatment of distant metastatic disease, as the first 131-I treatment ("first strike") has the highest chance of being curative [102]. The lower response rates from fractionated empiric fixed activity treatments are a result of lower radiation absorbed dose rates and reduced radiation absorbed doses delivered by second and subsequent treatments because of decreased 131-I uptake in the metastatic lesions (likely related to elimination of most radiosensitive tumor cell populations with the first treatment and survival of more radio-resistant and less-iodine avid clonal cell lines) [103].

The choice of empiric vs. dosimetry-guided 131-I therapy remains controversial, as there is no definitive published data to show the superiority of one approach versus the other. Although Deandreis et al. showed no survival advantage in metastatic DTC patients who received dosimetry-guided treatments vs. patients treated with repeated courses of empiric 131-I activity [104], the study has significant limitations due to the imperfect matching of patient cohorts in regard to age and preparation method (rhTSH stimulation vs. L-T4 withdrawal protocols) [105]. Klubo et al. also compared clinical outcomes for two patient cohorts treated either with empirically selected vs. dosimetry-determined 131-I activities and found that the rates of partial response, stable disease, and progression-free survival, as well as frequency of side effects, were not significantly different between the two groups. However, based on multivariate analysis, the dosimetry-guided treatment group was 70% less likely to progress (odds ratio 0.29; 95% CI 0.087–1.02; $p < 0.052$) and more likely to obtain a complete response (odds ratio 8.2; 95% CI 1.2–53.5; $p < 0.029$) [106]. Taking into consideration the limitations of retrospective studies, the advantages and disadvantages of empiric fixed activity versus dosimetry-guided treatments, the radiobiological principles, and thyroid cancer prognosis in the context of disease stage, this author considers that empiric fixed activity methods are adequate for the selection of 131-I activity for remnant ablation and adjuvant treatment, however, dosimetry-guided treatments may offer a distinct advantage for treatment of known metastatic disease. Scintigraphic identification of distant metastatic disease and therapeutic 131-I administration are the most important factors associated with significant improvement in survival and prolonged disease-free time interval [107–110].

7.12 Radioiodine Theranostics

The theranostic approach to ^{131}I administration involves the acquisition of a post-operative Dx radioiodine (^{123}I, ^{131}I, or ^{124}I) scan for planning ^{131}I therapy. Figure 7.1 presents the central role of radioiodine theragnostics in the management of thyroid cancer.

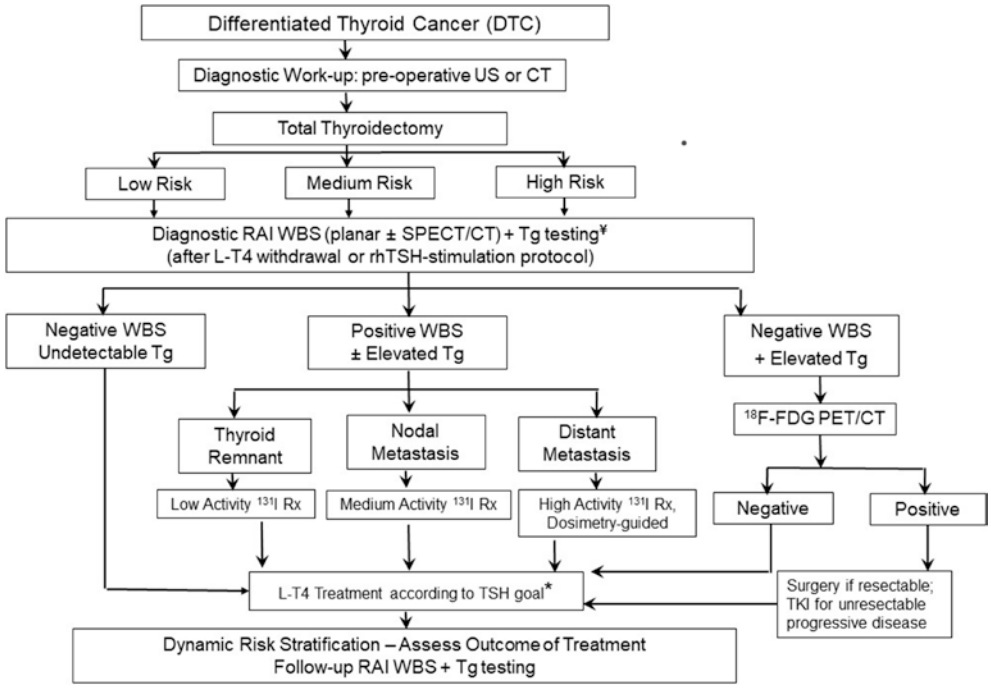

Fig. 7.1 Algorithm for radioiodine theragnostics for thyroid cancer management

Dx whole-body scans (WBS) are performed with the intent of identifying and localizing regional and distant metastatic disease, as well as evaluating the capacity of metastatic deposits to concentrate ^{131}I. Depending on institutional protocols, the findings on Dx WBS may alter management, such as providing guidance for additional surgery or altering the prescribed ^{131}I therapy, either by adjusting empiric ^{131}I activity, or performing dosimetry calculations for determining the maximum tolerated therapeutic ^{131}I activity (MTA) for therapy of distant metastatic disease. Also, unnecessary ^{131}I treatment may be avoided if Dx WBS finds no evidence of residual thyroid tissue or metastatic disease and the stimulated Tg is <1 ng/mL in the absence of interfering anti-Tg antibodies. Information acquired from DxWBS may also lead to additional functional metabolic imaging with ^{18}F-FDG PET/CT when non-iodine avid metastatic disease is suspected (based on Tg elevation out of proportion to the findings on DxWBS). Wherever available, it is preferable for post-operative Dx scanning to be performed using integrated multimodality imaging (i.e., single photon computed emission tomography/computed tomography (SPECT/CT). SPECT/CT imaging is particularly important for assessing focal radioiodine uptake in the neck and differentiating thyroid remnant versus nodal metastasis and for detecting metastases in normal-size cervical lymph nodes (that would not be visible on post-operative neck ultrasonography). Scintigraphic evaluation with Dx WBS can identify pulmonary micrometastases (which are too small to be detected on routine chest X-ray and may remain undetected on computer tomography) and can diagnose bone metastases at an early stage before cortical disruption is visible on bone X-rays or CT. Most importantly, since ^{131}I therapy is most effective for smaller metastatic deposits, early identification of regional

and distant metastases is important for successful therapy [111, 112]. In a group of 320 thyroid cancer patients referred for post-operative ^{131}I therapy, Dx WBS with SPECT/CT imaging detected regional metastases in 35% of patients, and distant metastases in 8% of patients. This information acquired changed staging in 4% of younger, and 25% of older patients [46]. Both imaging data and stimulated thyroglobulin levels acquired at the time of Dx WBS are consequential for ^{131}I therapy planning, providing information that changed clinical management in 29% of patients as compared to a management strategy based on clinical and surgical pathology information alone [5]. The benefits of integrating Dx WBS in the management algorithm of intermediate- and high-risk thyroid cancer for guiding ^{131}I therapeutic administration have been demonstrated in a group of 350 patients who were evaluated to assess treatment response with a median follow-up of 3 years after primary treatment (surgery and post-operative ^{131}I therapy): complete response (CR) to treatment was achieved in 88% patients with local-regional disease, and in 42% patients with distant metastases after a single ^{131}I therapeutic administration [48].

In all cases, ^{131}I administration should be followed by a post-treatment whole-body scan (PT-WBS) to determine therapeutic ^{131}I localization which is routinely used to complete post-operative staging. Hybrid imaging with SPECT/CT improves the accuracy of PT-WBS and should be done whenever possible, most importantly when DxWBS was not performed or when PT-WBS shows additional foci of activity as compared to Dx WBS [113]. A high level of concordance between Dx WBS and PT-WBS findings has been demonstrated in 2 large data series from Stanford University (98% concordance in a group of 280 patients) and the University of Michigan (92% concordance in a group of 303 patients) [39, 46]. Therefore, the information obtained with Dx WBS reasonably predicts ^{131}I therapeutic localization and can be used for ^{131}I therapy planning in the paradigm of thyroid cancer radiotheragnostics [114]. The theragnostic approach for the management of metastatic DTC is illustrated in Fig. 7.2.

Treatment response evaluation is integral to radiotheranostics, and the detection of elevated basal and/or stimulated Tg in the context of negative diagnostic radioiodine scan requires further evaluation with 18F-FDG PET/CT for early identification of non-iodine avid metastatic disease, which is unlikely to respond to repeated 131-I treatments [116]. In a study by Avram et al., only a minority of patients had iodine-avid structural incomplete response (8 patients, 2.3% of the entire cohort) and required repeated 131-I treatments. Meticulous follow-up and comprehensive imaging evaluation for patients with biochemical evidence of residual disease explain the low number of cases categorized as indeterminate (2.3%) and biochemically incomplete (1.4%) treatment responses in this study [48].

Integration of diagnostic radioiodine scintigraphy in the management algorithm of patients with thyroid cancer is feasible and advantageous because it permits 131-I therapy planning according to radiotheragnostic principles. The cost of diagnostic radioiodine scintigraphy is reasonable and approximately equal to or significantly less than the cost of most other imaging studies. According to a cost analysis by Van Nostrand et al., as of December 2013, the cost of a 131-I diagnostic whole-body scan was US $308, and compared favorably with Chest CT scan $411, Neck MRI $726, Neck PET-CT $1043, two rhTSH injections $2424. Neck US study is the least expensive study ($102), and in many instances needs to be supplemented by a US-guided FNA biopsy ($175) for definitive characterization of US study findings [117].

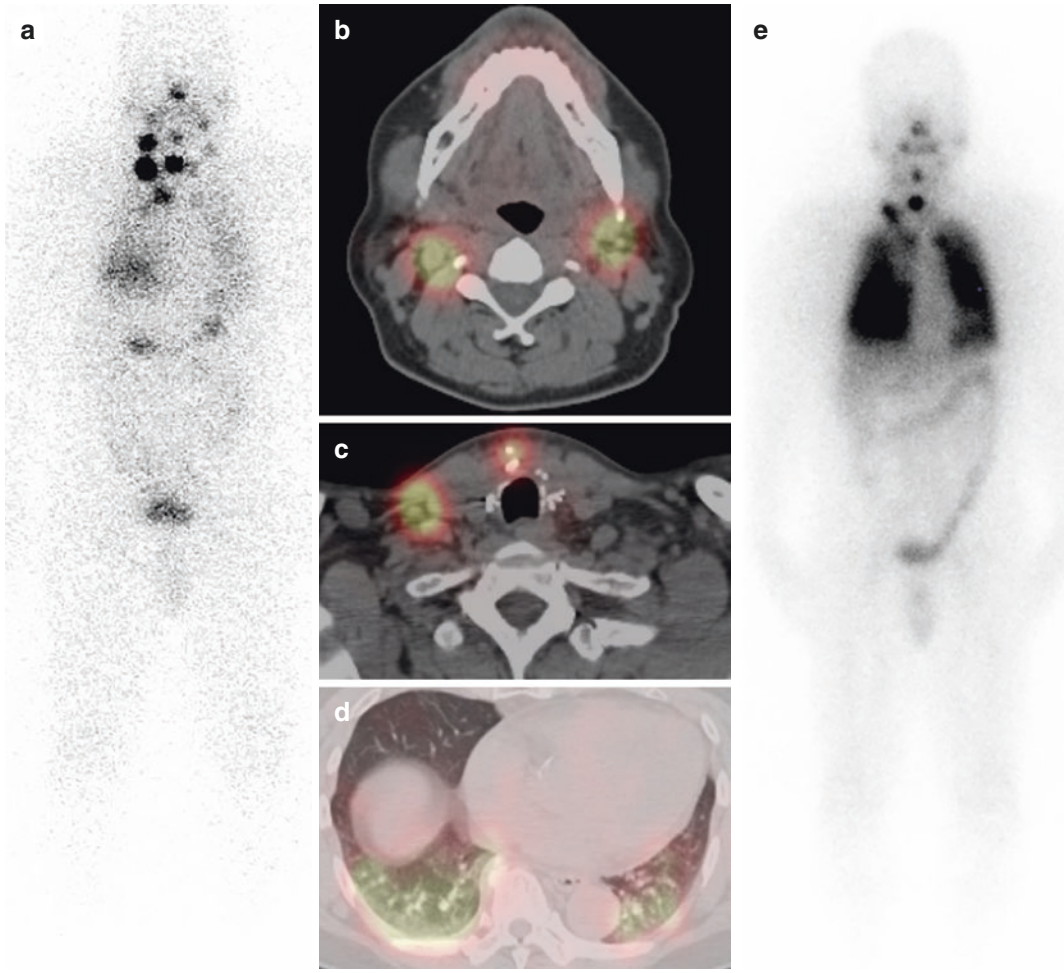

Fig. 7.2 Radioiodine theranostics for a 63-year-old man with regionally advanced thyroid cancer: 2.2 cm. PTC, 11+/11 lymph nodes resected in the surgical specimen of total thyroidectomy. Diagnostic 1 mCi ^{131}I WBS, anterior projection (**a**) depicts multifocal neck activity and diffuse lung activity. Neck SPECT/CT (**b**, **c**) demonstrates iodine-avid soft tissue nodules consistent with cervical nodal metastases. Chest SPECT/CT (**d**) demonstrates diffuse lung activity and branching pulmonary vasculature without definite lung nodules identified. The patient received dosimetry-guided 12.6 GBq (340 mCi) ^{131}I treatment and post-therapy WBS, anterior projection (**e**) obtained at 3 days demonstrates therapeutic ^{131}I localization to cervical lymph nodal metastases and diffuse miliary pulmonary metastatic disease. Reproduced with permission from [115]

7.13 Treatment of Advanced Disease

Distant metastases develop in about 10% of DTC patients, commonly in the lungs, bone, brain, liver and skin, and are the main cause of death (i.e., overall mortality 65% at 5 years and 75% at 10 years) [118].

The prognosis of metastatic DTC is variable, with two distinct phenotypes identified—indolent and aggressive [119]. Patients with iodine-avid metastatic DTC tend to have a more favorable prognosis with 10-year survival greater than 90%, while non-iodine avid metastatic DTC has a dire 10-year survival of 10% [120]. Younger patients and those with single-organ metastases and low disease burden have the best outcome. The mainstay of treatment is TSH suppression and ^{131}I therapy as long as the disease remains radioiodine avid. About two-thirds of patients

have radioiodine-avid distant metastases and one-third of them will achieve remission after multiple radioiodine treatments [111]. Approximately 15–20% of patients with metastatic DTC and most patients with Hurthle cell thyroid cancer are refractory to radioiodine (i.e., radioiodine-refractory) and overall survival for these patients ranges between 2.5 and 4.5 years [111, 121].

Determining when a patient no longer responds to ^{131}I can be challenging. Factors impacting the specific clinical situation such as age, tumor histology, stage, residual radioiodine avidity, and FDG avidity should be evaluated [122]. ^{18}F-FDG-PET/CT is particularly useful for the identification and localization of non-iodine avid metastastases and is used for evaluating patients with elevated Tg and negative DxWBS (i.e., Tg+/scan-) [123]. In this setting, having already established the lack of ^{131}I uptake on a DxWBS, a positive ^{18}F-FDG-PET/CT strongly supports the suspicion of ^{131}I negative/refractory disease, leading to changes in management by identifying patients unlikely to benefit from additional ^{131}I therapy and instead qualify for alternative therapy [124]. In addition, ^{18}F-FDG PET/CT has shown a prognostic value in metastatic DTC predicting the course of disease as aggressive or indolent [125]. In radioiodine refractory metastatic DTC there is a survival disadvantage for patients with a positive PET as compared with those with a negative PET [121].

7.14 Future Perspectives

Future studies addressing the benefits and limits of 131-I therapy in thyroid cancer must optimize the balance between 131-I treatment efficacy and minimization of potential side effects. Determining the objective and the target of 131-I therapy is essential for performing dosimetry and for assessing treatment the outcome, providing new compelling reasons for pre-therapeutic diagnostic scintigraphic imaging with low activities of 131-I or 124-I. ^{131}I therapy remains the only known cure for metastatic radioiodine-sensitive DTC and the use of redifferentiating strategies to permit additional ^{131}I treatment for patients with radioiodine-refractory metastatic disease represents a promising therapeutic approach that remains yet to be fully explored in future clinical trials.

References

1. https://seer.cancer.gov/statfacts/html/thyro.html. National Cancer Institute 2021 [03/16/2021].
2. American Thyroid Association (ATA) Guidelines Taskforce on Thyroid Nodules and Differentiated Thyroid Cancer, Cooper DS, Doherty GM, Haugen BR, Kloos RT, et al. Revised American Thyroid Association management guidelines for patients with thyroid nodules and differentiated thyroid cancer. Thyroid. 2009;19(11):1167–214.
3. Haugen BR, Alexander EK, Bible KC, Doherty GM, Mandel SJ, Nikiforov YE, et al. 2015 American Thyroid Association Management guidelines for adult patients with thyroid nodules and differentiated thyroid cancer: the American Thyroid Association Guidelines Task Force on Thyroid Nodules and Differentiated Thyroid Cancer. Thyroid. 2016;26(1):1–133.
4. Zerdoud S, Giraudet AL, Leboulleux S, Leenhardt L, Bardet S, Clerc J, et al. Radioactive iodine therapy, molecular imaging and serum biomarkers for differentiated thyroid cancer: 2017 guidelines of the French Societies of Nuclear Medicine, Endocrinology, Pathology, Biology, Endocrine Surgery and Head and Neck Surgery. Ann Endocrinol (Paris). 2017;78(3):162–75.
5. Avram AM, Esfandiari NH, Wong KK. Preablation 131-I scans with SPECT/CT contribute to thyroid cancer risk stratification and 131-I therapy planning. J Clin Endocrinol Metab. 2015;100(5):1895–902.
6. Kwak JY, Han KH, Yoon JH, Moon HJ, Son EJ, Park SH, et al. Thyroid imaging reporting and data system for US features of nodules: a step in establishing better stratification of cancer risk. Radiology. 2011;260(3):892–9.
7. Russ G, Bonnema SJ, Erdogan MF, Durante C, Ngu R, Leenhardt L. European thyroid association guidelines for ultrasound malignancy risk stratification of thyroid nodules in adults: the EU-TIRADS. Eur Thyroid J. 2017;6(5):225–37.
8. Cibas ES, Ali SZ. The 2017 Bethesda system for reporting thyroid cytopathology. Thyroid. 2017;27(11):1341–6.
9. Zulewski H, Giovanella L, Bilz S, Christ E, Haldemann A, Steinert H, et al. Multidisciplinary approach for risk-oriented treatment of low-risk papillary thyroid cancer in Switzerland. Swiss Med Wkly. 2019;149:w14700.
10. Ito Y, Miyauchi A, Oda H. Low-risk papillary microcarcinoma of the thyroid: a review of active surveillance trials. Eur J Surg Oncol. 2018;44(3):307–15.

11. Davies L, Roman BR, Fukushima M, Ito Y, Miyauchi A. Patient experience of thyroid cancer active surveillance in Japan. JAMA Otolaryngol Head Neck Surg. 2019;145(4):363–70.
12. Robbins KT, Shaha AR, Medina JE, Califano JA, Wolf GT, Ferlito A, et al. Consensus statement on the classification and terminology of neck dissection. Arch Otolaryngol Head Neck Surg. 2008;134(5):536–8.
13. Miller JE, Al-Attar NC, Brown OH, Shaughness GG, Rosculet NP, Avram AM, et al. Location and causation of residual lymph node metastasis after surgical treatment of regionally advanced differentiated thyroid cancer. Thyroid. 2018;28(5):593–600.
14. Roh JL, Park JY, Park CI. Total thyroidectomy plus neck dissection in differentiated papillary thyroid carcinoma patients: pattern of nodal metastasis, morbidity, recurrence, and postoperative levels of serum parathyroid hormone. Ann Surg. 2007;245(4):604–10.
15. Barczynski M, Konturek A, Stopa M, Nowak W. Prophylactic central neck dissection for papillary thyroid cancer. Br J Surg. 2013;100(3):410–8.
16. Brierley JD, Gospodarowicz MK, C W. TNM classification of malignant tumors. Oxford: Wiley; 2016.
17. Pacini F, Ladenson PW, Schlumberger M, Driedger A, Luster M, Kloos RT, et al. Radioiodine ablation of thyroid remnants after preparation with recombinant human thyrotropin in differentiated thyroid carcinoma: results of an international, randomized, controlled study. J Clin Endocrinol Metab. 2006;91(3):926–32.
18. Avram AM, Giovanella L, Greenspan B, Lawson SA, Luster M, Van Nostrand D, et al. SNMMI procedure standard/EANM practice guideline for nuclear medicine evaluation and therapy of differentiated thyroid cancer: abbreviated version. J Nucl Med. 2022;63(6):15N–35N.
19. American Cancer Society I. Key Statistics Thyroid Cancer 2014.
20. Clerc J, Verburg FA, Avram AM, Giovanella L, Hindie E, Taieb D. Radioiodine treatment after surgery for differentiated thyroid cancer: a reasonable option. Eur J Nucl Med Mol Imaging. 2017;44(6):918–25.
21. Tuttle RM, Ahuja S, Avram AM, Bernet VJ, Bourguet P, Daniels GH, et al. Controversies, consensus, and collaboration in the use of (131) I therapy in differentiated thyroid cancer: a joint statement from the American Thyroid Association, the European Association of Nuclear Medicine, the Society of Nuclear Medicine and Molecular Imaging, and the European Thyroid Association. Thyroid. 2019;29(4):461–70.
22. Van Nostrand D. The benefits and risks of I-131 therapy in patients with well-differentiated thyroid cancer. Thyroid. 2009;19(12):1381–91.
23. Jonklaas J, Sarlis NJ, Litofsky D, Ain KB, Bigos ST, Brierley JD, et al. Outcomes of patients with differentiated thyroid carcinoma following initial therapy. Thyroid. 2006;16(12):1229–42.
24. Carhill AA, Litofsky DR, Ross DS, Jonklaas J, Cooper DS, Brierley JD, et al. Long-term outcomes following therapy in differentiated thyroid carcinoma: NTCTCS registry analysis 1987-2012. J Clin Endocrinol Metab. 2015;100(9):3270–9.
25. Sawka AM, Thephamongkhol K, Brouwers M, Thabane L, Browman G, Gerstein HC. Clinical review 170: A systematic review and metaanalysis of the effectiveness of radioactive iodine remnant ablation for well-differentiated thyroid cancer. J Clin Endocrinol Metab. 2004;89(8):3668–76.
26. Ruel E, Thomas S, Dinan M, Perkins JM, Roman SA, Sosa JA. Adjuvant radioactive iodine therapy is associated with improved survival for patients with intermediate-risk papillary thyroid cancer. J Clin Endocrinol Metab. 2015;100(4):1529–36.
27. Yang Z, Flores J, Katz S, Nathan CA, Mehta V. Comparison of survival outcomes following post-surgical radioactive iodine versus external beam radiation in stage IV differentiated thyroid carcinoma. Thyroid. 2017;27(7):944–52.
28. Mazzaferri EL, Kloos RT. Clinical review 128: Current approaches to primary therapy for papillary and follicular thyroid cancer. J Clin Endocrinol Metab. 2001;86(4):1447–63.
29. Xiao J, Yun C, Cao J, Ding S, Shao C, Wang L, et al. A pre-ablative thyroid-stimulating hormone with 30-70 mIU/L achieves better response to initial radioiodine remnant ablation in differentiated thyroid carcinoma patients. Sci Rep. 2021;11(1):1348.
30. Potzi C, Moameni A, Karanikas G, Preitfellner J, Becherer A, Pirich C, et al. Comparison of iodine uptake in tumour and nontumour tissue under thyroid hormone deprivation and with recombinant human thyrotropin in thyroid cancer patients. Clin Endocrinol. 2006;65(4):519–23.
31. Freudenberg LS, Jentzen W, Petrich T, Fromke C, Marlowe RJ, Heusner T, et al. Lesion dose in differentiated thyroid carcinoma metastases after rhTSH or thyroid hormone withdrawal: 124I PET/CT dosimetric comparisons. Eur J Nucl Med Mol Imaging. 2010;37(12):2267–76.
32. Giovanella L, Duntas LH. MANAGEMENT OF ENDOCRINE DISEASE: the role of rhTSH in the management of differentiated thyroid cancer: pros and cons. Eur J Endocrinol. 2019;181(4):R133–R45.
33. Zanotti-Fregonara P, Hindie E. On the effectiveness of recombinant human TSH as a stimulating agent for 131I treatment of metastatic differentiated thyroid cancer. Eur J Nucl Med Mol Imaging. 2010;37(12):2264–6.
34. Plyku D, Hobbs RF, Huang K, Atkins F, Garcia C, Sgouros G, et al. Recombinant human thyroid-stimulating hormone versus thyroid hormone withdrawal in (124)I PET/CT-based dosimetry for (131)I therapy of metastatic differentiated thyroid cancer. J Nucl Med. 2017;58(7):1146–54.

35. Jeevanram RK, Shah DH, Sharma SM, Ganatra RD. Influence of initial large dose on subsequent uptake of therapeutic radioiodine in thyroid cancer patients. Int J Rad Appl Instrum B. 1986;13(3):277–9.
36. Huic D, Medvedec M, Dodig D, Popovic S, Ivancevic D, Pavlinovic Z, et al. Radioiodine uptake in thyroid cancer patients after diagnostic application of low-dose 131I. Nucl Med Commun. 1996;17(10):839–42.
37. Yeung HW, Humm JL, Larson SM. Radioiodine uptake in thyroid remnants during therapy after tracer dosimetry. J Nucl Med. 2000;41(6):1082–5.
38. Morris LF, Waxman AD, Braunstein GD. The non-impact of thyroid stunning: remnant ablation rates in 131I-scanned and nonscanned individuals. J Clin Endocrinol Metab. 2001;86(8):3507–11.
39. McDougall IR. 74 MBq radioiodine 131I does not prevent uptake of therapeutic doses of 131I (i.e. it does not cause stunning) in differentiated thyroid cancer. Nucl Med Commun. 1997;18(6):505–12.
40. Cholewinski SP, Yoo KS, Klieger PS, O'Mara RE. Absence of thyroid stunning after diagnostic whole-body scanning with 185 MBq 131I. J Nucl Med. 2000;41(7):1198–202.
41. Karam M, Gianoukakis A, Feustel PJ, Cheema A, Postal ES, Cooper JA. Influence of diagnostic and therapeutic doses on thyroid remnant ablation rates. Nucl Med Commun. 2003;24(5):489–95.
42. Rosario PW, Barroso AL, Rezende LL, Padrao EL, Maia FF, Fagundes TA, et al. 5 mCi pretreatment scanning does not cause stunning when the ablative dose is administered within 72 hours. Arq Bras Endocrinol Metabol. 2005;49(3):420–4.
43. Sisson JC, Avram AM, Lawson SA, Gauger PG, Doherty GM. The so-called stunning of thyroid tissue. J Nucl Med. 2006;47(9):1406–12.
44. Silberstein EB. Comparison of outcomes after (123) I versus (131)I pre-ablation imaging before radioiodine ablation in differentiated thyroid carcinoma. J Nucl Med. 2007;48(7):1043–6.
45. McDougall IR, Iagaru A. Thyroid stunning: fact or fiction? Semin Nucl Med. 2011;41(2):105–12.
46. Avram AM, Fig LM, Frey KA, Gross MD, Wong KK. Preablation 131-I scans with SPECT/CT in postoperative thyroid cancer patients: what is the impact on staging? J Clin Endocrinol Metab. 2013;98(3):1163–71.
47. Avram AM. Radioiodine scintigraphy with SPECT/CT: an important diagnostic tool for thyroid cancer staging and risk stratification. J Nucl Med. 2012;53(5):754–64.
48. Avram AM, Rosculet N, Esfandiari NH, Gauger PG, Miller BS, Cohen M, et al. Differentiated thyroid cancer outcomes after surgery and activity-adjusted 131I theragnostics. Clin Nucl Med. 2019;44(1):11–20.
49. Hocevar M, Auersperg M, Stanovnik L. The dynamics of serum thyroglobulin elimination from the body after thyroid surgery. Eur J Surg Oncol. 1997;23(3):208–10.
50. Spencer CA. Clinical review: Clinical utility of thyroglobulin antibody (TgAb) measurements for patients with differentiated thyroid cancers (DTC). J Clin Endocrinol Metab. 2011;96(12):3615–27.
51. Luster M, Clarke SE, Dietlein M, Lassmann M, Lind P, Oyen WJ, et al. Guidelines for radioiodine therapy of differentiated thyroid cancer. Eur J Nucl Med Mol Imaging. 2008;35(10):1941–59.
52. Verburg FA, Aktolun C, Chiti A, Frangos S, Giovanella L, Hoffmann M, et al. Why the European Association of Nuclear Medicine has declined to endorse the 2015 American Thyroid Association management guidelines for adult patients with thyroid nodules and differentiated thyroid cancer. Eur J Nucl Med Mol Imaging. 2016;43(6):1001–5.
53. McCowen KD, Adler RA, Ghaed N, Verdon T, Hofeldt FD. Low dose radioiodide thyroid ablation in postsurgical patients with thyroid cancer. Am J Med. 1976;61(1):52–8.
54. Johansen K, Woodhouse NJ, Odugbesan O. Comparison of 1073 MBq and 3700 MBq iodine-131 in postoperative ablation of residual thyroid tissue in patients with differentiated thyroid cancer. J Nucl Med. 1991;32(2):252–4.
55. Logue JP, Tsang RW, Brierley JD, Simpson WJ. Radioiodine ablation of residual tissue in thyroid cancer: relationship between administered activity, neck uptake and outcome. Br J Radiol. 1994;67(803):1127–31.
56. Bal C, Padhy AK, Jana S, Pant GS, Basu AK. Prospective randomized clinical trial to evaluate the optimal dose of 131 I for remnant ablation in patients with differentiated thyroid carcinoma. Cancer. 1996;77(12):2574–80.
57. Bal CS, Kumar A, Pant GS. Radioiodine dose for remnant ablation in differentiated thyroid carcinoma: a randomized clinical trial in 509 patients. J Clin Endocrinol Metab. 2004;89(4):1666–73.
58. Rosario PW, Reis JS, Barroso AL, Rezende LL, Padrao EL, Fagundes TA. Efficacy of low and high 131I doses for thyroid remnant ablation in patients with differentiated thyroid carcinoma based on post-operative cervical uptake. Nucl Med Commun. 2004;25(11):1077–81.
59. Pilli T, Brianzoni E, Capoccetti F, Castagna MG, Fattori S, Poggiu A, et al. A comparison of 1850 (50 mCi) and 3700 MBq (100 mCi) 131-iodine administered doses for recombinant thyrotropin-stimulated postoperative thyroid remnant ablation in differentiated thyroid cancer. J Clin Endocrinol Metab. 2007;92(9):3542–6.
60. Cherk MH, Kalff V, Yap KS, Bailey M, Topliss D, Kelly MJ. Incidence of radiation thyroiditis and thyroid remnant ablation success rates following 1110 MBq (30 mCi) and 3700 MBq (100 mCi) post-surgical 131I ablation therapy for differentiated thyroid carcinoma. Clin Endocrinol. 2008;69(6):957–62.
61. Maenpaa HO, Heikkonen J, Vaalavirta L, Tenhunen M, Joensuu H. Low vs. high radioiodine activity to

ablate the thyroid after thyroidectomy for cancer: a randomized study. PLoS One. 2008;3(4):e1885.
62. Kukulska A, Krajewska J, Gawkowska-Suwinska M, Puch Z, Paliczka-Cieslik E, Roskosz J, et al. Radioiodine thyroid remnant ablation in patients with differentiated thyroid carcinoma (DTC): prospective comparison of long-term outcomes of treatment with 30, 60 and 100 mCi. Thyroid Res. 2010;3(1):9.
63. Bal C, Chandra P, Kumar A, Dwivedi S. A randomized equivalence trial to determine the optimum dose of iodine-131 for remnant ablation in differentiated thyroid cancer. Nucl Med Commun. 2012;33(10):1039–47.
64. Caglar M, Bozkurt FM, Akca CK, Vargol SE, Bayraktar M, Ugur O, et al. Comparison of 800 and 3700 MBq iodine-131 for the postoperative ablation of thyroid remnant in patients with low-risk differentiated thyroid cancer. Nucl Med Commun. 2012;33(3):268–74.
65. Schlumberger M, Catargi B, Borget I, Deandreis D, Zerdoud S, Bridji B, et al. Strategies of radioiodine ablation in patients with low-risk thyroid cancer. N Engl J Med. 2012;366(18):1663–73.
66. Mallick U, Harmer C, Yap B, Wadsley J, Clarke S, Moss L, et al. Ablation with low-dose radioiodine and thyrotropin alfa in thyroid cancer. N Engl J Med. 2012;366(18):1674–85.
67. Kruijff S, Aniss AM, Chen P, Sidhu SB, Delbridge LW, Robinson B, et al. Decreasing the dose of radioiodine for remnant ablation does not increase structural recurrence rates in papillary thyroid carcinoma. Surgery. 2013;154(6):1337–44; discussion 44–5.
68. Castagna MG, Cevenini G, Theodoropoulou A, Maino F, Memmo S, Claudia C, et al. Post-surgical thyroid ablation with low or high radioiodine activities results in similar outcomes in intermediate risk differentiated thyroid cancer patients. Eur J Endocrinol. 2013;169(1):23–9.
69. Cheng W, Ma C, Fu H, Li J, Chen S, Wu S, et al. Low- or high-dose radioiodine remnant ablation for differentiated thyroid carcinoma: a meta-analysis. J Clin Endocrinol Metab. 2013;98(4):1353–60.
70. Fang Y, Ding Y, Guo Q, Xing J, Long Y, Zong Z. Radioiodine therapy for patients with differentiated thyroid cancer after thyroidectomy: direct comparison and network meta-analyses. J Endocrinol Investig. 2013;36(10):896–902.
71. Valachis A, Nearchou A. High versus low radioiodine activity in patients with differentiated thyroid cancer: a meta-analysis. Acta Oncol. 2013;52(6):1055–61.
72. Han JM, Kim WG, Kim TY, Jeon MJ, Ryu JS, Song DE, et al. Effects of low-dose and high-dose postoperative radioiodine therapy on the clinical outcome in patients with small differentiated thyroid cancer having microscopic extrathyroidal extension. Thyroid. 2014;24(5):820–5.
73. Zhang Y, Liang J, Yang X, Yang K, Lin Y. Low-dose radioiodine ablation in differentiated thyroid cancer with macroscopic extrathyroidal extension and low level of preablative-stimulated thyroglobulin. Nucl Med Commun. 2015;36(6):553–9.
74. Du P, Jiao X, Zhou Y, Li Y, Kang S, Zhang D, et al. Low versus high radioiodine activity to ablate the thyroid after thyroidectomy for cancer: a meta-analysis of randomized controlled trials. Endocrine. 2015;48(1):96–105.
75. Joung JY, Choi JH, Cho YY, Kim NK, Sohn SY, Kim SW, et al. Efficacy of low-dose and high-dose radioactive iodine ablation with rhTSH in Korean patients with differentiated thyroid carcinoma: the first report in nonwestern countries. Am J Clin Oncol. 2016;39(4):374–8.
76. Fatima N, Zaman MU, Zaman A, Zaman U, Tahseen R. Comparable ablation efficiency of 30 and 100 mCi of I-131 for low to intermediate risk thyroid cancers using triple negative criteria. Asian Pac J Cancer Prev. 2016;17(3):1115–8.
77. Ibrahim DR, Kelany M, Michael MM, Elsayed ZM. Low-dose versus high-dose radioactive iodine ablation of differentiated thyroid carcinoma: a prospective randomized study. Int J Cancer Ther Oncol. 2016;4(4):4415.
78. Shengguang Y, Ji-Eun C, Lijuan HL. I-131 for remnant ablation in differentiated thyroid cancer after thyroidectomy: a meta-analysis of randomized controlled evidence. Med Sci Monit. 2016;22:2439–50.
79. Ben Ghachem T, Yeddes I, Meddeb I, Bahloul A, Mhiri A, Slim I, et al. A comparison of low versus high radioiodine administered activity in patients with low-risk differentiated thyroid cancer. Eur Arch Otorhinolaryngol. 2017;274(2):655–60.
80. Lv RB, Wang QG, Liu C, Liu F, Zhao Q, Han JG, et al. Low versus high radioiodine activity for ablation of the thyroid remnant after thyroidectomy in Han Chinese with low-risk differentiated thyroid cancer. Onco Targets Ther. 2017;10:4051–7.
81. Ma C, Feng F, Wang S, Fu H, Wu S, Ye Z, et al. Chinese data of efficacy of low- and high-dose Iodine-131 for the ablation of thyroid remnant. Thyroid. 2017;27(6):832–7.
82. Qu Y, Huang R, Li L. Low- and high-dose radioiodine therapy for low−/intermediate-risk differentiated thyroid cancer: a preliminary clinical trial. Ann Nucl Med. 2017;31(1):71–83.
83. Seo M, Kim YS, Lee JC, Han MW, Kim ES, Kim KB, et al. Low-dose radioactive iodine ablation is sufficient in patients with small papillary thyroid cancer having minor Extrathyroidal extension and central lymph node metastasis (T3 N1a). Clin Nucl Med. 2017;42(11):842–6.
84. Jimenez Londono GA, Garcia Vicente A, Sastre Marco J, Pena Pardo FJ, Amo-Salas M, Caballero MM, Talavera Rubio MP, Gonzalez Garcia B, Disotuar Ruiz ND, Soriano Castrejon AM. Low-dose radioiodine ablation in patients with low-risk differentiated thyroid cancer. Eur Thyroid J. 2018;7:218–24.
85. Cai XY, Vijayaratnam N, McEwan AJB, Reif R, Morrish DW. Comparison of 30 mCi and 50

mCi I-131 doses for ablation of thyroid remnant in papillary thyroid cancer patients. Endocr Res. 2018;43(1):11–4.
86. Dehbi HM, Mallick U, Wadsley J, Newbold K, Harmer C, Hackshaw A. Recurrence after low-dose radioiodine ablation and recombinant human thyroid-stimulating hormone for differentiated thyroid cancer (HiLo): long-term results of an open-label, non-inferiority randomised controlled trial. Lancet Diabetes Endocrinol. 2019;7(1):44–51.
87. Vardarli I, Weidemann F, Aboukoura M, Herrmann K, Binse I, Gorges R. Longer-term recurrence rate after low versus high dose radioiodine ablation for differentiated thyroid cancer in low and intermediate risk patients: a meta-analysis. BMC Cancer. 2020;20(1):550.
88. Li F, Li W, Gray KD, Zarnegar R, Wang D, Fahey TJ 3rd. Ablation therapy using a low dose of radioiodine may be sufficient in low- to intermediate-risk patients with follicular variant papillary thyroid carcinoma. J Int Med Res. 2020;48(11):300060520966491.
89. Dong P, Wang L, Qu Y, Huang R, Li L. Low- and high-dose radioiodine ablation for low−/intermediate-risk differentiated thyroid cancer in China: large randomized clinical trial. Head Neck. 2021;43(4):1311–20.
90. Thyrogen Prescribing Information. https://www.accessdata.fda.gov/drugsatfda_docs/label/2014/020898s054lbl.pdf.
91. Genzyme. Thyrogen [package insert]. Cambridge, MA; 2008.
92. Singer MC, Marchal F, Angelos P, Bernet V, Boucai L, Buchholzer S, et al. Salivary and lacrimal dysfunction after radioactive iodine for differentiated thyroid cancer: American Head and Neck Society Endocrine Surgery Section and Salivary Gland Section joint multidisciplinary clinical consensus statement of otolaryngology, ophthalmology, nuclear medicine and endocrinology. Head Neck. 2020;42(11):3446–59.
93. Ylli D, Van Nostrand D, Wartofsky L. Conventional radioiodine therapy for differentiated thyroid cancer. Endocrinol Metab Clin N Am. 2019;48(1):181–97.
94. Van Nostrand D, Atkins F, Yeganeh F, Acio E, Bursaw R, Wartofsky L. Dosimetrically determined doses of radioiodine for the treatment of metastatic thyroid carcinoma. Thyroid. 2002;12(2):121–34.
95. Leblanc G, Tabah R, Liberman M, Sampalis J, Younan R, How J. Large remnant 131I ablation as an alternative to completion/total thyroidectomy in the treatment of well-differentiated thyroid cancer. Surgery. 2004;136(6):1275–80.
96. Santra A, Bal S, Mahargan S, Bal C. Long-term outcome of lobar ablation versus completion thyroidectomy in differentiated thyroid cancer. Nucl Med Commun. 2011;32(1):52–8.
97. Barbesino G, Goldfarb M, Parangi S, Yang J, Ross DS, Daniels GH. Thyroid lobe ablation with radioactive iodine as an alternative to completion thyroidectomy after hemithyroidectomy in patients with follicular thyroid carcinoma: long-term follow-up. Thyroid. 2012;22(4):369–76.
98. Benua RS, Cicale NR, Sonenberg M, Rawson RW. The relation of radioiodine dosimetry to results and complications in the treatment of metastatic thyroid cancer. Am J Roentgenol Radium Therapy, Nucl Med. 1962;87:171–82.
99. Lassmann M, Hanscheid H, Chiesa C, Hindorf C, Flux G, Luster M, et al. EANM Dosimetry Committee series on standard operational procedures for pre-therapeutic dosimetry I: blood and bone marrow dosimetry in differentiated thyroid cancer therapy. Eur J Nucl Med Mol Imaging. 2008;35(7):1405–12.
100. Atkins FB, Van Nostrand D, Wartofsky L. Dosimetrically determined prescribed activity of 131I for the treatment of metastatic differentiated thyroid carcinoma. In: Wartofsky L, Van Nostrand D, editors. Thyroid cancer: a comprehensive guide to clinical management. New York: Springer; 2016. p. 635–50.
101. Leeper RD. Thyroid cancer. Med Clin North Am. 1985;69(5):1079–96.
102. Dorn R, Kopp J, Vogt H, Heidenreich P, Carroll RG, Gulec SA. Dosimetry-guided radioactive iodine treatment in patients with metastatic differentiated thyroid cancer: largest safe dose using a risk-adapted approach. J Nucl Med. 2003;44(3):451–6.
103. Van Nostrand D. 131I treatment of distant metastases. In: Wartofsky L, Van Nostrand D, editors. Thyroid cancer: a comprehensive guide to clinical management. New York: Springer; 2016. p. 595–627.
104. Deandreis D, Rubino C, Tala H, Leboulleux S, Terroir M, Baudin E, et al. Comparison of empiric versus whole-body/-blood clearance dosimetry-based approach to radioactive iodine treatment in patients with metastases from differentiated thyroid cancer. J Nucl Med. 2017;58(5):717–22.
105. Tulchinsky M, Gross LJ. Comparison of empiric versus dosimetry-guided radioiodine therapy: the devil is in the details. J Nucl Med. 2017;58(5):863.
106. Klubo-Gwiezdzinska J, Van Nostrand D, Atkins F, Burman K, Jonklaas J, Mete M, et al. Efficacy of dosimetric versus empiric prescribed activity of 131I for therapy of differentiated thyroid cancer. J Clin Endocrinol Metab. 2011;96(10):3217–25.
107. Casara D, Rubello D, Saladini G, Masarotto G, Favero A, Girelli ME, et al. Different features of pulmonary metastases in differentiated thyroid cancer: natural history and multivariate statistical analysis of prognostic variables. J Nucl Med. 1993;34(10):1626–31.
108. Schlumberger M, Challeton C, De Vathaire F, Travagli JP, Gardet P, Lumbroso JD, et al. Radioactive iodine treatment and external radiotherapy for lung and bone metastases from thyroid carcinoma. J Nucl Med. 1996;37(4):598–605.
109. Samaan NA, Schultz PN, Hickey RC, Goepfert H, Haynie TP, Johnston DA, et al. The results of various modalities of treatment of well differentiated thyroid

carcinomas: a retrospective review of 1599 patients. J Clin Endocrinol Metab. 1992;75(3):714–20.
110. Orita Y, Sugitani I, Matsuura M, Ushijima M, Tsukahara K, Fujimoto Y, et al. Prognostic factors and the therapeutic strategy for patients with bone metastasis from differentiated thyroid carcinoma. Surgery. 2010;147(3):424–31.
111. Durante C, Haddy N, Baudin E, Leboulleux S, Hartl D, Travagli JP, et al. Long-term outcome of 444 patients with distant metastases from papillary and follicular thyroid carcinoma: benefits and limits of radioiodine therapy. J Clin Endocrinol Metab. 2006;91(8):2892–9.
112. Schmidt D, Linke R, Uder M, Kuwert T. Five months' follow-up of patients with and without iodine-positive lymph node metastases of thyroid carcinoma as disclosed by (131)I-SPECT/CT at the first radioablation. Eur J Nucl Med Mol Imaging. 2010;37(4):699–705.
113. Schmidt D, Szikszai A, Linke R, Bautz W, Kuwert T. Impact of 131I SPECT/spiral CT on nodal staging of differentiated thyroid carcinoma at the first radioablation. J Nucl Med. 2009;50(1):18–23.
114. Avram AM, Dewaraja YK. Thyroid cancer radiotheragnostics: the case for activity adjusted (131)I therapy. Clin Transl Imaging. 2018;6(5):335–46.
115. Avram AM, Zukotynski K, Nadel HR, Giovanella L. Management of differentiated thyroid cancer: the standard of care. J Nucl Med. 2022;63(2):189–95.
116. Wang W, Larson SM, Tuttle RM, Kalaigian H, Kolbert K, Sonenberg M, et al. Resistance of [18f]-fluorodeoxyglucose-avid metastatic thyroid cancer lesions to treatment with high-dose radioactive iodine. Thyroid. 2001;11(12):1169–75.
117. Van Nostrand D. To perform or not to perform radioiodine scans prior to 131I remnant ablation? PRO. In: Wartofsky L, Van Nostrand D, editors. Thyroid cancer: a comprehensive guide to clinical management. New York, NY: Springer; 2016. p. 245–54.
118. Cabanillas ME, McFadden DG, Durante C. Thyroid cancer. Lancet. 2016;388(10061):2783–95.
119. Ain KB. Papillary thyroid carcinoma. Etiology, assessment, and therapy. Endocrinol Metab Clin N Am. 1995;24(4):711–60.
120. Xing M, Haugen BR, Schlumberger M. Progress in molecular-based management of differentiated thyroid cancer. Lancet. 2013;381(9871):1058–69.
121. Robbins RJ, Wan Q, Grewal RK, Reibke R, Gonen M, Strauss HW, et al. Real-time prognosis for metastatic thyroid carcinoma based on 2-[18F]fluoro-2-deoxy-D-glucose-positron emission tomography scanning. J Clin Endocrinol Metab. 2006;91(2):498–505.
122. Giovanella L, van Nostrand D. Advanced differentiated thyroid cancer: when to stop radioiodine? Q J Nucl Med Mol Imaging. 2019;63(3):267–70.
123. Silberstein EB. The problem of the patient with thyroglobulin elevation but negative iodine scintigraphy: the TENIS syndrome. Semin Nucl Med. 2011;41(2):113–20.
124. Schleupner MC, Riemann B, Schafers M, Backhaus P, Vrachimis A. Impact of FDG-PET on therapy management and outcome of differentiated thyroid carcinoma patients with elevated thyroglobulin despite negative iodine scintigraphy. Nuklearmedizin. 2020;59(5):356–64.
125. Wang W, Larson SM, Fazzari M, Tickoo SK, Kolbert K, Sgouros G, et al. Prognostic value of [18F]fluorodeoxyglucose positron emission tomographic scanning in patients with thyroid cancer. J Clin Endocrinol Metab. 2000;85(3):1107–13.

8 Biomarkers and Molecular Imaging in Postoperative DTC Management

Domenico Albano, Francesco Dondi, Pietro Bellini, and Francesco Bertagna

8.1 Introduction

Differentiated thyroid carcinoma (DTC) is the most common endocrine cancer and its incidence has increased in the past decades. Generally, DTC has an indolent course with a favorable prognosis, except for cases with distant metastases at the time of diagnosis. For a long time, DTC was treated by thyroidectomy followed by radioiodine [iodine-131 (^{131}I)] therapy, with the theoretical result of the absence of residual benign thyroid tissue, letting thyroglobulin (Tg) be an ideal marker of disease.

Nowadays, recent American Thyroid Association (ATA) guidelines [1] suggest an individualized risk-adapted approach where the type and extent of surgery (lobectomy or total thyroidectomy), the indication and the goal of ^{131}I therapy (ablation, adjuvant, curative), replacement therapy with levothyroxine features (TSH suppressive or not) are individually personalized for each case [2].

For example, nowadays low to intermediate risk DTC patients are currently treated by thyroidectomy without radioiodine ablation or, in selected low risk, even by lobectomy alone. In these cases, the absolute value of Tg should be less significant for the follow-up due to the difficulties to discriminate between physiological and pathological Tg values, and the absence of a specific reference value [3, 4].

8.2 Biomarkers: Tg and TgAb

Postoperative risk stratification is based on the criteria reported by ATA guidelines [1].

Tg is a 660-kDa glycoprotein produced exclusively in the thyroid gland where it serves as the source for thyroxine (T4) and triiodothyronine (T3) production within the thyroid follicles. Small amounts of Tg are detected in the serum of healthy individuals as it is secreted alongside T4 and T3 [5]. Increased serum Tg levels are present during several disordered thyroid growths, increased thyroid activity, and glandular destruction such as in goiter, Graves' disease, and thyroiditis, or in DTC cells. Thus, the measurement of Tg for the initial evaluation of suspicious thy-

Supplementary Information The online version contains supplementary material available at https://doi.org/10.1007/978-3-031-35213-3_8.

D. Albano (✉) · F. Dondi · P. Bellini · F. Bertagna
Nuclear Medicine, University of Brescia and ASST Spedali Civili di Brescia, Brescia, Italy
e-mail: domenico.albano@unibs.it; francesco.bertagna@unibs.it

L. Giovanella (ed.), *Integrated Diagnostics and Theranostics of Thyroid Diseases*,
https://doi.org/10.1007/978-3-031-35213-3_8

roid nodules is not recommended, due to the overlap in Tg levels in patients with DTC and benign nodules [3, 4].

Absolute Tg concentrations are correlated with tumor load and are widely employed to assess the extension of the disease and evaluate the response to treatments. However, this single tumor marker measurement may not be exhaustive in the whole comprehension of disease status and treatment response, because it is not intrinsically inclusive of previous measurements and the overall trend.

During initial follow-up, the recommended interval for serum Tg measurement is about 6–12 months, unless in high-risk patients where more frequent measurements may be suggested.

Tg together with thyroglobulin autoantibodies (TgAb), neck ultrasound (US), and any additional imaging procedures (i.e., ^{131}I whole-body scintigraphy [WBS], computed tomography [CT], positron emission tomography [PET], and magnetic resonance imaging [MRI]) are mandatory for the monitoring of patients in the postoperative field, aiding in the early detection of persistent or recurrent disease and guiding the evaluation of dynamic risk.

The main limitation of Tg is the potential interference of TgAb which makes Tg not perfectly evaluable. More rarely, also heterophilic antibodies (HAb) may interfere with Tg measurement in vitro and cause false-positive Tg results. In DTC patients, the presence of TgAb and HAb is not so rare, with a prevalence described in up to 15–25% for TgAb and 1% for HAb [6].

Historically, Tg measurement was first performed by competitive radioimmunological assays (RIAs). However, RIAs were replaced by direct immunometric assays (IMAs), which are more sensitive, have a shorter incubation, a more robust labeled antibody reagent and a larger working range. Tg-IMAs are based on a two-site reaction that involves Tg capture by a solid-phase antibody followed by the addition of a labeled antibody that targets different epitopes on the captured Tg. Over the years, Tg assays have evolved to achieve superior sensitivities and a number of commercially available Tg-IMAs have functional sensitivities of 0.1–0.2 mg/L, referred to as high-sensitive (hsTg) or second-generation Tg-IMas [7]. Before the introduction of hsTg, thyroid hormone withdrawal or recombinant human TSH stimulation was necessary to reach the best degree of diagnostic sensitivity. Now, these procedures can be skipped in most cases with a significant improvement in patient quality of life and a reduction in costs.

When possible it is fundamental that consecutive Tg measurements be performed in the same laboratory using the same assay each time. If any change is unavoidable, a new baseline should be established and proceed with the same method.

A big problem of different IMAs is the intermethod variability, despite the introduction of the Certified Reference Material (CRM 457, currently called BCR 457) has partially reduced this variability. For this reason, it would be desirable to have assay-specific Tg cutoffs instead of fixed thresholds.

Moreover, the susceptibility of Tg-IMAs to antibodies-based interference is another limitation, causing an underestimation of Tg. Otherwise, TgAb concentration may become a surrogate tumor marker and guide patient management. Tumor recurrence can be anticipated by a rise in Tg antibodies with or without an increase in serum Tg.

Serum Tg concentrations are further influenced and regulated by the degree of thyroid stimulating hormone (TSH) stimulation. Measurements of Tg can be TSH suppressed while patients remain on suppressive doses of thyroid hormone, or TSH stimulated after thyroid hormone withdrawal or administration of recombinant human TSH (rhTSH).

Minor fluctuations between Tg measurements are possible and not necessarily referable to the recurrence or progression of the disease. However, a progressive increase in circulating Tg measurement strongly suggests recurrence/progression and should lead to further imaging tests to identify the site of the disease. The dynamic changes of Tg over time may be an alternative or complementary tumor marker, aside from the absolute Tg value. Tg kinetics may be expressed as Tg doubling time (Tg-DT) or Tg velocity

(Tg-vel). Tg doubling time (Tg-DT) was studied more and has been demonstrated as a valuable biomarker to predict loco-regional recurrences, distant metastases, and survival independently from the main prognostic variables (like gender, age, and TNM stage) [8]. In addition, Tg-DT may also help to select patients that will benefit from [18F]-FDG PET/CT [9]. About Tg-vel only initial evidences are available and further studies are mandatory [10].

8.2.1 Biomarkers Role in DTC Patients Treated by Total Thyroidectomy and ^{131}I

As previously discussed, Tg is a pivotal sensitive tool used in monitoring patients with DTC for the presence of residual or recurrent disease. In particular, Tg values have the highest sensitivity and specificity for the detection of recurrent disease after total thyroidectomy and ^{131}I ablation.

In the past, a measurement of stimulated Tg (after thyroid hormone withdrawal or rhTSH administration) every 6–12 months was suggested. Stimulated Tg < 1–2 ng/mL without evidence of structural disease (negative clinical examination, US, and/or other imaging modalities) predicted an excellent prognosis with a very low risk of recurrence and a normal life expectancy even in patients with high-risk disease [1]. More recently, with the development of Tg immunoassays more sensitive (hsTg), measurement of serum Tg concentrations of 0.1–0.2 ng/mL is possible. hsTg assays let to avoid the need for TSH stimulation, due to the fact that hsTg less than 0.1–0.2 ng/mL has a comparable negative predictive value (>95%) than sTg less than 1–2 ng/mL.

ATA guidelines classified response assessment after total thyroidectomy and radioiodine in different categories according to clinical, imaging, and serum results [1].

Response to therapy is assessed at each clinical appointment during surveillance. Careful clinical assessment and review of serial Tg and TgAb results allow us to follow patients during the course of the disease. An excellent response is defined in case of no evidence of disease on clinical exam and imaging and undetectable serum Tg measurements. A biochemical incomplete response is defined in a case of no clinical or imaging evidence of disease but with an elevated or rising Tg or TgAb concentration. Structural incomplete response is defined in case of evidence of disease in the thyroid bed, cervical nodes, or at distant sites in the presence of any Tg or TgAb value. Lastly, an indeterminate response category is for patients with non-specific or borderline biochemical or structural findings. Often patient surveillance with serial Tg and imaging will allow them to be recategorized into one of the above groups. Table 8.1 summarizes the response to therapy definitions according to ATA guidelines.

For patients undergoing total thyroidectomy and ^{131}I therapy that achieved an excellent response, an undetectable Tg during the follow-up may avoid performing imaging procedures. Instead in case of increasing Tg or TgAb levels, further investigations, like neck US and radioiodine WBS, should be performed [11].

8.2.2 Biomarkers Role in DTC Patients Treated by Total Thyroidectomy

A total or near-total thyroidectomy without ^{131}I ablation is now suggested in selected low- to intermediate-risk DTC. In this scenario, Tg is significantly influenced by the amount of residual thyroid remnants and the TSH level at the time of Tg measurement [12]. Thus, Tg potentially obscures possible tumor-related Tg levels and reduces the accuracy of dynamic risk stratification. Spencer et al. [13] speculated that Tg values under TSH suppression remain in the 0.1–0.5 mg/L range during long-term follow-up of these patients. Moreover, the amount of residual remnant thyroid tissue is strictly surgeon-dependent and widely variable, and chronic TSH suppression is no longer recommended in these patients. Tg reference intervals mathematically normalized to TSH level and residual thyroid tissue are needed to be validated. However, to guar-

Table 8.1 Response assessment after total thyroidectomy and radioiodine ablation according to ATA guidelines

Response	Definition	Imaging	Thyroglobulin ng/mL
Excellent	No evidence of disease (clinical, biochemical, and structural)	Negative	bTg < 0.2 OR sTg < 1
Incomplete biochemical	Abnormal Tg or rising TgAb. No evidence of structural disease	Negative	Tg > 1 OR sT > 10 OR rising TgAb
Incomplete structural	Evidence of structural disease	Positive	Any value
Indeterminate	Non-specific results	Indeterminate	bTg 0.2–1 OR sTg 1–10

bTg basal Thyroglobulin, *sTg* stimulated Thyroglobulin

antee reproducible results, stable TSH values are desirable or, at least, extremely low lot-to-lot variability and extremely good reproducibility are needed over a long time to guarantee reproducible results [3, 4, 14]. Dynamic evaluation of circulating Tg concentration may still provide useful information in such circumstances. A trend of decreasing Tg after surgery is usually reassuring, but general interpretation criteria for Tg in non-ablated DTC are lacking.

8.2.3 Biomarkers Role in DTC Patients Treated by Lobectomy

In DTC patients treated only by lobectomy, measuring Tg is not so useful as Tg levels will not depend on the presence or absence of tumor foci, but rather on the mass of the remaining thyroid lobe, TSH concentration, and current iodine status.

A recent meta-analysis based upon 7 studies for a total of 2455 patients demonstrated that circulating Tg was non-reliable in detecting early response and predicting recurrence in patients treated with lobectomy/hemithyroidectomy, especially those with a low initial ATA classification [15].

Thus, the benefit of Tg concentration in this setting is questionable. If performed, the results should be carefully interpreted, taking into account both the corresponding TSH value and the imaging findings (such as neck US). The options for follow-up of DTC patients treated by lobectomy are to perform periodic neck US and, if recurrence or metastasis is suspected, to confirm the diagnosis through a fine-needle biopsy or further examinations.

8.2.4 Patients with Positive TgAb

TgAb are present in approximately 10% of the general population and in up to 25–30% of patients with DTC [5]. Serum levels of TgAb are not correlated with the tumor load of the patient, but rather indicate the activity of the immune system [16]. However, TgAb interference may result in false low results in Tg-IMAs. TgAb interferences are variable in different patients and different IMAs and are independent of TgAb levels [17].

Tg RIAs are reported to be more resistant to TgAb interference; however, a significant number of falsely low and falsely high results have been described; moreover, the functional sensitivities of these assays are suboptimal in comparison with IMAs.

Recently, tandem mass spectrometry-liquid chromatography (MS/MS-LC) and Tg (mini)-recovery test has emerged as a promising method to overcome interferences in Tg measurement, but the current generation of MS/MS-LC assays had suboptimal functional sensitivity and yield false-negative results in a significant number of patients with evidence of structural disease and slightly detectable Tg concentrations in high-sensitive assays (0.1–0.5 ng/mL).

Thus, hsTg assays remain the mainstay of monitoring TgAb-negative patients, and also in patients with TgAb-positive with detectable Tg levels can be indicated.

Serum TgAb had an average disappearance time of 3 years after thyroid ablation for DTC, indicating that TgAb can be used as a "surrogate tumor marker." Similarly to Tg, the use of serial TgAb measurements as a surrogate tumor marker needs continuity of the laboratory method to perform an accurate comparison.

A consistent reduction in the serum TgAb level (especially when the reduction is more than 50% in the year after operation) indicates that the patient is likely to be free of disease, whereas a consistent rise or de novo appearance of serum TgAb raises suspicion of recurrence and prompts additional investigations; instead, an unchanged serum TgAb concentrations should be regarded as indeterminate and carefully monitored over time [6].

In summary, undetectable high-sensitive Tg and declining TgAb levels are both highly reassuring and predict favorable outcomes in TgAb-positive DTC patients after complete thyroid ablation and the lower, but still detectable Tg levels can be followed over time by high-sensitive Tg assay. No data are currently available to properly inform the management of TgAb-positive DTC patients treated by surgery alone without radioiodine ablation.

8.3 Molecular Imaging

8.3.1 Whole-Body Scintigraphy and SPECT/CT

8.3.1.1 Postoperative Setting

The last ATA guidelines [1] suggest that postoperative planar whole-body scintigraphy (WBS), after the administration of a diagnostic activity (1–5 mCi) of ^{131}I, may be useful for the assessment of differentiated thyroid cancer (DTC) when the extent of thyroid remnants or the presence of residual disease could not be accurately ascertained from surgical report or ultrasonography (US). In this setting, the specific choice of the dose of ^{131}I used to perform ^{131}I therapy can be made empirically or can be guided by the integration of postoperative WBS. This latter method is theoretically able to improve risk stratification and staging of DTC patients, influencing the clinical management of the patients in up to 25–50% of the cases [11, 18, 19]. However, there are no clear evidences to suggest the superiority of one method over the other.

One of the issues that need to be considered with the use of postoperative WBS is the so-called "stunning effect," resulting in a temporary suppression of iodine trapping function of the thyrocytes and thyroid cancer cells, as a result of the radiation given off by ^{131}I. In this setting, several studies have reported that the use of 5 mCi of ^{131}I before RAI treatment was independently associated with an increased risk of remnants ablation failure. However, these findings were not confirmed in other studies, resulting in heterogeneous insights. Recent improvements in technology, imaging acquisition, and imaging processing enable to use of lower ^{131}I doses, resulting in reduced risk of the stunning effect. In this setting, the possible negative impact of postoperative WBS on RAI therapeutic efficacy and on the success of remnant ablations may be reduced or avoided with the use of low-activity of ^{131}I (1–3 mCi at least 72 h before the therapeutic dose) or the use of alternative isotopes such as ^{123}I [20].

The use of single photon emission computed tomography/computed tomography (SPECT/CT) is one of the main factors that allow the reduction of ^{131}I dose and it has also demonstrated significant clinical benefit in terms of staging, risk stratification, and follow-up of patients with DTC, influencing the choice of the therapeutic dose to use. Notably, SPECT/CT is able to improve the diagnostic accuracy of planar WBS, reducing the number of equivocal foci interpretations. In this contest, it has demonstrated the ability to detect residual or unsuspected regional metastasis in about one-third of cases and distant metastases in about 10%. When coupled with the presence of high stimulated Tg values, postoperative diagnostic SPECT/CT underlined the presence of unsuspected nodal and distant metastasis resulting in a change in the estimated risk of recurrence and management. In addition, SPECT/CT is also able to perform three-dimensional imaging,

enabling the execution of dosimetric evaluation in selected cases [21, 22].

8.3.1.2 Posttherapy Setting

Planar WBS, usually obtained 3–10 days after ^{131}I therapy, is considered as an essential diagnostic tool in order to complete the staging, the risk stratification, the assessment of residual disease, the therapeutic planning, and the detection of recurrence in patients affected by DTC. Recent ATA guidelines [1] suggest that a posttherapy WBS (with or without the use of SPECT/CT) is recommended after ^{131}I treatment to complete the disease staging and document radioiodine avidity of any structural disease. The same guidelines suggest that WBS integrated by SPECT/CT after therapeutic radioiodine, and pre-ablation stimulated Tg measurement, remain the most accurate tools for the restaging of postoperative DTC and are fundamental elements of the risk stratification system. In practice, WBS allows the detection of possible unknown loco-regional and distant metastases, resulting in changing risk stratification that is able to customize additional therapy and subsequent follow-up. Notably, the presence of a negative diagnostic WBS is pivotal to underline the absence of persistent disease, to fully reassure the patients, and therefore to monitor them periodically simply by clinical examination and basal Tg measurement [11, 18].

The evaluation of the biodistribution of ^{131}I can be usually well defined with planar WBS imaging, however, this modality lacks anatomical information and has poor image resolution. As previously mentioned, the use of SPECT/CT can improve the diagnostic accuracy of WBS, resulting in accurate anatomic localization, reduction of the number of indeterminate findings, and correct assessment of size, localization, and avidity of metastatic lesions. These data are therefore able to guide further management decisions and, in particular, it has been reported that SPECT/CT was able to change patients' management in 25% of the cases, in particular for what concerns the frequency and intensity of follow-up studies. Interestingly, the incremental value of SPECT/CT in influencing the therapeutic approach appears to be greater in studies where its role has been reserved in situations with diagnostic uncertainty at posttherapy WBS or in advanced diseases with inconclusive WBS findings. In this field, the combination of posttherapy planar WBS and SPECT/CT of the neck and thorax had a sensitivity of 78% and a specificity of 100% for the assessment of DTC and furthermore the use of SPECT/CT can reduce the need for additional cross-sectional imaging. Interestingly, it was reported that a positive finding on SPECT/CT was more predictive of treatment failure than a positive finding on WBS [18].

The assessment of nodal localization of disease is mandatory for the correct staging of DTC. In this setting, WBS is mandatory for lymph node assessment and SPECT/CT has been demonstrated to be more accurate than WBS when evaluating nodal metastases, resulting again in a change in risk stratification [21, 22].

SPECT/CT has, however, some limitations, such as the presence of additional radiation exposure to the patient derived from the CT component (low-dose CT usually delivers to the patients a dose of 2–5 mSv.), the need for additional imaging time and the increased costs.

8.3.1.3 Response Assessment, Disease Monitoring, and Long-Term Follow-Up

The initial risk assessment of DTC patients is continuously modified and refined by the evaluation of response to treatment. Tg measurements, neck US and WBS (with both ^{123}I or ^{131}I) are used as primary tools for the follow-up of such subjects, having the potential to impact prognosis and risk stratification. However, at present no shared consensus on the routine use of ^{131}I WBS during the follow-up of DTC patients is available. In this setting, the aforementioned ATA guidelines suggest performing WBS in patients with high- or intermediate-risk of persistent disease, while it should not be routinely performed for the follow-up of other patients [1]. The use of WBS in low-risk patients should be strongly discouraged, especially in the presence of negative Tg values and neck US [11, 23].

A diagnostic WBS, performed 6–12 months after RAI therapy, can be useful for the follow-up

of patients with high- or intermediate-risk and should be performed with ^{123}I or ^{131}I. There is a strong agreement on the relevant role of WBS in patients with positive TgAb that reduce the evaluation of Tg, even in presence of negative US imaging, with extra-thyroid uptake at postoperative WBS, with large thyroid remnants precluding the execution of postoperative WBS and in selected cases based on individual risk profile [11, 24].

Moreover, WBS has been reported as a useful tool to select patients with a high risk of persistence/recurrence of disease, to assess patients with metastases and for the clear evaluation of patients with rising markers (Tg or TgAb). Notably, ^{131}I WBS performed after primary treatment of DTC has been reported as the only imaging modality associated with improved disease-specific survival. Furthermore, the use of rhTSH has shown to give reduce patients' discomfort and significantly improve the diagnostic performances of planar WBS [25–27].

As previously mentioned, also in the follow-up setting, SPECT/CT after WBS is usually recommended due to the incremental diagnostic value over planar imaging. SPECT/CT is associated with an increased number of patients with a diagnosis of metastatic lymph nodes and a decreased frequency of equivocal findings. In this setting, by providing precise localization and characterization of the residual thyroid tissue and ^{131}I-avid metastases, it strongly impacts the treatment approach for DTC patients, leading to a decrease in unnecessary 131I treatment in 20% of patients without disease [22].

WBS is also crucial to define the presence of iodine refractory disease, the condition when DTC has lost fully or partially the ability to concentrate ^{131}I despite the presence of disease.

8.3.2 PET/CT Imaging

8.3.2.1 Postoperative Setting

The effective role of ^{18}F-fluorodeoxyglucose [18F]-FDG) positron-emission tomography/CT (PET/CT) for the assessment of DTC remnants at the time of postoperative evaluation is yet unclear, with low evidences available in literature.

[18F]-FDG PET/CT might be useful, especially in high-risk patients, such as those with aggressive variants and poorly differentiated carcinoma, or in case of positive findings on other imaging modalities. In this setting, it has been reported that [18F]-FDG PET/CT can be very effective to search for distant metastases. Particularly, it can be sensitive for the evaluation of neck and mediastinal involvement and it may also be considered a prognostic tool in patients with metastatic disease, in order to identify subjects at higher risk for rapid disease progression and poor survival [1, 28].

8.3.2.2 Suspicious Relapse

In general, high-quality evidences about the role of [18F]-FDG PET/CT in studying DTC suspected relapse have been present. In particular, a pooled sensitivity ranging from 80% to 88% and a pooled specificity ranging from 84% to 90% were reported in the literature. In this setting, several factors may influence the sensitivity of [18F]-FDG PET/CT, such as tumor dedifferentiation, larger tumor burden and, with less evidences, TSH stimulation [29, 30].

The diagnostic performances of [18F]-FDG PET/CT may improve after TSH stimulation, however, it has been reported that sensitivity can be only marginally improved with such intervention and more studies are required to clearly identify the clinical benefit of this stimulation, in particular in patients with low Tg values. In this field, it has been described that [18F]-FDG PET/CT after TSH stimulation is able to detect more lesions than imaging performed on thyroid hormone treatment. However, the sensitivity to detect patients with at least one pathological site was not different in these two conditions and again the clinical benefit related to the identification of focal uptake at PET/CT scan remains to be proven. As a consequence, there are still no clear evidences that TSH stimulation improves the prognostic values of [18F]-FDG PET/CT [28, 31].

The last ATA guidelines recommend the use of [18F]-FDG PET/CT in order to assess the possible presence of DTC relapse in patients with

increasing Tg levels, negative US, and negative WBS imaging. Also in cases of patients with negative WBS and US but increasing levels of TgAb [18F]-FDG PET/CT has been proposed [1].

Interestingly, it has been reported that [18F]-FDG PET/CT is more sensitive than neck US in the detection of relapse in the retropharyngeal or retro-clavicular regions [28].

The best Tg cutoff able to define whether [18F]-FDG PET/CT has been indicated to be performed is still under debate. The aforementioned ATA guidelines suggest that PET/CT should be performed when Tg levels are higher than 10 ng/mL and concomitant negative ^{131}I imaging. But, it has been reported that true-positive findings are present in 10–20% of DTC patients with Tg levels lower than this threshold [32]. Recently, it has emerged the potential role of Tg kinetics (expressed as Tg doubling time and/or Tg velocity) to independently predict a positive [18F]-FDG PET/CT scan in patients with biochemical relapse of disease. In particular, the accuracy of [18F]-FDG PET/CT imaging significantly improves when the Tg doubling time is less than 1 year, irrespective of the absolute value of Tg [9, 33]. Further studies are needed to confirm or controvert these results.

Another potential field of application of [18F]-FDG PET/CT is in the presence of high TgAb levels, where Tg values cannot be reliably assessed; in presence of elevated TgAb values and a negative ^{131}I WBS a pooled sensitivity of 84% and a pooled specificity of 78% of [18F]-FDG PET/CT was reported [34].

Moreover, it was also described that a second empiric session of ^{131}I therapy and subsequent WBS were not diagnostically or therapeutically useful in patients with negative [18F]-FDG PET/CT scan but elevated Tg levels. This evidence suggests that the correct use of PET/CT imaging could be able to reduce unnecessary administrations of high 131I activities. In this scenario, the correct integration of ^{131}I imaging and [18F]-FDG PET/CT may optimize additional administrations of high ^{131}I activities and inform alternative strategies such as surgery or external beam radiation. Furthermore, the presence of 18F-FDG uptake on PET/CT imaging in metastatic patients is a major negative predictive factor for response to ^{131}I treatment and an independent prognostic factor for survival [18].

The presence of positive findings on [18F]-FDG PET/CT may change the clinical management of DTC patients in 20–40% of the cases. In this setting, in the presence of 18F-FDG positive lesions, alternative procedures instead of ^{131}I therapy may be considered [28].

8.3.2.3 Prognostic Role of PET Imaging

In general, more aggressive and high-grade DTC are characterized by higher [18F]-FDG uptake compared to low-grade and less aggressive tumors. The glycolytic rate of the most active lesion (sometimes expressed as maximum standardized uptake value, SUVmax) and the number of FDG-avid lesions are strongly associated with survival, even better than RAI uptake, histology, or immunohistochemical pattern [35–37].

On the other hand, a negative [18F]-FDG PET/CT scan is able to predict a favorable prognosis because it is associated with the absence of active DTC and the disappearance of TgAb over time. On the opposite, the presence of residual FDG-avid lesions is associated with more aggressive disease and persistently increased levels of TgAb [38, 39].

Recent studies showed a prognostic role of metabolic tumor volume (MTV) and total lesion glycolysis (TLG) in predicting overall survival and progression-free survival [40].

8.3.2.4 Assessment of Iodine Refractory Disease

In general, [18F]-FDG PET/CT helps address disease aggressiveness, detect distant metastases, and risk-stratify patients with iodine-refractory DTC and anaplastic cancers. It is known that while more differentiated thyroid cells tend to retain iodine and have lower glucose metabolism, undifferentiated cells tend to present with a lower ability to retain iodine but higher glucose metabolism. In this context, [18F]-FDG PET/CT is able to identify nodal localization or distant metastases of DTC patients that are not or only partially detected with ^{131}I WBS and as a consequence, the need to perform further ^{131}I therapy should be

reconsidered and avoided in these situations, given its low probability to alter the outcome of such patients. [18F]-FDG PET/CT may detect new iodine-negative localization of disease in patients with advanced DTC with stable ^{131}I WBS and rising Tg levels. In this scenario, more appropriate treatments other than RAI should be considered [28, 41, 42].

About the role of [18F]-FDG PET/CT for the prediction of systemic therapy in iodine refractory DTC, a significant association between average percent change in SUV and the response evaluation criteria in solid tumors (RECIST) response criteria were reported. Early [18F]-FDG PET/CT in patients on tyrosine kinase inhibitors (TKI) treatment could be an early indicator of response and could identify patients that are unlikely to respond to therapy. It has also been reported that [18F]-FDG imaging assessment at the baseline is able to predict radiological response but not clinical outcomes [43].

8.3.2.5 ^{124}I

^{124}I is an iodine isotope able to emit positron and it is, therefore, a suitable tracer to assess iodine metabolism with PET/CT imaging. The role of ^{124}I in the assessment of DTC is based on the assumption that this tracer is able to overcome some intrinsic limits of both ^{131}I and ^{123}I such as the reduced spatial resolution of SPECT/CT, poor image quality, and dose exposure. Theoretically, ^{124}I PET/CT could allow the selection of patients with rising Tg levels but negative neck US and [18F]-FDG PET/CT imaging, that will benefit from subsequent radioiodine in order to avoid inappropriate therapies. A high level of agreement between ^{124}I PET and ^{131}I WBS scan was reported in the literature, suggesting that ^{124}I PET/CT could be used for individualized treatment planning and staging in DTC patients. In this setting, data in the literature are however still controversial [1, 36].

It was reported that ^{124}I PET/CT is able to predict the response to high dose ^{131}I and would be a good diagnostic tool to support clinical decisions with high diagnostic accuracy. In particular, this imaging modality was able to reveal previously unknown lymph nodes and distant metastases [30, 44].

A negative ^{124}I PET/CT scan could suggest avoiding ^{131}I and performing further imaging to detect the localization of the non-iodine-avid disease. In contrast, it has also been reported that ^{124}I imaging had low sensitivity in detecting non-iodine avid metastases that were subsequently identified by post-therapeutic ^{131}I WBS. In this field, the high false-negative rate of rhTSH-stimulated ^{124}I PET/CT could preclude its use as a scouting procedure to prevent futile ^{131}I therapy. It is worth underlining that low diagnostic sensitivity of ^{124}I imaging was reported in the conditions of rhTSH stimulation, while in studies with high sensitivity the patients were on thyroid hormone withdrawal [45–47].

^{124}I PET/CT could also be useful for the assessment of post-operative DTC with high sensitivity, providing the detection of unknown metastases of disease and guiding subsequent ^{131}I [48].

8.3.2.6 Other PET Tracers

Somatostatin Analogs

DTC expresses somatostatin receptors 2, 3, and 5; thus, as a consequence PET/CT with labeled somatostatin analogs has been proposed as a diagnostic tool in such disease. In this setting, the comparison between ^{68}Ga-DOTATOC or ^{68}Ga-DOTANOC and [18F]-FDG PET/CT revealed similar sensitivity in a patient-based analysis. However, lesion-based analyses in multiple studies revealed a higher sensitivity for [18F]-FDG. Interestingly, it was reported that the accuracy of both modalities was not related to serum Tg levels, without significant differences in terms of accuracy between patients with low and high Tg [49–51].

When using ^{68}Ga-DOTANOC in patients with both negative ^{131}I WBS and [18F]-FDG PET/CT, it was reported that the presence of positive findings was significantly higher in poorly differentiated and oxyphilic carcinomas than in papillary or follicular tumors. In summary, these insights suggest that the diagnostic role of radiolabeled somatostatin analogs PET/CT in DTC is characterized by conflicting results and therefore it should not be considered in clinical practice [1].

More recently peptide receptor radionuclide therapy has been proposed as an alternative for the treatment of DTC and therefore ^{68}Ga-DOTATOC PET/CT was suggested as a guide to select patients for treatment. These insights are however in an embryonal phase and need therefore to be confirmed by other data [52].

Choline

It has been reported that PET/CT with radiolabeled choline may be useful in patients with metastatic DTC and negative [18F]-FDG PET/CT. This imaging modality can also be considered complementary to [18F]-FDG PET/CT, thereby increasing information about the status of the disease. Data in literature are, however, still in the early phases, and therefore this imaging modality should not be considered in clinical practice [53].

PSMA

There are only a few evidences in the literature on the role of labeled prostate-specific membrane antigen (PSMA) PET/CT for the assessment of DTC, underlying its potential usefulness for the assessment of metastatic radioiodine negative subjects. However, these insights need to be verified by further evidences [54].

NIS Imaging

^{18}F-tetrafluoroborate (^{18}F-FTB) and ^{18}F-fluorosulfate (^{18}F-FSO_3) are iodine analogs that are recently emerging as potential candidates to assess DTC given their ability to visualize sodium/iodide symporter (NIS) in preclinical and preliminary clinical applications. Even if in small samples, they revealed high sensitivity in some cases but their applications in DTC need, however, to be verified with further studies [55, 56].

8.4 Future Perspectives: Artificial Intelligence and Radiomics

In the last years, new knowledge and better technologies expanded the applications of artificial intelligence (AI) and extended it to medical problems: management of the malignant tumor represents one of the most important and promising fields of application of AI, particularly in the diagnosis of malignancy, in the prognostication and in the management [57–59].

Moreover, a rising interest in quantitative image analysis using techniques such as texture analysis has been developed. This has led to the introduction of radiomics, which has come to define large radiological image-derived feature sets, primed for exploration and analysis with data mining or machine learning approaches. Radiomics is a method that extracts a large number of features from radiographic medical images using data-characterization algorithms. The goal of both radiomics and texture analysis is to go beyond the size or human eye-based semantic descriptors, to enable the non-invasive extraction of quantitative radiological data to correlate them with clinical outcomes or pathological characteristics [59, 60].

But, there is great uncertainty about the actual clinical value of information derived from radiomic features as questions are raised on their reproducibility and interpretability in biological terms, beyond ethical concerns.

Regarding the postoperative field, a little number of studies that investigate the potential role of IA and/or radiomics are available.

The artificial neural network showed to have optimal accuracy in identifying factors that predict the presence of central nodal metastases [61], even better than traditional logistic regression analysis [62]. In a recent study [63], the application of machine learning algorithms showed to be superior to the classical US and clinical features in predicting central nodal metastases and after multivariate analysis and feature selection, the combination of young age, male gender, low serum thyroid peroxidase antibody, and US characteristics (like the presence suspected lymph nodes, size>1.1 cm and microcalcifications) were the most contributing predictors.

Furthermore, it has been reported that machine learning techniques could predict the presence of lymph node metastases with high sensitivity and specificity using only visual histopathological data derived from the primary tumor [64, 65].

The possible presence of skip metastases (a nodal disease in laterocervical levels without the involvement of the VI level), was also assessed reporting a model with high accuracy, specificity, and NPV. In this setting, the possibilities to better predict the presence of undetectable central node metastases and exclusion of skip metastases may help to choose when prophylactic lymphadenectomy of the VI level could be necessary [66].

Another promising application seems to be the prediction of disease recurrence: recent studies currently reported an accuracy of about 70–90% in the prediction of disease recurrence with an optimal NPV. According to the main international guidelines, thyroglobulin level after thyroidectomy, tumor size, and presence of contralateral nodal disease apparently are the most significant parameters derived by Machine Learning systems. More studies are needed to establish the best family of parameters or the combination of them for predicting the risk of recurrence. The possibility to predict DCT metastases and local recurrence could help in defining therapeutic and follow-up strategies.

It is worth underlining that despite a large number of works in the literature about the characterization of thyroid nodules and preoperative management of thyroid malignancy, no studies about the possible clinical usefulness of the analysis of radiomics features, a specific field of AI based on the extraction radiological and nuclear medicine imaging, in the postoperative management of DTC are actually available.

The application of promising machine learning techniques for the assessment of DTC has just started and more studies are necessary in order to create better models able to guide clinical practice.

References

1. Haugen BR, Alexander EK, Bible KC, Doherty GM, Mandel SJ, Nikiforov YE, Pacini F, Randolph GW, Sawka AM, Schlumberger M, Schuff KG, Sherman SI, Sosa JA, Steward DL, Tuttle RM, Wartofsky L. 2015 American Thyroid Association management guidelines for adult patients with thyroid nodules and differentiated thyroid cancer: the American Thyroid Association guidelines task force on thyroid nodules and differentiated thyroid cancer. Thyroid. 2016;26(1):1–133. https://doi.org/10.1089/thy.2015.0020.
2. Petranović Ovčariček P, Kreissl MC, Campenni A, de Keizer B, Tuncel M, Vrachimis A, Deandreis D, Giovanella L. SNMMI/EANM practice guideline vs. ETA consensus statement: differences and similarities in approaching differentiated thyroid cancer management-the EANM perspective. Eur J Nucl Med Mol Imaging. 2022; https://doi.org/10.1007/s00259-022-05935-1.
3. Knappe L, Giovanella L. Life after thyroid cancer: the role of thyroglobulin and thyroglobulin antibodies for postoperative follow-up. Expert Rev Endocrinol Metab. 2021;16(6):273–9. https://doi.org/10.1080/17446651.2021.1993060.
4. Giovanella L. Circulating biomarkers for the detection of tumor recurrence in the postsurgical follow-up of differentiated thyroid carcinoma. Curr Opin Oncol. 2020;32(1):7–12. https://doi.org/10.1097/CCO.0000000000000588.
5. Algeciras-Schimnich A. Thyroglobulin measurement in the management of patients with differentiated thyroid cancer. Crit Rev Clin Lab Sci. 2018;55(3):205–18. https://doi.org/10.1080/10408363.2018.1450830.
6. Verburg FA, Luster M, Cupini C, Chiovato L, Duntas L, Elisei R, Feldt-Rasmussen U, Rimmele H, Seregni E, Smit JW, Theimer C, Giovanella L. Implications of thyroglobulin antibody positivity in patients with differentiated thyroid cancer: a clinical position statement. Thyroid. 2013;23(10):1211–25. https://doi.org/10.1089/thy.2012.0606.
7. Giovanella L, Clark PM, Chiovato L, Duntas L, Elisei R, Feldt-Rasmussen U, Leenhardt L, Luster M, Schalin-Jäntti C, Schott M, Seregni E, Rimmele H, Smit J, Verburg FA. Thyroglobulin measurement using highly sensitive assays in patients with differentiated thyroid cancer: a clinical position paper. Eur J Endocrinol. 2014;171(2):R33–46. https://doi.org/10.1530/EJE-14-0148.
8. Giovanella L, Garo ML, Albano D, Görges R, Ceriani L. The role of thyroglobulin doubling time in differentiated thyroid cancer: a meta-analysis. Endocr Connect. 2022;11(4):e210648. https://doi.org/10.1530/EC-21-0648.
9. Albano D, Tulchinsky M, Dondi F, Mazzoletti A, Lombardi D, Bertagna F, Giubbini R. Thyroglobulin doubling time offers a better threshold than thyroglobulin level for selecting optimal candidates to undergo localizing [^{18}F]FDG PET/CT in non-iodine avid differentiated thyroid carcinoma. Eur J Nucl Med Mol Imaging. 2021;48(2):461–8. https://doi.org/10.1007/s00259-020-04992-8.
10. Albano D, Tulchinsky M, Dondi F, Mazzoletti A, Bertagna F, Giubbini R. The role of Tg kinetics in predicting 2-[^{18}F]-FDG PET/CT results and overall survival in patients affected by differentiated thyroid carcinoma with detectable Tg and negative

131I-scan. Endocrine. 2021;74(2):332–9. https://doi.org/10.1007/s12020-021-02755-5.
11. Campennì A, Barbaro D, Guzzo M, Capoccetti F, Giovanella L. Personalized management of differentiated thyroid cancer in real life - practical guidance from a multidisciplinary panel of experts. Endocrine. 2020;70(2):280–91. https://doi.org/10.1007/s12020-020-02418-x.
12. Giovanella L, Avram AM, Clerc J, Hindié E, Taïeb D, Verburg FA. Postoperative serum thyroglobulin and neck ultrasound to drive decisions about iodine-131 therapy in patients with differentiated thyroid carcinoma: an evidence-based strategy? Eur J Nucl Med Mol Imaging. 2018;45(12):2155–8. https://doi.org/10.1007/s00259-018-4110-4.
13. Spencer C, LoPresti J, Fatemi S. How sensitive (second-generation) thyroglobulin measurement is changing paradigms for monitoring patients with differentiated thyroid cancer, in the absence or presence of thyroglobulin autoantibodies. Curr Opin Endocrinol Diabetes Obes. 2014;21(5):394–404. https://doi.org/10.1097/MED.0000000000000092.
14. Wang W, Chang J, Jia B, Liu J. The blood biomarkers of thyroid cancer. Cancer Manag Res. 2020;6(12):5431–8. https://doi.org/10.2147/CMAR.S261170. Erratum in: Cancer Manag Res. 2022 Jan 05;14:49-50.
15. Giovanella L, Ceriani L, Garo ML. Is thyroglobulin a reliable biomarker of differentiated thyroid cancer in patients treated by lobectomy? A systematic review and meta-analysis. Clin Chem Lab Med. 2022;60(7):1091–100. https://doi.org/10.1515/cclm-2022-0154.
16. Feldt-Rasmussen U, Verburg FA, Luster M, Cupini C, Chiovato L, Duntas L, Elisei R, Rimmele H, Seregni E, Smit JW, Theimer C, Giovanella L. Thyroglobulin autoantibodies as surrogate biomarkers in the management of patients with differentiated thyroid carcinoma. Curr Med Chem. 2014;21(32):3687–92. https://doi.org/10.2174/0929867321666140826120844.
17. Giovanella L, Feldt-Rasmussen U, Verburg FA, Grebe SK, Plebani M, Clark PM. Thyroglobulin measurement by highly sensitive assays: focus on laboratory challenges. Clin Chem Lab Med. 2015;53(9):1301–14. https://doi.org/10.1515/cclm-2014-0813.
18. Giovanella L, Deandreis D, Vrachimis A, Campenni A, Ovcaricek PP. Molecular imaging and theragnostics of thyroid cancers. Cancers (Basel). 2022;14(5):1272. https://doi.org/10.3390/cancers14051272.
19. Avram AM, Esfandiari NH, Wong KK. Preablation 131-I scans with SPECT/CT contribute to thyroid cancer risk stratification and 131-I therapy planning. J Clin Endocrinol Metab. 2015;100(5):1895–902. https://doi.org/10.1210/jc.2014-4043.
20. Chen MK, Yasrebi M, Samii J, Staib LH, Doddamane I, Cheng DW. The utility of I-123 pre-therapy scan in I-131 radioiodine therapy for thyroid cancer. Thyroid. 2012;22:304–9.
21. Avram AM. Radioiodine scintigraphy with SPECT/CT: an important diagnostic tool for thyroid cancer staging and risk stratification. J Nucl Med. 2012;53:754–64.
22. Lee SW. SPECT/CT in the treatment of differentiated thyroid cancer. Nucl Med Mol Imaging. 2017;51(4):297–303. https://doi.org/10.1007/s13139-017-0473-x.
23. Lamartina L, Deandreis D, Durante C, Filetti S. ENDOCRINE TUMOURS: imaging in the follow-up of differentiated thyroid cancer: current evidence and future perspectives for a risk-adapted approach. Eur J Endocrinol. 2016;175(5):R185–202. https://doi.org/10.1530/EJE-16-0088.
24. Verburg FA, Mäder U, Reiners C, Hänscheid H. Long-term survival in differentiated thyroid cancer is worse after low-activity initial post-surgical 131I therapy in both high- and low-risk patients. J Clin Endocrinol Metab. 2014;99(12):4487–96. https://doi.org/10.1210/jc.2014-1631.
25. Alzahrani AS, AlShaikh O, Tuli M, Al-Sugair A, Alamawi R, Al-Rasheed MM. Diagnostic value of recombinant human thyrotropin-stimulated ^{123}I whole-body scintigraphy in the follow-up of patients with differentiated thyroid cancer. Clin Nucl Med. 2012;37(3):229–34. https://doi.org/10.1097/RLU.0b013e31823ea463.
26. Barwick T, Murray I, Megadmi H, Drake WM, Plowman PN, Akker SA, Chew SL, Grossman AB, Avril N. Single photon emission computed tomography (SPECT)/computed tomography using Iodine-123 in patients with differentiated thyroid cancer: additional value over whole body planar imaging and SPECT. Eur J Endocrinol. 2010;162(6):1131–9. https://doi.org/10.1530/EJE-09-1023.
27. Spanu A, Solinas ME, Chessa F, Sanna D, Nuvoli S, Madeddu G. 131I SPECT/CT in the follow-up of differentiated thyroid carcinoma: incremental value versus planar imaging. J Nucl Med. 2009;50(2):184–90. https://doi.org/10.2967/jnumed.108.056572.
28. Piccardo A, Trimboli P, Foppiani L, Treglia G, Ferrarazzo G, Massollo M, Bottoni G, Giovanella L. PET/CT in thyroid nodule and differentiated thyroid cancer patients. The evidence-based state of the art. Rev Endocr Metab Disord. 2019;20(1):47–64. https://doi.org/10.1007/s11154-019-09491-2.
29. Schütz F, Lautenschläger C, Lorenz K, Haerting J. Positron emission tomography (PET) and PET/CT in thyroid cancer: a systematic review and meta-analysis. Eur Thyroid J. 2018;7:13–20.
30. Zampella E, Klain M, Pace L, Cuocolo A. PET/CT in the management of differentiated thyroid cancer. Diagn Interv Imaging. 2021;102(9):515–23. https://doi.org/10.1016/j.diii.2021.04.004.
31. Ma C, Xie J, Lou Y, Gao Y, Zuo S, Wang X. The role of TSH for 18F-FDG-PET in the diagnosis of recurrence and metastases of differentiated thyroid carcinoma with elevated Tg and negative scan: a meta-analysis. Eur J Endocrinol. 2010;163:177–83.

32. Bertagna F, Albano D, Bosio G, Piccardo A, Dib B, Giubbini R. 18F-FDG-PET/CT in patients affected by differentiated thyroid carcinoma with positive thyroglobulin level and negative 131I whole body scan. It's value confirmed by a bicentric experience. Curr Radiopharm. 2016;9(3):228–34. https://doi.org/10.2174/1874471009666160523145005.
33. Giovanella L, Trimboli P, Verburg FA, Treglia G, Piccardo A, Foppiani L, et al. Tg levels and Tg doubling time independently predict a positive (18) F-FDG PET/CT scan in patients with biochemical recurrence of differentiated thyroid carcinoma. Eur J Nucl Med Mol Imaging. 2013;40:874–80.
34. Kim SJ, Lee SW, Pak K, Shim SR. Diagnostic performance of PET in thyroid cancer with elevated anti-Tg Ab. Endocr Relat Cancer. 2018;25:643–52.
35. Robbins RJ, Wan Q, Grewal RK, Reibke R, Gonen M, Strauss HW, et al. Real-time prognosis for metastatic thyroid carcinoma based on 2-[18F]fluoro-2-deoxy-D-glucose-positron emission tomography scanning. J Clin Endocrinol Metab. 2006;91:498–505.
36. Treglia G, Giovanella L. Prognostic role of FDG-PET/CT in differentiated thyroid carcinoma: where are we now? J Med Imaging Radiat Oncol. 2015;59:278–80.
37. Deandreis D, Al Ghuzlan A, Leboulleux S, Lacroix L, Garsi JP, Talbot M, et al. Do histological, immunohistochemical, and metabolic (radioiodine and fluorodeoxyglucose uptakes) patterns of metastatic thyroid cancer correlate with patient outcome? Endocr Relat Cancer. 2011;13(18):159–69.
38. Marcus C, Antoniou A, Rahmim A, Ladenson P, Subramaniam RM. Fluorodeoxyglucose positron emission tomography/computerized tomography in differentiated thyroid cancer management: importance of clinical justification and value in predicting survival. J Med Imaging Radiat Oncol. 2015;59:281–8.
39. Bogsrud TV, Hay ID, Karantanis D, Nathan MA, Mullan BP, Wiseman GA, et al. Prognostic value of 18 F-fluorodeoxyglucose-positron emission tomography in patients with differentiated thyroid carcinoma and circulating antiTg auto-antibodies. Nucl Med Commun. 2011;32:245–51.
40. Albano D, Dondi F, Mazzoletti A, Bellini P, Rodella C, Bertagna F. Prognostic role of 2-[18F]FDG PET/CT metabolic volume parameters in patients affected by differentiated thyroid carcinoma with high thyroglobulin level, negative 131I WBS and positive 2-[18F]-FDG PET/CT. Diagnostics (Basel). 2021;11(12):2189. https://doi.org/10.3390/diagnostics11122189.
41. Iwano S, Kato K, Ito S, Tsuchiya K, Naganawa S. FDG PET performed concurrently with initial I-131 ablation for differentiated thyroid cancer. Ann Nucl Med. 2012;26:207–13.
42. Piccardo A, Foppiani L, Morbelli S, Bianchi P, Barbera F, Biscaldi E, Altrinetti V, Villavecchia G, Cabria M. Could [18]F-fluorodeoxyglucose PET/CT change the therapeutic management of stage IV thyroid cancer with positive (131)I whole body scan? Q J Nucl Med Mol Imaging. 2011;55(1):57–65.
43. Marotta V, Ramundo V, Camera L, Del Prete M, Fonti R, Esposito R, Palmieri G, Salvatore M, Vitale M, Colao A, Faggiano A. Sorafenib in advanced iodine-refractory differentiated thyroid cancer: efficacy, safety and exploratory analysis of role of serum thyroglobulin and FDG-PET. Clin Endocrinol. 2013;78(5):760–7. https://doi.org/10.1111/cen.12057.
44. Capoccetti F, Criscuoli B, Rossi G, Ferretti F, Manni C, Brianzoni E. The effectiveness of 124I PET/CT in patients with differentiated thyroid cancer. Q J Nucl Med Mol Imaging. 2009;53:536–45.
45. Freudenberg LS, Jentzen W, Müller SP, Bockisch A. Disseminated iodine-avid lung metastases in differentiated thyroid cancer: a challenge to 124I PET. Eur J Nucl Med Mol Imaging. 2008;35:502–8.
46. Kist JW, de Keizer B, van der Vlies M, Brouwers AH, Huysmans DA, van der Zant FM, THYROPET study group; other members of the THYROPET study group are John M.H. de Klerk, et al. 124I PET/CT to predict the outcome of blind 131I treatment in patients with biochemical recurrence of differentiated thyroid cancer: results of a multicenter diagnostic cohort study (THYROPET). J Nucl Med. 2016;57:701–7.
47. Khorjekar GR, Van Nostrand D, Garcia C, O'Neil J, Moreau S, Atkins FB, et al. Do negative 124I pretherapy positron emission tomography scans in patients with elevated serum Tg levels predict negative 131I posttherapy scans? Thyroid. 2014;24:1394–9.
48. Santhanam P, Taieb D, Solnes L, Marashdeh W, Ladenson PW. Utility of I-124 PET/CT in identifying radioiodine avid lesions in differentiated thyroid cancer: a systematic review and meta-analysis. Clin Endocrinol. 2017;86:645–51.
49. Middendorp M, Selkinski I, Happel C, Kranert WT, Grünwald F. Comparison of positron emission tomography with [(18)F] FDG and [(68)Ga] DOTATOC in recurrent differentiated thyroid cancer: preliminary data. Q J Nucl Med Mol Imaging. 2010;54:76–83.
50. Traub-Weidinger T, Putzer D, von Guggenberg E, Dobrozemsky G, Nilica B, Kendler D, et al. Multiparametric PET imaging in thyroid malignancy characterizing tumour heterogeneity: somatostatin receptors and glucose metabolism. Eur J Nucl Med Mol Imaging. 2015;42:1995–2001.
51. Kundu P, Lata S, Sharma P, Singh H, Malhotra A, Bal C. Prospective evaluation of (68)Ga-DOTANOC PET-CT in differentiated thyroid cancer patients with raised thyroglobulin and negative (131)I-whole body scan: comparison with (18)F-FDG PETCT. Eur J Nucl Med Mol Imaging. 2014;41:1354–62.
52. Versari A, Sollini M, Frasoldati A, Fraternali A, Filice A, Froio A, Asti M, Fioroni F, Cremonini N, Putzer D, et al. Differentiated thyroid cancer: a new perspective with radiolabeled somatostatin analogues for imaging and treatment of patients. Thyroid. 2014;24:715–26.
53. Piccardo A, Trimboli P, Puntoni M, Foppiani L, Treglia G, Naseri M, Bottoni GL, Massollo M, Sola S, Ferrarazzo G, Bruzzone M, Catrambone U, Arlandini A, Paone G, Ceriani L, Cabria M, Giovanella L. Role of 18F-choline positron emission tomography/

computed tomography to detect structural relapse in high-risk differentiated thyroid cancer patients. Thyroid. 2019;29(4):549–56. https://doi.org/10.1089/thy.2018.0552.
54. Verburg FA, Krohn T, Heinzel A, Mottaghy FM, Behrendt FF. First evidence of PSMA expression in differentiated thyroid cancer using 68GaPSMA-HBED-CC PET/CT. Eur J Nucl Med Mol Imaging. 2015;42:1622–3.
55. Jiang H, DeGrado TR. [18F]Tetrafluoroborate ([18F]TFB) and its analogs for PET imaging of the sodium/iodide symporter. Theranostics. 2018;8(14):3918–31. https://doi.org/10.7150/thno.24997.
56. Jiang H, Schmit NR, Koenen AR, Bansal A, Pandey MK, Glynn RB, Kemp BJ, Delaney KL, Dispenzieri A, Bakkum-Gamez JN, Peng KW, Russell SJ, Gunderson TM, Lowe VJ, DeGrado TR. Safety, pharmacokinetics, metabolism and radiation dosimetry of ^{18}F-tetrafluoroborate (^{18}F-TFB) in healthy human subjects. EJNMMI Res. 2017;7(1):90. https://doi.org/10.1186/s13550-017-0337-5.
57. Liew C. The future of radiology augmented with artificial intelligence: a strategy for success. Eur J Radiol. 2018;102:152–6. https://doi.org/10.1016/j.ejrad.2018.03.019.
58. Nakata N. Recent technical development of artificial intelligence for diagnostic medical imaging. Jpn J Radiol. 2019;37(2):103–8. https://doi.org/10.1007/s11604-018-0804-6.
59. Rizzo S, Botta F, Raimondi S, Origgi D, Fanciullo C, Morganti AG, Bellomi M. Radiomics: the facts and the challenges of image analysis. Eur Radiol Exp. 2018;2(1):36. https://doi.org/10.1186/s41747-018-0068-z.
60. Corrias G, Micheletti G, Barberini L, Suri JS, Saba L. Texture analysis imaging "what a clinical radiologist needs to know". Eur J Radiol. 2022;146:110055. https://doi.org/10.1016/j.ejrad.2021.110055.
61. Esce AR, Redemann JP, Sanchez AC, Olson GT, Hanson JA, Agarwal S, Boyd NH, Martin DR. Predicting nodal metastases in papillary thyroid carcinoma using artificial intelligence. Am J Surg. 2021;222(5):952–8. https://doi.org/10.1016/j.amjsurg.2021.05.002.
62. Ozden S, Er S, Saylam B, Yildiz BD, Senol K, Tez M. A comparison of logistic regression and artificial neural networks in predicting central lymph node metastases in papillary thyroid microcarcinoma. Ann Ital Chir. 2018;89:193–8.
63. Wu Y, Rao K, Liu J, Han C, Gong L, Chong Y, Liu Z, Xu X. Machine learning algorithms for the prediction of central lymph node metastasis in patients with papillary thyroid cancer. Front Endocrinol (Lausanne). 2020;21(11):577537. https://doi.org/10.3389/fendo.2020.577537.
64. Kim SY, Kim YI, Kim HJ, Chang H, Kim SM, Lee YS, Kwon SS, Shin H, Chang HS, Park CS. New approach of prediction of recurrence in thyroid cancer patients using machine learning. Medicine (Baltimore). 2021;100(42):e27493. https://doi.org/10.1097/MD.0000000000027493.
65. Park YM, Lee BJ. Machine learning-based prediction model using clinico-pathologic factors for papillary thyroid carcinoma recurrence. Sci Rep. 2021;11(1):4948. https://doi.org/10.1038/s41598-021-84504-2.
66. Zhu S, Wang Q, Zheng D, Zhu L, Zhou Z, Xu S, Shi B, Jin C, Zheng G, Cai Y. A novel and effective model to predict skip metastasis in papillary thyroid carcinoma based on a support vector machine. Front Endocrinol (Lausanne). 2022;5(13):916121. https://doi.org/10.3389/fendo.2022.916121.

9 Definition of Radioactive Iodine Refractory Thyroid Cancer and Redifferentiation Strategies

M. Finessi, V. Liberini, and D. Deandreis

9.1 Definition of Radioiodine Refractory Thyroid Cancer

Differentiated thyroid cancer (DTC) arises from follicular cells and includes papillary and follicular cancers that represent the majority (>90%) of all thyroid cancers [1]. It represents a heterogeneous disease, with a very wide range of clinical presentation and prognosis.

Mostly of DTC are represented by indolent tumors with an excellent prognosis but the 5-year survival greatly varies according to the disease stage at diagnosis, ranging from 99.9% in case of localized thyroid cancer to 56.2% in case of distant metastases and patient age, that shifted from 45 years to 55 years for prognostic stratification into the recent TNM system [2]. Accordingly to the initial presentation and on the basis of histological findings [1] patients are also stratified in different classes of risk of recurrence: low (risk of recurrence <5%), intermediate (risk of recurrence ranging from 5 to 30%), and high risk (risk of recurrence >30–40%), according to American Thyroid Association classification [1]. The first-line treatment approach to DTC is represented by surgery, radioactive iodine (RAI) and suppressive therapy with L-thyroxine (L-T4) with achievement of excellent response in a high pourcentage of patients without distant metastases.

Metastatic disease is present in 4% up to 10% of DTC patients [3] and may be discovered at the time of initial disease or during follow-up [2]. The presence of distant metastases represents the leading cause of cancer-related death and the most challenging situation to treat. Radioactive iodine (RAI) therapy with [131I]I is the main treatment modality, in the case of persistent or metastatic disease frequently in association with other treatment modalities such as surgery, thermal ablation and external beam radiation therapy [1]. About 50% of metastatic patients obtain complete remission or stabilization of the disease over a long-term period with RAI therapy. Unfortunately, another 50%, develop an RAI refractory disease [4] with 5-year disease-spe-

M. Finessi
Nuclear Medicine Unit, Department of Diagnostic Imaging and Interventional Radiology, AOU Città della Salute e della Scienza, Turin, Italy
e-mail: mfinessi@cittadellasalute.to.it

V. Liberini
Nuclear Medicine Unit, Department of Medical Sciences, University of Turin, AOU Città della Salute e della Scienza, Turin, Italy
e-mail: liberini.v@ospedale.cuneo.it

D. Deandreis (✉)
Nuclear Medicine Unit, Department of Diagnostic Imaging and Interventional Radiology, AOU Città della Salute e della Scienza, Turin, Italy

Nuclear Medicine Unit, Department of Medical Sciences, University of Turin, AOU Città della Salute e della Scienza, Turin, Italy

Nuclear Medicine Division, Gustave Roussy, Villejuif, France
e-mail: desiree.deandreis@gustaveroussy.fr

L. Giovanella (ed.), *Integrated Diagnostics and Theranostics of Thyroid Diseases*,
https://doi.org/10.1007/978-3-031-35213-3_9

cific survival ranging from 60% to 70% and 10-year survival of around 10%, respectively.

RAI refractory disease definition is still challenging and includes wide clinical presentations and heterogeneous clinical conditions notably, patients with high volume and rapidly progressive disease or patients with low volume and slow disease progression after the failure of RAI treatment. According to radioactive iodine uptake ATA guidelines [1] classified RAI refractory thyroid cancer in four categories: (1) malignant/metastatic structurally evident disease that does not ever concentrate RAI (no uptake outside the thyroid bed at the first therapeutic whole-body scan (WBS)), (2) tumor tissue that loses the ability to concentrate RAI after previous evidence of RAI avid disease (in the absence of stable iodine contamination), (3) RAI concentration in some lesions but not in others, (4) metastatic disease that progresses despite significant concentration of RAI. Further proposals also include patients with 2-deoxy-2-[18F]-fluoro-D-glucose ([18F]FDG) avid lesions at Positron Emission tomography/computed tomography (PET/CT) as a condition related to scarce response to RAI and patients that do not reach complete response after a fixed cut-off of 22.2. GBq of cumulative activity of RAI [5, 6]. The therapeutic decision to discontinue RAI therapy is nevertheless critical and should be based on several elements: the clinical presentation of the disease, the presence and the entity of RAI uptake, the entity of metabolic and morphological response to previous RAI treatment, the trend of serum thyroglobulin (Tg) value, the morphological progression slope, the cumulated activity, and RAI side effects.

9.1.1 Clinical Presentation

Patient age, tumor differentiation, histological subtype, tumor burden, and molecular patterns are the most defined predictive factors of tumor response to RAIT. Older patients (> 40 years) with poorly differentiated carcinomas or with most aggressive histology (such as Tall cells variants, hurtle cells, poorly differentiated) and with multiple and macro-metastases present poorer overall survival (OS) compared to younger patients with well-differentiated tumors and micro-metastases, who can be cured by RAI [7].

In 2006, Durante et al. [8] retrospectively evaluated a cohort of 444 patients with distant metastases from papillary and follicular thyroid carcinoma (223 with lung metastases only, 115 with bone metastases only, 82 with both lung and bone metastases, and 24 with other sites of disease) and observed that RAIT was highly effective in patients younger than 40 years with micro-metastases from papillary thyroid cancer; while patients older than 40 years with macro-metastases were associated with poor prognosis, even in presence of RAI uptake. In case of no objective response, RAIT should be abandoned, and other treatment modalities should be preferred.

In 2017, also Deandreis et al. [7] in a retrospective study on the optimal management of RAI treatment in patients with metastatic disease found out that male sex, age over 40 years at the diagnosis of distant metastases, follicular histology, macro- or multiple metastases, and the presence of both lung and bone metastases had a negative impact on OS.

In particular, bone lesions from thyroid cancer are often lytic with a large skeletal burden, sometimes with extension into surrounding soft tissues, and are less responsive to RAI compared to lung metastases [9]. The spine is the most frequent site, and spinal metastases can be the first manifestation of follicular thyroid cancer [9–11]. A recent review on bone metastases in thyroid cancer [12] underlines that the factors causing low RAI efficacy are principally large skeletal burden and high absorbed dose required to achieve an effective treatment. Complete response to RAI in case of bone metastases can be achieved but only in case of high iodine uptake and focal uptake in the absence of evident lesions on morphological imaging.

From a molecular point of view, several mechanisms are involved in NIS expression and several are responsible for NIS expression loss. Firstly, Thyroid Stimulating Hormone (TSH) regulates NIS expression through stimulation of the TSH receptor (TSHR), which activates

adenylyl cyclase accumulating cyclic AMP (cAMP) that induces NIS transcription by stimulating thyroid-specific transcriptional factors (TTFs), such as paired box 8 (PAX8) [13].

Genetic and epigenetic alterations of RTK/BRAF/MAPK/ERK and PI3K/AKT-mTOR pathways are responsible for lower NIS signaling and subsequent RAI refractoriness (Fig. 9.1) and higher expression of glucose transporter especially GLUT1, responsible for 18F-FDG uptake [14, 15].

The mutation of v-raf murine sarcoma viral oncogene homolog B1 (BRAF-V600E) is the most frequent mutation in papillary thyroid cancer (around 60% of cases) and it is strongly correlated to the loss of NIS expression [16] both directly driving histone deacetylation of the H3 and H4 lysine residues of the sodium/iodide symporter (NIS) promoter, preventing its transcription [14, 17] and indirectly, repressing paired box gene 8 (PAX8) binding to the NIS promoter by activation of Transforming growth factor β (TGFβ)/Smad3 signalling [14, 18]. These mechanisms lead to tumor dedifferentiation, high risk of recurrence, and distant metastasis [14]. In follicular cancer, RAS is the most frequent mutation, but it is mostly related to a well-differentiated tumor forms. RET/PTC rearrangement has also been reported and related to a decreased NIS expression in thyroid cells [19].

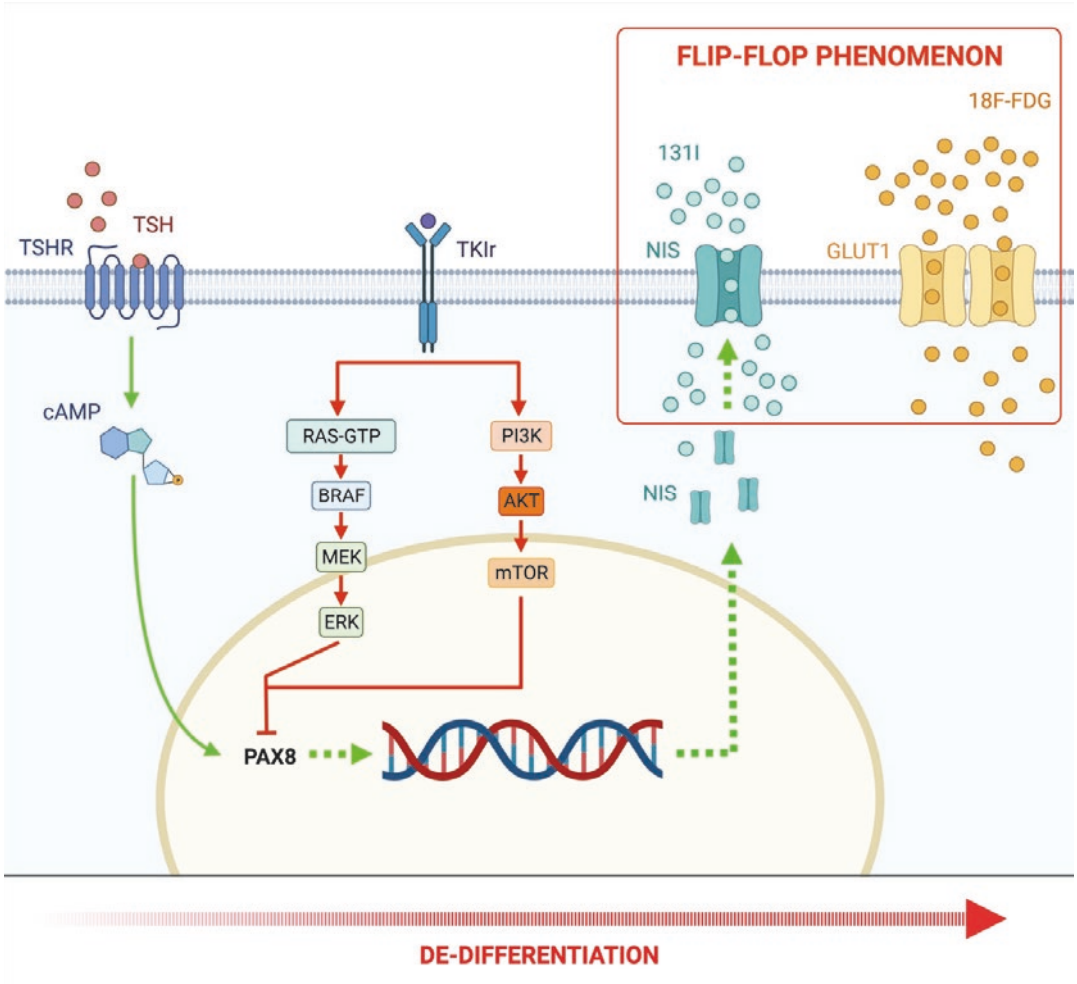

Fig. 9.1 Principle mechanisms involved in NIS expression and "*flip-flop phenomenon*." Created with BioRender.com

9.1.2 Radioactive Iodine Treatment

A great debate is still of actuality also on the best approach to RAI uptake evaluation and administration modalities in metastatic patients.

In 2013, the Council of the European Union with the directive 2013/59 EURATOM [20], following the "ALARA" ("As Low As Reasonably Achievable") concept, stated that for all medical exposure of patients for radio-therapeutic purposes, including metastatic DTC, exposures of target volumes shall be individually planned. Considering the approach between empiric compared to dosimetry determined activities of radioactive iodine, after more than 60 years of RAI use for thyroid cancer. However, the optimal activity to be administered is still unknown, especially in metastatic patients, and the American Thyroid Association (ATA) guidelines [1] suggest activities variably between 3.7 and 7.4 GBq higher for bone metastases compared to lung metastases.

The empirical approach is based on the administration of fixed activities (from 3.7 to 7.4 GBq) according to clinical factors and tumor burden: this approach is widespread as it is easier to manage, with low patient discomfort and shorter hospitalization. Most of the data available are based on this approach. Typically, lower activities are administrated in case of multiple lung lesions and higher activities in case of bone metastases with or without lung involvement. Treatment is usually repeated in case of objective benefit every 6–12 months or disappearance of RAI uptake [21]. However, it does not take into account tumor biology and repeated fractionated lower activities may lead to changes in tumor biology or different lesion biokinetics as described by Samuel et al. [22].

Dosimetric evaluation could be provided by both Maximum Tolerated Activity (MTA) calculation or lesional dosimetry [21]: the first one, originally proposed by Benua and Leeper et al. [23, 24], allows the administration of the highest therapeutic activity to the lesions with the respect of absorbed dose limit to the blood marrow of 2 Gy and whole-body retention of 80 mCi at 48 h.

This approach could allow administering higher activities avoiding toxicity. Nevertheless, higher activities could not be effective if a significant absorbed dose is not delivered to the tumors. Lesional dosimetry can evaluate the absorbed dose delivered to the tumoral lesions assessed by [131I]I SPECT/CT or [124I]I PET/CT imaging, but is not feasible in all lesions and presents some limits in case of disseminated metastases, such as miliary pulmonary metastases, irregularly shaped lesions, lesions without a correlate in morphological imaging and lesions with low radioiodine uptake [21]. Neverthless it is not has been yet demonstrated if the simulated absorbed dose calculated by pre-therapeutic dosimetry is equivalent to the dose delivered after the therapeutic administration.

PET imaging is probably the best approach to quantify tracer concentration and, if available, a pre-therapeutic theranostic approach with [124I]I PET lesion dosimetry is feasible [25], allowing the assessment of absorbed radiation doses to the tumors and the normal organs.

Previous studies demonstrated that response can be achieved by an effective delivered dose of 85 Gy for lung and lymph nodes [26–29], instead, to achieve response there is a great variation in absorbed dose for bone metastases ranging from 85 to 650 Gy [28].

The evaluation of the response to the first RAI treatment is another crucial point in the history of DTC patients: high-risk patients with complete response after initial therapy presented no differences in recurrence or DTC-related mortality rates compared to low-risk patients, but the DTC recurrence rate increased with an increasing number of RAIT cycles required to achieve complete response ($p = 0.001$) and the DTC-related mortality increased in high-risk patients from four RAIT cycles as demonstrated by Thies et al. [30].

According to different approaches for RAI treatment in metastatic disease, tumor response rates are very heterogenous [21] and variables among the studies; the different studies are not comparable and the superiority of a specific method to the others cannot be defined. In the last years, two retrospective studies compared

the impact on overall survival (OS) and progression-free survival (PFS) of the dosimetric and the empiric approach. In a retrospective analysis conducted on patients with locoregionally advanced DTC or metastatic DTC treated with either dosimetric approach (n = 43) or empiric approach (n = 44), Klubo-Gwiezdzinska et al. [31] demonstrated higher efficacy of Maximum Tolerated Activity based on the dosimetric approach compared to the empiric approach in a patient with locally advanced DTC with a similar safety profile. Patients treated by dosimetric approach tended to be 70% less likely to progress (odds ratio, 0.29; 95% confidence interval, 0.087–1.02; p = 0.052) and more likely to obtain complete response (CR) (odds ratio, 8.2; 95% confidence interval, 1.2–53.5; p = 0.029) with only a trend of association with longer PFS for dosimetry-based approach. On the other hand, there were no statistical differences in response rate and PFS in the subgroup of patients with distant metastases (p = 0.422). In 2017, Deandreis et al. [7] in a retrospective study found no differences in OS in patients with metastatic DTC treated with whole-body/−blood clearance (WB/BC) dosimetric approach compared to empiric approach based on the administration of fixed activities of 3.7 GBq. Patients treated according to the dosimetric approach received a significantly higher median cumulative activity compared to patients treated with the empiric approach (24.2 GBq vs 14.8 GBq, p < 0.0001). No statistical differences in OS, both at 5 and 10 years, were found stratifying patients for age and metastases extension (p = no significance) with the worst prognosis for older patients (>40 years), multiple bones, and lung lesions.

A retrospective study evaluated 1229 low-intermediate and high-risk patients including 135 with distant metastases [30]. The endpoint was to evaluate the impact of the number of radioiodine therapies required to achieve complete remission on the risk of recurrence, disease-specific mortality, and life expectancy. Complete remission was defined based on the stimulated thyroglobulin assay and the negativity of diagnostic [131I]I WBS. In the entire population after a median follow-up of 9 years (0.1–31.8 years), a total of 896 patients achieved remission after a median of only one RAI treatment (range 1–11) and only 10 patients achieved complete remission after 5 or more treatments. The median value of the cumulative activity needed to achieve complete remission in the entire population was 370 MBq, and only 1.3% needed a cumulative activity above 22.2 GBq. Among the 135 patients with distant metastases, only 25 achieved disease complete remission and only 4 after a total of 5 or more treatments and therefore cumulative activity above 22.2 GBq.

Recently, Kaewput et al. [32] retrospectively investigated the outcomes and complications in 176 DTC patients who received RAI treatment with a cumulative dose exceeding or equal to 22.2 GBq (median 33.3 GBq, range 22.2–81.4 GBq): 67% of patients had locoregional metastasis (n = 118), whereas 27% of them (n = 48) had distant metastases at presentation. Remission criteria were no clinical and imaging evidence of disease and low serum thyroglobulin levels during TSH suppression of <0.2 ng/mL or of <1 ng/mL after stimulation in the absence of interfering antibodies. Only 9.1% of patients (n = 16) met remission criteria at the end of treatment, 53.4% presented stable disease (n = 94), 19.3% presented at least 1 metastasis without [131I]I uptake (n = 34), 11.9% manifested progressive disease (n = 21), and 6.3% died during the follow-up (n = 11). In all series, 1.1% of patients (n = 2) developed second primary malignancy, 10.8% (n = 14) were suspected of bone marrow suppression, 3.9% (n = 7) developed permanent salivary gland dysfunction. Although the complications after receiving RAI treatment with a cumulative dose greater than 600 mCi were low and not severe, the patients with disease remission were less than 10%. They concluded by suggesting that the decision to administer further treatments (>22.2 GBq) should be made on an individual basis, because beneficial effects may be controversial with increased toxicity (remission rate < 10%).

9.1.3 The Role of [18F]FDG PET/CT in the Definition of Rai Refractory DTC

[18F]FDG uptake in tumoral lesions is an essential tool, not only from a diagnostic point of view to detect metastatic disease in case of thyroid cancer relapse but also from a prognostic point of view being a criterion taken into account to define and predict RAI refractory thyroid tumor [14, 33, 34].

Dedifferentiation of DTC cancer reduces expression of NIS, losing the ability to concentrate RAI and simultaneously increasing [18F]FDG uptake, likely for an upregulation of glucose transporter-1 (GLUT1) [35]. This phenomenon, called "*flip-flop*," could be observed not only in different patients but also in different tumor sites in the same patient. For this phenomenon, [18F]FDG PET/CT could be an early predictor of reduced RAI therapy response.

[18F]FDG PET/CT scan is at this moment contemplated by American Thyroid Association (ATA) guidelines in the relapse of disease setting in high-risk DTC patients with elevated serum Tg and negative RAI imaging [1] or in the initial staging in poorly differentiated thyroid cancers and invasive Hurthle cell carcinomas, but also in known metastatic disease to evaluate the extension of the disease and to study disease heterogeneity.

In 2012, Leboulleux et al. [33] suggested that [18F]FDG PET/CT should be performed eventually before empiric RAI administration, which should be performed only in patients without significant [18F]FDG uptake. Authors compared the sensitivities of WBS post-RAI and [18F]FDG PET/CT in 47 patients with no evidence of disease and elevated Tg or Tg antibodies (Tg-Ab) levels. Post-therapy WB scan and [18F]FDG PET/CT were discordant in 18 patients: WBS was negative in 17 patients with positive [18F]FDG PET/CT, while [18F]FDG PET/CT was negative in only 1 patient with abnormal WBS, with significantly higher sensitivities for metastatic disease localization (65% vs 18%, 97% vs 22%, and 88% vs 16% for PET and RAI WBS, respectively ($p < 0.01$).

In 2006, Robbins et al. [34] demonstrated that [18F]FDG uptake is an independent negative prognostic factor and that both [18F]FDG SUVmax and the number of lesions are strongly correlated with poor survival ($P < 0.001$). Deandreis et al. [36] confirmed these results in a retrospective study including 80 patients with metastatic thyroid cancer and showed that [18F]FDG uptake was the only significant prognostic factor for survival ($p = 0.02$) and the prognosis was significantly related to both SUVmax and the number of [18F]FDG avid lesion ($p = 0.03$ and 0.009, respectively). Furthermore, patients with both [18F]FDG and RAI avid lesions have a prognosis similar to patients with [18F]FDG-only avid lesions.

[18F]FDG PET/CT could be a good predictor of prognosis, not only for qualitative assessment but also for quantitative analysis/parameters, such as metabolic tumor volume (MTV) and total lesion glycolysis (TLG). A retrospective study in 2018 by Manohar et al. [37] demonstrated in 62 RAI refractory DTC metastatic patients that [18F]FDG PET/CT, with both qualitative and quantitative analyses, could be considered as an imaging biomarker for prognosis of OS and PFS by identifying the imaging phenotype of patients with aggressive disease; in fact, higher than median values of MTV and TLG were associated with worse OS ($P = 0.06$) and PFS ($P = 0.007$).

9.2 Treatment and Management of RAI Refractory Thyroid Cancer

Despite patients with RAI refractory DTC could be asymptomatic for several years and with slowly progressive disease, they present a 10-year survival rate of 10% from the time of detection of metastasis [38] and conventional treatment like chemotherapy and/or external beam radiation therapy presented scarce efficacy associated with poor tolerability. In patients with multiple metas-

tases, Tyrosine Kinase Inhibitors (TKI) systemic treatment are recommended in case of documented tumor progression and high tumor burden [8].

Usually, eligible patients for enrollment in the phase-3 trials have measurable, pathologically confirmed differentiated thyroid cancer, evidence of RAI refractory disease and independently reviewed radiologic evidence of progression within 12–14 months [38].

Multitargeted TKI including Sorafenib and Lenvatinib is actually authorized in RAI refractory DTC treatment [39].

Sorafenib is an oral multikinase inhibitor with anti-proliferative and antiangiogenic effects approved for the treatment of advanced kidney and hepatocellular carcinomas [40, 41]. It targets several molecular signals like rat sarcoma gene (RAS) and BRAF/MEK/ERK signalling pathways, ligand-dependent RET/PTC receptor tyrosine kinase activation, and pathways involving vascular endothelial growth factor (VEGF), platelet-derived growth factor (PDGF) and their receptors that are involved in the pathogenesis of thyroid cancer [42]. In a multicenter, randomized, double-blind, placebo-controlled, phase 3 trial (DECISION trial) Sorafenib showed a significantly longer median PFS compared with placebo (10.8 vs 5.8 months $p < 0{,}0001$). improved PFS was observed irrespective of mutations [40].

Lenvatinib is an oral, multitargeted tyrosine kinase inhibitor of the VEGFRs 1, 2, and 3, FGFRs 1 through 4, PDGFR α, RET, and KIT [38, 41]. A phase 3, randomized, double-blind, placebo-controlled, multicenter trial (SELECT trial) demonstrated a median PFS of 18.3 months in patients treated with Lenvatinib compared to 3.6 months in the placebo arm ($p < 0.001$) with a higher response rate (64.8% vs 1.5%; $p < 0.001$) [38].

Also Vandetanib, a tyrosine kinase inhibitor of RET, VEGFR, and EGFR signalling approved in Canada, Europe, Switzerland, and the USA for the treatment of medullary thyroid cancer in patients with unresectable locally advanced or metastatic disease, was investigated in a randomized, double-blind, phase 2 trial in patients with locally advanced or metastatic differentiated thyroid carcinoma (papillary, follicular, or poorly differentiated) [43]. In this phase 2 trial, patients treated with Vandetanib presented a longer median PFS compared to patients treated with placebo (11.1 vs 5.9 months, one-sided $p = 0.008$, two-sided $p = 0.017$).

Another TKI, Cabozantinib, is under investigation in phase III trials for patients with RAI refractory DTC unresponsive to previous VEGFR therapy [14].

Moreover, several TKIs such as Axitinib, Motesanib, Sunitinib, Pazopanib, Dovitinib, Imatinib, Selumetinib, Dabrafenib, and Vemurafenib [44], have been studied but none of them has been FDA approved yet.

Despite TKIs demonstrating good performance in terms of PFS, they present a high rate of incidence of treatment-related adverse events that sometimes lead to treatment interruption dose reduction, or withdrawal for the great impact on the quality of life. Several adverse events are described for different types of TKI such as hand-foot skin reaction, diarrhea, alopecia, rash or desquamation, fatigue, weight loss, hypertension, QTc prolongation, proteinuria, arterial and venous thromboembolic effects, renal and hepatic failure. Furthermore, TKIs should be continued until evidence of tumoral progression or until the appearance of severe adverse events: once stopped for adverse effects, tumoral cells start to grow rapidly and progression of the disease can become more rapid [42].

If routine morphological imaging and RECIST criteria are used to evaluate the response to TKI, [18F]FDG PET/CT could be proposed as a reliable tool to identify no responders patients to avoid useless treatments or to modulate drugs dosage in case of clinical benefit but in presence of adverse events [45–47]. Regarding the evaluation of response to TKIs in advanced RAI refractory DTC with [18F]FDG PET/CT, some studies are available but with discordant results.

Kloos et al. [48] in 2009, in phase II clinical trial of Sorafenib, investigated as a secondary

endpoint, the metabolic response with [18F]FDG PET/CT in 14 patients, every 8 weeks on therapy when possible (median time points was 3: range 2 to 5). The authors did not find clear correlation between metabolic response, assessed by variation in SUVmax and MTV compared to baseline, and objective tumor response, assessed by RECIST criteria.

Also Leboulleux et al. [43], in the Vandetanib phase II trial investigated the role of [18F]FDG PET-CT at baseline and within 3 weeks after the start of treatment in 79 patients (37 patients in the Vandetanib group and 42 patients in the placebo group) to assess early tumor response evaluating SUVmax variations. Vandetanib group compared to placebo group demonstrated stable disease in 89% ($n = 33$) and 81% of cases ($n = 35$), respectively, whereas progressive disease occurred in 11% ($n = 4$) and 12% of patients ($n = 5$), respectively. Tg levels did not change during Vandetanib treatment, so no correlation could be made between the changes in thyroglobulin concentrations or [18F]FDG uptake and disease control. One limit of [18F]FDG PET/CT evaluation could be the execution time (within 3 weeks) that might be too early to detect any change in [18F]FDG uptake.

In 2013, Marotta et al. [49] evaluated early metabolic response to Sorafenib in 11 RAI refractory DTC patients that underwent [18F]FDG-PET/CT assessment at baseline and after 15 days of treatment. Patients with progressive disease showed an average baseline SUVmax significantly higher compared to patients with clinical benefit (stable disease + partial response) ($p = 0.001$) and, despite SUVmax reduction being evident in all patients, group of responders presented more robust SUVmax variation compared to non-responders' group ($p = 0.002$). Instead, no significant association was found between PFS and SUVmax, neither for the baseline average value ($p = 0.07$) nor for early reduction ($p = 0.01$).

Lin et al. [50] in a prospective study, assessed efficacy and safety of Apatinib in 10 patients with RAI refractory DTC and found, as a secondary endpoint, a significant decrease in SUVmax after both 4 and 8 weeks of treatment ($p = 0.032$ and 0.020, respectively).

More recently, Ahmaddy et al. [51] retrospectively investigated the role of [18F]FDG PET/CT semiquantitative parameters in the assessment of functional tumor response to Lenvatinib in 22 RAI refractory DTC patients that underwent [18F]FDG PET/CT scan before and after 3 and 6 months of treatment. They assessed their prediction of PFS and disease-specific survival (DSS) and demonstrated that responders' patients showed a decline in all semiquantitative PET parameters, and a lack of metabolic response was associated with a worse outcome in terms of PFS and DSS. Furthermore, they concluded that semiquantitative parameters such as standard uptake value (SUV)peak, SUVmax, metabolic tumor volume (MTV), and total lesion glycolysis (TLG) both at 3 and 6 months were significantly higher in patients with disease progression and could serve as additional markers for monitoring early tumor response and outcome.

Despite promising results of [18F]FDG PET/CT in the evaluation of early response to TKIs treatment of RAI refractory DTC, studies available are heterogeneous. For these reasons, a standardization of [18F]FDG PET/CT acquisition and evaluation is necessary, with the design of clinical trials act to confirm the promising role of [18F]FDG PET/CT in the evaluation of response to TKIs (Figs. 9.2 and 9.3).

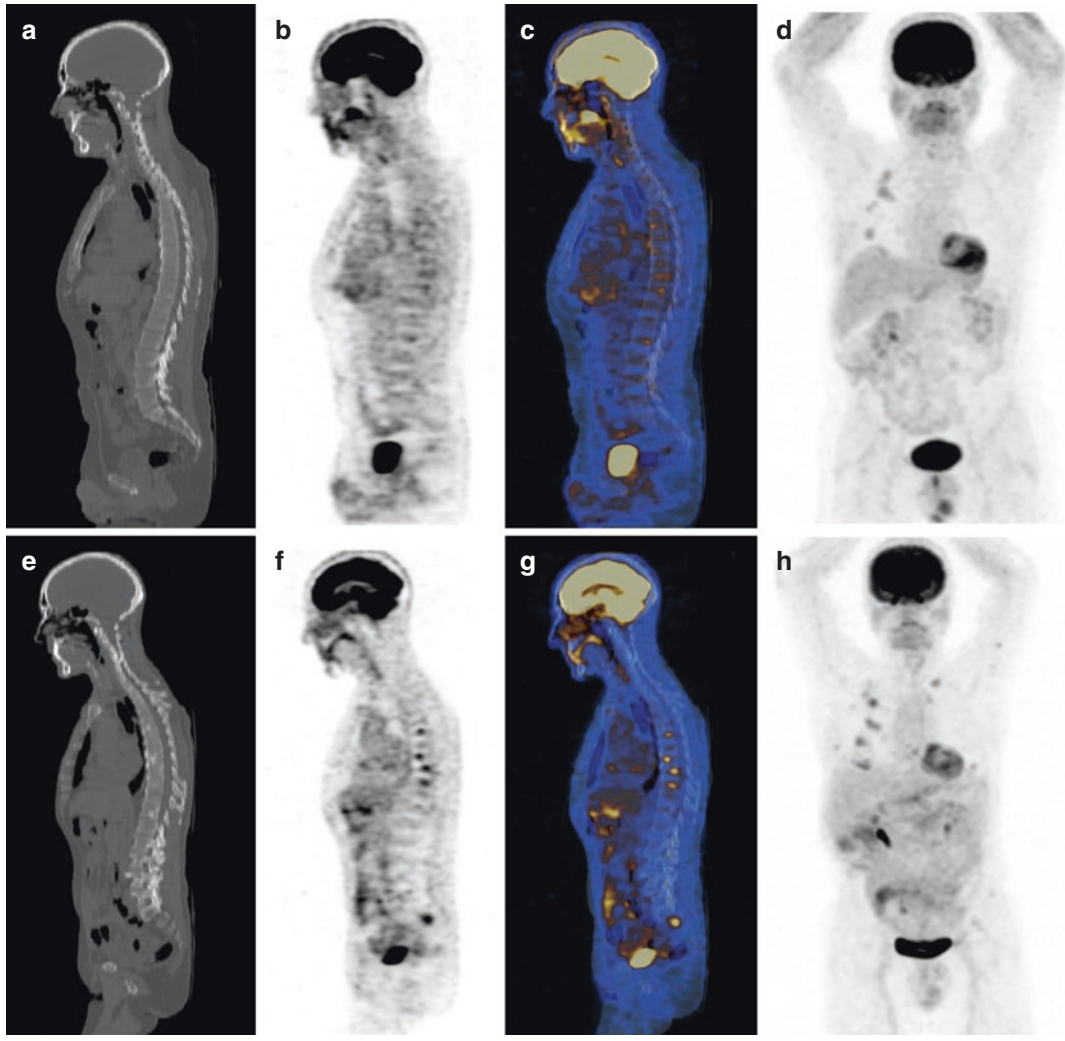

Fig. 9.2 Serial [18F]FDG PET/CT scans of a 62-year-old male patient with radioiodine-negative metastasized poorly differentiated thyroid carcinoma before (**a**–**d**) as well as at 24 months (**e**–**h**) after the start of TKI therapy (lenvatinib, 10 mg daily). Previously, the patients underwent thyroidectomy (pT3N1M1), radioiodine ablation (3.7 GBq), and PRRT (17.0 MBq of 177Lu-DOTATATE and 4.8 MBq of 90Y-DOTATATE). The follow-up PET/CT scan (**e**–**h**) demonstrates an increased tracer uptake in the known right pleuro-parietal thickening (**d** and **h**) and the appearance of several new FDG avid sclerotic bone lesion (**e**–**g**) in the dorsal and lumbar vertebrae. Moreover, the patient presented a progressive increase in serum Tg levels (from 3899 ng/mL at baseline PET/CT to 43600 ng/mL at follow-up PET/CT). The PET/CT findings associated with Tg increasing suggest disease progression

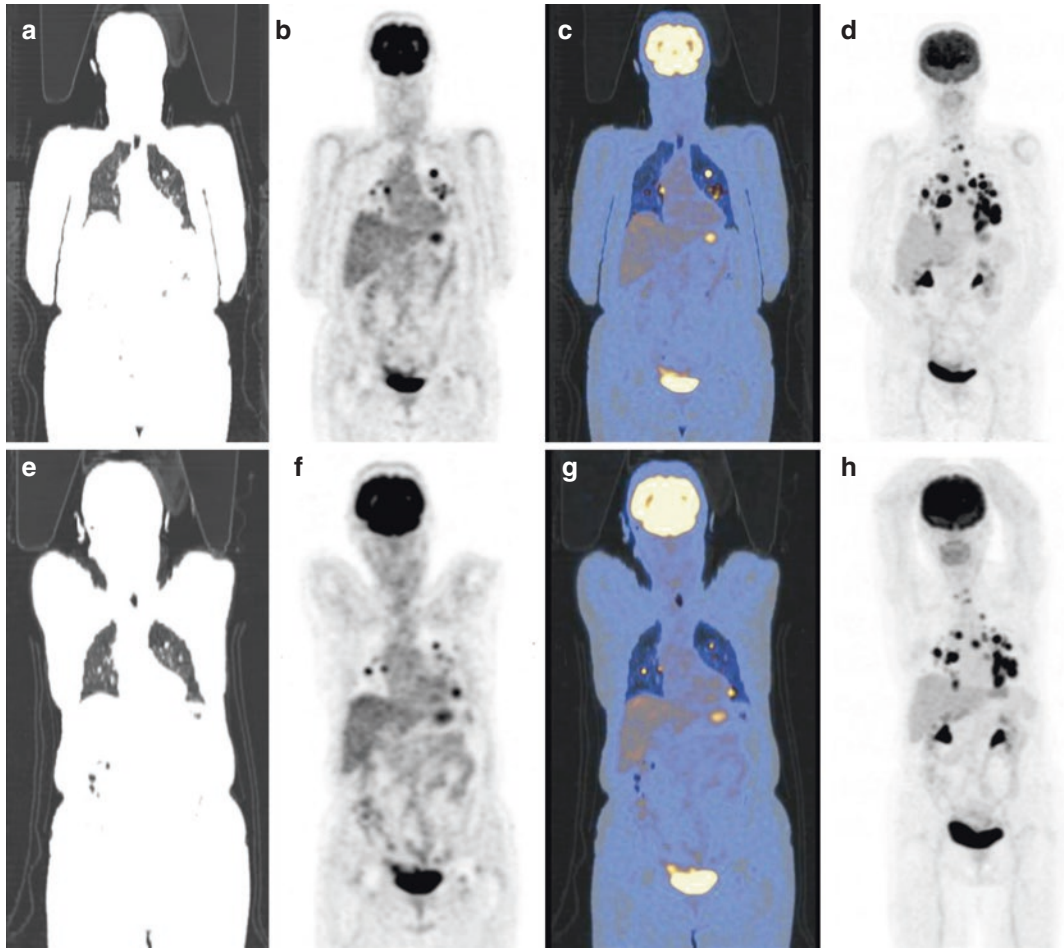

Fig. 9.3 Serial [18F]FDG PET/CT scans of an 82-year-old female patient with radioiodine-negative metastasized papillary thyroid carcinoma before (**a**–**d**) as well as at 12 months (**e**–**h**) after the start of TKI therapy (lenvatinib, 10 mg daily). Previously, the patients underwent thyroidectomy and three consecutive radioiodine ablations (11.8 GBq). The follow-up PET/CT scan (**e**–**h**) demonstrates a partially decreased tracer uptake in the lung and mediastinal lymph nodes metastases. Moreover, the patient presented stable non-measurable Tg levels, but with stable high levels of Tg-Ab (> 4000 UI/mL). The PET/CT findings suggest a partial metabolic response to the TKI therapy

9.3 Redifferentiation Strategies

In case of refractory thyroid cancer, a further step is the possibility to pharmacologically manipulate target(s) expression and to **reinduce the expression of differentiation genes with the final aim of improving the efficacy of radioactive iodine treatment.**

Several agents, including retinoic acid (RA), peroxisome proliferator-activated receptor-gamma (PPARγ) agonists, and histone deacetylase (HDAC) inhibitors have been proposed in the last years as redifferentiation drugs in RAI refractory DTC patients, but with limited clinical impact [16].

More recently, some studies suggested that a pretreatment with TKI in RAI refractory DTC thyroid cancer can restore iodine trapping in these tumors ("re-differentiation" agents), restoring RAI both avidity and efficacy [52, 53].

In vitro studies have demonstrated that the activation of MAPK intracellular pathway

involved in tumor proliferation and neoangiogenesis reduces the expression and activity of NIS with subsequent reduction of RAI avidity in DTC lesions. The activation of the MAPK pathway through MEK and ERK activation has been found in mutated tumors harboring BRAF, NRAS, or RET/PTC mutations. According to preclinical data in mice, blockage of hyperactivated pathways could lead to a re-expression of NIS on the cell membrane [54, 55].

The *first-in-human* trial published in 2013 demonstrated the potential of target therapy to reinduce a significant RAI uptake through the inhibition of MAPK cascade in patients treated by Selumetinib (MEK inhibitor) 4 weeks before RAI treatment [56] in 20 patients with RAI refractory DTC. RAI uptake evaluated by 124I PET/CT was restored in 12/20 patients and when calculated activities required to achieve a presumed absorbed dose >2000 cGy in the metastatic lesions were ≤ 11.1 GBq, patients were treated with a personalized 131I activity after recombinant human rhTSH administration Finally, 8/12 patients were treated with 5 partial responses and 3 stable diseases at 6 months follow-up. Nevertheless, RAI uptake reinduction was observed in only 4/9 patients harboring BRAF mutation and only 1 patient among them was treated with RAI and achieved an objective response: On the other hand, 5/5 patients with NRAS mutation showed reinduction of RAI uptake and all were treated with 131I with an objective response. The remaining 2 treated patients had a wild type and RET/PTC mutated thyroid carcinoma respectively. The low efficacy of redifferentiation strategy by selumetinib in BRAF mutated tumors was mainly related to a sub-optimal inhibition of the MAPK pathway. Consequently, specific BRAF inhibitors (i.e., dabrafenib, vemurafenib, or trametinib) may induce a sustained MAPK pathway inhibition and have been tested, as single agents or in combination, in redifferentiation clinical trials in BRAF mutated tumors.

In 2015, Rothenberg et al. [57] tested 4 weeks of treatment with Dabrafenib (BRAF inhibitor) in 10 patients harboring BRAFV600 mutation and without RAI uptake at WBS whole-body scan within 14 months before the inclusion in the trial. Six among 10 patients showed new [131I]I RAI uptake foci and were consequently treated with a fixed activity of 5.5 GBq achieving 2 partial responses and 4 stable diseases at 3 months radiological restaging evaluation.

In 2019, Dunn et al. [58] investigated 4 weeks of treatment with Vemurafenib, (BRAF inhibitor), in 10 patients with BRAFV600 mutation. Six patients presented uptake reinduction at [124I]I PET/CT, but only four met the lesional dosimetry threshold and were treated with [131I]I. All 4 patients did not present disease progression at 6 months follow-up, 2 of them achieving a partial response and 2 stable diseases, respectively. Many other clinical trials are ongoing (EudraCT No 2015-002269-47, NCT03244956 NCT04554680, NCT04619316) and many other targets are under investigation. In particular, the hypothesis is that higher efficacy in terms of objective response could be achieved using the combination of different drugs targeting MEK and BRAF to induce a more robust MAPK pathway inhibition [59]. Recently, for example, Tchekmedyian et al. from Memorial Sloan Kettering Cancer Center hypothesized that combined inhibition of BRAF and HER3 using vemurafenib and the human monoclonal antibody CDX-3379, respectively, could potently inhibit MAPK activation and restore radioactive iodine (RAI) avidity in patients with BRAF-mutant RAIR thyroid cancer. Seven patients were included, 5/7 patients had increased RAI uptake after treatment and in 4/7 patients this increased uptake warranted therapeutic 131I with 2 partial responses after 131I and 2 progression of disease at 6 months after RAI treatment [60].

Despite very promising perspectives, there are still several open questions to define the best approach, in particular, the most appropriate therapy sequence and drug combination, the role of a direct effect of short-term target therapy alone on tumor response, molecular pretreatment schedule, 131I activity to be administered and the duration of response.

9.4 Conclusions

RAI refractory DTC is a changeling clinical situation. Despite patients could be asymptomatic for several years, their survival rate rapidly decreases from the time of detection of metastasis and other treatment modality must be applied. The definition of RAIR tumor could be based on several factors, including clinical biological and molecular with an impact on RAI uptake and response to treatment. Standardized and reliable criteria for the choice of stopping RAI in these patients is still a challenge. TKIs are mostly preferred in the treatment planning of these patients for their impact on PFS, but they present a high rate of incidence of treatment-related adverse events that severely impact the quality of life and sometimes lead to treatment interruptions, reductions, or withdrawals that could invalidate treatment efficacy.

[18F]FDG PET/CT could be a useful tool in several steps of RAI refractory DTC patients management: firstly, as baseline evaluation to define the RAI refractoriness conditions and as a prognostic factor of OS and PFS and, during TKIs administration, could serve to assess response to treatment. To confirm the multi-level role of [18F]FDG PET/CT in RAI refractory DTC patients management, more homogeneous data are required to confirm these promising observations with the necessity of prospective, multicentre clinical trials. In the future, the association between RAI and TKI treatment according to the first experience on redifferentiation strategies is very promising for the best management of these patients.

References

1. Haugen BR, Alexander EK, Bible KC, Doherty GM, Mandel SJ, Nikiforov YE, et al. 2015 American Thyroid Association management guidelines for adult patients with thyroid nodules and differentiated thyroid cancer: the American Thyroid Association guidelines task force on thyroid nodules and differentiated thyroid cancer. Thyroid. 2016;26(1):1–133.
2. Tuttle M, Morris L, Haugen B, Shah J, Sosa J, Rohren E, et al. Thyroid differentiated and anaplastic carcinoma (Chapter 73). In: Amin M, Edge S, Greene F, Byrd DX, Brookland R, Washington M, et al., editors. AJCC cancer staging manual. 8th ed. New York, NY: Springer Publishing; 2017.
3. National Cancer Institute: Surveillance, Epidemiology and ERP. Cancer stat facts: thyroid cancer. [cited 2020 Dec 16]. https://seer.cancer.gov/statfacts/html/thyro.html.
4. Aashiq M, Silverman DA, Na'ara S, Takahashi H, Amit M. Radioiodine-refractory thyroid cancer: molecular basis of redifferentiation therapies, management, and novel therapies. Cancers (Basel). 2019;11(9):1–15.
5. Pacini F. Which patient with thyroid cancer deserves systemic therapy and when? Best Pract Res Clin Endocrinol Metab. 2017;31(3):291–4.
6. Schlumberger M, Brose M, Elisei R, Leboulleux S, Luster M, Pitoia F, et al. Definition and management of radioactive iodine-refractory differentiated thyroid cancer. Lancet Diabetes Endocrinol. 2014;2(5):356–8.
7. Deandreis D, Rubino C, Tala H, Leboulleux S, Terroir M, Baudin E, et al. Comparison of empiric versus whole-body/-blood clearance dosimetry–based approach to radioactive iodine treatment in patients with metastases from differentiated thyroid cancer. J Nucl Med. 2017;58(5):717–22.
8. Durante C, Haddy N, Baudin E, Leboulleux S, Hartl D, Travagli JP, et al. Long-term outcome of 444 patients with distant metastases from papillary and follicular thyroid carcinoma: benefits and limits of radioiodine therapy. J Clin Endocrinol Metab. 2006;91(8):2892–9.
9. Pittas AG, Adler M, Fazzari M, Tickoo S, Rosai J, Larson SM, et al. Bone metastases from thyroid carcinoma: clinical characteristics and prognostic variables in one hundred forty-six patients. Thyroid. 2000;10(3):261–8.
10. Kushchayeva YS, Kushchayev SV, Carroll NM, Felger EA, Links TP, Teytelboym OM, et al. Spinal metastases due to thyroid carcinoma: an analysis of 202 patients. Thyroid. 2014;24(10):1488–500.
11. Schlumberger M, Challeton C, De Vathaire F, Travagli JP, Gardet P, Lumbroso JD, et al. Radioactive iodine treatment and external radiotherapy for lung and bone metastases from thyroid carcinoma. J Nucl Med. 1996;37(4–6):598–605.
12. Iñiguez-Ariza NM, Bible KC, Clarke BL. Bone metastases in thyroid cancer. J Bone Oncol. 2020;21:100282. https://doi.org/10.1016/j.jbo.2020.100282.
13. Al-Jundi M, Thakur S, Gubbi S, Klubo-Gwiezdzinska J. Novel targeted therapies for metastatic thyroid cancer—a comprehensive review. Cancers (Basel). 2020;12(8):1–37.
14. Aashiq M, Silverman DA, Na'ara S, Takahashi H, Amit M. Radioiodine-refractory thyroid cancer: molecular basis of Redifferentiation therapies, management, and novel therapies. Cancers (Basel). 2019;22:2382.
15. Paladino S, Melillo RM. Novel mechanism of radioactive iodine refractivity. Thyroid cancer. J Natl Cancer Inst. 2017:109.

16. Liu J, Liu Y, Lin Y, Liang J. Radioactive iodine-refractory differentiated thyroid cancer and redifferentiation therapy. Endocrinol Metab (Seoul). 2019;34:215–25.
17. Zhang Z, Liu D, Murugan AK, Liu Z, Xing M. Histone deacetylation of NIS promoter underlies BRAFV600E-promoted NIS silencing in thyroid cancer. Endocr Relat Cancer. 2014;21:161–73.
18. Costamagna E, Garcia B, Santisteban P. The functional interaction between the paired domain transcription factor Pax8 and Smad3 is involved in transforming growth factor-beta repression of the sodium/iodide symporter gene. J Biol Chem. 2004;279:3439–46.
19. Kogai T, Sajid-Crockett S, Newmarch LS, Liu YY, Brent GA. Phosphoinositide-3-kinase inhibition induces sodium/iodide symporter expression in rat thyroid cells and human papillary thyroid cancer cells. J Endocrinol. 2008;199:243–52.
20. European Commission. Council Directive 2013/59/Euratom of 5 December 2013. Off J Eur Union 2014;(December 2003):1–73.
21. Finessi M, Liberini V, Deandreis D. Dosimetrically determined activities in advanced differentiated thyroid carcinoma – controversies. Q J Nucl Med Mol Imaging. 2019;63(3):258–66.
22. Samuel A, Rajashekharrao B, Shah D. Pulmonary metastases in children and adolescents with well-differentiated thyroid cancer. J Nucl Med. 1998;8(39):1531–6.
23. Benua R, Cicale N, Sonenberg M, Rawson R. The relation of radioiodine dosimetry to results and complications in the treatment of metastatic thyroid cancer. Am J Roentgenol Radium Therapy, Nucl Med. 1962;87:171–82.
24. Benua R, Leeper R. A method and rationale for treatment of thyroid carcinoma with the largest, safe dose of 131-I. In: Medeiros-Neto G, Gaitan E, editors. Frontiers in thyroidology. New York: Plenum Medical; 1986. 1317p.
25. Nagarajah J, Janssen M, Hetkamp P, Jentzen W. Iodine symporter targeting with 124 I/ 131 I theranostics. J Nucl Med. 2017;58(Supplement 2):34S–8S.
26. Maxon H, Thomas S, Hertzberg V, Kereiakes J, Chen I, Sperling M, et al. Relation between effective radiation dose and outcome of radioiodine therapy for thyroid cancer. N Engl J Med. 1983;309(16):937–41.
27. Maxon HI, Englaro E, Thomas S, et al. Radioiodine-131 therapy for well differentiated thyroid cancer: a quantitative radiation dosimetric approach-outcome and validation in 85 patients. J Nucl Med. 1992;33:1132–6.
28. Jentzen W, Verschure F, van Zon A, van de Kolk R, Wierts R, Schmitz J, et al. 124I PET assessment of response of bone metastases to initial radioiodine treatment of differentiated thyroid cancer. J Nucl Med. 2016;57(10):1499–504.
29. Jentzen W, Hoppenbrouwers J, van Leeuwen P, van der Velden D, van de Kolk R, Poeppel TD, et al. Assessment of lesion response in the initial radioiodine treatment of differentiated thyroid cancer using 124I PET imaging. J Nucl Med. 2014;55(11):1759–65.
30. Thies E, Tanase K, Maeder U, Luster M, Buck AK, Hänscheid H, et al. The number of 131 I therapy courses needed to achieve complete remission is an indicator of prognosis in patients with differentiated thyroid carcinoma. Eur J Nucl Med Mol Imaging. 2014;41:2281–90.
31. Klubo-Gwiezdzinska J, Van Nostrand D, Atkins F, Burman K, Jonklaas J, Mete M, et al. Efficacy of dosimetric versus empiric prescribed activity of 131I for therapy of differentiated thyroid cancer. J Clin Endocrinol Metab. 2011;96(10):3217–25.
32. Kaewput C, Pusuwan P. Outcomes following I-131 treatment with cumulative dose exceeding or equal to 600 mCi in differentiated thyroid carcinoma patients. World J Nucl Med. 2020;20(1):54–6.
33. Leboulleux S, El Bez I, Borget I, Elleuch M, Déandreis D, Al Ghuzlan A, et al. Postradioiodine treatment whole-body scan in the era of 18-fluorodeoxyglucose positron emission tomography for differentiated thyroid carcinoma with elevated serum thyroglobulin levels. Thyroid. 2012;22(8):832–8.
34. Robbins RJ, Wan Q, Grewal RK, Reibke R, Gonen M, Strauss HW, et al. Real-time prognosis for metastatic thyroid carcinoma based on 2-[18F]fluoro-2-deoxy-D-glucose-positron emission tomography scanning. J Clin Endocrinol Metab. 2006;91(2):498–505.
35. Grabellus F, Nagarajah J, Bockisch A, Schmid KW, Sheu SY. Glucose transporter 1 expression, tumor proliferation, and iodine/glucose uptake in thyroid cancer with emphasis on poorly differentiated thyroid carcinoma. Clin Nucl Med. 2012;37(2):121–7.
36. Deandreis D, Al Ghuzlan A, Leboulleux S, Lacroix L, Garsi JP, Talbot M, Lumbroso J, Baudin E, Caillou B, Bidart JMSM. Do histological, immunohistochemical, and metabolic (radioiodine and fluorodeoxyglucose uptakes) patterns of metastatic thyroid cancer correlate with patient outcome? Endocr Relat Cancer. 2011;18(1):159–69.
37. Manohar PM, Beesley LJ, Bellile EL, Worden FP, Avram AM. Prognostic value of FDG-PET/CT metabolic parameters in metastatic radioiodine-refractory differentiated thyroid cancer. Clin Nucl Med. 2018;43(9):641–7.
38. Schlumberger M, Tahara M, Wirth LJ, Robinson B, Brose MS, Elisei R, et al. Lenvatinib versus placebo in radioiodine-refractory thyroid cancer. N Engl J Med. 2015;372(7):621–30.
39. Bible KC, Ryder M. Evolving molecularly targeted therapies for advanced-stage thyroid cancers. Nat Rev Clin Oncol. 2016;13(7):403–16.
40. Brose MS, Nutting CM, Jarzab B, Elisei R, Siena S, Bastholt L, et al. Sorafenib in radioactive iodine-refractory, locally advanced or metastatic diff erentiated thyroid cancer: a randomised, double-blind, phase 3 trial. Lancet. 2014;384(9940):319–28.
41. Felicetti F, Nervo A, Piovesan A, Berardelli R, Marchisio F, Gallo M, et al. Tyrosine kinase inhibitors rechallenge in solid tumors: a review of literature and

a case description with lenvatinib in thyroid cancer. Expert Rev Anticancer Ther. 2017;17:1093.
42. Valerio L, Pieruzzi L, Giani C, Agate L, Bottici V, Lorusso L, et al. Targeted therapy in thyroid cancer: state of the art. Clin Oncol. 2017;29(5):316–24.
43. Leboulleux S, Bastholt L, Krause T, de la Fouchardiere C, Tennvall J, Awada A, et al. Vandetanib in locally advanced or metastatic differentiated thyroid cancer: a randomised, double-blind, phase 2 trial. Lancet Oncol. 2012;13(9):897–905.
44. Naoum GE, Morkos M, Kim B, Arafat W. Novel targeted therapies and immunotherapy for advanced thyroid cancers. Mol Cancer. 2018;17:51.
45. Abgral R, Leboulleux S, Deandreis D, et al. Performance of (18)fluorodeoxyglucose-positron emission tomography and somatostatin receptor scintigraphy for high Ki67 (≥10%) well-differentiated endocrine carcinoma staging. J Clin Endocrinol Metab. 2011;96(3):665–71.
46. Salvatori M, Biondi B, Rufini V. Imaging in endocrinology: 2-[18F]-fluoro-2-deoxy-d-glucose positron emission tomography/computed tomography in differentiated thyroid carcinoma: clinical indications and controversies in diagnosis and follow-up. Eur J Endocrinol. 2015;173(3):R115–30. http://www.eje--online.org/content/173/3/R115.abstract
47. Boellaard R, Delgado-Bolton R, Oyen WJG, Giammarile F, Tatsch K, Eschner W, et al. FDG PET/CT: EANM procedure guidelines for tumour imaging: version 2.0. Eur J Nucl Med Mol Imaging. 2014;42(2):328–54.
48. Kloos RT, Ringel MD, Knopp MV, Hall NC, King M, Stevens R, et al. Phase II trial of sorafenib in metastatic thyroid cancer. J Clin Oncol. 2009;27(10):1675–84.
49. Marotta V, Ramundo V, Camera L, Del PM, Fonti R, Esposito R, et al. Sorafenib in advanced iodine-refractory differentiated thyroid cancer: efficacy, safety and exploratory analysis of role of serum thyroglobulin and FDG-PET. Clin Endocrinol. 2013;78(5):760–7.
50. Lin Y, Wang C, Gao W, Cui R, Liang J. Overwhelming rapid metabolic and structural response to apatinib in radioiodine refractory differentiated thyroid cancer. Oncotarget. 2017;8:42252.
51. Ahmaddy F, Burgard C, Beyer L, Koehler VF, Bartenstein P, Fabritius MP, et al. 18F-FDG-PET/CT in patients with advanced, radioiodine refractory thyroid cancer treated with Lenvatinib. Cancers (Basel). 2021;13(2):317.
52. Gild M, Topliss D, Learoyd D, Parnis F, Tie J, Hughes B, et al. Clinical guidance for radioiodine refractory differentiated thyroid cancer. Clin Endocrinol. 2018;88(4):529–37.
53. Leboulleux S, Dupuy C, Lacroix L, Attard M, Grimaldi S, Corre R, et al. Redifferentiation of a BRAFK601E-mutated poorly differentiated thyroid cancer patient with dabrafenib and trametinib treatment. Thyroid. 2019;29(5):735–42.
54. Nagarajah J, Le M, Knauf J, Al E. Sustained ERK inhibition maximizes responses of BrafV600E thyroid cancers to radioiodine. J Clin Invest. 2016;126(11):4119–24.
55. Chakravarty D, Santos E, Ryder M, et al. Small-molecule MAPK inhibitors restore radioiodine incorporation in mouse thyroid cancers with conditional BRAF activation. J Clin Invest. 2011;121(12):4700–11.
56. Ho AL, Grewal RK, Leboeuf R, Sherman EJ, Pfister DG, Deandreis D, Pentlow KS, Zanzonico PB, Haque S, Gavane S, Ghossein RA, Ricarte-Filho JC, Domínguez JM, Shen R, Tuttle RM, Larson SMFJ. Selumetinib-enhanced radioiodine uptake in advanced thyroid cancer. N Engl J Med. 2013;368(7):623–32.
57. Rothenberg SM, McFadden DG, Palmer EL, Daniels GH, Wirth LJ. Redifferentiation of iodine-refractory BRAF V600E-mutant metastatic papillary thyroid cancer with dabrafenib. Clin Cancer Res. 2015;21(5):1028–35.
58. Dunn LA, Sherman EJ, Baxi SS, et al. Vemurafenib redifferentiation of BRAF mutant, RAI-refractory thyroid cancers. J Clin Endocrinol Metab. 2019;104:1417–28.
59. Buffet C, Wassermann J, Hecht F, et al. Redifferentiation of radioiodine-refractory thyroid cancers. Endocr Relat Cancer. 2020;27(5):R113–32.
60. Tchekmedyian V, Dunn L, Sherman E, Baxi SS, Grewal RK, Larson S, et al. Enhancing radioiodine incorporation in BRAF-mutant, radioiodine-refractory thyroid cancers with vemurafenib and the anti-ErbB3 monoclonal antibody CDX-3379: results of a pilot clinical trial. Thyroid. 2022;32(3):273–82.

10 Integrated Diagnostics and Theragnostics of Medullary Thyroid Carcinoma and Related Syndromes

Christelle Fargette, Alessio Imperiale, Luca Giovanella, and David Taïeb

10.1 Medullary Thyroid Carcinoma and Related Syndromes

10.1.1 Medullary Thyroid Carcinoma

Medullary thyroid carcinoma (MTC) is a rare neoplasm derived from calcitonin-secreting cells of the thyroid (C cells). MTC accounts for 3–10% of all thyroid carcinomas, which has remained stable over the last 20 years. It also represents 0.4–1.3% of all thyroid nodules [1]. MTC can occur sporadically (about 70%) or as part of multiple endocrine neoplasia type 2 (MEN2) syndromes. MEN2 is an autosomal dominant disease caused by germline activating point mutations in the *RET* proto-oncogene.

MTC typically arises from the posterior upper-thirds of the thyroid lobes, characterized by the largest concentration of C cells and high propensity for regional lymph node metastases. MEN2-related MTC is characterized by bilateral C-cell hyperplasia (CCH) and is considered a pre-neoplastic lesion. Multifocality also occurs in sporadic cases (predominantly in large tumors) in the absence of CCH via intrathyroidal diffusion (5.6% of multifocal sporadic MTC) [2].

When serum calcitonin is routinely assayed as a screening test in patients with thyroid disorders, MTC can be suspected in the presence of hypercalcitoninemia. However, increased calcitonin levels can also be seen in patients with chronic renal failure, CCH due to thyroiditis, or from medications such as acid-lowering drugs. In such cases, additional procalcitonin measurement recently proved to significantly increase diagnostic accuracy [3]. Usually, the diagnosis of primary MTC is very likely for calcitonin levels >100 pg/mL (and unlikely for calcitonin levels <20 pg/mL) [4]. Calcitonin levels correlate with tumor mass and differentiation. A dedifferentiated MTC, however, can secrete carcinoembryonic antigen (CEA), which can be used as a marker for follow-up. Patients with MTC can present with a thyroid mass, with less frequent local symptoms (neck fullness/pain, dysphagia,

C. Fargette · D. Taïeb (✉)
Department of Nuclear Medicine, La Timone University Hospital, CERIMED, Aix-Marseille University, Marseille, France
e-mail: david.taieb@ap-hm.fr

A. Imperiale
Department of Nuclear Medicine and Molecular Imaging, Institut de Cancérologie Strasbourg Europe (ICANS), IPHC, UMR 7178, CNRS/University of Strasbourg, Strasbourg, France
e-mail: a.imperiale@icans.eu

L. Giovanella
Clinic of Nuclear Medicine and Molecular Imaging, Imaging Institute Southern Switzerland, Ente Ospedaliero Cantonale, Bellinzona, Switzerland

Clinic of Nuclear Medicine, University Hospital of Zurich, Zurich, Switzerland
e-mail: Luca.Giovanella@eoc.ch

L. Giovanella (ed.), *Integrated Diagnostics and Theranostics of Thyroid Diseases*,
https://doi.org/10.1007/978-3-031-35213-3_10

dyspnea, or hoarseness), or with exceptional systemic symptoms (bone pain, flushing, weight loss, and/or diarrhea) due to the presence of distant metastases secreting high levels of calcitonin. The diagnosis of MTC can be confirmed by a fine-needle aspiration (FNA) biopsy of the thyroid lesions and immunohistochemistry (positive for calcitonin) and/or calcitonin measurement on fine-needle washouts.

10.1.2 Multiple Endocrine Neoplasia Type 2

Multiple Endocrine Neoplasia Type 2 (MEN2) is a rare autosomal dominant syndrome caused by mutations in the RET proto-oncogene. MEN2 is divided into two groups, depending on their clinical features: MEN2A (95% of MEN2, including the former subgroup of familial MTC) and MEN2B (5%) [5, 6]. Some MEN2A mutations can lead to an earlier and possibly more aggressive disease compared to others (for example, the *RET* 634 mutation) [5], as outlined in the American Thyroid Association (ATA) classification of risk of *RET* variants. A recent study reported that overall survival was no difference between patients with high and moderate ATA risk levels based on age at thyroidectomy, suggesting that the *RET* codon might not influence the natural history of the disease, but only the onset of the disease [7]. Data from a large consortium on MEN2B suggests that this might not be true for the *RET* M918T codon mutation, as the overall survival was drastically worse when compared to other mutations. As detailed later, this might explain why the M918T variant could theoretically be able to induce aggressive MTC in comparison to other *RET* variants (on a somatic level).

MEN2 patients are younger at diagnosis of MTC compared to sporadic cases and can present with pathognomonic findings such as a family history of MTC, presence of nostalgia paresthetica (hyperpigmented macular pruritic skin that can occur in cases of MEN2A with *RE*T 634 codon mutation), pheochromocytoma (in 10–50% of cases depending on RET mutation and age at last follow-up), and primary hyperparathyroidism (in roughly 10–20% of cases of MEN2A only). Among less common clinical signs, MEN2B is also associated with mucosal neuromas, marfanoid habitus, and a more aggressive form of MTC with disease onset during their first year of life [6, 8, 9]. Of note, MEN2 can be found in individuals without a family history, known as de novo mutations (e.g., 15% of MEN2A and >80% of MEN2B). A definitive diagnosis of MEN2 is made by *RET* sequencing (positive in more than 98% of cases). Somatic RET mutations are identified in 23–60% of MTC, independent of MEN2. The M918T *RET* mutation is the most frequent in tumors larger than 3 cm and predicts a more aggressive phenotype of the tumor [10]. Genetic testing is recommended for all recently detected cases of MTC and for all first-degree relatives of a patient with a *RET* mutation [5].

MEN2-related PHEOs occur most often during young adult to mid-adult life. They are almost always confined to the adrenal medullas and unlikely to be metastatic. MEN2-related PHEOs are characterized by increased plasma concentrations of metanephrine (indicating that they consistently produce epinephrine, with or without norepinephrine) [11]. In PHEOs that exclusively produce norepinephrine, MEN2 can be excluded [12]. The presence of bilateral PHEO is highly suggestive of hereditary PHEO but is not restricted to the MEN2 phenotype (e.g., *MAX*). In all cases of PHEO, assessment of serum calcitonin, calcium, and PTH is recommended as PHEO could be the first clinical manifestation of MEN2. Elevated levels of serum calcitonin (usually greater than 100 pg/ml) enable diagnosis of MTC and therefore MEN2-related PHEO.

pHPT is rarely the first manifestation. Diagnosis is established by detecting mild hypercalcemia with either mild elevations in PTH or (inappropriately) normal PTH levels. Assessment of serum calcitonin should be recommended in patients younger than 40 years of age. Nowadays, pHPT is diagnosed at an early stage and is often due to a single parathyroid adenoma. pHPT in MEN2 is usually associated with RET mutations in codon 634.

A definitive diagnosis of MEN2 is made by RET sequencing (positive in 98% of cases). Genetic testing should be recommended in patients with phenotypic abnormalities and in all cases of MTC.

10.2 Role of Imaging According to Different Clinical Situations

Successful management of MTC and MEN2 heavily relies on the patient's age, the tumor stage at initial diagnosis, and the medical team's experience. The role of imaging is to guide the clinician's approach toward thyroid surgery, reveal the extent of the lymph node dissection, and determine the management plan for metastatic disease. There are several points that must be considered.

10.2.1 Prophylactic Thyroidectomy for MTC Does Not Require any Preoperative Imaging

In MEN2A cases diagnosed by genetic screening, prophylactic total thyroidectomy can cure almost 100% of patients [5, 13, 14]. The optimal timing of prophylactic thyroidectomy is based on the type of *RET* mutations: moderate, high, or highest risk of MTC aggressiveness [5]. No imaging study is mandatory prior to prophylactic thyroidectomy since the thyroid gland is pathologically normal or limited to C-cell hyperplasia in patients who do not have an elevated serum calcitonin. However, it is suggested to have a preoperative neck ultrasound (US) and calcitonin assessment prior to prophylactic thyroidectomy, and plasma metanephrines should be measured to rule out pheochromocytoma (PHEO). In MEN2B, prophylactic thyroidectomy is rarely observed as most patients have de novo *RET* mutations. MEN2B familial cases are infrequent, however, MEN2B patients may have children who test positive for *RET* germline mutation and these children should have a prophylactic total thyroidectomy before the age of 1 [5].

10.2.2 Indications of Imaging for Persistent/Recurrent MTC

Although total thyroidectomy with systematic nodal dissection is routinely performed, approximately 20% of patients will present with persistent/recurrent disease (frequently patients who had nodal metastases at initial diagnosis). Here, postoperative serum calcitonin measurement plays a central role in detecting persistent or recurrent disease. Although these patients undergo an adequate initial surgery, the ability to cure is rare due to lymph node involvement.

In patients with structural disease in the neck, reoperation should be carefully discussed. The extent of reoperative surgery depends on the initial surgery and ranges from a systematic compartment-oriented to a modified functional radical neck dissection. An exhaustive imaging work-up and serum calcitonin levels should be performed prior to reoperative surgery.

In persistent MTC, imaging is usually delayed until serum calcitonin rises to approximately 100–200 pg/mL.

^{18}F-FDOPA PET/CT is currently the best molecular (functional) imaging modality for evaluating patients with persistent/recurrent MTC [15].

Hoegerle et al. were the first to demonstrate the utility of ^{18}F-FDOPA PET to localize persistent MTC [16]. This was confirmed by several studies with a wide range of sensitivity, ranging from 47% to 83% [17–20]. Differences in technical aspects and inclusion criteria could explain the heterogeneity in the sensitivity values reported, as well as the gold standard used to define positive lesions. In MTC, tracer uptake is often moderate and retention can be reduced (Fig. 10.1) [21]. Therefore, it may be recommended to increase duration of PET acquisition (5–10 min per bed position on the neck) and to begin acquisition 15–20 min post-injection. Although these practical considerations are essential for PET sensitivity, most studies have reported similar findings with standard imaging protocols [22].

In 2009, the ATA MTC guidelines recommended performing an ^{18}F-FDOPA PET/CT in

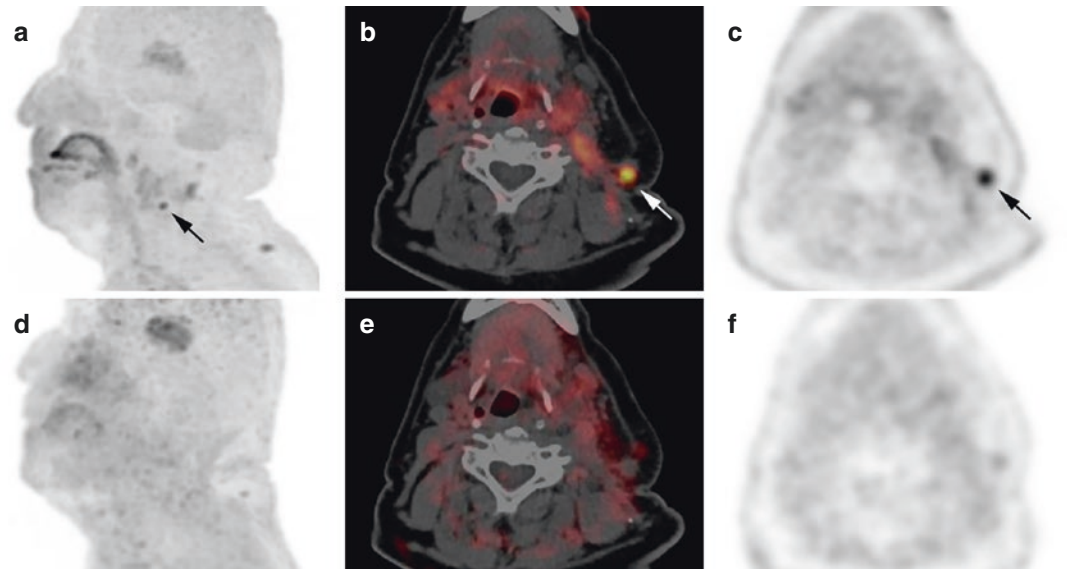

Fig. 10.1 Persistent disease in a sporadic MTC patient evaluated by dual-time point ^{18}F-FDOPA PET/CT. (**a**–**c**) PET/CT acquisition performed at 15 min post-injection. (**d**–**f**) PET/CT acquisition performed at 60 min post-injection. ^{18}F-FDOPA PET/CT shows a LN located in the left lateral compartment on early phase PET/CT (**a**–**c**, arrows) followed by decreased uptake on delayed images (**d**–**f**). This case illustrates the role of early acquisition phase in MTC patients

MTC patients with persistent/recurrent serum calcitonin >150 pg/mL [23], however, this recommendation was not made in the 2015 revised version [5]. The European Association of Nuclear Medicine (EANM) did not endorse the revised recommendations due to contradictions between versions, no new evidence against the use of ^{18}F-FDOPA PET/CT, the amount of scientific evidence in the literature, and quality of images that can be obtained with an optimal imaging protocol [24, 25]. A recent study has shown that ^{18}F-FDOPA PET/CT can accurately help determine the involved lymph node compartments in relapsed MTC, and could therefore guide the surgical strategy [26]. Furthermore, ^{18}F-FDOPA PET/CT can also detect PHEO that can coexist with MTC in MEN2 patients, although biochemical testing should be used to diagnose PHEO. Based on 2 meta-analyses and several original articles, ^{18}F-FDOPA PET is considered the best radiopharmaceutical for the detection of persistent/recurrent MTC on both patient- and lesion-based analyses [27, 28]. Overall, the per-patient detection rate of ^{18}F-FDOPA PET/CT is estimated to 60–70% and heavily depends on serum calcitonin levels and tumor behavior. The main limitation of ^{18}F-FDOPA PET/CT is that it relies on a poor spatial resolution that leads to underestimation of millimetric nodes. However, one study showed that ^{18}F-FDOPA PET/CT performed better than whole-body MRI and whole-body CT [29]. The cutoff value of 150 pg/mL for calcitonin **should not** be taken **as a strict** value that determines ^{18}F-FDOPA PET/CT sensitivity but rather as a clinically relevant value for the timing of reoperative surgery. ^{18}F-FDOPA PET/CT, together with neck US, can show the involved neck compartments/levels and help to determine the optimal surgical strategy (extended versus limited neck dissection). Therefore, there is no evidence to disqualify the use of ^{18}F-DOPA in countries where ^{18}F-DOPA is approved and implemented. In a recent prospective study that included 36 MTC patients, ^{18}F-DOPA PET/CT led to modification in treatment strategies in nearly 40% of cases [30].

10.2.3 ^{18}F-FDOPA PET/CT Prior Initial Surgery

Accurate preoperative staging of MTC is important for treatment selection and prognostication. Neck US should first be performed for assessing thyroid nodules and cervical lymph nodes, and it can also be used to guide fine-needle aspiration cytology (FNAC). It is less sensitive for evaluating the central neck compared to the lateral neck compartment due to the location of the thyroid gland. In subcentimeter MTC with no evidence of nodal extension on neck US, no additional imaging is needed (apart from abdominal CT/MRI along with biochemical assays like plasma or urine metanephrines to rule out PHEO). In supracentimeter MTC, the work-up is more exhaustive and usually includes a cervicothoracoabdominal CT. However, CT remains less sensitive and specific than neck US for depicting cervical lymph nodes, and the risk of mediastinal and lung metastases is almost nonexistent in these cases. In contrast, a cervicothoracoabdominal CT can complement neck US for both detecting potential mediastinal metastases and ruling out lung metastases or PHEO in cases of MTC with suspected lymph node metastases in US. Certain patients with positive LNs in the upper mediastinum, but without distant metastasis, may benefit from mediastinal dissection. Furthermore, in patients with distant metastasis, a less extended neck surgery should be considered to avoid local and lateral neck complications.

Finally, a preoperative work-up should be more exhaustive and include ^{18}F-FDOPA PET/CT in MTC patients with highly elevated serum calcitonin values (>500 ng/ml) [31]. Patients must undergo plasma or urine metanephrines to rule out PHEO in addition to an abdominal CT/MRI.

Although ^{18}F-FDOPA PET/CT can detect MTC and LN metastases, its role prior to initial therapeutic thyroidectomy must be further evaluated (Figs. 10.2 and 10.3).

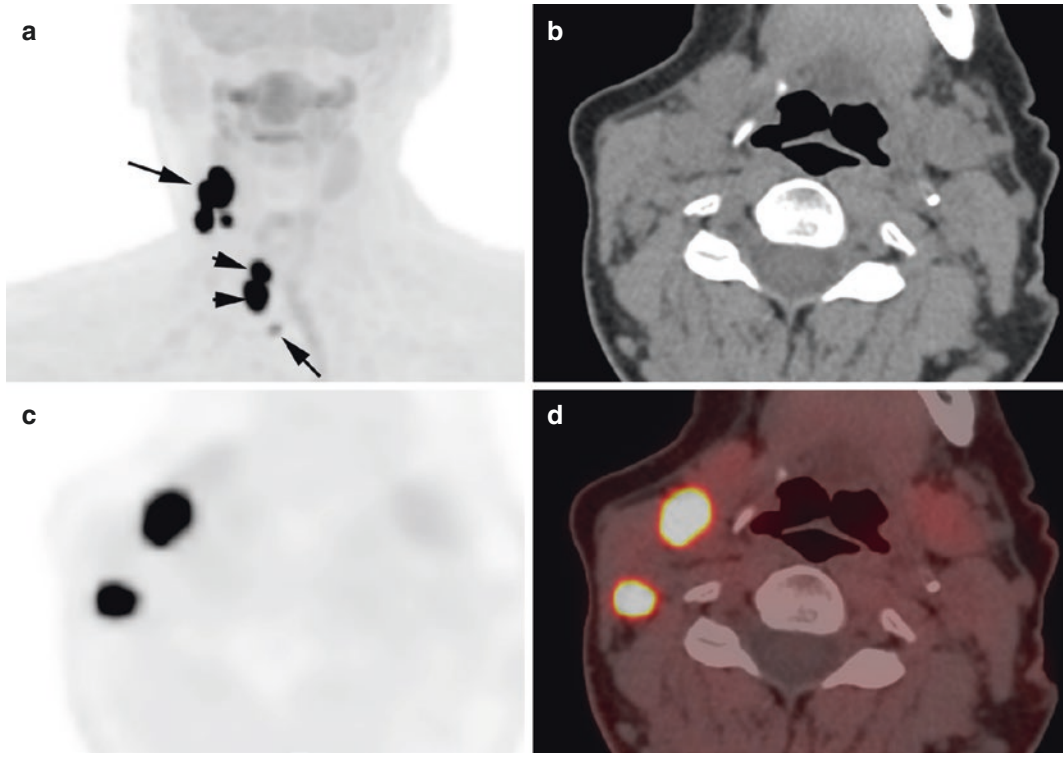

Fig. 10.2 ^{18}F-FDOPA PET at initial diagnosis of MTC in a sporadic case. ^{18}F-FDOPA PET/CT shows 2 right MTC (**a**, arrowheads) and LN in the central and right lateral neck compartments (**b–d**, arrows)

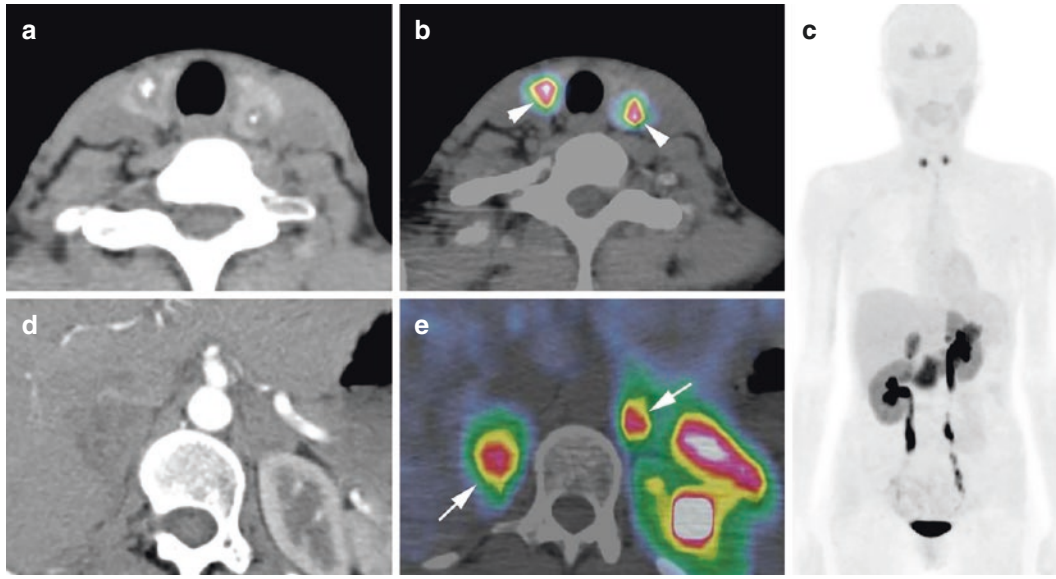

Fig. 10.3 ^{18}F-FDOPA PET at initial diagnosis of MTC in a MEN2 patient. ^{18}F-FDOPA PET/CT shows a bilateral MTC (**a**–**c**, arrowheads) and a bilateral pheochromocytoma (**c**–**e**, arrows)

A recent study from an experienced surgical team has evaluated the impact of neck US and contrast-enhanced ^{18}F-FDOPA PET/CT prior to initial surgery in 50 MTC patients [32]. All patients underwent total thyroidectomy with bilateral central neck dissection and bilateral lateral lymphadenectomy (including level V) regardless of serum CT levels and imaging findings in the neck. The only criterion for modifying this strategy was the presence of positive LNs in the mediastinum and distant metastasis on ^{18}F-FDOPA PET/CT. Nodal, central, and lateral compartment-based sensitivities were 43%, 6%, and 56% for neck US and 57%, 28%, and 75% for ^{18}F-FDOPA PET/CT. Missed patients with lateral LN involvement had small metastases (5.6 ± 5.1 mm), illustrating that the small size of LN metastasis affects PET sensitivity due to a partial volume effect. One could argue that this possible underestimation of small lateral LN could lead to a systematic bilateral lateral neck dissection. However, it is important to consider that LN can also occur in the upper mediastinum and patients do not benefit from systematic mediastinal dissection. Additionally, in cases of negative imaging findings, lateral neck dissection revealed negative LN in a large proportion of cases, even those with serum CT > 85 pg/mL (42% in the series of Brammen et al) [32]. Also, lateral neck dissection can be performed during a second surgical procedure without additional morbidity, if needed. Brammen et al. also argue that the use of ^{18}F-FDOPA PET/CT results in increased patient radiation exposure of approximately 25 mSv. However, this statement reflects historical data as it is widely accepted that the effective dose from radiopharmaceuticals in adults is 0.025 mSv/MBq [33] with an additional radiation dose from CT depending on scan parameters (ranging from 2 to 5 mSv). Currently, no guidelines recommend performing ^{18}F-FDOPA PET/CT prior to initial surgery due to scarce literature [5, 31, 34, 35]. Of note, all patients should undergo genetic testing for *RET* mutations and have PHEO excluded preoperatively by measurements of plasma or urinary metanephrines.

10.3 ^{18}F-FDG PET and Prognostication

Recent data have shown that a patient's genotype is a determinant of the age of MTC occurrence but has no impact on multivariate analysis of overall survival or time to distant metastatic disease [7]. The tumor stage is a critical prognostic

factor in MTC. Recently, new TNM staging has been proposed for a more accurate risk stratification and potential treatment selection. One major change included placing only metastatic disease in stage IV (T4 and N1b being downstaged), which led to a revised 5-year disease-specific survival rate in this group of 40% compared to 82% in the current AJCC TNM staging [36].

Serum calcitonin and CEA doubling times are powerful prognosticators and they may guide the timing and choice of diagnostic imaging procedures.

The role of imaging is to evaluate the risk of disease presence in certain locations and to provide prognostic information. The management of metastatic disease heavily depends on tumor behavior and location of metastasis. Imaging of MTC remains, however, a challenge due to the high frequency of disseminated and micrometastatic disease. ^{18}F-FDG PET/CT is considered suboptimal in assessing the extent of disease, even if certain tumors exhibit a high tracer uptake (59% per-patient sensitivity, 95% confidence interval: 54–63%) [37]. However, it has a unique prognostic value [38]. Survival is significantly reduced in ^{18}F-FDG-positive MTC compared to F-FDG negative MTC, regardless of ^{18}F-FDOPA PET/CT results. ^{18}F-FDG PET/CT sensitivity is increased in patients with shorter biomarker doubling times [39]. Additionally, in one small study, imaging biomarkers such as intratumoral textural features and volumetric parameters (total lesion glycolysis, TLG) obtained from ^{18}F-FDG PET/CT were found to be independent parameters for overall survival prediction in MTC patients treated with Vandetanib [40]. Some authors have proposed performing PET/CT with both ^{18}F-FDG and ^{18}F-FDOPA in patients with metastasis to better characterize tumor behavior [41].

10.4 Peptide Receptor Targeting and Theragnostic Approaches

NETs usually overexpress somatostatin receptor type 2 (SST2) and therefore, can be targeted by radiolabeled somatostatin analogs (SSAs) for imaging. The current importance of somatostatin analogs as theragnostic radiopharmaceuticals lie in their dual application as imaging agents (^{68}Ga) and therapeutic radioisotopes (such as ^{90}Y and ^{177}Lu). The impressive results obtained from the NETTER-1 study, which compared ^{177}Lu-DOTATATE (4 administrations of 7.4 GBq) with an augmented dose of octreotide long-acting release (60 mg) in patients with progressive, somatostatin receptor expressing mid-gut NETs (ileal in 75% of cases), has provided a powerful impetus for a wider application of peptide receptor radionuclide therapy (PRRT) in NETs. Overall, the diagnostic performance of PET/CT using ^{68}Ga-SSA in recurrent MTC seems to be inferior compared to ^{18}F-FDOPA PET/CT [42] due to the variable SST2 expression in MTC [43]. However, ^{68}Ga-SSA performs better than ^{18}F-FDG PET [44], can provide complementary informations to ^{18}F-FDOPA, especially in the detection of bone metastases [45] and may impact on therapeutic strategies [46]. These results suggest that PRRT can be a treatment option in a subset of MTC patients [47]. In vitro receptor autoradiography has revealed that SST2 antagonists can bind more receptor sites than agonists, therefore, opening new opportunities for imaging and PRRT with SST antagonists in MTC [48].

Specific overexpression of cholecystokinin 2 (CCK2)/gastrin receptors has been demonstrated to be expressed in MTC. The safety of the use of 111In-DOTA-minigastrin analogue (*CP04*) for diagnostic purposes has been demonstrated in the setting of a phase 1 trial. Of note, there is a high *stomach* (S) uptake is attributed to the high density of CCK2R located on enterochromaffin-like cells in corpus mucosa of the *stomach.* CCK-2/gastrin receptor imaging is expected to become a valuable diagnostic method for the specific non-invasive staging and monitoring of MTC patients [49]. The treatment of recurrent and disseminated disease with CCK2R analogs could also represent an interesting tool, especially for patients that progress after targeted therapies such as selective anti-RET TKI.

The expanded use of PSMA (for prostate-specific membrane antigen) imaging has shown uptake in nonprostatic benign and malignant

entities including cases of recurrent MTC [50, 51]. Since PSMA targeting represents a theragnostic approach, it could be interesting to evaluate the expression of PSMA in a series of MTC with various tumor stages and genotypes.

10.5 Immuno-PET for CEA Targeting

Medullary thyroid carcinoma is a prime example of CEA-secreting tumors. The most sophisticated approach for CEA targeting is the pre-targeted method with bispecific monoclonal antibodies (bsmAbs) [52]. One approach consists of first administrating a bispecific antibody that recognizes CEA at one site and a peptide at the other site. After this, a radiolabeled bivalent peptide is administered, which is eventually bound by 2 bsmAbs, thereby forming a ternary complex that has been shown to improve tumor uptake (the affinity enhancement system). This approach was initially developed for radioimmunotherapy in relapsed MTC [53], however, its use is currently being questioned after the recent introduction of tyrosine kinase inhibitors [54]. Recently, the same approach has been developed for PET imaging (immuno-PET) with promising results [55, 56].

10.6 Future Perspectives

Future prospective studies are needed to better address whether PET/CT could enhance risk stratification and personalize approaches to MTC patients. Targeted molecular therapies that inhibit RET and other tyrosine kinase receptors involved in angiogenesis have shown antitumor effects with improved progression-free survival in advanced MTC. However, it is still not clear which patients will benefit the most from these treatments. It would be of particular interest to utilize PET imaging to gauge patient responses to targeted therapies (patient selection, optimal timing, and effective molecular therapeutic targets).

The future of diagnostic and therapeutic nuclear medicine in MTC will depend on the identification of new MTC cell-specific targets. Novel CCK-2 receptor ligands show promise for MTC imaging and represent potential theragnostic approaches in selected cases [57]. Molecular imaging using 18F-AV-45 PET by its virtue of detecting amyloid deposition should also be evaluated for disease subtyping of MTC [58].

In conclusion, theragnostic approaches in combination with new future therapies, will undoubtedly uncover novel imaging techniques to effectively defeat these tumors.

Declaration of Interest The authors declare that there is no conflict of interest that could be perceived as prejudicing the impartiality of the research reported.

Funding This research did not receive any specific grant from any funding agency in the public, commercial, or not-for-profit sector.

References

1. Costante G, et al. Predictive value of serum calcitonin levels for preoperative diagnosis of medullary thyroid carcinoma in a cohort of 5817 consecutive patients with thyroid nodules. J Clin Endocrinol Metab. 2007;92:450–5. https://doi.org/10.1210/jc.2006-1590.
2. Essig GF Jr, et al. Multifocality in sporadic medullary thyroid carcinoma: an international multicenter study. Thyroid. 2016;26:1563–72. https://doi.org/10.1089/thy.2016.0255.
3. Giovanella L, et al. Procalcitonin as an alternative tumor marker of medullary thyroid carcinoma. J Clin Endocrinol Metab. 2021;106:3634–43. https://doi.org/10.1210/clinem/dgab564.
4. Scheuba C, et al. Sporadic hypercalcitoninemia: clinical and therapeutic consequences. Endocr Relat Cancer. 2009;16:243–53. https://doi.org/10.1677/ERC-08-0059.
5. Wells SA Jr, et al. Revised American Thyroid Association guidelines for the management of medullary thyroid carcinoma. Thyroid. 2015;25:567–610. https://doi.org/10.1089/thy.2014.0335.
6. Castinetti F, Moley J, Mulligan L, Waguespack SG. A comprehensive review on MEN2B. Endocr Relat Cancer. 2018;25:T29–39. https://doi.org/10.1530/ERC-17-0209.
7. Voss RK, et al. Medullary thyroid carcinoma in MEN2A: ATA moderate- or high-risk RET mutations do not predict disease aggressiveness. J Clin Endocrinol Metab. 2017;102:2807–13. https://doi.org/10.1210/jc.2017-00317.
8. Zenaty D, et al. Medullary thyroid carcinoma identified within the first year of life in children with hered-

itary multiple endocrine neoplasia type 2A (codon 634) and 2B. Eur J Endocrinol. 2009;160:807–13. https://doi.org/10.1530/EJE-08-0854.
9. Raue F, Dralle H, Machens A, Bruckner T, Frank-Raue K. Long-term survivorship in multiple endocrine neoplasia type 2B diagnosed before and in the new millennium. J Clin Endocrinol Metab. 2017; https://doi.org/10.1210/jc.2017-01884.
10. Romei C, et al. Low prevalence of the somatic M918T RET mutation in micro-medullary thyroid cancer. Thyroid. 2012;22:476–81. https://doi.org/10.1089/thy.2011.0358.
11. Eisenhofer G, et al. Measurements of plasma methoxytyramine, normetanephrine, and metanephrine as discriminators of different hereditary forms of pheochromocytoma. Clin Chem. 2011;57:411–20.
12. Pacak K, Eisenhofer G, Ilias I. Diagnosis of pheochromocytoma with special emphasis on MEN2 syndrome. Hormones. 2009;8:111–6.
13. Skinner MA, et al. Prophylactic thyroidectomy in multiple endocrine neoplasia type 2A. N Engl J Med. 2005;353:1105–13. https://doi.org/10.1056/NEJMoa043999.
14. Prete FP, et al. Prophylactic thyroidectomy in children with multiple endocrine neoplasia type 2. Br J Surg. 2018;105:1319–27. https://doi.org/10.1002/bjs.10856.
15. Schutz F, Lautenschlager C, Lorenz K, Haerting J. Positron emission tomography (PET) and PET/CT in thyroid cancer: a systematic review and meta-analysis. Eur Thyroid J. 2018;7:13–20. https://doi.org/10.1159/000481707.
16. Hoegerle S, et al. 18F-DOPA positron emission tomography for tumour detection in patients with medullary thyroid carcinoma and elevated calcitonin levels. Eur J Nucl Med. 2001;28:64–71.
17. Treglia G, Rufini V, Salvatori M, Giordano A, Giovanella L. PET imaging in recurrent medullary thyroid carcinoma. Int J Mol Imaging. 2012;2012:324686. https://doi.org/10.1155/2012/324686.
18. Beheshti M, et al. The value of 18F-DOPA PET-CT in patients with medullary thyroid carcinoma: comparison with 18F-FDG PET-CT. Eur Radiol. 2009;19:1425–34.
19. Beuthien-Baumann B, Strumpf A, Zessin J, Bredow J, Kotzerke J. Diagnostic impact of PET with 18F-FDG, 18F-DOPA and 3-O-methyl-6-[18F] fluoro-DOPA in recurrent or metastatic medullary thyroid carcinoma. Eur J Nucl Med Mol Imaging. 2007;34:1604–9.
20. Luster M, et al. Clinical value of 18-fluorine-fluorodihydroxyphenylalanine positron emission tomography/computed tomography in the follow-up of medullary thyroid carcinoma. Thyroid. 2010;20:527–33.
21. Soussan M, et al. Added value of early 18F-FDOPA PET/CT acquisition time in medullary thyroid cancer. Nucl Med Commun. 2012;33:775–9. https://doi.org/10.1097/MNM.0b013e3283543304.
22. Santhanam P, Taieb D. Role of (18) F-FDOPA PET/CT imaging in endocrinology. Clin Endocrinol. 2014;81:789–98. https://doi.org/10.1111/cen.12566.
23. American Thyroid Association Guidelines Task Force, et al. Medullary thyroid cancer: management guidelines of the American Thyroid Association. Thyroid. 2009;19:565–612. https://doi.org/10.1089/thy.2008.0403.
24. Treglia G, et al. The 2015 Revised American Thyroid Association guidelines for the management of medullary thyroid carcinoma: the "evidence-based" refusal to endorse them by EANM due to the "not evidence-based" marginalization of the role of Nuclear Medicine. Eur J Nucl Med Mol Imaging. 2016;43:1486–90. https://doi.org/10.1007/s00259-016-3404-7.
25. Verburg FA, et al. Why the European Association of Nuclear Medicine has declined to endorse the 2015 American Thyroid Association management guidelines for adult patients with thyroid nodules and differentiated thyroid cancer. Eur J Nucl Med Mol Imaging. 2016;43:1001–5. https://doi.org/10.1007/s00259-016-3327-3.
26. Archier A, et al. (18)F-DOPA PET/CT in the diagnosis and localization of persistent medullary thyroid carcinoma. Eur J Nucl Med Mol Imaging. 2016;43:1027–33. https://doi.org/10.1007/s00259-015-3227-y.
27. Lee SW, Shim SR, Jeong SY, Kim SJ. Comparison of 5 different PET radiopharmaceuticals for the detection of recurrent medullary thyroid carcinoma: a network meta-analysis. Clin Nucl Med. 2020;45:341–8. https://doi.org/10.1097/RLU.0000000000002940.
28. Treglia G, et al. Detection rate of recurrent medullary thyroid carcinoma using fluorine-18 dihydroxyphenylalanine positron emission tomography: a meta-analysis. Acad Radiol. 2012;19:1290–9. https://doi.org/10.1016/j.acra.2012.05.008.
29. Terroir M, et al. F-18-Dopa positron emission tomography/computed tomography is more sensitive than whole-body magnetic resonance imaging for the localization of persistent/recurrent disease of medullary thyroid cancer patients. Thyroid. 2019;29:1457–64. https://doi.org/10.1089/thy.2018.0351.
30. Califano I, Pitoia F, Chirico R, De Salazar A, Bastianello MJ. Prospective study on the clinical relevance of (18)F-DOPA positron emission tomography/computed tomography in patients with medullary thyroid carcinoma. Endocrine. 2022;77:143–50. https://doi.org/10.1007/s12020-022-03062-3.
31. Filetti S, et al. Thyroid cancer: ESMO Clinical Practice Guidelines for diagnosis, treatment and follow-updagger. Ann Oncol. 2019;30:1856–83. https://doi.org/10.1093/annonc/mdz400.
32. Brammen L, et al. Medullary thyroid carcinoma: do ultrasonography and F-DOPA-PET-CT influence the initial surgical strategy? Ann Surg Oncol. 2018; https://doi.org/10.1245/s10434-018-6829-3.
33. ICRP. Radiation dose to patients from radiopharmaceuticals: a compendium of current informa-

tion related to frequently used substances. ICRP Publication 128. Ann ICRP. 2015;44.
34. Bozkurt MF, et al. Guideline for PET/CT imaging of neuroendocrine neoplasms with (68)Ga-DOTA-conjugated somatostatin receptor targeting peptides and (18)F-DOPA. Eur J Nucl Med Mol Imaging. 2017;44:1588–601. https://doi.org/10.1007/s00259-017-3728-y.
35. Giovanella L, et al. EANM practice guideline for PET/CT imaging in medullary thyroid carcinoma. Eur J Nucl Med Mol Imaging. 2020;47:61–77. https://doi.org/10.1007/s00259-019-04458-6.
36. Adam MA, Thomas S, Roman SA, Hyslop T, Sosa JA. Rethinking the current American Joint Committee on Cancer TNM Staging System for medullary thyroid cancer. JAMA Surg. 2017; https://doi.org/10.1001/jamasurg.2017.1665.
37. Treglia G, Villani MF, Giordano A, Rufini V. Detection rate of recurrent medullary thyroid carcinoma using fluorine-18 fluorodeoxyglucose positron emission tomography: a meta-analysis. Endocrine. 2012;42:535–45. https://doi.org/10.1007/s12020-012-9671-6.
38. Verbeek HH, et al. Clinical relevance of 18F-FDG PET and 18F-DOPA PET in recurrent medullary thyroid carcinoma. J Nucl Med. 2012;53:1863–71. https://doi.org/10.2967/jnumed.112.105940.
39. Kauhanen S, et al. Complementary roles of 18F-DOPA PET/CT and 18F-FDG PET/CT in medullary thyroid cancer. J Nucl Med. 2011;52:1855–63. https://doi.org/10.2967/jnumed.111.094771.
40. Werner RA, et al. Volumetric and texture analysis of pretherapeutic (18)F-FDG PET can predict overall survival in medullary thyroid cancer patients treated with Vandetanib. Endocrine. 2018; https://doi.org/10.1007/s12020-018-1749-3.
41. Marzola MC, et al. Dual PET/CT with (18)F-DOPA and (18)F-FDG in metastatic medullary thyroid carcinoma and rapidly increasing calcitonin levels: comparison with conventional imaging. Eur J Surg Oncol. 2010;36:414–21.
42. Treglia G, et al. Comparison of 18F-DOPA, 18F-FDG and 68Ga-somatostatin analogue PET/CT in patients with recurrent medullary thyroid carcinoma. Eur J Nucl Med Mol Imaging. 2012;39:569–80. https://doi.org/10.1007/s00259-011-2031-6.
43. Yamaga LYI, et al. 68Ga-DOTATATE PET/CT in recurrent medullary thyroid carcinoma: a lesion-by-lesion comparison with 111In-octreotide SPECT/CT and conventional imaging. Eur J Nucl Med Mol Imaging. 2017;44:1695–701. https://doi.org/10.1007/s00259-017-3701-9.
44. Pajak C, Cadili L, Nabata K, Wiseman SM. (68)Ga-DOTATATE-PET shows promise for diagnosis of recurrent or persistent medullary thyroid cancer: a systematic review. Am J Surg. 2022;224:670–5. https://doi.org/10.1016/j.amjsurg.2022.03.046.
45. Asa S, et al. Evaluation of F-18 DOPA PET/CT in the detection of recurrent or metastatic medullary thyroid carcinoma: comparison with GA-68 DOTA-TATE PET/CT. Ann Nucl Med. 2021;35:900–15. https://doi.org/10.1007/s12149-021-01627-2.
46. Serfling SE, et al. Somatostatin receptor-directed molecular imaging for therapeutic decision-making in patients with medullary thyroid carcinoma. Endocrine. 2022; https://doi.org/10.1007/s12020-022-03116-6.
47. Hayes AR, et al. Metastatic medullary thyroid cancer: the role of 68Gallium-DOTA-somatostatin analogue PET/CT and peptide receptor radionuclide therapy. J Clin Endocrinol Metab. 2021;106:e4903–16. https://doi.org/10.1210/clinem/dgab588.
48. Reubi JC, Waser B, Maecke HR, Rivier JE. Highly increased 125i-Jr11 antagonist binding in vitro reveals novel indications for Sst2 targeting in human cancers. J Nucl Med. 2016; https://doi.org/10.2967/jnumed.116.177733.
49. Erba PA, et al. A novel CCK2/gastrin receptor-localizing radiolabeled peptide probe for personalized diagnosis and therapy of patients with progressive or metastatic medullary thyroid carcinoma: a multicenter phase I GRAN-T-MTC study. Pol Arch Intern Med. 2018;128:791–5. https://doi.org/10.20452/pamw.4387.
50. Arora S, et al. Recurrent medullary thyroid carcinoma on 68Ga-prostate-specific membrane antigen PET/CT: exploring new theranostic avenues. Clin Nucl Med. 2018;43:359–60. https://doi.org/10.1097/RLU.0000000000002010.
51. Arora S, et al. Prostate-specific membrane antigen imaging in recurrent medullary thyroid cancer: a new theranostic tracer in the offing? Indian J Nucl Med. 2018;33:261–3. https://doi.org/10.4103/ijnm.IJNM_10_18.
52. Boerman OC, van Schaijk FG, Oyen WJ, Corstens FH. Pretargeted radioimmunotherapy of cancer: progress step by step. J Nucl Med. 2003;44:400–11.
53. Salaun PY, et al. Phase II trial of anticarcinoembryonic antigen pretargeted radioimmunotherapy in progressive metastatic medullary thyroid carcinoma: biomarker response and survival improvement. J Nucl Med. 2012;53:1185–92. https://doi.org/10.2967/jnumed.111.101865.
54. Wells SA Jr, et al. Vandetanib in patients with locally advanced or metastatic medullary thyroid cancer: a randomized, double-blind phase III trial. J Clin Oncol. 2012;30:134–41. https://doi.org/10.1200/JCO.2011.35.5040.
55. Bodet-Milin C, et al. Immuno-PET using anticarcinoembryonic antigen bispecific antibody and 68Ga-labeled peptide in metastatic medullary thyroid carcinoma: clinical optimization of the pretargeting parameters in a first-in-human trial. J Nucl Med. 2016;57:1505–11. https://doi.org/10.2967/jnumed.116.172221.
56. Bodet-Milin C, et al. Anti-CEA pretargeted immuno-PET shows higher sensitivity than DOPA PET/CT in detecting relapsing metastatic medullary thyroid carcinoma: post hoc analysis of the iPET-MTC study. J Nucl Med. 2021;62:1221–7. https://doi.org/10.2967/jnumed.120.252791.

57. Rottenburger C, et al. Cholecystokinin 2 receptor agonist (177)Lu-PP-F11N for radionuclide therapy of medullary thyroid carcinoma: results of the lumed phase 0a study. J Nucl Med. 2020;61:520–6. https://doi.org/10.2967/jnumed.119.233031.

58. Li C, et al. Targeting amyloids with [(18)F]AV-45 for medullary thyroid carcinoma positron emission tomography/computed tomography imaging: a pilot clinical study. Mol Pharm. 2022;19:584–91. https://doi.org/10.1021/acs.molpharmaceut.1c00680.

Correction to: Integrated Thyroid Imaging: Ultrasound and Scintigraphy

Simone A. Schenke, Daniel Groener, Michael Grunert, and Alexander R. Stahl

Correction to: Chapter 4 in: Luca Giovanella, Integrated Diagnostics and Theranostics of Thyroid Diseases, https://doi.org/10.1007/978-3-031-35213-3_4

The original version of the chapter has been revised. The chapter was previously published with an error in correctly representing a detail of thyroid embryogenesis within the reference. The necessary correction has been made in the chapter to accurately reflect the information.

The corrected sentence now reads as "During embryonic development, the thyroid gland arises from endodermal tissue at the pharyngeal floor".

The updated version of the chapter can be found at https://doi.org/10.1007/978-3-031-35213-3_4

L. Giovanella (ed.), *Integrated Diagnostics and Theranostics of Thyroid Diseases*,
https://doi.org/10.1007/978-3-031-35213-3_11